Option Valuation of Smart Grid Technology Projects under Endogenous and Exogenous Uncertainty

A thesis submitted to

Imperial College London

for the degree of Doctor of Philosophy

by

Spyridon (Spyros) Giannelos

October 2016

Department of Electrical and Electronic Engineering

Imperial College London

Declaration of Originality

This is to certify:

- The material contained in this thesis is my own work.
- Other work is appropriately referenced.

The copyright of this thesis rests with the author and is made available under a Creative Commons Attribution Non-Commercial No Derivatives licence. Researchers are free to copy, distribute or transmit the thesis on the condition that they attribute it, that they do not use it for commercial purposes and that they do not alter, transform or build upon it. For any reuse or redistribution, researchers must make clear to others the licence terms of this work.

Abstract

Electricity demand and renewables penetration are set to increase worldwide over the coming decades as part of the global decarbonisation effort. As a result, distribution networks are expected to face challenges related to increased peaks and undesirable voltage excursions. Hence, significant network reinforcements may be required over the next decades. However, a very significant challenge in realizing this transition is the increased uncertainty that surrounds future distributed generation and load connections in terms of size, location and timing. This uncertainty inadvertently will give rise to the prospect of inefficient investments and stranded assets given that current planning practices remain deterministic. It follows that new planning frameworks are needed that allow the quantification of option value and achieve reduction of stranding risk by encouraging cost-efficient strategic investments through smart technologies under both endogenous and exogenous sources of uncertainty.

This thesis presents multi-epoch stochastic optimization models, for the distribution network planning problem, that consider a set of investment options with different techno-economical characteristics so as to reflect the multitude of choices available to planners in a realistic setting characterized by endogenous or exogenous uncertainty. These optimization models are rendered tractable through the use of novel decomposition schemes that effectively help manage the associated increased computational burden. The corresponding simulation results validate that smart technologies constitute valuable options for enabling cost effective integration of distributed generation units and underline the importance of early investment in such assets under decision-dependent uncertainty. In addition, the results emphasize that deterministic approaches systematically undervalue the flexibility that smart assets provide, thereby posing a barrier to the advent of the flexible smart grid paradigm.

.

Table of contents

Abstract 4

Table of contents 5

List of publications 8

Abbreviations 9

Acknowledgements 10

Dedication 11

Chapter 1 Introduction 12

1.1 Contribution to the Autonomic Power System (APS) project 12

1.2 Motivation 12

1.3 Smart Grid Technologies 14

1.3.1 Voltage rise effect 15

1.4 Option Value of Smart Grid Technologies 26

1.5 Decision-Dependent Uncertainty 28

1.6 Benders Decomposition 32

1.7 Original research contributions 35

1.8 Thesis Structure 36

Chapter 2 Option Value of Smart Technologies under Exogenous Uncertainty 37

2.1 Integration of renewables to distribution networks via Storage and DLR 37

2.1.1 Problem Description 37

2.1.2 Results of the optimization studies 42

2.1.3 Mathematical Formulation 49

2.1.4 Solution Methodology 59

2.2 Integration of solar PV to distribution networks via SOP, CVC, DSR, APGC . 60

2.2.1 Problem Description 61

2.2.2 Results of the optimization studies 66

2.2.3 Mathematical formulation 78
2.2.4 Solution Methodology 89
Chapter 3 Option Value under Endogenous Uncertainty with Immediate Resolution 92
3.1 Immediate & Local DDU resolution (applied to distribution) 92
3.1.1 Problem description 92
3.1.2 Results of the optimization studies 96
3.1.3 Mathematical Formulation 104
3.1.4 Solution Methodology 117
3.2 Immediate & Global DDU resolution 121
3.2.1 Problem description 122
3.2.2 Results of the optimization studies 123
3.2.3 Mathematical Formulation 129
3.2.4 Solution Methodology 130
3.3 Immediate & Local DDU resolution (applied to transmission) 132
3.3.1 Problem description 132
3.3.2 Results of the optimization studies 138
3.3.3 Mathematical formulation 141
3.3.4 Solution Methodology 142
Chapter 4 Option Value under Endogenous Uncertainty with Gradual Resolution 146
4.1 Gradual & Global DDU resolution 146
4.1.1 Problem description 147
4.1.2 Results of the optimization studies 149
4.1.3 Mathematical Formulation 153
4.1.4 Solution Methodology 165
4.2 Gradual & Local resolution of DDU 167
4.2.1 Problem description 168
4.2.2 Results of the optimization studies 169

4.2.3 Mathematical Formulation 173
4.2.4 Solution Methodology 183
Chapter 5 Concluding remarks and further work 184
5.1 Summary and future goals 184
5.2 Prospects for future work 186
References 190

List of publications

- S. Giannelos, I. Konstantelos and G. Strbac, “Stochastic optimization-based valuation of smart grid options under firm DG contracts,” *2016 IEEE International Energy Conference (ENERGYCON),* Leuven, 2016, pp. 1-7.

- S. Giannelos, I. Konstantelos and G. Strbac, "Option Value of Demand Side Response schemes under Decision Dependent Uncertainty," in *IEEE Transactions on Power Systems* [to be submitted]

- S. Giannelos, I. Konstantelos and G. Strbac, “Option value of Soft Open Points in distribution networks,” *PowerTech, 2015 IEEE,* Eindhoven, 2015, pp 1-6.

- S. Giannelos, I. Konstantelos and G. Strbac, “A New Class of Planning Models for Option Valuation of Storage Technologies under Decision-Dependent Innovation Uncertainty,” *PowerTech, 2017 IEEE,* Manchester [to be submitted].

- I. Konstantelos, S. Giannelos and G. Strbac, "Strategic Valuation of Smart Grid Technology Options in Distribution Networks," in *IEEE Transactions on Power Systems* , vol.PP, no.99, pp.1-1

Abbreviations

AC OPF: Alternating Current Optimal Power Flow

APGC: Active Power Generation Curtailment

AVC: Automatic Voltage Control

CVC: Coordinated Voltage Control

DG: Distributed Generation

DC OPF: Direct Current Optimal Power Flow

DDU: Decision – Dependent Uncertainty (Endogenous Uncertainty)

DSR: Demand Side Response

DLR: Dynamic Line Rating

DNO: Distribution Network Operator (electricity networks)

GB: Great Britain

MILP: Mixed Integer Linear Programming problem

MINLP: Mixed Integer Non Linear Programming problem

NAC: Non-Anticipativity Constraint

NOP: Normally-open point

OFGEM: Office of Gas and Electricity Markets

OLTC: On-Load Tap Changer unit

PV: PhotoVoltaic

SOP: Soft Open Point

VOLL: Value of Lost Load

Acknowledgements

I would like to thank Professor Goran Strbac for giving me the opportunity to conduct the PhD under his supervision, for all the opportunities to participate in top conferences around the world and publish in the most well-known and respected journals, for his fundamental guidance as well as for his constant feedback. Finally, I would like to express my gratitude for his offer for the position of the Research Associate and the opportunity to further participate in various projects.

I would like to thank Dr. Ioannis Konstantelos for his substantial feedback and insightful inputs at every step of the research that led to higher quality overall output, as well as for his feedback and guidance on how to best structure publications in top journals and how to optimally tackle complex problems that arose during the research.

I would also like to thank my colleagues in the Control and Power research group for our fruitful discussions on research topics relevant to the thesis as well as my Professor at National Technical University of Athens, Nikos Hatziargyriou, for our discussion that led to me applying for a PhD under the supervision of Professor Goran Strbac and for his personal interest in my work throughout the duration of the PhD.

Finally, I would like to express my deepest gratitude to my parents, brother and relatives for sending their positive energy throughout my PhD.

Dedication

To the entire Mathematical Optimization community
that is making the world a better place.

Chapter 1 Introduction

1.1 *Contribution to the Autonomic Power System (APS) project*

APS is a multi-disciplinary project with a focus on the electricity system of 2050 [1]. This system is expected to be characterised by increased uncertainty around the availability of generation (due to increased presence of renewable generating units), significant consumer participation in the system operation and considerable presence of low carbon demand (electric vehicles and heat pumps) as well as of smart technologies such as the ones presented in the thesis. The resulting "autonomic" system will have the ability to yield the optimal decisions relevant to network operation and act upon them on its own ('self-manage') in real-time.

The goal of this research, which contributes to the Work Package (WP) "Autonomic Economics" [2] that is one of the four WP components of APS and was led by Professor Goran Strbac, is to prove the concepts, methods and systems that could deliver such an autonomic power system. To this end, focus is placed on novel methodologies and mathematical models for economic decision making built around the concept of option value of smart technologies.

1.2 *Motivation*

Investments constitute the central idea in the process of transitioning from the traditional passive power distribution system to a smart distribution grid. This transition is expected to continue at a high pace and on a global scale as it is driven by many factors, as the ones presented below.

First and foremost, **climate change** is a very important key driver for this transition. Governments and inter-governmental organisations are becoming more and more motivated to propose legislation that will promote measures for deceleration of climate change and avoidance of its consequences. For example, the UK government has pledged an 80% reduction, from 1990 levels, in greenhouse gas emissions by the year 2050 [3] while the

European Council has dictated a 20% reduction in CO2 emission as well as a 20% uptake (comparing to 1990 levels) of renewables in total energy consumption by 2020 [4]. Since smart grids can allow more renewables to connect to the system while at the same time improve the utilization of existing infrastructure it can be concluded that the consequences of climate change may be ameliorated or even avoided at a cost smaller than following a traditional passive investment approach.

Secondly, the availability of **information and communication technology** and especially of cheap and well-established technology that can be easily integrated into the system can help realize this paradigm shift. What remains is to gain understanding of how this technology will operate in a coordinated fashion and how the corresponding investment decision making process can unfold under uncertainty.

The transition to a smart grid is also driven by the desire to prevent a further **degradation in infrastructure utilization**. For example, currently the annual utilization of thermal generation assets in the UK is about 55% [5] with generators running at low levels during spring and summer and relatively higher levels during winter when demand is greater. It is expected that significant amounts of renewables are to be added to the system to cover the increasing demand, which will partially stem from the electrification of transport and heat sectors. However, although the installed capacity of the renewable generating units may displace energy produced by conventional plants, it may not be able to displace proportional amounts of installed capacity of conventional plants because of the intermittency of the resource (wind, sun). For instance, during periods of low wind speed some conventional plants will have to operate to cover the missing wind generation. This means that more thermal units will have to be built to cover the increased demand despite building more renewable generating units. Another factor leading to the reduction of asset utilization constitutes the increased uncertainty that may lead to assets that are used less time than initially planned.

Thus, according to relevant studies the utilization of generating assets may drop to 35% by 2025 and even less than 25% by 2035 [5]. For similar reasons the utilization of network assets (lines, substations etc.) may reduce significantly because the need to accommodate the rising power flows will stimulate significant equipment upgrades that will essentially be utilized to securely accommodate some rare peaks. With the use of smart

technologies considerable increases in peaks may be averted and the stranding risk can decrease, thereby potentially achieving to prevent the downward trend in asset utilization.

The current thesis is **motivated** by the desire to facilitate the process of transition to a smart grid in order to allow greater integration of renewables thereby tackling climate change while at the same time preventing further degradation of asset utilization and avoiding stranded assets. The thesis also responds to the call made by OFGEM in RIIO-ED1 for the consideration of option value when forming investment decisions [6] and for greater levels of innovation stating in particular the following. "*The consideration of smart grid solutions will need to be at the heart of the DNO's business plan […]. We expect a well-justified business plan to clearly demonstrate how DNOs have considered alternative solutions in their cost benefit analysis […] and include an assessment of the option value of proposed smart grid investments*". This response is provided in the form of the presentation of novel investment decision frameworks based on the concept of option value of smart technologies. In addition OFGEM recognizes that "*we currently do not fully understand smart grids and the uncertainty around low carbon technology take-up"* Providing many examples can assist OFGEM in understanding these new developments; this also constitutes a motivation for the current work.

1.3 *Smart Grid Technologies*

Smart technologies have long been recognized as an alternative to conventional reinforcements in distribution networks [7]. In this thesis a range of technologies are considered, such as APGC of a DG unit [8], SOP [9], [10], [11], DSR [12], [13], CVC [14], storage [15] and DLR [16], [17]. The operation of the former four is presented in paragraph 1.3.1 as well as in section 2.2 where the eradication of the voltage rise effect is achieved under exogenous uncertainty. The operation of the DSR scheme is also analysed under endogenous uncertainty in Chapter 3 and Chapter 4 for achieving the safe accommodation of increased power flows. Storage technology is analysed under both endogenous and exogenous uncertainty and involves charging and discharging of energy at different time periods with the aim of keeping power flows within thermal limits. Finally, DLR is presented in section 2.1 and is shown to assist in eradicating the stranding risk (along with storage) tied to first epoch conventional investments by informing the network operator

about the possibility to allow power flows that are on an annual average 30% greater than those indicated by the static thermal rating. This inadequacy of conservative static rating values has been observed in practice [18], [19], [20].

1.3.1 *Voltage rise effect*

DNOs are responsible for delivering electricity to consumers within statutory voltage limits [21] as follows:

- The steady-state voltage magnitude for networks of voltage level between 1kV to 33kV should be kept within +/- 6% of the nominal voltage. These limits are used in the case study shown in section 2.2.

- The steady-state voltage magnitude for networks of voltage level below 1kV (low-voltage) should be kept within +10/- 6% of the nominal voltage.

Any deviation outside these limits may be hazardous for the connected equipment. This is particularly relevant nowadays due to the increasing DG penetration in distribution networks [22] and its effect on voltage magnitudes. Following, the voltage rise effect and possible ways of tackling it are analyzed.

Figure 1.1 shows a diagram of a simplified traditional distribution network where the power flows from the substation towards the load. In this case, equation (1.1) holds.

$$\overrightarrow{V_1} = \overrightarrow{V_2} + \vec{I}(R + jX) \tag{1.1}$$

The current $\vec{I}$ can be expressed as $\overrightarrow{I_2} = \overrightarrow{(P_2 - jQ_2)}/\overrightarrow{V_2^*}$ given that it is $\overrightarrow{S_2} = \overrightarrow{V_2}\overrightarrow{I_2^*}$. Thus, (1.1) can be written as follows.

$$\overrightarrow{V_1} - \overrightarrow{V_2} = \frac{\overrightarrow{(P_2 - jQ_2)}}{\overrightarrow{V_2^*}}(R + jX) \tag{1.2}$$

Equation (1.2) is equivalent to (1.3).

$$\overrightarrow{V_1} - \overrightarrow{V_2} = \frac{RP_2 + XQ_2 + j(XP_2 - RQ_2)}{\overrightarrow{V_2^*}} \tag{1.3}$$

Taking $\overrightarrow{V_2}$ as a reference ($\overrightarrow{V_2} = V_2$) the complex number $\overrightarrow{V_1} - \overrightarrow{V_2}$ can be represented as a vector on the complex x-y plane with coordinates ($\frac{RP_2+XQ_2}{V_2}, \frac{XP_2-RQ_2}{V_2}$). Since the angle difference between $\overrightarrow{V_1}, \overrightarrow{V_2}$ is usually very small, the vector is practically tangent on the horizontal axis, meaning that (1.3) can be simplified to (1.4), i.e. only the abscissa is kept.

$$\overrightarrow{V_1} - \mathrm{V}_2 = \frac{RP_2 + XQ_2}{V_2} \tag{1.4}$$

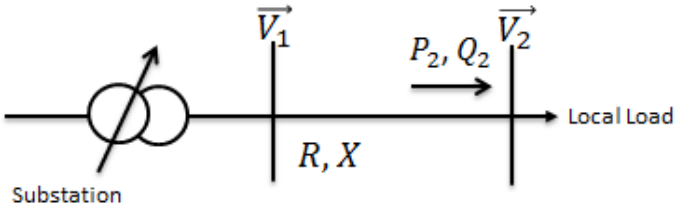


Figure 1.1 Traditional distribution network with unidirectional power flows. The R, X symbolize line resistance and reactance values respectively while $P_2, Q_2, \overrightarrow{V_2}$ are the active and reactive power flows and voltage respectively at bus 2 (load bus).

If a DG unit is connected to the load bus (Figure 1.2), then the voltage difference $\overrightarrow{V_1} - \overrightarrow{V_2}$ can be expressed as in (1.5), based on the assumption that the DG operates at unity power factor (i.e. it does not produce or absorb reactive power); such operation has been common practice for DG units [14], [23] as DNOs normally require the DG owners to maintain a constant power factor close to unity for both commercial reasons (to ensure the availability of the generator's full real power output [24]) and technical reasons [25] (if small DG units attempt to correct voltage drops by injecting large reactive power, then this may result in high currents and potential overheating of the DG unit, triggering the over-current protection and disconnecting the DG from the network).

$$\overrightarrow{V_1} - \mathrm{V}_2 = \frac{R\left(P_2 - P_g\right) + XQ_2}{V_2} \tag{1.5}$$

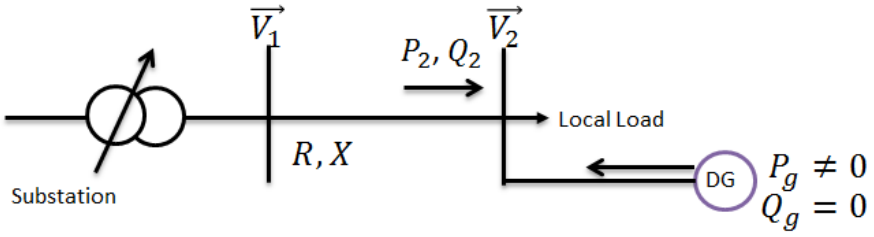


Figure 1.2 Distribution network after the connection of a DG unit operating at unity power factor (i.e. no reactive power generation/absorption capability).

At the 11kV level (i.e. the voltage level of the networks examined in the thesis) the voltage difference $\overrightarrow{V_1} - \overrightarrow{V_2}$ is affected equally by both terms because $R/X \approx 1$. Note that at 0.4kV the voltage difference $\overrightarrow{V_1} - \overrightarrow{V_2}$ is affected more by the term $(P_2 - P_g)$ than by Q_2 because the ratio of the line resistance R to line reactance X is high.

The voltage rise effect can occur during time periods when the load is small (assume the extreme condition that $P_2 = 0, Q_2 = 0$) and the DG output is very high (assume it is maximum i.e. $P_g = P_g^{max}$, where P_g^{max} is the installed capacity of the DG unit). For example, a solar PV unit reaches the maximum output at time periods around midday and especially in hot summer days. During such periods it is $P_2 - P_g \ll 0$ i.e. the numerator of the right-hand-side of (1.5) becomes negative. Hence, it becomes $|V_1| < |V_2|$ and the power flows from the load to the substation with the potential that the load voltage may at some period exceed its upper statutory limit i.e.$|V_2| > |V_2^{max}|$. Equation (1.6) describes such a situation where the voltage at the load bus has reached its upper statutoty limit.

$$\overrightarrow{V_1} - V_2^{max} = \frac{R\left(0 - P_g^{max}\right) + X \cdot 0}{V_2^{max}} \tag{1.6}$$

Equation (1.6) can be solved for P_g^{max} leading to (1.7). This shows that the left-hand side (installed capacity of all the DG units that are connected to the load bus) can increase by reducing line resistance R. The latter can be realized by **line reconductoring** i.e. replacing the existing conductors with thicker cables of higher cross-sectional area and, therefore, lower resistance. Hence, reconductoring can help tackle the voltage rise effect and this has actually been the method traditionally utilized by the industry. It is a "passive solution"

because once the line is reconductored no further action or real-time management is needed to take place.

$$P_g^{max} = \left(\mathrm{V}_2^{\max} - \overrightarrow{V_1}\right)\frac{\mathrm{V}_2^{\max}}{R} \tag{1.7}$$

Under the current EU legislation, DNOs provide firm connections to new DG. However, a review of grid access regimes with a shift to non-firm connections is becoming increasingly relevant [8] in order to allow cost-effective solutions to deal with network constraints. In this context, the **APGC service** can provide an alternative solution to reconductoring as it can allow an increase in the installed capacity of the connected DG capacity P_g^{max}. In this case (1.5) takes the form of (1.9) when considering APGC.

$$\overrightarrow{V_1} - V_2 = \frac{R\left(P_2 - [P_g - P_g^{curt}]\right) + XQ_2}{V_2} \tag{1.8}$$

At the extreme case when the load is zero and the DG output is maximum it is $P_2 = 0$, $Q_2 = 0$ and $P_g = P_g^{max}$. Solving for P_g^{max}, equation (1.9) is yielded, which, when compared to (1.7) indicates the possibility of increase in P_g^{max} that can connect to the system.

$$P_g^{max} = P_g^{curt} + \left(\mathrm{V}_2^{\max} - \overrightarrow{V_1}\right)\frac{\mathrm{V}_2^{\max}}{R} \tag{1.9}$$

The connection of a **reactive power compensator** can provide an alternative solution to reconductoring as it can allow for an increase in the installed capacity of the connected DG capacity P_g^{max}. Figure 1.3 illustrates a situation where the reactive compensator and the DG unit can absorb / generate reactive power (the DG unit does not operate at unity power factor). In the case of voltage rise effect, absorbing reactive power has the effect of reducing the bus voltage and it is the desirable function. Thus, equation (1.5) takes the form of (1.10).

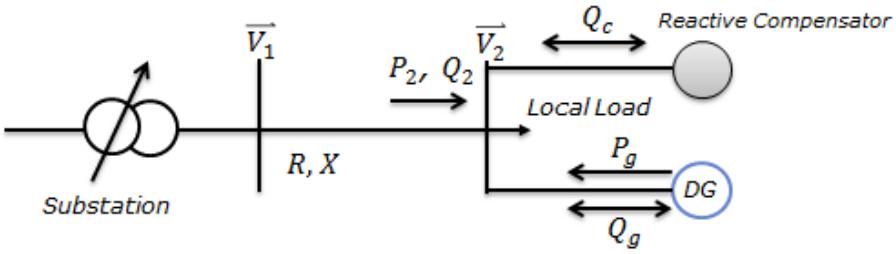


Figure 1.3 Connection of a reactive compensator, which can generate or absorb reactive power. Also, the DG unit is shown to be able to generate or absorb reactive power.

$$\overrightarrow{V_1} - \mathrm{V}_2 = \frac{R(P_2 - P_g) + X(Q_2 + Q_c + Q_g)}{V_2} \tag{1.10}$$

At the extreme case when the load is zero and the DG output is maximum it is $Q_2 = 0, P_2 = 0, P_g = P_g^{max}$. Thus, (1.11) holds. Solving for the installed capacity of the DG unit P_g^{max} yields (1.12) that, when compared to (1.7), indicates an increase in P_g^{max}. In cases where the value for line reactance (X) is relatively close to that of line resistance (R), as in the 11kV network, this technique can be effective as opposed to low-voltage grids where $R \gg X$.

$$\overrightarrow{V_1} - \mathrm{V}_2^{\max} = \frac{R(0 - P_g^{max}) + X(0 + Q_c + Q_g)}{\mathrm{V}_2^{max}} \tag{1.11}$$

$$P_g^{max} = (\mathrm{V}_2^{\max} - \overrightarrow{V_1})\frac{\mathrm{V}_2^{\max}}{R} + \frac{XQ_c + XQ_g}{R} \tag{1.12}$$

In section 2.2, **SOP technology** plays the role of reactive compensator thereby positively contributing to the eradication of the voltage rise effect. In particular SOPs can control the active power flow between two buses that are connected with a line where a normally-open point switch is placed. This can be done by absorbing some kW of power at one terminal and releasing the same amount (or possibly reduced due to losses inside SOP, which are however small) at the other SOP terminal. Note that SOPs cannot transfer reactive power between two adjacent feeders. The term "transfer of reactive power" that sometimes is used for SOPs, as in [26], actually refers to the situation where reactive power generation takes place in one terminal and absorption at the other SOP terminal. Obviously, if the SOP sets both of its ports to absorb (as in section 2.2) or to generate reactive power then this cannot be characterized as a transfer.

In this work both SOP functionalities are modelled i.e. reactive power compensation and transfer of active power for the eradication of the voltage rise effect. Note that both functionalities are possible because a SOP consists of a power-electronics converter (voltage-sourced converter, VSC) which is a single unit placed on the line and allows for rapid control of active and reactive power in all four quadrants of the P-Q plane (i.e. both absorption and generation functions). The reactive power control at each terminal is independent of the other terminal, whereas the active power flows from one terminal to the other. Implementation details of the power electronic converters are out of the scope of the current work but the interested reader can gain insight from published works such as [26]. In conclusion, although SOPs have been characterized as a mature technology, given the commercial availability of power electronic converters [7], at present there are limited, if any, operational examples of their deployment across European networks and there is also a gap in existing modelling capabilities for the strategic evaluation of such flexible assets [27].

The **DSR technology** can also provide an alternative solution to reconductoring as it can increase the installed capacity of the connected DG capacity P_g^{max}. The DSR can allow the planner (DNO) to reschedule (i.e. switch off or reduce) the customer's electricity demand. Note that to allow this to happen, a prior agreement between the planner and the customer needs to be established with the customer receiving some form or financial remuneration. [28]. Then, demand rescheduling is meant to lead to voltage constraints being respected at all times [12]. This is realized by shifting the flexible load of a bus from periods of relatively small (or zero) DG generation to "critical" periods of relatively high DG generation. As a result the net power injections at the bus during these critical periods are reduced, thereby eliminating the voltage rise effect.

When a DSR is deployed at the load bus (bus 2), equation (1.5) is expressed as (1.13) with $P_2' = P_2 + P_{DSR}$, where P_{DSR} is the power that is connected to the bus. At the extreme case when the hourly load is zero and the DG output is maximum it is $Q_2 = 0, P_2 = 0, P_g = P_g^{max}$, equation (1.14) holds. It has been assumed that although the hourly load P_2 is zero, the load that is connected by the DSR is not zero (this can happen when, for instance smart dishwashers whose operation was deferred are put into power, with the other load at the bus being zero). Solving for P_g^{max} results in (1.15), which when compared with (1.7)

indicates an increase in the amount of installed capacity of the DG units that can connect to the grid.

$$\overrightarrow{V_1} - \mathrm{V}_2 = \frac{R\left(P_2{}' - P_g\right) + XQ_2}{V_2} \tag{1.13}$$

$$\overrightarrow{V_1} - \mathrm{V}_2^{\max} = \frac{R\left(0 + P_{DSR} - P_g^{max}\right) + X \cdot 0}{\mathrm{V}_2^{max}} \tag{1.14}$$

$$P_g^{max} = P_{DSR} + \left(\mathrm{V}_2^{\max} - \overrightarrow{V_1}\right)\frac{\mathrm{V}_2^{max}}{R} \tag{1.15}$$

The term **Coordinated Voltage Control (CVC) scheme** refers to schemes that compute and alter the value of the voltage-target V_{TAR} of the AVC-relay (located in the substation transformer) based on real-time measurements of network parameters [14], [29]. In particular, this approach involves the remote measurement of voltage V_2 of the load-bus and when $|V_2| = |V_2^{max}|$ the information is transmitted in real-time to the substation where V_{TAR} gets decreased and therefore V_1 is reduced (via tap operation) to its minimum value V_1^{min} resulting in the reduction of V_2 as well (because during the voltage rise effect it is $|V_1| < |V_2|$).

The relationship between V_1 and V_{TAR} is illustrated in Figure 1.4, where V_1 is called V_{VT}, and is the voltage at the secondary side of the transformer. This voltage is continuously compared to V_{TAR} [30], which is also known as setpoint [31] and represents the desired voltage magnitude at the secondary of the transformer. When V_{VT} is outside of an allowed range (deadband) around V_{TAR}, for at least a certain amount of time (in the order of seconds [32]) the AVC-relay sends a signal to the OLTC transformer that changes its taps resulting in V_{VT} returning to a value within the deadband of V_{TAR} [31]. The OLTC unit is a mechanical switching arrangement that adjusts the transformer turns-ratios based on the instructions taken from the AVC relay. This unit can perform this operation whilst the transformer is in use. Note that the value for V_{TAR} varies depending on the characteristics of the network. However, traditionally it has been set at a fixed value ("fixed voltage target

policy") that is usually relatively higher than 11kV in order to ensure that even under the heaviest load conditions the voltage at remote buses remains above the lower statutory limit. This can be seen in Figure 1.5 for the case of the "initial setpoint" where it can be observed that heavy load conditions (no DG presence) can lead to greater voltage drop along the line.

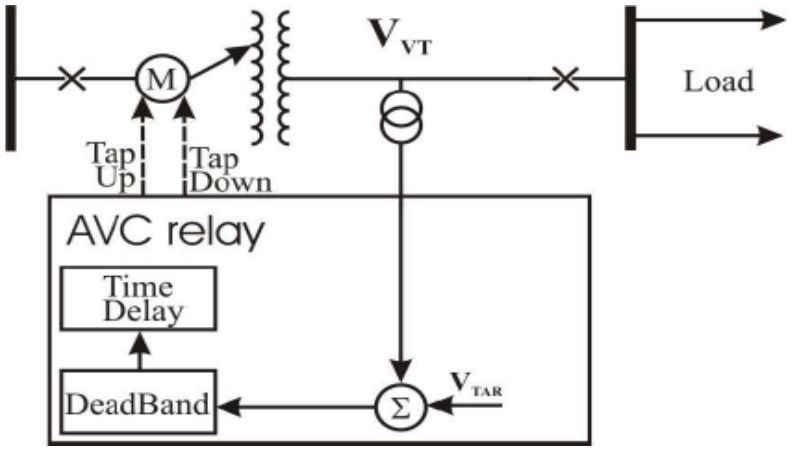


Figure 1.4 Traditional Automatic Voltage Control mechanism

Dianitta In the event that a renewable-DG unit connects to the remote load-bus, keeping the same value for the voltage-target as that prior to the DG connection may lead to the development of the voltage rise effect as it is shown in Figure 1.5 (for the case of the "initial setpoint"), where with the lowest demand (with DG) the voltage at the remote bus may exceed the upper statutory limit. Thus, it becomes necessary to change the value for the voltage target ("New Setpoint") thereby eliminating the voltage-rise effect in the event of high DG output and low load [33]. Note that it is essential to make an accurate calculation of the new value for the voltage-target ("New Setpoint") because changing it may correct the voltage magnitude at some critical buses but distort it in other areas of the network. In this thesis, the optimal voltage target value is obtained through mathematical optimization. In practice, this accuracy can be achieved through measurement of the voltage magnitude at critical buses and transmission of this information back to the substation for the estimation of V_{TAR} so that the voltage magnitudes across the network remain within statutory limits.

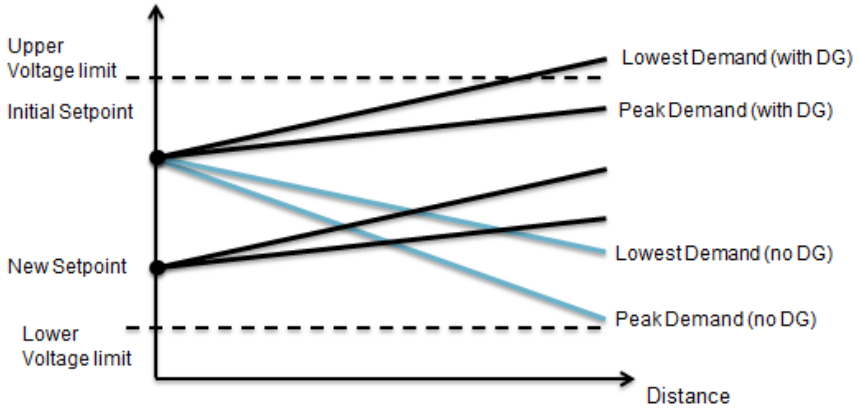


Figure 1.5 Effect of the selection of the voltage setpoint on the network voltage levels.

The connection of a CVC scheme can also provide an alternative solution to reconductoring by allowing for an increase in the installed capacity P_g^{max} of the connected DG. At the extreme case during periods when the load is zero and the DG output is maximum it is $Q_2 = 0, P_2 = 0, P_g = P_g^{max}$. Thus, (1.16) holds, which when compared with (1.7) indicates an increase in the amount of installed capacity of the DG units that can connect to the grid.

$$P_g^{max} = \left(\mathrm{V}_2^{\max} - \overrightarrow{V_1^{min}}\right) \cdot \frac{\mathrm{V}_2^{\max}}{R} \tag{1.16}$$

In [14] a mathematical formulation of a centralized CVC scheme is presented where real-time information from all buses is sent back to the substation. In addition, the CVC scheme is compared with other voltage control schemes, such as APGC and reactive power compensation, showing that CVC can achieve voltage regulation under high DG penetration. In [34] the voltage-rise effect caused by high PV penetration is resolved through the use of a CVC scheme applied to a network that hosts various distributed energy storage systems.

1.3.2 *Concise description of smart technologies*

All smart technologies assist in eradicating the stranding risk tied to the first epoch conventional investment decisions due to smaller build time, thereby rendering wait - and – see strategies cost-effective.

Demand Side Reponse (DSR):

- Achieves the safe accommodation of increased power flows by allowing the planner to reschedule (i.e. switch off / reconnect) the customers' electricity demand within a period of a day, after a prior agreement has been established with the customers receiving some form or financial remuneration.

- Allows the treatment of the voltage rise effect by shifting the flexible load of a bus from periods of relatively small (or zero) DG generation to "critical" periods of relatively high DG generation. As a result the net power injections at the bus during these critical periods are reduced, thereby eliminating the voltage rise effect.

Storage:

- Involves charging and discharging energy at different time periods with the aim of keeping power flows within thermal limits.

Dynamic Line Rating:

- Informs the network operator about the possibility to allow power flows that can be, on an annual average, 30% greater than those indicated by the static thermal line rating which is typically very conservative thereby restricting to an unnecessary extent the power flows.

Reconductoring:

- Involves replacing the existing conductors with thicker ones of higher cross-sectional area and lower resistance.

- Helps tackle the voltage rise effect and, additionally, leads to increased thermal line capacity, thereby allowing for greater DG penetration at a higher cost.

- Involves high stranding risk under uncertainty.

- It has been the method traditionally utilized by the industry. It is a "passive solution" because once the line is reconductored no further action or real-time management is needed to take place.

Active Power Generation Curtailment (APGC):

- Can allow for greater DG penetration.

Soft Open Point (SOP):

- It can allow for effectively tackling the voltage rise effect.

- It can absorb reactive power at any of its two terminals, which has the effect of reducing the bus voltage. It can also generate reactive power at any of its two terminals. These functions can be performed independently between the terminals e.g. generation of some kVAr at one terminal, absorbtion of a different amount of kVar at the other terminal, or absorbtion at both terminals or generation at both terminals.

- It can control the active power flow between two buses that are connected with a line where a normally-open point switch is placed. This can be done by absorbing some kW of power at one terminal and releasing the same amount (potentially reduced due to losses inside SOP, which are however small) at the other SOP terminal. Figure 2.19 illustrates this SOP operation.

- It cannot transfer reactive power between two adjacent feeders because of a DC element within the converter (AC/DC – DC/AC).

- Consists of a power-electronics converter (voltage-sourced converter, VSC) which is a single unit placed on the line and allows for rapid control of active and reactive power in all four quadrants of the P-Q plane (i.e. both absorption and generation functions).

Coordinated Voltage Control (CVC):

- Refers to schemes that update in real-time the value of the voltage-target of the AVC-relay (located in the substation transformer) based on real-time measurements of network parameters. In particular, the CVC technique involves the remote measurement of load voltages and when one approaches the upper statutory voltage limit the information is transmitted in real-time to the substation where the voltage-target value gets decreased (and therefore the voltage at the substation gets reduced via tap operation) resulting in the

reduction of the load voltage as well thereby effectively eradicating the voltage-rise effect. Figure 2.18 illustrates this CVC operation.

1.4 *Option Value of Smart Grid Technologies*

Smart technologies are characterized by two types of flexibility. First of all, most of them may have broader nonlocalized effects, meaning that investment achieves to improve DG (or load) hosting capability not only of a single line or busbar but of a larger network area. For example, when the DSR reduces the load or the voltage magnitude at the bus of connection this may alleviate the flow on the entire feeder and affect the voltage profile of neighbouring buses as well. As a further example, when the CVC technology reduces the substation voltage it affects the voltage pattern across the entire network. On the other hand, conventional reconductoring may affect the voltage pattern of neighboring buses but the thermal rating is only upgraded for the particular line section that is reconductored. It becomes evident that smart technologies have wider nonlocalized effects than conventional ones and this extra flexibility allows for dealing with uncertainty. For instance, it can allow for providing a natural hedge when future DG or load deployment patterns are characterized by locational uncertainty. In this case, a single smart technology investment may alleviate the stress on multiple lines regardless of the location of connection of DG/load, whereas a conventional investment could easily turn out as a stranded asset in the event of unfavourable realization of uncertainty.

Secondly, smart technologies typically have faster commissioning times than conventional reinforcements as lengthy planning permissions, asset reinforcement activities and public works can be avoided. Rapid deployment of smart assets can render "wait-and-see" investment strategies cost-effective and viable because investment will no longer be required prior to the resolution of uncertainty, thereby relieving the need for first-epoch conventional commitments which, for this reason, are highly susceptible to stranding risks. Since smart technologies can be deployed in a contingent fashion, they can be viewed as investment options under uncertainty, whose value (*option value*) reflects the investment and / or operational cost savings generated by adopting a "smart" investment strategy over a traditional one that relies on conventional reinforcements alone [35], [36]. In other words, the term "option value" incorporates the valuation of both aforementioned types of

flexibility that smart technologies hold. Since under deterministic planning the latter flexibility is lost, the "option value" is not defined for such a type of planning.

In the context of the current thesis the term "option" characterizes i) the investment in any number of assets of a particular technology and ii) when the resulting investment decision making process has the form of a strategy. The former means that the "option value" of a technology is found, rather than of single assets of that technology. This calculation allows for the evaluation of the benefits of the overall technology. The latter means that in the first epoch (current time when the strategy is formed) of the horizon the decision maker does not know whether or not particular future investments will eventually be undertaken as this will depend on the realization of uncertainty. In contrast, investing in a smart technology cannot be characterized as an "option" for a deterministic planner because at the current time the planner knows exactly when future investments will take place. Note that in this work the "option value" is obtained for "smart options" rather than for conventional ones; smart assets can be viewed as interim investment options in the sense that they can be very useful in 'buying time' in the interim until conventional large-volume reinforcements can become operational.Finally, notice that as in the case of option valuation of financial contracts [37], the option value is always nonnegative as investment in such options is not obligatory.

Although stochastic optimization is utilized in the current work for obtaining the option value of smart technologies, it is important to mention efforts that have been made to consider the dynamic investment problem under uncertainty through Real Options Analysis [36], [38]. For example the flexibility that FACTS devices possess (ability to resell them at a lower value and ability to relocate them due to their modular design, if uncertainties unfold unfavourably) is evaluated through the Least Squares Monte Carlo method [39]. This technique is also used in [40] to estimate the value of flexibility that storage technology can provide in Combined Heat and Power plants to respond to real time market signals. Methodologies other than the aforementioned include Binomial Trees, or application of the Black-Scholes model [41], [42].

Valuation approaches such as the ones noted above are becoming increasingly relevant. However their application scope is limited to a small number of candidate investment strategies defined a priori, while, in reality, a large number of strategic opportunities can arise in all irreversible dynamic decision processes due to the inter-

temporal resolution of uncertainty and the possibility for managerial flexibility. This is certainly the case for distribution network planning, which entails decisions with respect to numerous asset types and possible investment timings. To this end, the use of mathematical optimization is essential for the identification of the optimal investment strategy across all possible investment combinations [35], [43]. Obviously, mathematical optimization can also be used to obtain the option value by comparing a set of pre-defined strategies as in [44] rather than examining all possible investment combinations. Undoubtedly, such practice allows for reduced solution times. However, in the thesis no strategies have been pre-defined thereby allowing for a more realistic examination of possible investment combinations of the available technologies.

In conclusion, although much has been written about the importance of incorporating option value in investment appraisals and the concept is gaining traction with industry and institutions worldwide (see, for example,[45], [46]), the proposed methodology formalizes the effort to fully quantify the value of smart technologies when facing uncertainty.

1.5 *Decision-Dependent Uncertainty*

Although much has been written about the importance of uncertainty modelling in distribution network planning [47] the concept of DDU has not yet been investigated in the context of electric power systems, where uncertainty sources are exogenous i.e. sources the resolution of which cannot be affected by actions taken by the planner. However, the importance of incorporating sources of DDU, where the planner's actions have an impact on uncertainty resolution, has been gaining traction in other research fields such as gas and oil exploitation and portfolio planning of research projects, as presented below.

In particular, [48] involves the stochastic planning of an offshore site that consists of oil-fields that are uncertain in size and initial deliverability (Figure 1.6). These sources of uncertainty are endogenous because they can be resolved only after the deployment of drilling-platforms ontop of the fields for oil extraction and further processing. Without these investments the actual values of size and initial deliverability cannot become available – only estimates exist. In this example, the uncertainty resolves *immediately* and *locally*. In particular, *immediate DDU resolution* means that if an investment in a drilling-platform is

made at an epoch e, then complete DDU resolution will be made by the end of e. In other words no more uncertainty will surround the actual value of size and deliverability starting from epoch $e + 1$. *Local DDU resolution* means that investing in a drilling-platform on a field F leads to the resolution of the DDU that only F exhibits. The uncertainty that other fields may exhibit is not affected at all.

The authors in [49] describe the general principles that govern problems that exhibit both endogenous and exogenous sources of uncertainty. For instance, one main characteristic of such problems is the increased cardinality of the scenario set as it consists of all possible combinations of realizations of the endogenous and exogenous uncertain parameters; for each realization of an exogenous uncertain parameter there are all the possible realizations of the uncertain endogenous parameters. An additional consideration is that any two scenarios remain indistinguishable if both the endogenous and exogenous uncertainties have not been resolved.

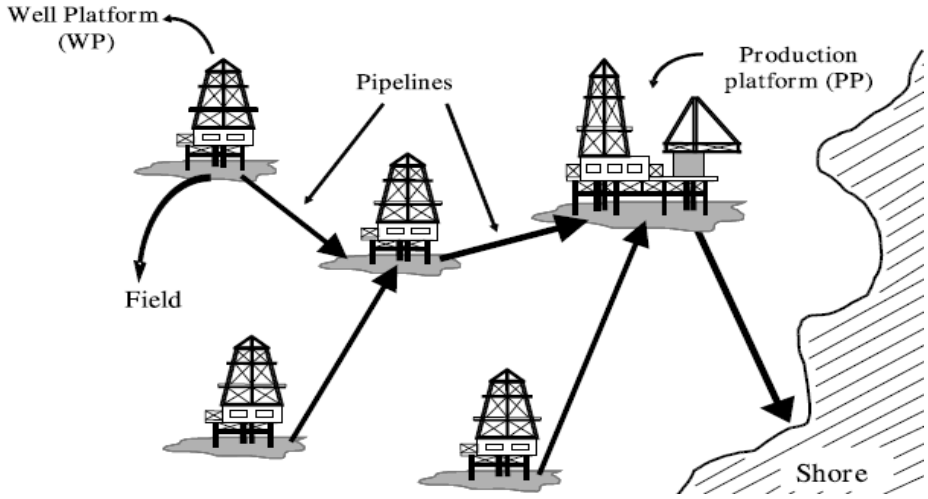


Figure 1.6 Offshore oil production site [48] consisting of five oil fields, from each of which oil can be extracted using well (i.e. drilling) platforms which are connected with each other through pipelines. Then, the oil that is extracted is sent to the production platform, which then sends it to the shore through pipelines for sale.

References [50] and [51] demonstrate case studies where the uncertainty resolution is *gradual*. In particular, the former involves a single oilfield that is uncertain in a number of its characteristics. Every source of uncertainty becomes resolved after some action has been made. For example, when the total number of oil wells drilled exceeds some threshold value a one source of uncertainty resolves, and if a threshold $b > a$ is reached then another DDU

resolution takes place. As a further example, when the total number of years of oil production exceeds a threshold c another source of DDU becomes resolved and so on. Although the individual sources of DDU become resolved immediately, the design of the problem is such that for the complete resolution of uncertainty a number of investments are required that span over more than one epochs i.e. gradually. A similar analysis applies to [52] with the difference being that in the latter case the uncertainty involves Research and Development projects, each of which exhibits DDU around some characteristics. Then, one source of uncertainty is partially resolved when the aggregate investment made in a project reaches some threshold value, and when the aggregate investment rises above a higher threshold another source of uncertainty gets resolved.

In [53] another case study exhibiting gradual DDU resolution is presented. In particular, a number of processing units are deployed in a factory, with each one being uncertain around its productivity level. In order to partially resolve the uncertainty for each unit it is necessary to either operate it during one epoch or to make some form of investment. The partial resolution of DDU will then yield two possible values for the productivity level (e.g. 69% or 81%). If the unit is operated for an extra epoch or more investment is made in it then the uncertainty will resolve completely and two extra possible values will be observed depending on the previously observed value. That is, 69% or 73% (if previously the value 69% was observed) and 79% or 81% (if previously 81% was observed). This is a case of *gradual* DDU resolution as it is impossible for it to be resolved completely in one epoch. Moreover, the resolution happens *locally* i.e. independently of the resolution of DDU relating to other processing units.

The aforementioned references to case studies exhibiting DDU constitute a very small part of the existing work in the area of distribution planning under uncertainty; the overwhelming majority of the corresponding literature involves problems that exhibit exogenous uncertainty. In such problems, the optimal decisions and the uncertainty resolution are independent of each other. In addition, the non-anticipativity constraints (NACs) are unconditional resulting in a fixed structure of the scenario tree (i.e. the tree that describes the uncertainty resolution), which is given as an input to the problem. Thus, the resulting decision tree (i.e. the tree that depicts the optimal investment strategy) has a shape that is exactly similar to that of the scenario tree. Note that the NACs are constraints that force the investment and operational decisions corresponding to two scenarios to be

identical from the beginning of the horizon up until a certain epoch when some information arrives that distinguishes them (uncertainty resolution). For example, the uncertainty around parameter ξ_1, in Figure 1.7 [48], is resolved at epoch 2 and for ξ_2 it is resolved in epoch 3, while the horizontal dotted lines represent the application of NACs that link those nodes whose decision variables x_e^s (scenario s, epoch e) are forced to be identical (indistinguishable nodes). Examples of exogenously uncertain problems include both case studies presented in Chapter 2. For instance, in section 2.2 the uncertainty around the amount of PV capacity that is connected to the system is exogenous as it resolves simply with the passage of time i.e. independently of optimal decisions. Thus, the scenario tree shown in Figure 2.12 is given as an input and it is identical to the decision tree shown in Figure 2.16.

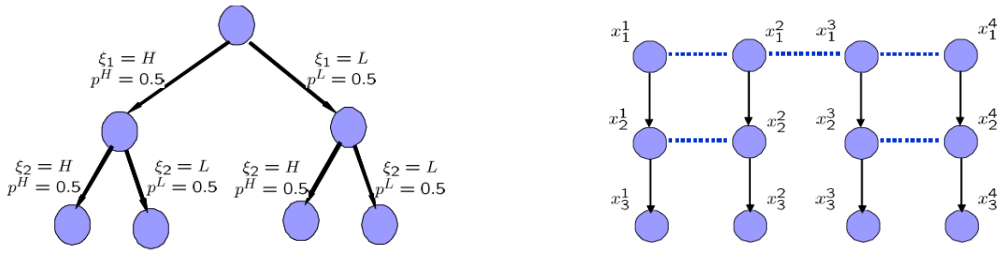


Figure 1.7 Equivalent representations [48] of uncertainty resolution using a scenario tree. The representation shown on the left corresponds to node-variable stochastic formulations, while that on the right deals with scenario-variable ones.

On the contrary, all case studies presented in Chapter 3 and Chapter 4 involve stochastic optimization problems that exhibit DDU. Such problems require the explicit inclusion of NACs as well as that of auxiliary variables and constraints in order to define a variable structure of the decision tree that enables decision-dependent information discovery. These NACs are conditionally applied based on the optimal value of decision variables indicating that uncertainty resolution is dependent on optimal decisions. It follows that the use of a scenario-variable formulation becomes necessary [54] leading to significantly increased problem size. Several methods have been proposed (see the literature references noted above) in an effort to address such a computational issue, most of which constitute iterative decomposition techniques as well as branch-and-bound algorithms. In the thesis it is shown that Benders decomposition can also be effectively applied and can also be modified to take advantage of the special structure of DDU formulations.

1.6 *Benders Decomposition*

Benders Decomposition constitutes an iterative decomposition algorithm that can be applied to MILP problems characterized by a number of variables and constraints that negatively affect the solution time as well as the memory that is consumed during the implementation of the problem. According to this decomposition methodology, the original problem is broken down into a master MILP subproblem and a continuous operational subproblem [55]. The master solves the investment part of the original problem while approximating the operational subproblem and the optimal solution that is yielded is passed as an input to the operational subproblem, which is then optimally solved. Part of its solution involves the dual variables corresponding to the "coupling constraints" (i.e. those that couple the investment variables in the operational subproblem with the inputs from the master subproblem). These are passed as inputs to the master subproblem of the next Benders iteration so that they can be used to construct linear constraints ("Benders cuts") that are appended to the master problem.

In particular, the original problem has a structure similar to (1.1)-(1.4), where the integer decision variables x_i (representing investment decisions) are treated as the complicating ones [56] whereas the continuous variables y_j pertain to operational decisions. Note that the remaining symbols are input parameters with $c_i, d_j > 0$ representing costs.

$$\min_{x_i, y_j} \left\{ \sum_{i=1}^{n} c_i x_i + \sum_{j=1}^{m} d_j y_j \right\} \tag{1.1}$$

$$\sum_{i=1}^{n} a_{li} x_i + \sum_{j=1}^{m} e_{lj} y_j = b_l \qquad l = 1, \dots, q \tag{1.2}$$

$$x_i^{down} \leq x_i \leq x_i^{up} \quad , \quad x_i \in \mathbb{N} \qquad i = 1, \dots, n \tag{1.3}$$

$$y_i^{down} \leq y_j \leq y_j^{up} \, , \quad y_j \in \mathbb{R} \qquad j = 1, \dots, m \tag{1.4}$$

The operational subproblem is defined by the objective function (1.5) subject to (1.2), (1.4), (1.6), where $x_i^{(k)}$ are known values and the x_i used in this subproblem are all continuous decision variables.

$$\min_{y_j} \left\{ \sum_{j=1}^{m} d_j y_j \right\} \tag{1.5}$$

$$x_i = x_i^{(k)} : \lambda_i \qquad i = 1, \dots, n \tag{1.6}$$

The investment master subproblem is defined by the objective function (1.7) subject to (1.3), (1.8), (1.9), where a^{down} is a lower bound on scalar variable a and is specifically determined based on the particular problem (in this thesis, it is given a value zero as it represents operational cost that cannot be negative). In addition, k represents the Benders iteration index and as it increases an extra Benders cut (i.e. the linear constraint (1.8)) is appended to the master problem. Note that $x_i^{(k)}$ is guaranteed not to yield infeasibility of the operational subproblem because of the existence of slack variables incorporated in (1.7)-(1.8). Also $\lambda_i^{(k)}$ is an input parameter representing the marginal change to (1.5) after relaxing (1.6) i.e. it constitutes gradient information given to the master and indicating if further improvement can be made to (1.5) through new investment.

$$\min_{x_i, a} \left\{ \sum_{i=1}^{n} c_i x_i + a \right\} \tag{1.7}$$

$$a \geq \sum_{j=1}^{m} d_j y_j^{(k)} + \sum_{i=1}^{n} \lambda_i^{(k)} \left(x_i - x_i^{(k)} \right) \qquad k = 1, \dots, v \tag{1.8}$$

$$a \geq a^{down} \qquad i = 1, \dots, n \tag{1.9}$$

The first iteration of the algorithm starts by solving (1.7) subject to (1.3) and (1.9). This problem yields zero as the optimal value for the investment variables and a because no

Benders cuts have been appended (i.e. no information from the operational subproblem has arrived to create the need for investments) as the operational subproblem has not yet been called to run. Then, the operational subproblem (i.e. (1.5) subject to (1.4), (1.2) and (1.6)) is solved yielding a high cost because the absence of investments does not allow much of the system load to be served (cost of energy not supplied). Then, the upper and lower bounds are estimated and compared to evaluate whether or not they are sufficiently close to each other, meaning that the algorithm converged to the optimal solution. Otherwise, the iteration index is increased by one and the master problem is solved with the addition of Benders cut constraints. In particular (1.7) subject to (1.3), (1.9) and (1.8), which is the Benders cut constraint and where the $y_j^{(1)}, \lambda^{(1)}, x^{(1)}$ are used as inputs from the previous iteration. Note that after a number of v iterations, the Benders cut constraint appears in the formulation corresponding to iterations $1, \dots, v$. The lower and upper bounds are defined as follows:

$$Z_{up}^{(k)} = \sum_{i=1}^{n} c_i x_i^{(k)} + \sum_{j=1}^{m} d_j y_j^{(k)} \tag{1.10}$$

$$Z_{down}^{(k)} = \sum_{i=1}^{n} c_i x_i^{(k)} + a^{(k)} \tag{1.11}$$

Note that the feasible region for the master problem is initially drawn based on (1.3) and (1.9). In the second iteration the first Benders cut constraint (see (1.8)) is added in the formulation resulting in the restriction of the feasible region. With more cuts being added to the formulation, the feasible region more and more starts to take the shape of the feasible region of the original problem. At the same time, the lower and upper bounds to the original problem's objective function come closer and closer, until the algorithm converges. Figure 1.8 illustrates Benders decomposition methodology.

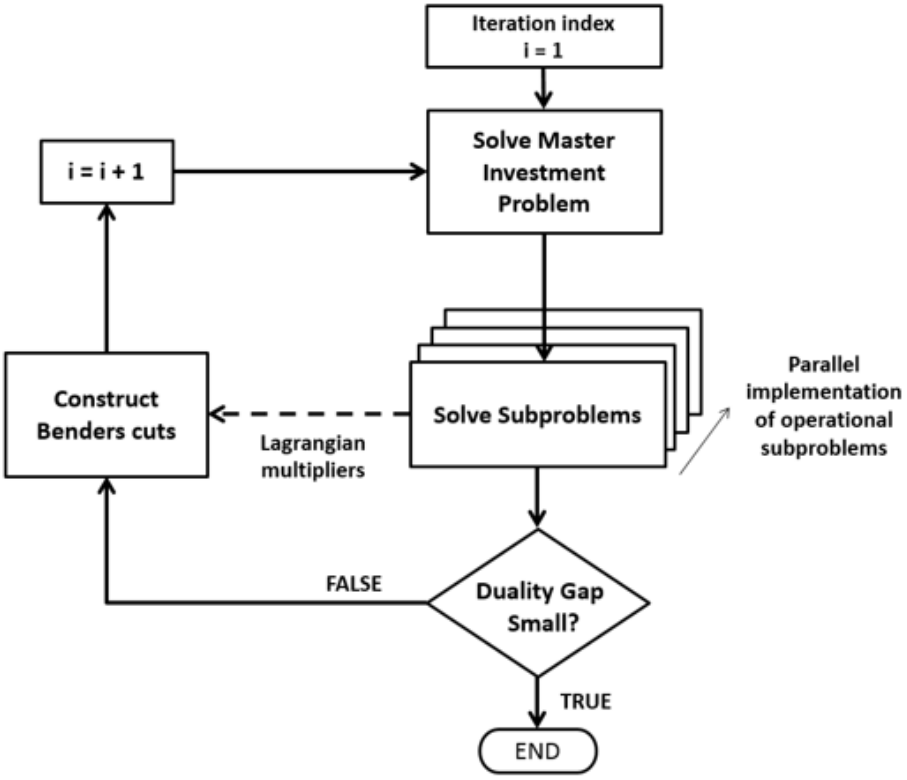


Figure 1.8 Benders Decomposition approach where each iteration starts with solving the master problem and then proceeds on with the parallel implementation of the operational subproblems as long as the duality gap is not as sufficiently small as to yield convergence of the algorithm. Note that each iteration proceeds by successively adding Benders cuts in the master problem.

1.7 *Original research contributions*

This thesis has made significant contributions in the area of electricity network planning under endogenous and exogenous uncertainty, as follows.

- Formulation of a stochastic planning methodology for obtaining the option value of various portfolios of smart grid technologies under endogenous and exogenous sources of uncertainty (see Chapter 2, Chapter 3 and Chapter 4).

- Presentation of mathematical formulations for investment and operation of smart technologies, with emphasis on SOP and CVC, in a disjunctive optimisation model (see Chapter 2)

- Demonstration of the strategic "wait-and-see" flexibility that smart technologies can provide as well as their exclusion when uncertainty is ignored, highlighting the shortcomings of deterministic planning standards (see Chapter 2).

- Application of Benders multicut decomposition algorithm in the context of distribution planning when considering storage and DLR assets (see Chapter 2).

- Presentation of the mathematical formulation for distribution planning problems that exhibit DDU that is resolved in a combination of possible ways: locally, globally, immediately and globally (see Chapter 3 and Chapter 4).

- Showcase of the way by which the investment planning process interacts with the revelation of DDU (see Chapter 3 and Chapter 4).

- Application of Benders decomposition variants (monocut and multicut) to planning problems under DDU (see Chapter 3 and Chapter 4).

- Presentation of a novel extension of Benders decomposition algorithm that allows for improved computational performance for planning problems under DDU (see Chapter 3 and Chapter 4).

- Showcase of the importance of early investments in smart technologies under DDU (see Chapter 3 and Chapter 4).

- Application of the DDU concept to transmission system planning (see Chapter 3).

1.8 *Thesis Structure*

This thesis is organized in five chapters focused on the methodology for calculating the option value of investing in smart technologies under exogenous (Chapter 2) and endogenous (Chapter 3 and Chapter 4) uncertainty. Endogenous uncertainty that resolves in an *immediate* manner is presented in Chapter 3, while *gradual* resolution is demonstrated in Chapter 4. Finally, Chapter 5 summarizes the main findings and sets the goals for future work. Note that although much of the relevant literature review is incorporated in Chapter 1, there are references to relevant work within each chapter.

Chapter 2 Option Value of Smart Technologies under Exogenous Uncertainty

2.1 *Integration of renewables to distribution networks via Storage and DLR*

In this section a case study is presented that applies to a distribution network that undergoes load and DG capacity growth over a six-year horizon. In order to accommodate the resulting rising power flows the planner has the possibility to invest in conventionally upgrading lines and / or investing in DLR and /or in energy storage. However, the way by which optimal investment decisions will be made is not straightforward due to uncertainty. In particular, the sources of uncertainty, which are the growth in load and DG capacity, are of exogenous type (i.e. they resolve with the passage of time without requiring any action taken from the planner). The results show that the deployment of storage and DLR in the system allows not only for accommodating the rising power flows but also for eradication of the first-epoch stranding risk (i.e. the risk of first-epoch investment decisions turning out to be stranded assets) thereby yielding significant cost savings underlying that smart technologies can constitute flexible options that allow network planners to deal effectively with uncertainty and generate significant savings. Conducting the studies involves modelling the problem in a stochastic optimization programming formulation and using the Benders multicut decomposition technique to produce results within reasonable solution times. Finally, the methodology for obtaining the option value of the presented smart technologies is presented with relevant insights and explanations being provided.

2.1.1 *Problem Description*

Figure 2.1 depicts the reference overhead radial distribution network under study. There are eleven buses, with bus 1 representing the substation which allows energy imports from the main system, while some of the remaining buses accommodate load whose annual peak (in the first epoch) is 30kW. From the second epoch onwards the peak load at *all* buses grows over the study horizon, as shown in Figure 2.2. Note that all load-buses have identical demand profiles as in Figure 2.3 [74], which illustrates the annual load factor profile. In

particular, let $d_{n,t}$ be the demand at bus n during time period t, l_t be the load factor during time period t and $\hat{d}_n$ be the annual peak load at bus n. Then it is $d_{n,t} = l_t \cdot \hat{d}_n$, i.e. the hourly load factor expresses the hourly demand as the percentage (%) of the annual peak demand. Hence, with the increase in peak load, the corresponding hourly values for $d_{n,t}$ increase proportionally.

Also, the eleventh bus starts to accommodate a DG wind unit from the second epoch onwards (i.e. the DG unit is not operational in the first epoch) with installed capacity that grows as shown in Figure 2.2; a deterministic time series is used to capture annual variability in its operational pattern [61], as seen in Figure 2.4. Note that high values in Figure 2.2 (occurring around winter) coincide with high values in Figure 2.4 i.e. some time periods are characterized by both increased demand (during winter in the UK) and by high wind speeds meaning high DG output given the dependence of the latter on the wind speed. This fact renders the DLR system highly useful as the high DG output coincides with high dynamic line rating, thereby reducing the need for line upgrades for avoiding DG output curtailment.

Regarding the scenario tree, shown in Figure 2.2, it can be seen that there is 45% chance of moving from node 1 to node 2 where there is a large amount of DG penetration taking place as well as high load growth. There is also 45% chance of moving from node 1 to node 4 where low DG penetration and low load-growth take place. Depending on whether the system has arrived at node 2 or at node 4 (optimistic and pessimistic states, respectively, for DG and load-growth), there is 70% chance of moving to subsequent nodes of optimistic (node 5) and pessimistic (node 10) states for DG and load growth.

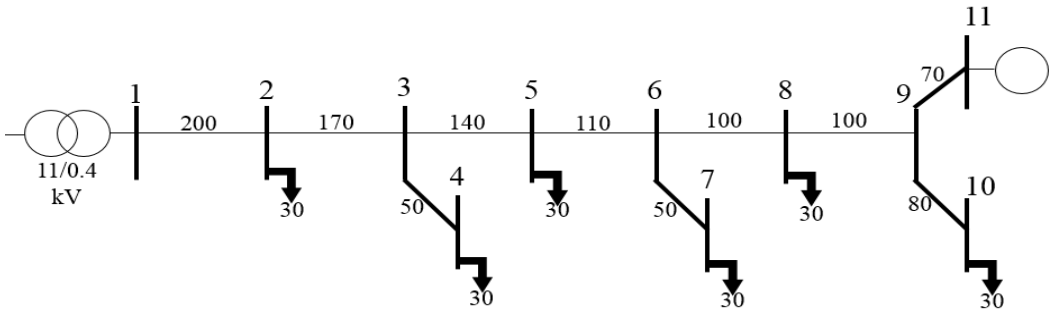


Figure 2.1 Schematic diagram of the distribution network showing line ratings (numbers above each line, in kW), peak load (numbers to which the arcs point, in kW), bus indices (numbers above each bus) and the location of connection of the DG-wind unit (bus 11), which becomes operational at the second epoch.

The load growth leads to increased power flows, the safe accommodation of which requires investments. Note that without resorting to any investments a significant amount of load needs to be curtailed over the six-year horizon with the greatest amount of curtailment taking place across scenarios S1 and S2 at 336MWh and 32MWh respectively; these amounts refer to the entire six-year horizon spanned by each corresponding scenario. The planner has a range of technologies available for investment shown in Table 2.1.

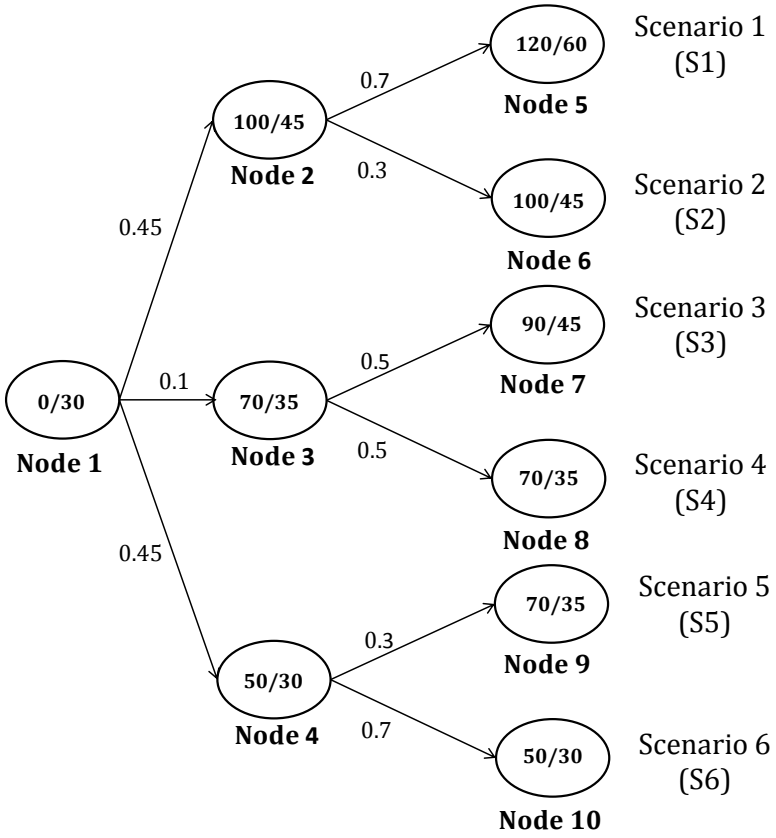


Figure 2.2 Scenario-tree describing the uncertainty around the capacity of the DG unit (kW) and the peak load (kW) at each bus. The values for these parameters are depicted inside each node in the form X/Y where X is the former value and Y is the latter one.

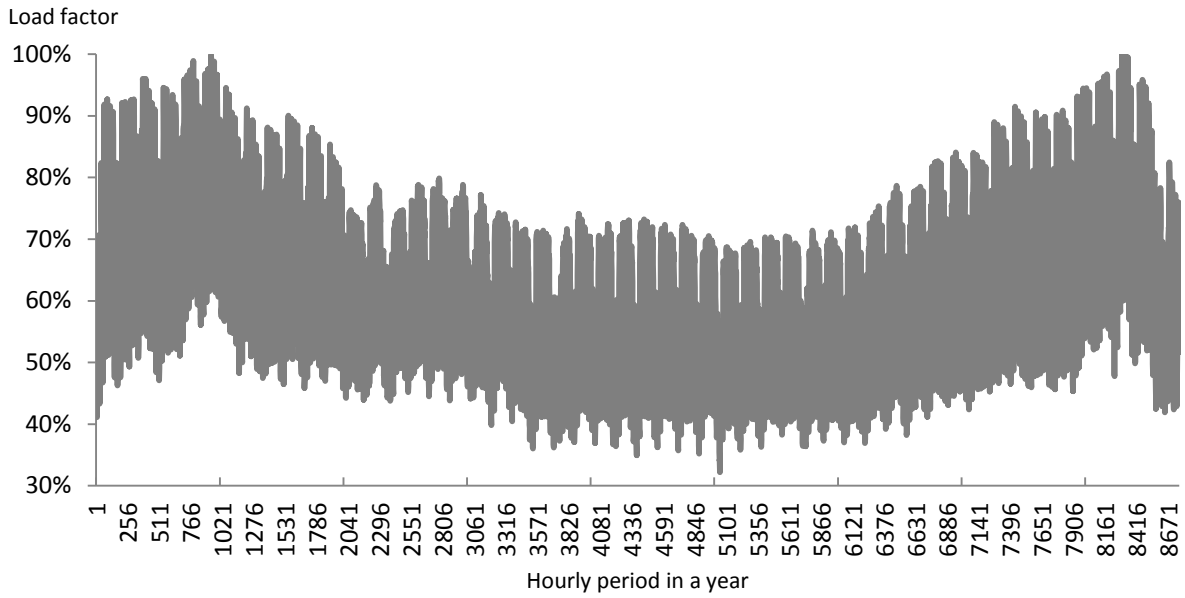


Figure 2.3 Annual pattern for the load factor.

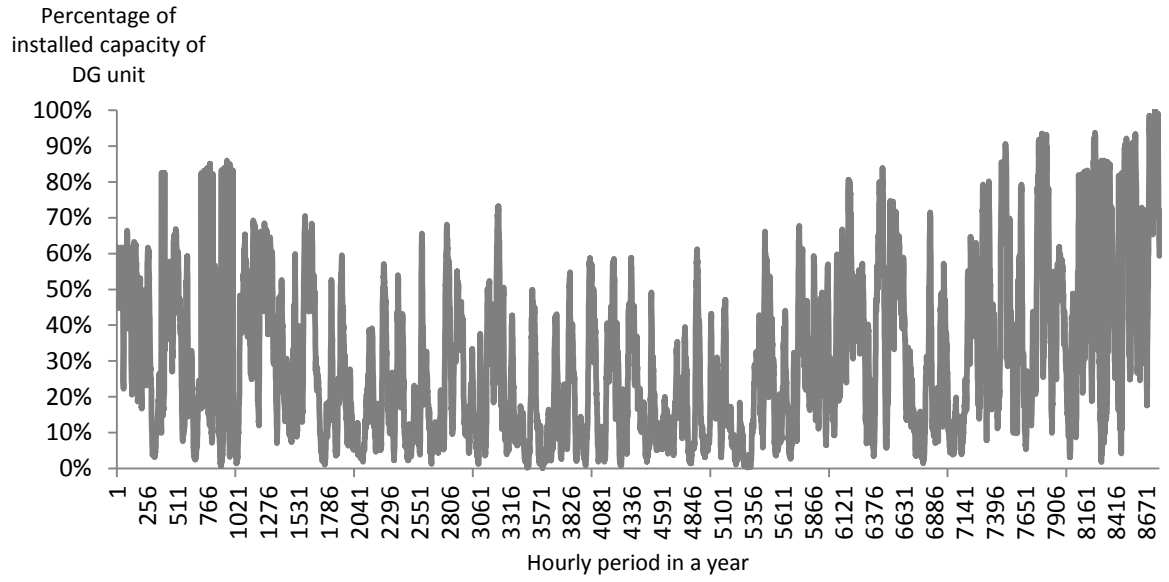


Figure 2.4 Annual pattern for the normalized output of the DG – wind unit.

Technology	Build time (epochs)	Investment cost (£k)
Conventional reinforcement alternative #1 (+100 kW)	1	130 /year/line
Conventional reinforcement alternative #3 (+200 kW)	1	250 /year/line
Dynamic Line Rating (DLR)	0	20 /year - line
Storage (500kWh/ 500kW)	0	150 /year - bus

Table 2.1 Investment cost and build-time for the available technologies for investment.

Regarding the candidate technologies for investment, it can be observed that a storage unit has 500kWh energy capacity (i.e. 500kW of power can be stored in the unit for the duration of one hour) and 500kW power capability meaning that this amount can be charged/discharged into/from the storage unit over an hour. Note that losses in the stored energy from one time period to the next are ignored.

In addition, the deployment of a DLR system on a line has the sole purpose of allowing the calculation of the actual (i.e. dynamic) line thermal rating. Figure 2.5 shows the annual duration curve for the DLR capacity factor, which is a number by which the static line thermal rating is multiplied so as to yield the value for the dynamic line rating. For example, assume that at a particular hourly period the DLR capacity factor is 1.5 and the line has static rating 100kW. Then, the dynamic line rating at that hour is 150kW i.e. a power flow of 150kW can flow through a line whose static rating is just 100 kW. Obviously this rating is continuously changing as wind speed and temperature fluctuate throughout the day.

In particular, this factor is relatively high during hourly periods corresponding to large values of the normalized wind output time series (see Figure 2.4) on the basis that wind speed has the most significant effect on thermal line ratings [19]; Figure 2.4, which actually corresponds to the DG output, is an indication of the wind speed given that the output of DG-wind units is a function of wind speed. In addition, the effect of temperature has also been taken into account by giving relatively lower values to the DLR capacity factor for time periods belonging to the summer season; 29% average increase over the static rating is achieved over a year [18], [19].

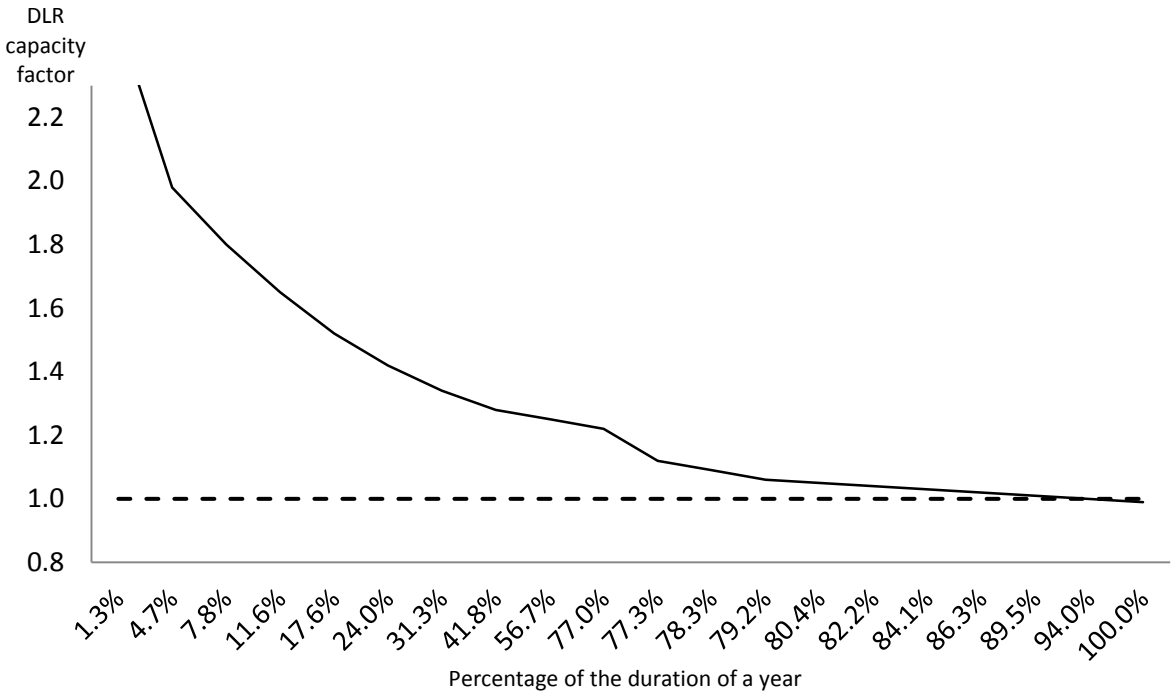


Figure 2.5 Annual duration curve for the dynamic line rating capacity factor (continuous line). The dashed line illustrates the static line rating capacity factor. The horizontal axis shows the percentage (%) of the year (8760 hours) that the DLR capacity factor is greater than the depicted value on the vertical axis. For instance, 77% of the duration of a year the DLR capacity factor is greater than or equal to 1.2. Note that it has been assumed that identical meteorological conditions apply at all buses across the system.

Note that for a very short period of time during summer (high temperatures and dry weather) the DLR capacity factor is lower than the static one. This fact does not have any effect on the results of the current case study (because during summer the demand is low and, as a result, the power flows) but it is useful for the operator to know for matters of security especially in locations where the power flows are high during summer [62].

2.1.2 *Results of the optimization studies*

Figure 2.6 displays the optimal investment strategy if only the conventional technology is available to the planner. Note that wind curtailment (i.e. it is 0%) is not allowed in any of the studies of this paragraph. The resulting total expected system cost is £5.33m. In particular, a total of 700kW of line upgrades are decided for investment in the first epoch, while an additional 300kW capacity is decided at node 2. Note that the

corresponding investments become operational in the subsequent epoch, i.e. at epochs 2 and 3 respectively, because of the one-epoch build-time as presented in Table 2.1. Table 2.2 shows the maximum power flows passing through each line thereby allowing for comprehension of the logic behind each investment decision. For example, lines 1-2 and 2-3 are upgraded by 200kW each because across scenario S1 the maximum power flows, occurring at node 5, are 338kW and 281kW respectively and the initial static thermal rating of the lines stands at 200kW and 170kW respectively (at most one investment per line is allowed). A similar logic applies to all other investment decisions depicted in the figure. Notice that the first-epoch decisions are subject to significant stranding risk meaning that nodes other than 2 and 5 involve smaller power flows, thus, not requiring the full upgraded capacity. In the scenario involving the greatest stranding risk (S6 i.e. nodes 1→4→10), with probability 31.5%, no line upgrade is needed as all power flows are safely accommodated.

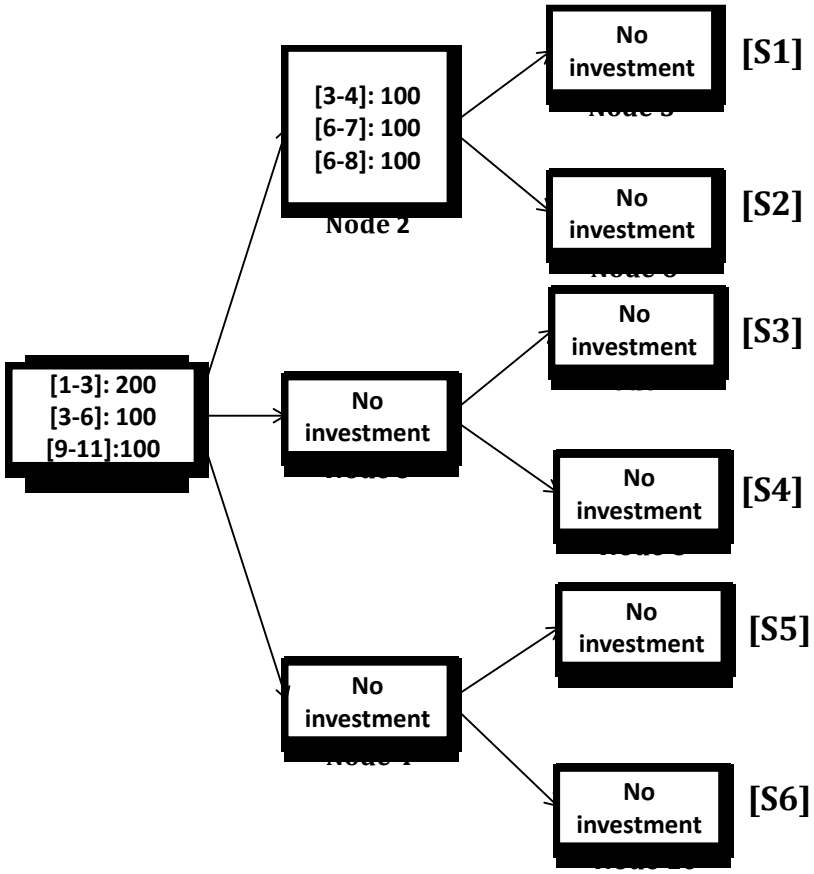


Figure 2.6 Optimal investment strategy in the case where only the conventional technology is available to the planner. The [x-y]:100 means that the decision is taken to reinforce all lines between buses x and y by 100kW. For example [1-3]:200 is equivalent to [1-2]:200 and [2-3]:200. Similarly, [3-6]:100 is equivalent to [3-5]:100 and [5-6]:100. Such a conventional investment becomes operational in the subsequent epoch. The brackets at the rightmost corner show to which scenarios the depicted investment paths correspond.

	1-2:200	2-3:170	3-4:50	3-5:140	5-6:110	6-7:50	6-8:100	8-9:100	9-10:80	9-11:70
N2	253	211	45	168	125	45	83	77	45	100
N3	203	169	36	135	101	36	67	52	36	70
N4	170	141	30	113	84	30	56	36	30	50
N5	338	281	60	224	167	60	110	90	60	120
N7	253	211	45	168	125	45	83	68	45	90

Table 2.2 Maximum power flows (kW), in absolute value, per line for scenario-tree nodes $N_i, i \in \{2..7\}$ of the scenario tree depicted in Figure 2.2. The nodes within the sets $\{N_3, N_8, N_9\}, \{N_2, N_6\}$ and $\{N_4, N_{10}\}$ exhibit identical power flows, according to the scenario tree, as they involve identical values for the uncertain parameters. Thus, only the power flows for one node per set are depicted.

Figure 2.7 shows the optimal investment strategy for a network planner who has both the DLR and the conventional technologies available for investment; the resulting total expected system cost is £1.93m and the total expected percentage of curtailment of DG-wind output is 0% (now allowed).

Comparing to Figure 2.6, it can be seen that there are lower levels of stranding risk due to the reduction of the amount of kW decided for investment in the first-epoch (from 700kW to 200kW). In addition, the total number of conventional investment decisions sees a 50% decline from 8 to 4 across all scenarios. This is achieved by deploying a large number of DLR systems across the network so that they inform the system operator about whether or not it is possible to pass power of greater (during windy periods with low temperature) or lower (during dry periods of high temperature) magnitude than that stipulated by the static line rating. This is particularly favourable for the output of the DG unit because when the wind is blowing intensely (i.e. the DG output may be higher than the line 9-11 rating), the DLR system informs about the ability to pass more power through 9-11.

The logic behind the investment decisions can be understood by observing Table 2.2, which also applies to this study. For example, line 1-2 has an initial rating of 200kW (see Figure 2.1) and at the first node a decision to conventionally upgrade it by 100kW is taken. Thus, at nodes 2 and 5 the static rating of this line is 300kW. During some periods of the year, at node 5, the power flow through this line exceeds 300kW and by deploying a DLR

system the actual dynamic rating becomes known to be in excess of 300kW. For example, at some period the DLR capacity factor stands at 1.22 leading to a value of $200\text{kW} \cdot 1.22 + 100\text{kW} = 344\text{kW}$ dynamic line rating value. Note that despite the deployment of DLR systems, the first-epoch conventional investment decisions are still necessary for satisfying the system load.

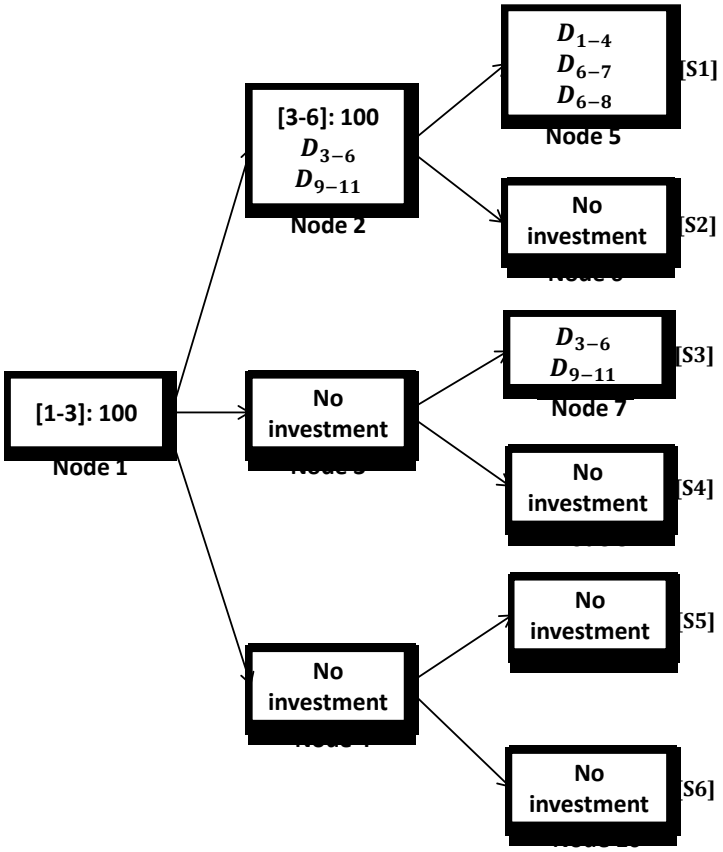


Figure 2.7 Optimal investment strategy for a network planner with two investment technologies available: DLR and conventional reinforcement. The D_{x-y} signifies the decision to invest in DLR on all lines between buses x, y. For example D_{3-6} is equivalent to D_{3-5} and D_{5-6} . Similarly, D_{1-4} is equivalent to $D_{1-2}, D_{2-3}, D_{3-4}$. Investments in DLR become operational at the same epoch the investment decision was made. The brackets at the rightmost corner show to which scenarios the depicted investment paths correspond.

Figure 2.8 shows the optimal investment strategy for a network planner who has both storage and conventional technologies available for investment leading to a total expected system cost of £1.99m. Note that the total expected percentage (%) of curtailment of DG-wind output is 0% achieved through storage operation (bus 11) where the unit charges with DG-wind output at times when without the storage unit there would be

curtailement of DG output due to insufficient capacity of line 9-11. Table 2.3 shows the maximum power flows per scenario-tree node.

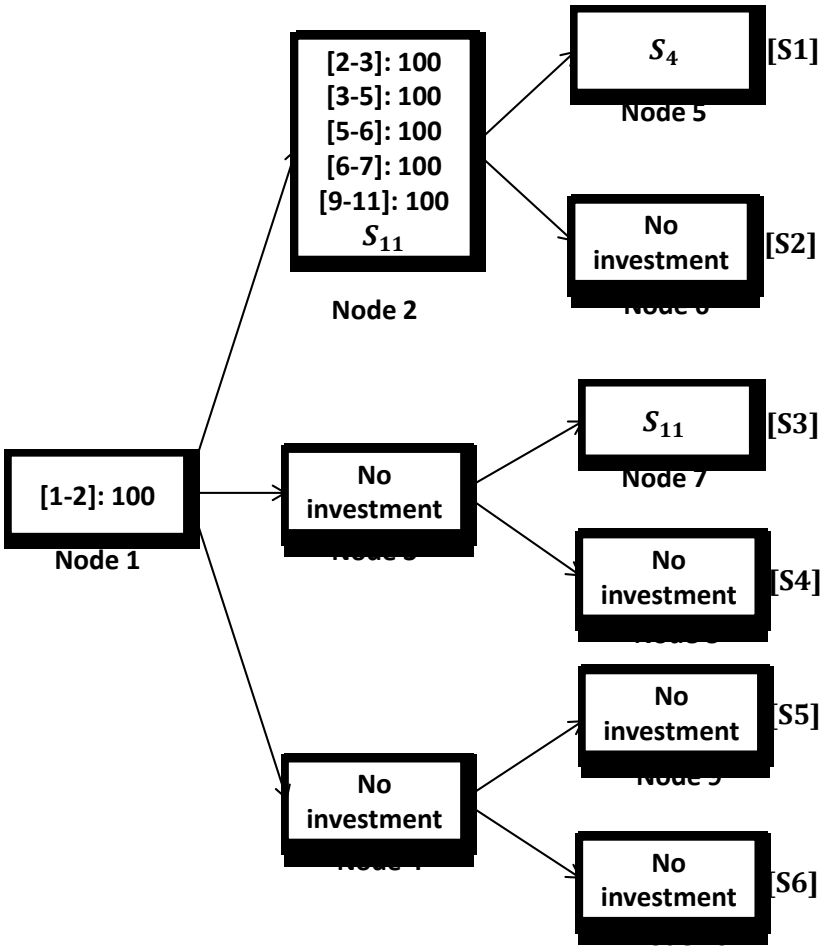


Figure 2.8 Optimal investment strategy for a network planner with two investment technologies available: Storage and conventional reinforcement.

	1-2: 200	2-3: 170	3-4: 50	3-5: 140	5-6: 110	6-7: 50	6-8: 100	8-9: 100	9-10: 80	9-11:70
N2	213	170	45	140	110	45	34	63	45	70
N3	204	169	36	135	101	36	67	53	36	70
N4	170	141	30	113	84	30	56	35	30	50
N5	300	250	50	200	150	60	100	90	60	120
N6	254	211	45	168	126	45	83	78	45	100
N7	215	170	45	140	110	45	87	63	45	70

Table 2.3 Maximum power flows (kW), in absolute value, per line for each of the ten scenario-tree nodes of the scenario tree depicted in Figure 2.2. The resulting power flows for only six nodes are shown because according to the scenario tree, nodes 3, 8, 9 as well as nodes 4, 10 exhibit identical power flows as they involve identical values for the uncertain parameters and no investment in storage is undertaken. Thus, only the power flows for one of the nodes in each of the aforementioned groups are depicted.

There is no coordinated use of the two storage units at node 5; that at bus 4 serves only the accommodation of the increased bus-4 load, while that in bus 11 serves the accommodation of the increased flows along the main feeder.

Figure 2.9 shows the optimal investment strategy for a network planner who has all three technologies (DLR, storage, conventional upgrade) available for investment. Note that after solving a study with storage units of 500kW/500kWh it is seen that this size constitutes and overinvestment and units of smaller size suffice. Thus, 15kW / 15kWh storage units (at a cost of £22k/year per unit) are considered as candidates for investment. Notice that the storage capacity is not a variable to be optimized as it can be seen in paragraph 2.1.3.

The resulting total expected system cost is £1.02m and the total expected percentage (%) of curtailment of DG-wind output is 0% (not allowed). Notice that this is the only study where no first-epoch investment decisions are made meaning that the corresponding stranding risk is completely eradicated. Thus, at all nodes of the second epoch the increased power flows are accommodated solely via the presence of all deployed DLR and storage assets (no line has been upgraded). For example, lines 1-2, 2-3, 3-5, 5-6 and 9-11 are each fitted with a DLR system informing the operator that it is possible to allow maximum power flows of a magnitude that is approximately higher than their static rating. In addition, the

storage units operate as a complement to the DLR systems, in periods where the power flows are greater than the corresponding dynamic line rating, by discharging power necessary to feed system load resulting in the reduction of power coming from the substation.

By comparing between the total expected cost of the strategies shown in the previous figures (i.e. £5.33m, £1.99m, £1.93m, £1.02m) one can quantify the option value of the portfolio of smart technologies consisting of DLR and storage as well as the option value of each individual technology. The former amounts to £5.33m – £1.02m = £4.31m and represents the [63] expected savings (expected net benefit) due to the ability to invest in DLR and storage assets. Notice that the combined portfolio corresponds to an option value that is less than the sum of the individual ones because when each technology is solely present in the system the entire benefit that it brings is entirely attributed to it whereas when both DLR and storage technologies are deployed the benefit is attributed to both of them and in some sense they "share" the benefit.

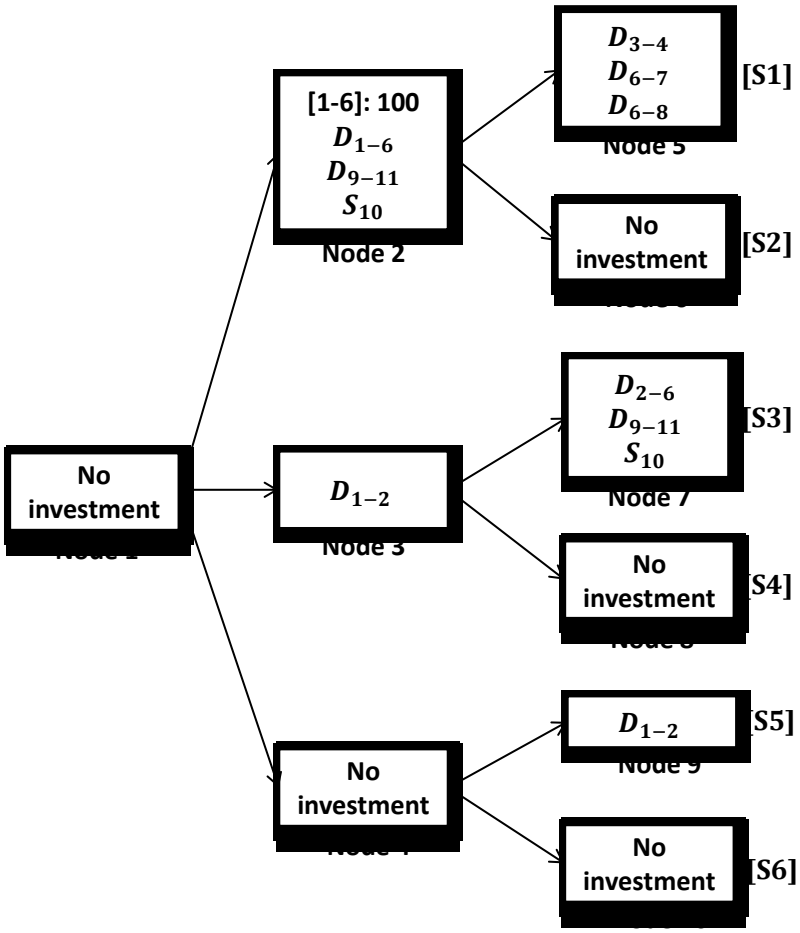


Figure 2.9 Optimal investment strategy for a network planner with three investment technologies available: Storage, DLR and conventional reinforcement. The S_x signifies the decision to invest in storage at bus x. The D_{x-y} signifies the decision to invest in DLR on the the line between buses x, y. The [x-y]:100 means that the decision is taken to reinforce the line between buses x and y by 100kW. Such a conventional investment becomes operational in the subsequent epoch as opposed to investments in smart technologies that become operational at the same epoch. The brackets at the rightmost corner show to which scenarios the depicted investment paths correspond.

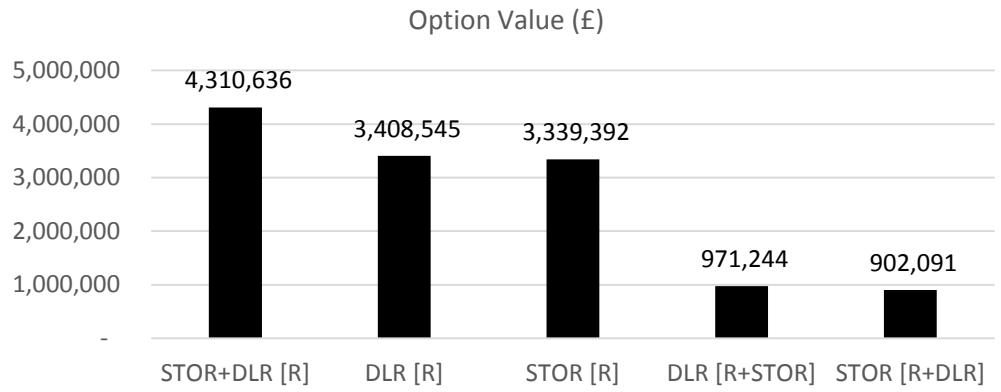


Figure 2.10 Option Value (OV), expressed in £, for each type of smart technology (storage, DLR) as well as of the portfolio consisting of DLR and storage technologies together. Note X+Y[Z], where X,Y,Z investment technologies, is the option value of X+Y under the influence of Z (i.e. when Z is also optimally deployed in the system).

2.1.3 *Mathematical Formulation*

The nomenclature for the mathematical formulation follows.

Sets and indices

Ω_{DG} Set of renewable DG units, indexed g^*.

Ω_M Set of scenario-tree nodes, indexed m.

Ω_L Set of distribution lines, indexed l.

Ω_G Set of generation units and substations, indexed g. It is $\Omega_{DG} \subseteq \Omega_G$.

Ω_N Set of system buses, indexed n.

Ω_O Set of conventional investment alternatives, indexed o.

Ω_T Set of demand periods in a year, indexed t.

Input Parameters

γ_s	Investment cost for a storage unit deployment $(£/year)$.
γ_o	Investment cost for a line upgrade with o $(£/year)$.
γ_l	Investment cost for deploying a DLR system $(£/year)$.
δ_t	Duration of one period (hours).
η	Efficiency of storing energy in a storage unit between periods $t-1$, t.
ε_m	Epoch to which node m belongs.
π_m	Probability of scenario tree node m occurring.
$\zeta_{t,g}$	Percentage (%) of the installed capacity of unit g. For $g \in \Omega_G - \Omega_{DG}$ (i.e. substations and thermal units) it is $\zeta_{t,g} = 1, \forall t$. Otherwise, $\zeta_{t,g}$ is a real number $\in [0,1]$.
c	Cost of curtailing DG output $(£/kWh)$.
$d_{m,t,n}$	Demand at bus n, in m, t (kW).
$\tilde{S}_{m,n}^{i-1}$	Parameter that holds the value of $\tilde{S}_{m,n}$ from Benders iteration $i-1$.
$F_{m,l,o}^{i-1}$	Parameter that holds the value of $\tilde{F}_{m,l,o}$ from Benders iteration $i-1$.
$\tilde{D}_{m,l}^{i-1}$	Parameter that holds the value of $\tilde{D}_{m,l}$ from Benders iteration $i-1$.
F_l	Initial static thermal rating of line l (kW).
$I_{n,g}$	Bus-to-generation incidence matrix. Its elements are equal to 1 when g is connected to n. Otherwise, they are equal to zero.
k_D	Build-time for deployment of the DLR system (epochs).
k_s	Build-time for deployment of a storage unit (epochs).
k_L	Build-time for line upgrade becoming operational (epochs).
$K_{m,g}$	Installed capacity of unit g at node m (kW).
$L_{n,l}$	Bus-to-line incidence matrix. Its elements are equal to 1 when n is the receiving bus of l, and -1 when it is the sending bus. Otherwise they are 0.

R_t DLR capacity factor (%) in t.

Ξ Maximum power (kW) that a storage unit can charge/ discharge in t.

Ψ Maximum energy capacity (kWh) that a storage unit can have in t. It is $\Psi \geq \Xi$.

Q_o Capacity corresponding to line upgrade alternative o (kW).

r Annual interest rate.

r_{ε_m} Cumulative discount factor for investment cost corresponding to ε_m.

τ_{ε_m} Cumulative discount factor for operational cost corresponding to ε_m.

u_l Sending bus of line l.

v_l Receiving bus of line l.

X_l Reactance for line l (pu).

$\Phi_k(m)$ Time-ordered set containing all parent nodes of node m from the first epoch up to $\varepsilon_m - k$, where k build-time. E.g. according Figure 2.2, node 5 has nodes 2 and 1 as its parent nodes in epochs 2 and 1 respectively. Thus, it is $\Phi_1(5) = 1, \Phi_2(5) = 2$.

Decision Variables

a_m^i Variable $\in \mathbb{R}_+$ corresponding to node m for the approximation of the expected operational cost at Benders iteration i.

$\theta_{t,n}$ Variable $\in \mathbb{R}$ representing the voltage angle at t for bus n (rad). It is $\theta_{t,1} = 0$ (i.e. bus 1 acts as a reference).

$\lambda_{m,l,o}^i$ Dual variable $\in \mathbb{R}$ yielded from the operational subproblem for m related to conventional investment at Benders iteration i.

$\mu_{m,l}^i$ Dual variable $\in \mathbb{R}$ yielded from the operational subproblem for m, related to DLR investment at Benders iteration i.

$\rho_{m,n}^i$ Dual variable $\in \mathbb{R}$ yielded from the operational subproblem for m,

	related to storage investment at Benders iteration i.
ω_m^i	Objective function of the operational subproblem for m at Benders iteration i.
Δ_l	Continuous variable representing $\widetilde{D}_{m,l}$ in the operational subproblem corresponding to node m.
ξ_m	Total investment cost for m.
$\Phi_{l,o}$	Continuous variable representing $\tilde{F}_{m,l,o}$ in the operational subproblem corresponding to node m.
Π_n	Continuous variable representing $\tilde{S}_{m,n}$ in the operational subproblem corresponding to node m.
$B_{m,l,o}$	Binary decision to upgrade line l by o at m.
$D_{m,l}$	Binary decision to invest in a DLR system at line l at m.
$\widetilde{D}_{m,l}$	Continuous state variable aggregating all investment decisions $D_{m,l}$ while considering their corresponding build-times.
$E_{t,n}$	Continuous variable $\in \mathbb{R}_+$ for storage capacity at t, n .
$S_{m,n}$	Binary decision to invest in storage at bus n at m.
$\tilde{S}_{m,n}$	Continuous state variable aggregating all investment decisions $S_{m,n}$ while considering their corresponding build-times.
$F_{m,l,o}$	Continuous variable for the capacity (on top of F_l) by which line l is upgraded by o at m (kW).
$\tilde{F}_{m,l,o}$	Continuous state variable aggregating all investment decisions $F_{m,l,o}$ while considering their corresponding build-times.
$F_{t,l}$	Variable $\in \mathbb{R}$ for the power flow across line l at t (kW). Negative values indicate that the power goes from the receiving bus of the line to the sending bus.

$J_{t,n}$ Continuous variable $\in \mathbb{R}$ equal to power charged / discharged by the storage unit located at n. Positive values indicate that the storage unit acts as a load (i.e. charges with power) and, otherwise, as a generator.

$P_{t,g}$ Continuous variable $\in \mathbb{R}_+$ for the output of g at t (kW).

The planning problem is formulated as a mixed integer linear problem, where binary variables are used to denote investment decisions. The planner's objective is to minimize the total expected system cost while having the choice to invest in conventional line reinforcement, in DLR and in storage technologies. Note that at most one DLR system can be installed on a line and at most one storage unit can be deployed at a bus while a line can be upgraded at most once (i.e. with any of the two available alternatives) across each scenario; investments are driven by the need to respect the thermal limits of the lines due to the increasing demand.

The mathematical formulation is based on Benders Decomposition, in which the original problem is decomposed into a master subproblem and several operational subproblems; each corresponding to a scenario-tree node m. The former problem models investment decision and approximates operation, while the latter problems model the operation of the power system. In particular, the problem presented in section 2.1.1 consists of one master subproblem and ten operational subproblems (each corresponds to a scenario-tree node) solved in parallel. Note that decomposition reduces the dimension of operational variables as in $P_{t,g}$ instead of $P_{m,t,g}$ (without decomposition). At every iteration of the algorithm the master subproblem is first solved and the 'trial' investment decisions it yields are passed, as inputs, onto the operational subproblems. In turn, these generate Lagrange multipliers that are used by the master of the subsequent iteration to construct $|\Omega_M|$ extra constraints known as the Benders cuts. As the Benders iteration index increases more Benders cuts are gradually appended to the master problem. Ultimately, the algorithm converges when the difference between the lower and the upper bounds, to the original problem's objective function, is sufficiently close to zero. The lower bound (2.1) is essentially the objective function of the master problem, while the upper bound (2.2) is equal to the objective function of the original problem.

$$z_{lower}^{i} = \sum_{m} (\pi_m r_{\varepsilon_m} \xi_m^i + a_m^i) \tag{2.1}$$

$$z_{upper}^{i} = \sum_{m} (\pi_m r_{\varepsilon_m} \xi_m^i) + \sum_{m} \pi_m \omega_m^i \tag{2.2}$$

At each Benders iteration i the master problem contains all investment-related variables and constraints as follows:

$$\min \sum_{m} (\pi_m r_{\varepsilon_m} \xi_m + a_m^i) \tag{2.3}$$

$$\xi_m = \sum_{l} \sum_{o} B_{m,l,o} \gamma_o + \sum_{n} S_{m,n} \gamma_s + \sum_{l} D_{m,l} \gamma_l \qquad \forall m \tag{2.4}$$

$$\tilde{F}_{m,l,o} = \sum_{\phi \in \Phi_{k_L}(m)} F_{\phi,l,o} \qquad \forall m, l, o \tag{2.5}$$

$$\tilde{D}_{m,l} = \sum_{\phi \in \Phi_{k_D}(m)} D_{\phi,l} \qquad \forall m, l \tag{2.6}$$

$$\tilde{S}_{m,n} = \sum_{\phi \in \Phi_{k_S}(m)} S_{\phi,n} \qquad \forall m, n \tag{2.7}$$

$$F_{m,l,o} = Q_o B_{m,l,o} \qquad \forall m, l, o \tag{2.8}$$

$$a_m^i \geq \pi_m \omega_m^{i-1} + \sum_{l,o} \pi_m \lambda_{m,l,o}^{i-1} \left(\tilde{F}_{m,l,o} - \tilde{F}_{m,l,o}^{i-1}\right) + \sum_{l} \pi_m \mu_{m,l}^{i-1} \left(\tilde{D}_{m,l} - \tilde{D}_{m,l}^{i-1}\right) + \sum_{n} \pi_m \rho_{m,n}^{i-1} \left(\tilde{S}_{m,n} - \tilde{S}_{m,n}^{i-1}\right) \quad \forall m \qquad (2.9)$$

The objective function (2.3) describes the minimization of the sum of the discounted expected investment cost and the approximation of the total expected operation cost, denoted by $\sum_m a_m^i$. The total investment cost per node is shown in (2.4). Equations (2.5)-(2.7) define the state variables for the investment decisions taking into account the corresponding build-time required until the investment becomes operational. For example, according to the scenario tree shown in Figure 2.2 it is $\tilde{F}_{5,l,o} = F_{2,l,o} + F_{1,l,o}$ as nodes 1 and 2 are the parent nodes for node 5 in epochs 1 and 2 respectively. Constraint (2.8) allows the variable $F_{m,l,o}$ to take on a value equal to the capacity (kW) of one of the available investment alternatives. Finally, (2.9) represents the Benders cut corresponding to node m, where α_m^i is the estimate for the operational cost at iteration i corresponding to node m. In the right-hand-side of the inequality the first term, $\pi_m \omega_m^{i-1}$, is the total expected operational cost corresponding to Benders iteration $i-1$, where ω_m^{i-1} is a parameter holding the optimal objective function value of the operational subproblem corresponding to m. The remaining terms in the right hand side of (2.9) incorporate the information about the impact that the change (between iterations i and $i-1$) in the investment decisions has on the optimal objective function value of the operational subproblem. The formulation for the operational subproblem corresponding to Benders iteration i with node m as an input follows.

$$\omega_m^i = min\left\{\sum_t \sum_{g^*} \tau_{\varepsilon_m} \delta_t c(K_{m,g^*} \zeta_{t,g^*} - P_{t,g^*})\right\} \qquad (2.10)$$

$$E_{t,n} = \eta E_{t-1,n} + \delta_t J_{t,n} \quad \forall t, n \qquad (2.11)$$

$$E_{t,n} \leq \Psi \cdot \Pi_n \qquad \forall t, n \qquad (2.12)$$

$$|J_{t,n}| \leq \Xi \cdot \Pi_n \qquad \forall t, n \qquad (2.13)$$

$$P_{t,g} \leq K_{m,g}\zeta_{t,g} \qquad \forall t, g \qquad (2.14)$$

$$F_{t,l} = \frac{\theta_{t,u_l} - \theta_{t,v_l}}{X_l} \qquad \forall t, l \qquad (2.15)$$

$$|F_{t,l}| \leq F_l R_t \Delta_l + (1 - \Delta_l)F_l + \sum_o \Phi_{l,o} \qquad \forall t, l \qquad (2.16)$$

$$\sum_g P_{t,g} I_{n,g} + \sum_l F_{t,l} L_{n,l} = d_{m,t,n} + J_{t,n} \qquad \forall t, n \qquad (2.17)$$

$$\Delta_l = \widetilde{D}^i_{m,l} : \mu^i_{m,l} \qquad \forall n \qquad (2.18)$$

$$\Phi_{l,o} = \tilde{F}^i_{m,l,o} : \lambda^i_{m,l,o} \qquad \forall l, o \qquad (2.19)$$

$$\Pi_n = \tilde{S}^i_{m,n} : \rho^i_{m,n} \qquad \forall n \qquad (2.20)$$

According to (2.10) the objective function is equal to the discounted cost of curtailment of the output of the renewable DG unit. Note that in (2.3) and (2.10) cumulative discounting factors $r_{\varepsilon_m}, \tau_{\varepsilon_m}$ are used as the capital and operational costs are given per annum. Thus, when for example a storage unit is deployed at a certain node its annual investment cost needs to be paid starting from the epoch to which the node belongs until the end of the horizon. Summing these discounted annual investment costs leads to the

derivation of the total investment cost corresponding to the particular investment. This discounting factor is expressed as in (2.21), where k is the number of years per epoch (in the problem of section 2.1.1 it is $k = 2$) and $|\Omega_E|$ is the number of epochs for the considered horizon. Thus $k \cdot |\Omega_E|$ is the number of years in the horizon. For example, referring to Figure 2.2, assume that an investment decision is made at node m =4 that belongs to epoch $\varepsilon_4 = 2$ of the three-epoch horizon ($|\Omega_E| = 3$ i.e. there are $k \cdot |\Omega_E|$ =6 years in the horizon). Then, the cumulative discounting factor is found by summing from year $k \cdot \varepsilon_4 - k$ =2 to year $k \cdot |\Omega_E| - 1 = 5$, i.e. $r_2 = \frac{1}{(r+1)^2} + \frac{1}{(r+1)^3} + \frac{1}{(r+1)^4} + \frac{1}{(1+r)^5}$ and with r=5% it yields 3.37. That is, the first epoch consists of years 0 and 1, the second epoch consists of years 2 and 3 and so on. The assumption that holds is that the lifetime of the assets is greater than the horizon, otherwise the summation would span until the year that marks the end of the asset life; there are no other costs to be paid after the end of the horizon.

$$r_{\varepsilon_m} = \sum_{i=k\cdot\varepsilon_m}^{k|\Omega_E|-1} \frac{1}{(r+1)^{i-k}} \qquad \forall e \qquad (2.21)$$

Regarding the operational costs, the cumulative discounting factor is defined by (2.22) accounting for the fact that payments corresponding to node m are paid for all years that make up m and not after that. For example, the cumulative discounting factor corresponding to node $m = 4$, which belongs to epoch $\varepsilon_4 = 2$, is $\tau_2 = \frac{1}{(1+r)^2} + \frac{1}{(1+r)^3}$ and with $r = 5\%$ it yields 1.77 (dimensionless).

$$\tau_{\varepsilon_m} = \sum_{i=k\cdot\varepsilon_m}^{k\cdot\varepsilon_m+1} \frac{1}{(r+1)^{i-k}} \qquad \forall e \qquad (2.22)$$

Constraint (2.11) determines the energy capacity of a storage unit at t as equal to its capacity at $t-1$ plus/minus the energy charged/discharged to/from the storage unit, where η is the efficiency factor for the energy stored in the unit from period $t-1$ to t. The bounds for storage capacity $E_{t,n}$ and storage power $J_{t,n}$ are shown in (2.12)-(2.13) respectively. Notice that $E_{t,n}$ can only assume nonnegative real values while $J_{t,n}$ can take on positive (signifying charging of the storage unit i.e. it behaves like a load) and negative (signifying

discharging of the storage unit) real values. In addition, in order to prevent energy storage from wasting its stored content at the end of the year it has been set that $E_{8760,n} = 0, \forall n$, where 8760 is the last hourly period of a year.

According to (2.14) and when g refers to the substation (in this case it is $\zeta_{t,g} = 1, \forall t$), it is ensured that the power drawn from the grid is within the limits of the transformer whereas when g refers to a renewable DG unit the maximum output of the unit is defined in terms of its installed capacity and resource (sun, wind) variability as dictated by parameter $\zeta_{t,g}$.

Constraint (2.15) defines the power flows according to the DC power flow model [64]. Note that the AC equations for the power that flows from bus n to m are $p_{nm} = |V_n|^2 g_{nm} - |V_n||V_m| g_{nm} \cos(\theta_n - \theta_m) - |V_n||V_m| b_{nm} \sin(\theta_n - \theta_m)$ and $q_{nm} = -|V_n|^2 b_{nm} + |V_n||V_m| b_{nm} \cos(\theta_n - \theta_m) - |V_n||V_m| g_{nm} \sin(\theta_n - \theta_m)$, where θ_n, θ_m are the corresponding voltage angles with $|V_i|$ voltage magnitudes. Assuming that under normal operating conditions the voltage angle difference is small (i.e. $\sin(\theta_n - \theta_m) \approx \theta_n - \theta_m$ and $\cos(\theta_n - \theta_m) = 1$), bus voltage magnitudes are approximately 1 $p.u.$ (i.e. $|V_i| = 1, \forall\ bus\ i$) and that line reactance is far greater than line resistance (i.e. $x_{nm} \gg r_{nm}$ and so $b_{nm} = \frac{-x_{nm}}{r_{nm}^2 + x_{nm}^2} = -\frac{1}{x_{nm}}$, $g_{nm} = \frac{r_{nm}}{r_{nm}^2 + x_{nm}^2} = 0$), then the aforementioned equations become $p_{nm} = -b_{nm}(\theta_n - \theta_m) = \frac{\theta_n - \theta_m}{x_{nm}}$, $q_{nm} = 0$.

Constraint (2.16) states that power flows are bounded by the line's static thermal rating F_l when no DLR has been deployed in the line, or are bounded by the line's dynamic (i.e. actual) rating when a DLR unit has been installed on the line. The last term of the right-hand side of this constraint adds to the line's thermal rating any upgraded capacity (by any of the available investment alternatives). Notice that the DLR system is modelled to inform about the actual rating with respect to the initial static thermal rating and not the upgraded one in case any line upgrade has taken place. This modelling is made to guarantee linearity of the constraint.

In addition, (2.17) imposes system energy balance while considering actions from storage assets: The active power flows coming into a bus are equal to those coming out of the bus, at every period. Finally, the last three equalities guarantee that the output of the master subproblem can inform the corresponding variables in the operational subproblems;

Lagrange multipliers are obtained from these constraints and used to construct the Benders cut constraints to be applied to the master problem of the next iteration. Note that the value of these multipliers is negative (to indicate a reduction in the objective value of the operational subproblem) or zero. Note also that in the master problem the investment variables are binary variables (i.e. the problem is mixed-integer linear), whereas all variables in the operational subproblem formulation are continuous so that the Benders decomposition can be applicable.

Equation (2.23) shows the formula used for the calculation of the percentage (%) of wind curtailment at node m. This calculation does not apply to node 1 as the DG-wind installed capacity there is zero. The expected wind curtailment is equal to $\sum_m \pi_m \widetilde{W_m}$.

$$\widetilde{W_m} = \frac{\delta_t \sum_{t,g^*}(\zeta_{t,g^*} K_{m,g^*}) - \delta_t \sum_{t,g^*} P_{t,g^*}}{\delta_t \sum_{t,g^*}(\zeta_{t,g^*} K_{m,g^*})} \qquad \forall m - \{1\} \qquad (2.23)$$

2.1.4 *Solution Methodology*

As it is mentioned in section 2.1.3, the problem is solved via Benders decomposition in which the original mixed-integer linear problem is broken down into a master subproblem and many continuous and linear operational subproblems, the number of which equals the number of nodes in the scenario tree. Note that every node spans the duration of one epoch that, in turn, consists of two years, with each year containing 8760 hourly periods (i.e.$|\Omega_T| = 8760,\ \delta_t = 1\ \forall t$). Table 2.4 shows the corresponding solution times indicating the effect on them that the consideration of storage has.

Available technologies in the respective study	**Solution time**
R (see Figure 2.6)	9 mins
R and DLR (see Figure 2.7)	13 mins
R and Storage (see Figure 2.8)	4 hours
R, DLR and Storage (see Figure 2.9)	9 hours

Table 2.4 Solution times corresponding to the case studies presented in section 2.1.2.

2.2 *Integration of solar PV to distribution networks via SOP, CVC, DSR, APGC*

In this section a case study is presented that applies to an 11kV distribution network that undergoes PV-generation capacity growth over a six-year horizon, resulting in the development of the voltage rise effect in various buses across the network. In order to keep voltages within statutory limits the planner has the possibility to invest in conventionally reconductoring lines and / or a number of smart technologies such as Coordinated Voltage Control (CVC) and Soft Open Points (SOP). However, the way by which optimal investment decisions will be made is not straightforward due to uncertainty. In particular the sources of uncertainty, which are the growth in PV capacity connected to the system as well as the location of connection, are of exogenous type (i.e. resolve with the passage of time without requiring any action taken from the planner).

The results show that the deployment of smart technologies in the system allows not only for accommodating PV while respecting the statutory voltage limits but also for eradication of the first-epoch stranding risk (i.e. the risk of first-epoch investment decisions turning out to be stranded assets) thereby yielding significant cost savings underlying that smart technologies can constitute flexible options that allow network planners to deal effectively with uncertainty and generate significant savings. In addition, it is shown that corresponding deterministic plans completely ignore smart technologies and solely focus on conventional ones with the majority of investments taking place in the first epoch. Such practices may hinder the transition to a smarter grid as the technologies that will help realize it are not eventually deployed, while in addition the first-stage stranding risk is increased as investments carried out in the first epoch may turn out to be stranded assets.

Conducting the studies involves modelling the problem in a stochastic optimization programming formulation that includes significant nonlinear component, thereby utilizing linearization methodologies along with formulation simplifications to yield an optimal or near-optimal investment strategy. Finally, the methodology for obtaining the option value of the presented smart technologies along with that of various technology portfolios is presented with relevant insights and explanations being provided.

Note that most existing models in the field of distribution planning regard the deployment pattern of DG sources either as a non-stochastic input parameter or as a variable

to be optimized [65], [47]. Although integrated resource planning would lead to efficient system development, in many jurisdictions there is no coordination between DG deployment and network planners; in such cases future connection patterns should be modeled as stochastic parameters as in the current section; in the UK, systems of installed capacity less than 4kW are not required to inform the DNO for their connection while larger systems almost always gain connection as part of the decarbonisation effort [66]. Such stochasticity poses a challenge to DNOs as they cannot accurately determine in advance where voltage and/or thermal violations may occur resulting in potential asset stranding.

Distribution planning is an active research topic with most publications traditionally focusing on deterministic network design frameworks [27], [67], [68]. However, results in this section show that deterministic planning suggests that none of the smart technologies should be part of the investment solution as opposed to stochastic planning that favours combined smart technology deployment resulting in significant economic savings that are quantified through the concept of option value.

2.2.1 *Problem Description*

Figure 2.11 depicts the 11kV overhead distribution network, based on [69], used in the present case study. This network belongs to the category of semi-urban networks as the limiting factor for DG integration is the voltage rise effect, as in the case of rural networks. In contrast, DG integration in urban networks is limited by the fault current level i.e. the amount of current that can safely flow through the network due to a fault that has occurred [28]. Also, observe that the network under study is of radial structure with overhead feeders, like rural networks, achieved through normally-open points (NOP). Urban networks, on the other hand, are mostly meshed consisting of heavy-loaded underground cables with load being concentrated in small largely-populated areas. Note that NOP constitutes a switching device connecting two adjacent feeders to provide alternative routes of electricity supply in case of planned or unplanned power outages [26], [70], [71].

The network shown in Figure 2.11 consists of 15 buses, 14 lines and 10 NOPs. Statutory voltage limits at all buses are assumed to be 1.06 pu and 0.94 pu for a base voltage of 11kV, which constitutes an idealization. In the first epoch, all demand is satisfied

through energy imports from the main grid via the 33/11kV primary substation (bus 1). However, an uncertain amount of distributed PV generation is to be connected over the study horizon, which consists of three epochs each of 2-year duration. As shown in the figure there are a total of 7 buses that may accommodate some PV capacity; 4 buses in both Feeder-1 (F-1) and its lateral, and 3 buses in Feeder-2 (F-2).

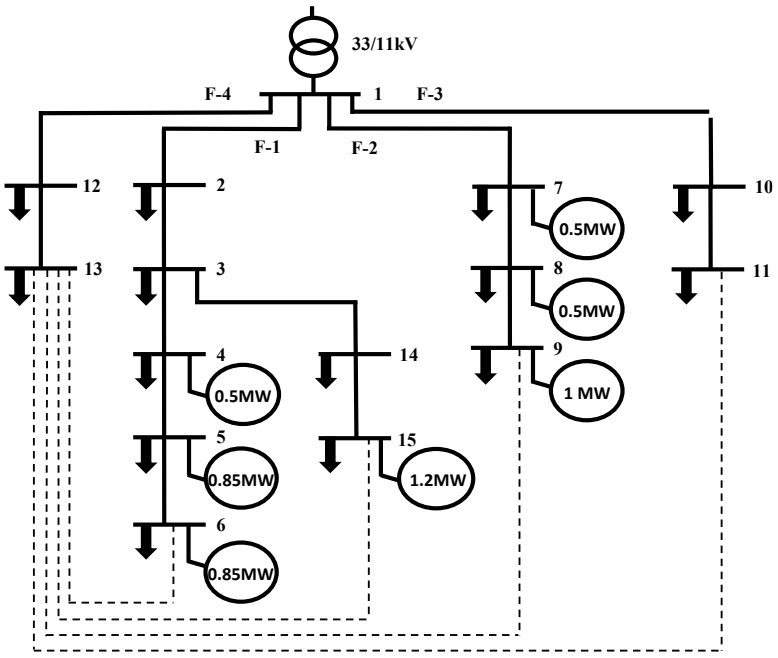


Figure 2.11 Schematic diagram of the 11kV distribution network showing prospective DG connection points, installed capacities, and all NOPs (dotted lines) corresponding to bus 13. Similar NOPs exist for buses 6,9,11, and 15, but are not shown for visual clarity purposes.

The exact temporal and locational deployment pattern is not known a priori; expert opinion has been utilized to construct the scenario tree shown in Figure 2.12 to describe future PV evolution. It consists of 7 nodes comprising 4 scenario paths. For example, scenario S1 consists of the transition across the scenario tree nodes 1→2→4. Transition probabilities are shown above each arc. Note that for clarity, the interior of each node shows the aggregate PV capacity installed and the set of buses that the commissioned PV units connect to. Also, above each node a value is depicted for the voltage target of the AVC relay that controls the OLTC transformer at the primary substation.

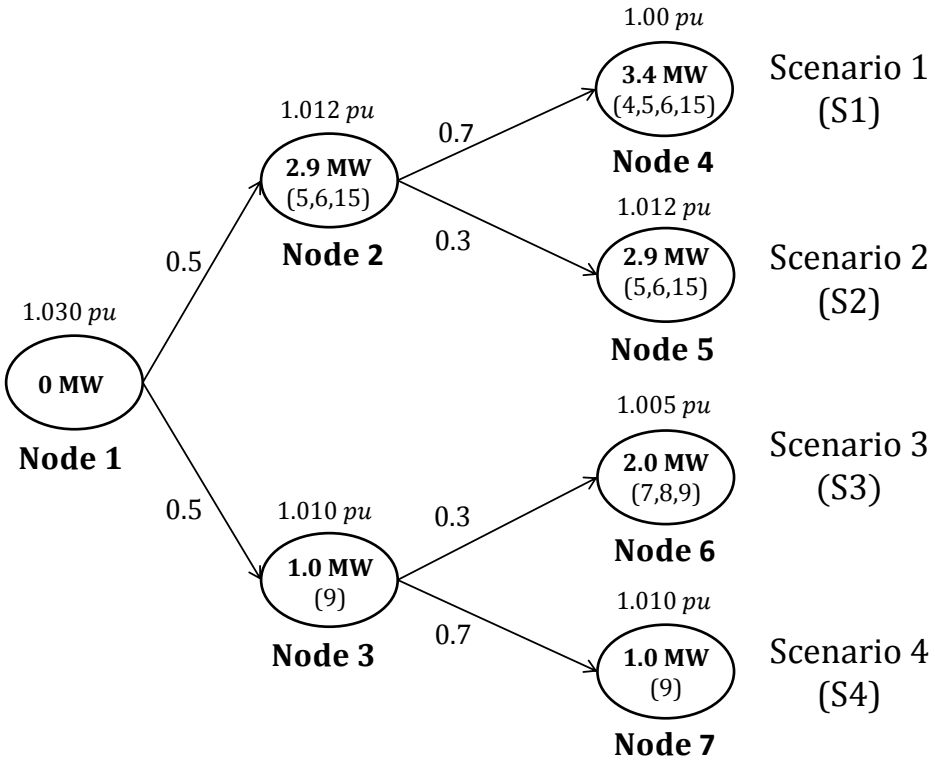


Figure 2.12 Scenario tree describing the uncertainty around PV deployment.

As can be seen, the uncertainty is not only around the magnitude of the DG penetration, but also around the location of these connections. The scenario tree is constructed following appropriate consultation with developers and system experts based on the following logic. In the first epoch, i.e. root node, there is no PV deployed in the system. However, in the subsequent epochs there will be PV deployment in either feeder F-1 or F-2. The uncertainty around which one of these two feeders will be fitted with PV is resolved in the second epoch transition. In the case of a node 1 → node 2 transition, buses 5, 6 and 15 on F-1 are fitted with PV. Subsequent transitions in the third epoch will determine whether this will remain unchanged (as described by scenario S2) or additional PV capacity will be added on bus 4. Note that the general philosophy [24] is that PV is first built in the most distant buses and may eventually be deployed at buses closer to the substation.

In the absence of CVC, it has been assumed that a fixed voltage target policy applies to the AVC relay scheme. In such a case, the voltage target is kept fixed at a value selected traditionally above 1 pu to prevent voltage drops at remote buses [72] and this applies for all scenario-tree nodes as it can be seen in Figure 2.12. It has been assumed that this value is

changed by the Distribution Network Operator at an interval of one epoch based on the connected PV capacity to the system. For example, those scenario-tree nodes that correspond to higher PV capacity have higher potential for voltage rise and hence the voltage target value is selected to be closer to 1 pu than in other nodes. However, under the presence of DG the fixed voltage target schemes may need to be replaced by CVC schemes which can allow for accurate real-time computation of the voltage target value (rather than setting it to a fixed value) based on the actual information of voltage magnitudes across the network [72]. Note that it has been assumed that there is no load growth in subsequent epochs and that all buses have identical load profile and magnitude. Also, it is assumed that all load power factors are time-independent (stay the same throughout the day) and equal to 0.9 meaning that with a load angle of 25.84 degrees it is $\cos(25.84) = 0.9$ and that the relation between the real and reactive powers is $\mathrm{Q} = \mathrm{P}\tan(25.84) = \mathrm{P} \cdot 0.4843$.

The planner has a range of potential solutions for addressing the voltage rise problem, shown in Table 2.5. Note that the active power generation curtailment (APGC) of PV units is a service that the PV owners provide to the network operator in exchange for a payment of $£100/\mathrm{MWh}$.

Technology	Build time (epochs)	Investment cost (£k)
Demand Side Response	0	60 /year/bus
Coordinated Voltage Control	0	540 /year/whole system
Soft Open Point	0	450 /year/NOP
Reconductoring	1	320/year/line km

Table 2.5 Investment cost and build time for the available technologies for investment.

The DSR technology allows the optimal time-shifting of the flexible load, which amounts to 30% of the total hourly load of each bus. In particular, resolving the voltage rise effect involves shifting the flexible load from periods of small (or zero) PV generation to 'critical' periods of relatively higher PV generation. The resulting effect is the reduction of the net power injections and the restoration of the voltage magnitude within statutory limits.

The CVC technology can measure the actual voltage values at all buses in the network, enabling the optimal hourly regulation of the substation voltage target value. The

SOP allows optimal control of the active power flow through its two terminals and optimal reactive compensation at any of its two terminals; 90% efficiency (in transporting active power from one terminal to the other) with 135kW and 135kVAr capacity being used for these two operations. The reconductoring technology involves the replacement of the existing conductor with a new line of lower resistance and reactance values. All existing lines have conductors of 35mm^2 with R/X factor equal to 2 and resistance equal to 0.9 Ω/km [73]. The candidate conductor for reconductoring has a cross-sectional area of 300mm^2 with resistance equal to 0.0892 Ω/km and R/X factor equal to 1. Also, DG units do not perform reactive management (unity power factor operation i.e. $Q_{m,t,g} = 0 \; \forall \; m, \forall \; t, \forall g \in \; \Omega_{DG}$).

The analysis is focused on 5 typical days, which are used to represent the duration of one year. Each day is characterized by daily patterns for demand and PV output (Figure 2.13) corresponding to a particular season and for a location outside London [74]. From this figure it can be observed that summer is the season with the highest PV generation levels and very low demand levels. Note that since there are four seasons in a year, the use of four typical days would be representative in our analysis. However, since the voltage rise effect is more intense during some periods in the summer than during others (this season exhibits high PV output and low load levels in the UK) it has been deemed appropriate to consider an extra typical day that corresponds to a hot summer day with relatively higher insolation and lower demand levels than other summer days. The consideration of this extra day adds to the accuracy of the representation of the risk of voltage rise complications within a year. The annual frequency of each typical day has been estimated according to [75]; 48 days for the autumn-day and spring-day respectively, 155 days for the winter-day, 70 days for the summer-day and 44 days for the high-summer-day.

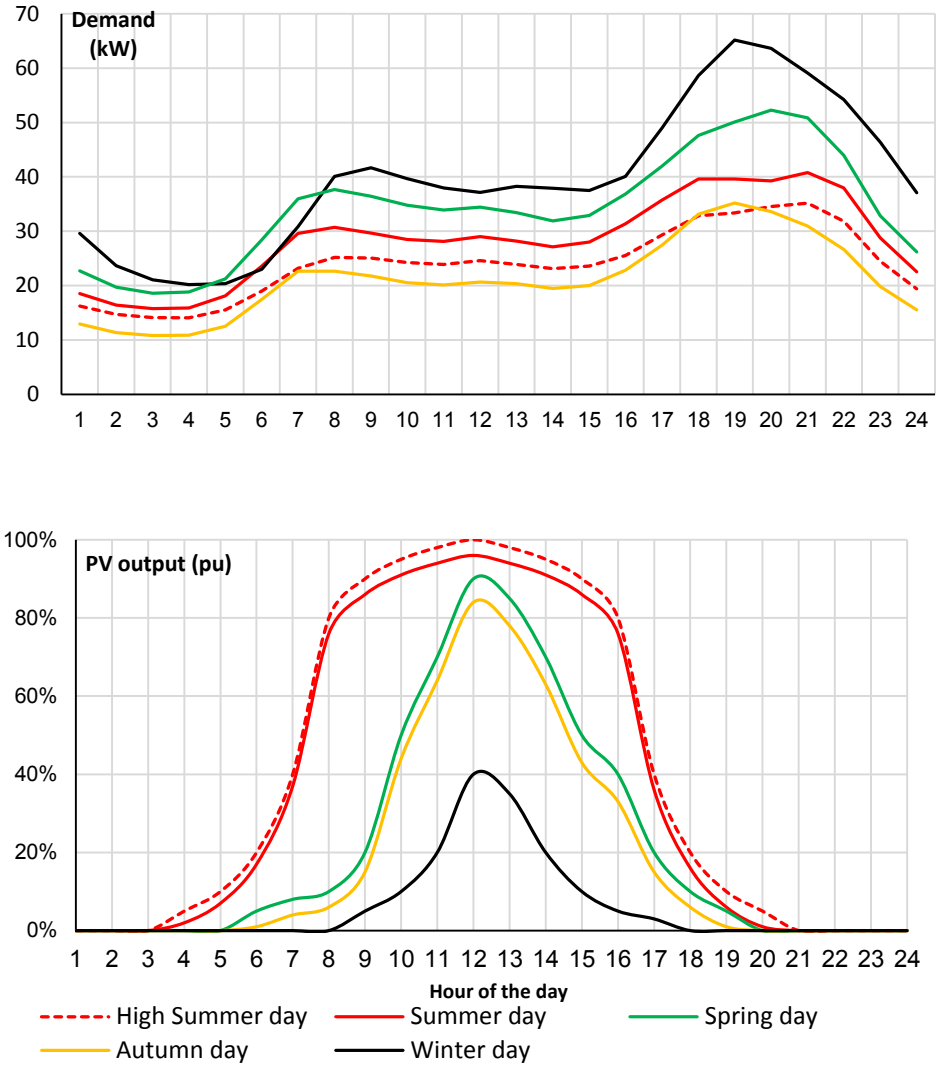


Figure 2.13 Patterns per typical day, for demand (above) and generation of a PV unit expressed as a percentage of its installed capacity.

2.2.2 *Results of the optimization studies*

Figure 2.14 displays the optimal investment strategy for a stochastic planner if line reconductoring is the sole available investment alternative and firm DG connections apply i.e. no APGC is allowed. It can be observed that a large number of conventional investments are needed in the first epoch to guarantee that no voltage-rise complications will take place at any time in the future. In particular, the entire feeder F-1 and most of feeder F-2 are reconductored. This is particularly risky, however, because in the event that node 2 occurs, the reconductoring of F-2 will turn out stranded. The resulting total expected system cost is

£818k and consists purely of the investment component as both DSR and APGC are not available thereby leading to zero operational costs.

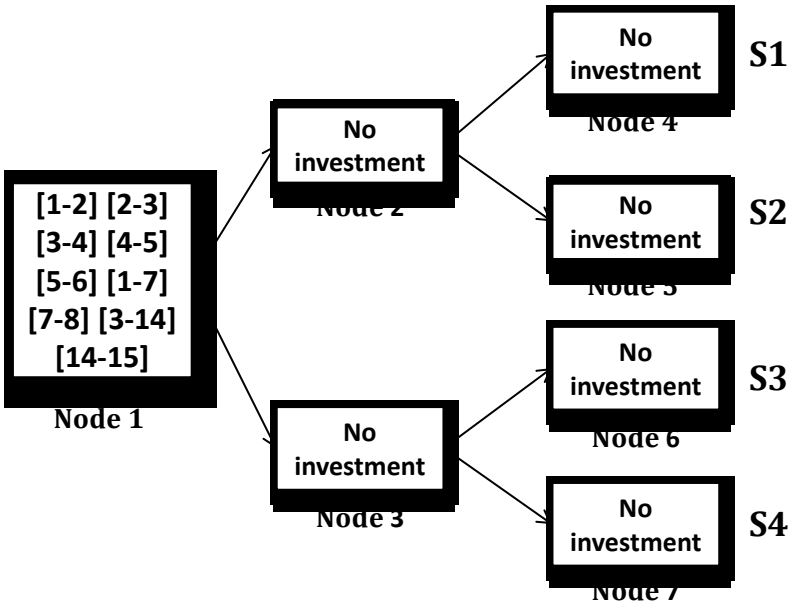


Figure 2.14 Optimal investment strategy for a stochastic planner in the case where only the conventional technology is available. Note that APGC is not available. The [x-y] means that the decision is taken to reconductor the line between buses x and y. Such a conventional investment decision becomes operational in the subsequent epoch. The S_i are the scenarios to which the depicted investment paths correspond.

Note that the following notation applies in this section: D(n) represents the decision to invest in DSR at bus n, SOP(a-b) represents the decision to invest in a SOP at the NOP of buses a and b, while CVC denotes the decision for installation of a CVC scheme in the substation. The [a-b] represents the decision to invest in reconductoring of line a- b.

Figure 2.15 illustrates the optimal investment strategy for a stochastic planner if line reconductoring as well as the APGC service are available to the planner. Comparing to the previous figure, the number of first-epoch conventional investment decisions has reduced because the availability of the APGC service has made it possible to defer these decisions by one epoch. It can also be seen that the decisions are more relevant to the uncertainty resolution meaning that 1-7 as well as 3-4, 4-5, 14-15 are reconductored conditionally on uncertainty resolution. Note that the reconductoring of 14-15 leads to the reduction of the voltage magnitude at bus 15.

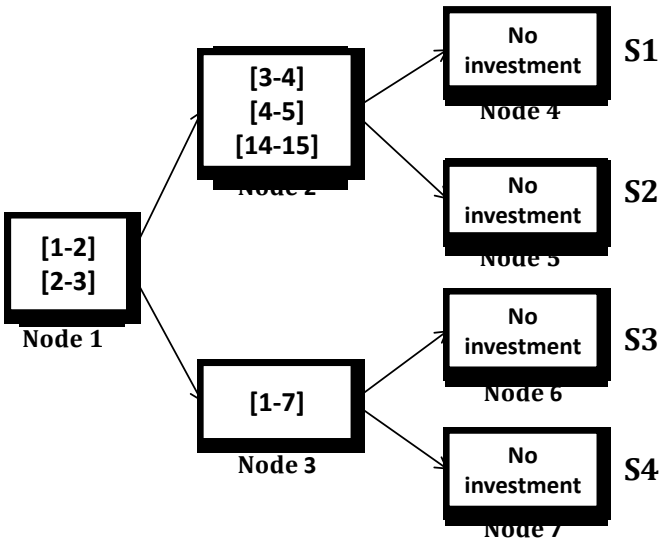


Figure 2.15 Optimal investment strategy for a stochastic planner in the case where only the conventional technology is available. Note that APGC is available.

The resulting total expected system cost is £512k and the total expected percentage of PV curtailment amounts to 14.9%. Table 2.6 presents information on the total cost, which is the summation of investment cost and operation cost, per scenario, as well as the percentage of curtailed energy produced from PVs. The operational cost is equal to the cost of PV curtailment as no DSR investment is present in the solution. Notice that the first two scenarios involve identical investment decisions and, thus, investment costs. Their operational costs differ though because of different PV curtailment amouns due to different voltage setpoints at nodes 4 and 5 respectively; with node 5 having a higher setpoint value the entire voltage pattern across the feeders is at higher levels, thereby leading to a more intense voltage rise effect and greater need for PV curtailment.

	Total Cost (£k)	**Investment Cost (£k)**	**Operational Cost (£k)**	**PV Curtailment (%)**
S1	666.7	354.6	312.1	14.4
S2	688.0	354.6	334.0	16.8
S3	379.6	239.4	140.2	14.2
S4	339.4	239.4	100.0	14.8
E	**512.6**	**297.5**	**215.3**	**14.9**

Table 2.6 Total costs per scenario for the strategy shown in Figure 2.15. The last row displays expected values.

Also, observe that scenarios S3 and S4 not only do they involve fewer investments but also lower absolute value of PV curtailment (not shown in the table), thereby corresponding to lower operational costs than S1 and S2. However, since the total maximum possible generation is also lower (due to smaller PV installed capacity levels), the PV curtailment stands at around the same level as in S1 and S2. Notice that the amount of PV curtailment decided at each node is optimally obtained based on the available costs and the voltage setpoints at each node (fixed voltage target policy) and no explicit stipulation has been included to limit the possible amount of PV curtailment below a certain bound.

Figure 2.16 presents the optimal investment strategy if the planner can consider all conventional and smart technologies, including APGC. It is evident that comparing to the previous strategies the availability of smart technologies to the stochastic planner radically affects both the timing and the type of the optimal investment decisions. Far fewer decisions to invest in conventional assets can be observed because of high deployment of smart grid assets; only lines 1-2 and 2-3 are chosen for reconductoring. Furthermore, no first-epoch capital commitments are made enabling the planner to commit only after the locational uncertainty of future PV development is resolved (e.g. separate strategies for the node 1 → node 2 and node 1 → node 3 branches), thereby significantly reducing the scope for asset stranding.

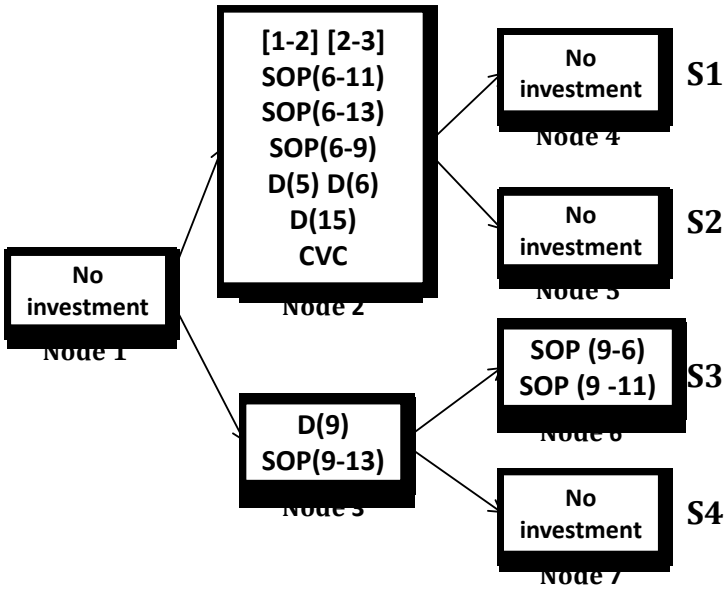


Figure 2.16 Optimal investment strategy for a stochastic planner in the case where all technologies (SOP, DSR, CVC, Reconductoring, APGC) are available.

The resulting total expected system cost is £444.2k with an average amount of PV curtailment (%) of 8.4%. Table 2.7 displays the total cost and the percentage of PV curtailment per scenario. Note that the cost of DSR operation is a very small part of operational costs, which can therefore be seen as purely PV curtailment costs.

Comparing to Table 2.6 it can be seen that the PV curtailment cost per scenario reduced due to a greater number of smart technologies deployed in the system that operate in an active manner (e.g. controlling the power flows through SOPs, or changing the load pattern through DSRs). Notice also that although the investment costs for S1 and S2 increased, the operational costs exhibit significant reduction due to drop in PV curtailment, thereby driving the total scenario costs down. Also observe the remarkable decline in PV curtailment levels for S3 and S4 without resorting to any conventional investment.

	Total Cost (£k)	**Investment Cost (£k)**	**Operational Cost (£k)**	**PV Curtailment (%)**
S1	742.2	488.7	253.4	11.8
S2	721.5	488.7	232.8	11.7
S3	207.1	168.9	38.2	3.9
S4	128.9	91.8	37.1	5.6
E	**444.2**	**301.8**	**142.4**	**8.4**

Table 2.7 Total costs per scenario for the strategy shown in Figure 2.16. The last row displays expectation values.

Notice that various types of smart technologies are deployed so as to assist with the eradication of the voltage rise effect. For instance, at node 2 of Figure 2.16 with PV units being installed in buses 5, 6 and 15, the DSR units are placed at exactly these buses in order to perform load shifting operations. Since adding an extra DSR scheme at another bus would very little alleviate the voltage rise effect at the aforementioned buses, other technologies are deployed and particularly CVC which reduces the voltage levels across the entire network and, as a result, in the aforementioned buses. The intensity of the voltage rise effect is such that SOPs are also required for further assistance. By deploying SOPs 6-9, 6-11 and 6-13 the voltage rise effect is completely eradicated. Observe that a SOP is not

deployed at 6-15 because buses 6 and 15 are both locations where the appearance of voltage rise effect takes place at the same hourly periods (around midday). Thus, a SOP between these two buses would not have the desired effects because when drawing power from bus 6 it would act as a load there (having a positive effect on buses 5 and 6) but exacerbate the situation at bus 15 by acting as an extra generator. The optimal mix of investment decsions at node 2 is completed by reconductoring lines 1-2 and 2-3, which become operational at the subsequent epoch. This investment leads to the reduction of the voltage magnitude across the entire section from bus 3 to bus 6, and bus 14 to bus 15, thereby achieving voltage reduction at the desired buses. If these reconductoring investments do not take place, then at node 4 there will be far greater amount of PV curtailment leading to an increase in total expected costs by 15%.

By comparing between the total expected cost of the strategies shown in Figure 2.14 and Figure 2.16 one can quantify the option value of the portfolio of smart technologies consisting of CVC, APGC, SOP and DSR. This value amounts to £818.0k – £444.2k = £373.8k i.e. 45% cost reduction and represents the expected savings (expected net benefit) due to the ability to invest in smart grid assets. If APGC is available (i.e. comparing Figure 2.15 to Figure 2.16), the option value of CVC, SOP and DSR is equal to £512.6k – £444.2k = £68.4k, corresponding to a 13% cost reduction. Note that APGC does not entail direct investment costs but can be interpreted as a policy decision to curtail renewable energy output for a penalty when needed. Similarly, one can quantify the option value of each different technology.

These option values are depicted in Figure 2.17 as a function of the availability for investment of other smart and conventional technologies. As an example, the option value of CVC with the availability of reconductoring (REC) and APGC represents the net benefit accrued from optimally investing in CVC, APGC and reconductoring compared to a system with optimal investments in APGC and reconductoring (i.e. without CVC). The main message of this figure is that when more technologies are added into the portfolio of available technologies for investment, the option value of any particular smart technology starts reducing because more technologies share the generated economic benefit; how this benefit is shared is determined by the corresponding investment costs and the way by which the technologies are modelled in the mathematical formulation. This ultimately means that the sum of option values of individual technologies (i.e. when only one technology is

available to the planner) is greater than the option value of the combined portfolio (i.e. when all technologies are available to the planner) as the latter accounts for complementary interactions between individual assets. For example, the option value of the entire portfolio of technologies is found to be equal to £373.8k, which is smaller than the sum of the option values of each type of smart technology when deployed alone, namely being £310k + £126k + £122k + £38k = £596k.

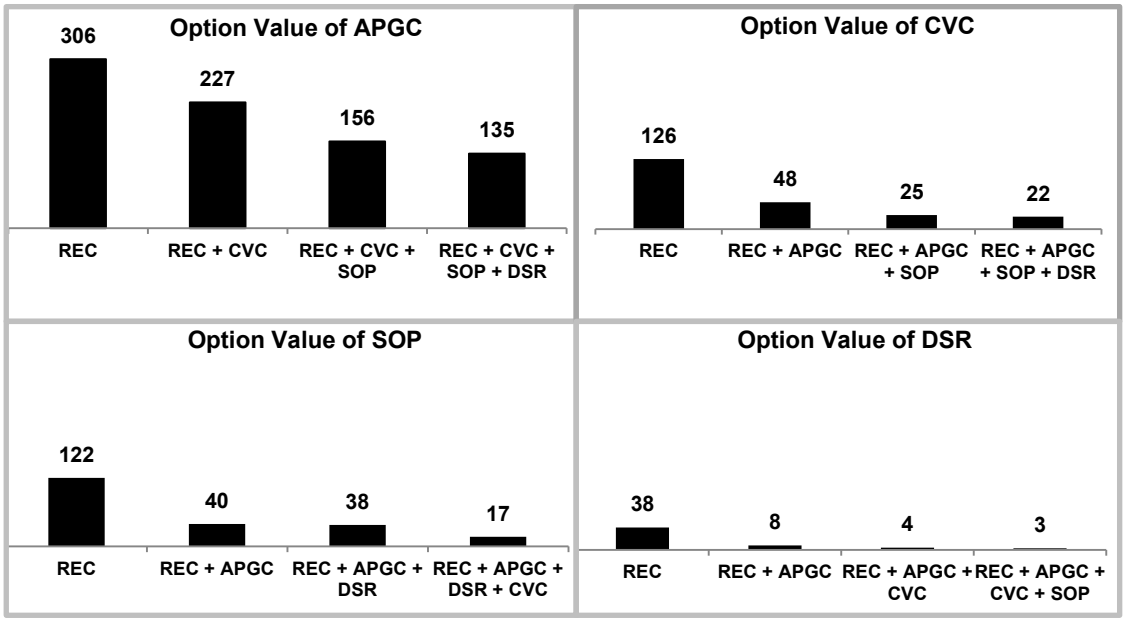


Figure 2.17 Option Value (£k) of a smart technology as a function of the availability of other technologies (REC refers to reconductoring).

Note that the concept of option value does not reflect the extra benefit from optimally investing in a smart technology at a system where other technologies have already been *optimally* deployed. For instance, one could falsely claim that the option value of CVC when SOP and reconductoring are available can be found by optimally solving the system with only SOP and reconductoring available (study 1), and then running a second study (study 2) but with the additional availability of CVC while fixing the investment decisions for SOP and reconductoring to those indicated by study 1. In contrast, the methodology followed in this work is that both studies 1 and 2 are solved independently of each other (i.e. without forcing some solutions to be identical to each other) and then subtracting the total expected costs. The superiority of this methodology over the former one is that it involves subtraction of optimal objective function values rather than subtraction of an optimal value from a suboptimal one (as in the case of forcing some decisions to be equal to those of

another study). Notice that the option value of each smart technology under no availability of other technologies is not presented because in the particular system none of these technologies alone (with the exception of APGC that resorts to extensive PV curtailment) is sufficient enough to be able to completely resolve the voltage rise effect.

For the specific case study, the most valuable technology is APGC, followed by CVC, SOP and DSR. In particular, APGC is shown to entail considerable option value since it enables cost-beneficial PV curtailment across the entire network and carries no investment cost. For example while with only reconductoring available (as seen in Figure 2.14) nine conventional decisions are made in the first epoch with the addition of APGC this number drops to two (Figure 2.15) as the rest are deferred or avoided. Similar situations arise with the rest combinations of technologies. Regarding CVC and SOP, these also turn out to be highly valuable due to their ability to increase network controllability across the entire network and across adjacent feeders respectively. Their deployment results in reduced PV curtailment and deferral or avoidance of first-epoch conventional reinforcement. DSR is shown to embed comparatively low levels of strategic flexibility as it has to be targeted at a specific bus and has little effect on nearby buses. This means that it cannot affect the entire voltage pattern of the feeder, as can the SOP, APGC or CVC technologies. As a consequence, many DSR investments are required in various buses along with extra investments. It can be concluded that the order of option values (i.e. which technology has the highest option value, and which technologies follow etc.) is determined by the input data (e.g. investment costs) and the mathematical modelling of each smart technology in the formulation.

Figure 2.18 illustrates an example of CVC operation corresponding to node 2 of Figure 2.16, where a voltage violation at bus 6 occuring during the summer-high day is resolved by reducing the substation voltage during hours of high PV output. In particular, the exact same solution that is depicted in Figure 2.16 is analysed when the CVC is not deployed at node 2. In this case, the substation voltage is at 1.012 pu, which is the fixed setpoint at the substation (see node 2 in Figure 2.12), resulting in bus-6 voltage magnitude exceeding the upper statutory limit of 1.06 pu. When the CVC is deployed, the voltage setpoint becomes controllable and for the purpose of tackling the voltage rise effect it gets reduced appropriately so that the voltage at bus 6 comes within the statutory limits (1.06

pu). This is a clear demonstration of CVC's ability to alleviate constraints at different parts of the network through enhanced controllability.

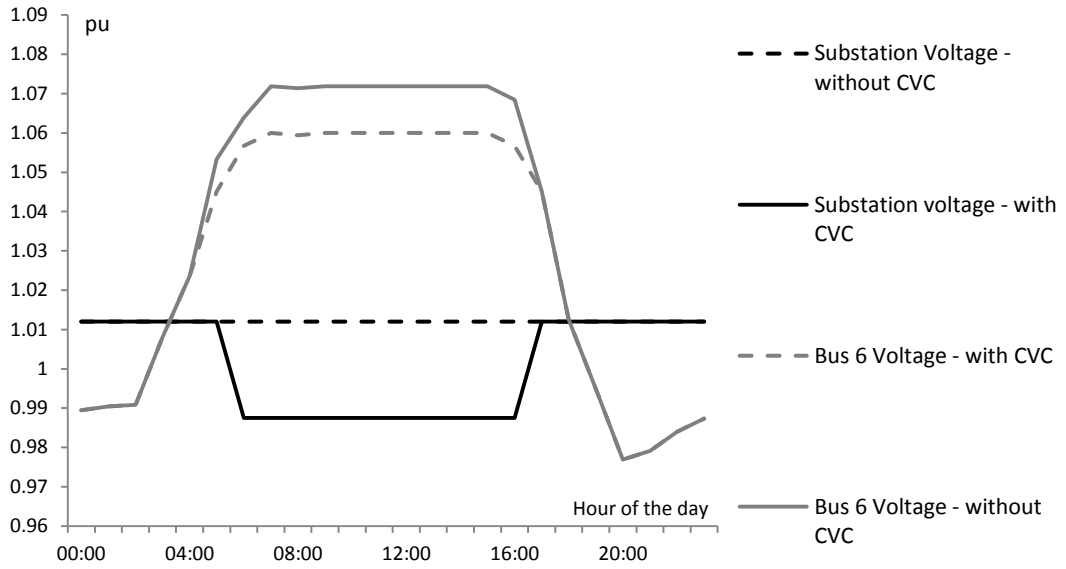


Figure 2.18 Impact of CVC operation on the substation voltage and on bus 6 voltage at scenario-tree node 2, in the high summer day (referring to Figure 2.16). Note that power flows follow the ACOPF model.

The basic operating principle of SOP technology for tackling the voltage rise effect is depicted in Figure 2.19, which corresponds to node 4 of Figure 2.16. At this node there are three SOPs deployed in the system, namely at NOPs 6-9, 6-11 and 6-13 and a PV unit deployed at bus 6 (see Figure 2.12). Figure 2.19 focuses solely on SOP 6-9. It can be seen that around midday hours of the summer-high day (very low demand levels) the voltage – rise effect occurs at bus 6. In particular, the dashed voltage line shows the voltage magnitude exceeding the 1.06 pu, which is the upper statutory voltage limit. This voltage profile is generated by solving a study with similar investment and operational decisions as the one shown in Figure 2.16 but without the presence of SOP at NOP 6-9 at node 4. This shows the importance of the operation of just one SOP device in the collective attempt to resolve the voltage rise effect. Figure 2.19 also shows the voltage profile that respects the upper statutory limit of 1.06 pu (see the black straight line). This profile is obtained from the output of the study shown in Figure 2.16. In particular, the second and third (from above) lines (both are dashed) show the initial demand at feeders F-1 and F-2 respectively. Since all buses have the same load profile the demand at F-1 is equal to the multiplication of

the profile of a single bus by 7 (there are seven buses in F-1). Similarly, the demand profile at F-2 is equal to the multiplication of the demand profile of a single bus by 3 (there are three buses in F-2). The SOP distorts these profiles because it draws active power from bus 6 (i.e. it acts as a load at F-1) and releases the same power (after applying a 90% efficiency factor) to bus 9, acting as a generator (i.e. negative load) at F-2. The new total F-1 demand is depicted in the first line (from above), while that in F-2 is shown in the fourth line from above. This transfer of active power re-sets the power flows to gain their natural 'unidirectional' flow which is from the substation to the load rather than from the load to the substation. Note that SOPs cannot transfer reactive power from one bus to the other. However, they can perform reactive compensation at any of these two buses. In this particular case, the SOP absorbs reactive power (shown negative in the figure) at bus 6. Thus, the SOP performs two functions at the same time: transfer of active power and absorption of reactive power. When the voltage rise effect is no longer an issue, the system topology returns to its initial configuration state, with the SOP ending its operation.

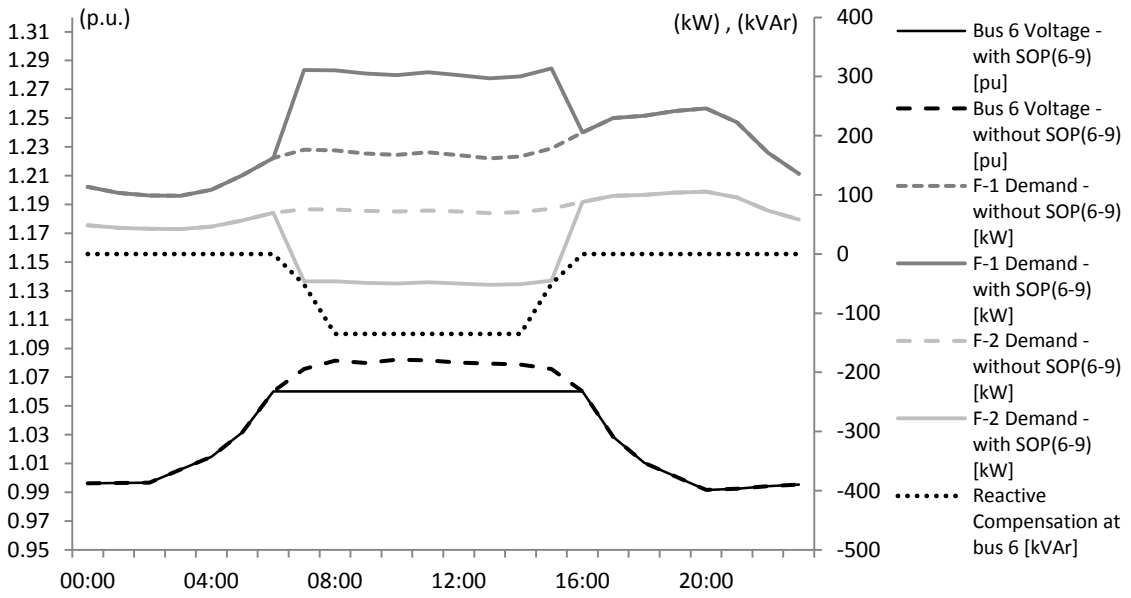


Figure 2.19 Demonstration of the operation of the SOP deployed at NOP 6-9 at scenario-tree node 4, during the high summer day (referring to Figure 2.16). The depicted voltage profiles correpond to the left axis, while the profiles for demand as well as reactive compensation correspond to the right axis. Note that power flows follow the ACOPF model.

So far the studies have pertained to stochastic planning. This type of planning involves identifying the optimal investment strategy that results in the minimization of the

total expected system cost across the horizon. Figure 2.20 illustrates the optimal investment plans under deterministic planning. This type of planning involves finding the optimal investment schedule for each of the four scenarios (S1 – S4, as seen in Figure 2.12) by applying the model described in section 2.2.3 and setting the scenario probability equal to one (i.e. no uncertainty - perfect future information).

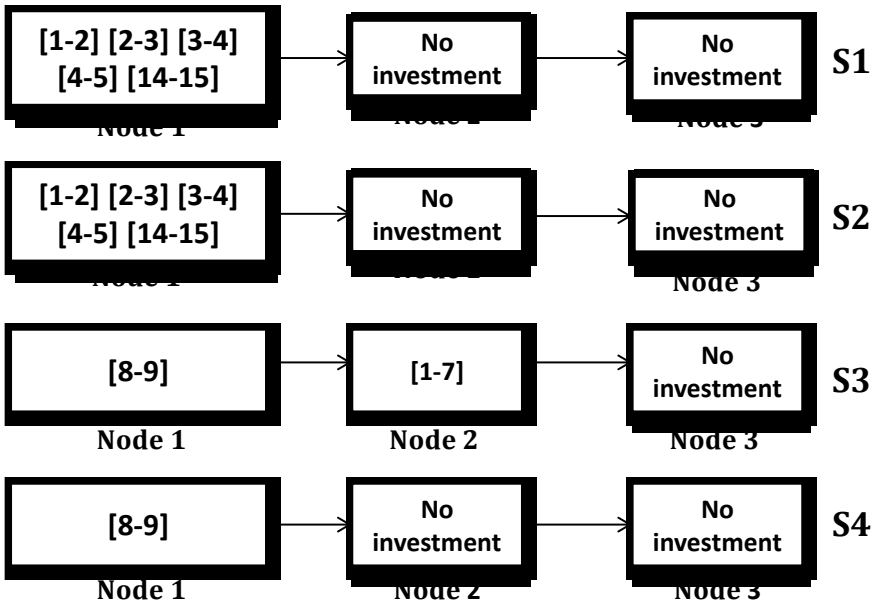


Figure 2.20 Optimal investment plans when each scenario is solved individually and all technologies are available to the planner.

It can be seen that all four investment plans are dominated by decisions to undertake conventional rather than smart investments, with the vast majority of commitments made in the first epoch. This is particularly problematic because making the decision to invest in conventional reinforcements 'here and now' and assuming that there is no uncertainty may lead a significant portion of these investments to become stranded assets. That is, although the planner considers deterministic growth in PV capacity, in reality the eventual scenario realization is uncertain. Hence, in the event that some PV connections do not materialize according to the scenario considered, some of the capital decisions may prove to be inefficient. For example, if the planner decides to follow the optimal investment schedule for scenario S2 (PV units are deployed at buses 5, 6, and 15) and in reality S3 (PV units are deployed at buses 7, 8, and 9) materializes instead, then all first-epoch decisions taken for S2 will turn out to be stranded investments. This is because line reconductoring is a commitment that entails little strategic potential for agility while smart technologies such as

CVC and SOP are flexible in the sense that even if another realization occurs it is more difficult for them to turn out to be stranded assets. For example, assume that the deterministic planner estimates that S2 will realize but instead of reconductoring a CVC is deployed. Then, even if S3 was realized instead of S2, the CVC would not turn out to be a stranded asset because it would still be able to assist in tackling the voltage rise effect by reducing the voltage appropriately. Similarly, a SOP deployed at NOP 6-9 would be able to operate in either case and would not become a stranded investment.

Notice that it is remarkable that despite the availability of DSR, SOP and CVC technologies, they are all deemed unattractive and, thus, fully ignored because a deterministic planner neglects the strategic benefits that accompany these technologies. Ignoring these technologies hinders the attempt to transform the current network to a smart grid and certainly discourages innovation. Table 2.8 presents information on the total cost, as well as its cost components, and the percentage of curtailed energy produced from PVs per scenario.

Regarding Figure 2.20, by comparing Table 2.8 with Table 2.6 and Table 2.7 it can be seen that the deterministic planner decides to make use of much less PV curtailment than the stochastic planner. Note that the maximum PV generation per scenario is identical for both the stochastic and the deterministic planners because it depends on the installed PV capacity. What is different for each planner is the amount of PV curtailment. For instance, according to Table 2.6 around 17% of PV output is curtailed, as opposed to 12% (see Table 2.7) and just 2.4% (Table 2.8). These differences can be attributed to the PV curtailment at node 2 (see Figure 2.15) where only the reconductored lines 1-2 and 2-3 are operational, while SOPs, DSRs and CVC are in Figure 2.16. In contrast in Figure 2.20, lines 1-2, 2-3, 3-4 and 4-5 are operational at node 2 revealing that smart technologies appearing at node 2 in Figure 2.16 are not sufficient to tackle the voltage rise effect by themselves, thereby prompting the planner to make use of an extra smart technology, the APGC. In other words, smart technologies can support the planner in managing the risk of stranded conventional assets by constituting *interim investment options* that defer large capital commitments on a conditional basis; as PV penetration increases, conventional investments will need to be made at some point but this point can be deferred owing to smart technologies.

Note that reconductoring has been modelled so that new conductors exhibit very low resistance and reactance values rendering it very effective and, therefore, not requiring the

assistance of APGC. This is the reason why at node 2 in Figure 2.20 the PV curtailment is very low; there is no practical need to curtail PV output. Obviously, the stochastic planner in Figure 2.15 and Figure 2.16 could opt to invest in conventional reinforcement in the first epoch. However, that did not happen because it would affect all four scenarios resulting in significant cost increases that would be far greater than making use of APGC at node 2.

	Total Cost (£k)	**Investment Cost (£k)**	**Operational Cost (£k)**	**PV Curtailment (%)**
S1	478.9	454.6	24.3	1.1
S2	501.0	454.6	46.4	2.4
S3	168.7	148.5	20.2	1.9
S4	129.3	90.9	38.4	5.8

Table 2.8 Total costs per scenario for the investment plans shown in Figure 2.20.

2.2.3 *Mathematical formulation*

The nomenclature for the mathematical formulation follows.

Sets and indices

Ω_C Set of normally-open points, indexed c.

Ω_{DG} Set of renewable distributed-generation (DG) units, indexed g.

Ω_E Set of epochs, indexed e.

Ω_L Set of distribution lines, indexed l.

Ω_M Set of scenario tree nodes, indexed m.

Ω_N Set of system buses, indexed n.

Ω_{TH} Set of thermal units & substations, indexed g.

Ω_Q Set of typical days, indexed q.

Ω_{T_q} Set of demand periods corresponding to q, indexed t.

ε_m Epoch to which scenario tree node m belongs.

$\Phi_k(m)$ Time-ordered set containing all parent nodes of node m, from the first epoch up to epoch $\varepsilon_m - k$

Input Parameters

γ_l Investment cost $(£/year)$ for reinforcing line l.

γ_c Investment cost $(£/year)$ for CVC deployment.

γ_D Investment cost $(£/year)$ for DSR deployment.

γ_S Investment cost $(£/year)$ for SOP deployment.

δ_t Duration of one period (hours).

λ Consumer payments for DSR flexibility $£/(kWh)$.

η_f SOP efficiency in transporting active power (%).

π_m Probability of scenario-tree node m occurring.

$\Psi_{n,t}$ Tangent of the load angle at bus n at period t.

$\zeta_{t,g}$ Time series representing intermittency of the renewable DG unit g, expressed as a percentage of installed capacity.

b_l^A Line susceptance before reconductoring (pu).

b_l^N Line susceptance after reconductoring (pu).

c^c Cost of curtailing DG output $(£/kWh)$.

$\overline{D}_{t,n}$ Maximum load that can be shifted to t at bus n (kW).

$d_{t,n}$ Real power demand at bus n, period t (kW).

F_l Initial capacity of line l (kW).

F_{max} Extra capacity, obtained from reconductoring, relative to existing capacity (kW).

$f_{t,n}$ Percentage of the initial load that is available, at bus n at period t, for shifting to a period $\tau \neq t$.

g_l^A	Line conductance before reconductoring (pu).
g_l^N	Line conductance after reconductoring (pu).
$I_{n,g}$	Equals 1 if g is connected to bus n. Otherwise, it equals zero.
k_L	Build time for reconductoring $(epochs)$.
k_C	Build time for CVC $(epochs)$.
k_D	Build time for DSR $(epochs)$.
k_S	Build time for SOP $(epochs)$.
N_q	Times of occurrence of day q in a year.
n_c^a	Primary terminal of SOP installed at c.
n_c^b	Secondary terminal of SOP installed at c.
$P_{m,g}^{max}$	Maximum real power stable generation of g (kW).
P_c^{max}	Real power capacity of SOP installed at c. (kW).
Q_c^{max}	Reactive power capacity of SOP installed at c. $(kVar)$.
$r_{\varepsilon_m}^I$	Cumulative discount factor for investment cost.
$r_{\varepsilon_m}^O$	Cumulative discount factor for operational cost.
$S_{m,g}^{max}$	Installed capacity of $g \in \Omega_{TH}\ U\ \Omega_{DG}$ at m (kVA).
u_l	Sending bus of line l.
v_l	Receiving bus of line l.
V_{set_m}	Voltage target value at the AVC relay of the substation OLTC transformer at node m (pu).
V_{min}	Minimum voltage statutory limit (pu).
V_{max}	Maximum voltage statutory limit (pu).
V_{min}^{cvc}	Minimum voltage attainable by CVC (pu).
V_{max}^{cvc}	Maximum voltage attainable by CVC (pu).

Decision Variables

$\theta_{m,t,n}$	Voltage angle at t corresponding to bus n (rad). It is $\theta_{m,t,1} = 0$.
$\xi^{d}_{m,t,n}$	Load at m, n shifted away from period t (kW).
$\xi^{c}_{m,t,n}$	Load at m, n shifted to period t (kW).
ω^{I}_{m}	Investment cost (£).
ω^{O}_{m}	Operational cost (£).
$B_{m,l}$	Binary variable for deciding to reconductor l at m.
$\tilde{B}_{m,l}$	State variable corresponding to $B_{m,l}$.
C_m	Binary variable for deciding to invest in CVC at m.
$\tilde{C}_m$	State variable corresponding to C_m.
$D_{m,n}$	Binary variable for deciding to invest in DSR at m, n.
$\widetilde{D}_{m,n}$	State variable corresponding to $D_{m,n}$.
$F_{m,l}$	Continuous variable for the extra capacity due to reconductoring l at m (kW).
$\tilde{F}_{m,l}$	State variable corresponding to $F_{m,l}$.
$G_{m,t,c}$	Real power drawn by SOP at terminal n^{a}_{c} (kW).
$H^{Q}_{m,t,c,n}$	Reactive power drawn by SOP at bus n $(kVAr)$.
$P_{m,t,g}$	Real power output of unit g at m, t (kW).
$P^{s}_{m,t,l}$	Variable $\in \mathbb{R}$ for the real power flow at the sending bus of l at m, t (kW).
$P^{r}_{m,t,l}$	Variable $\in \mathbb{R}$ for the real power flow at the receiving bus of l at m, t (kW).
$Q_{m,t,g}$	Reactive power output of unit g at m, t $(kVar)$.
$Q^{s}_{m,t,l}$	Variable $\in \mathbb{R}$ for the reactive power flow at the sending bus of l at m, t

	$(kVAr)$.
$Q^{r}_{m,t,l}$	Variable ∈ ℝ for the reactive power flow at the receiving bus of l at m, t $(kVAr)$.
$S_{m,c}$	Binary variable for SOP investment decision at m, c.
$\tilde{S}_{m,c}$	State variable corresponding to $S_{m,c}$.
$V_{m,t,n}$	Voltage magnitude at bus n at m, t (pu).
$V^{CVC}_{m,t}$	Substation voltage target regulated by CVC (pu).
$V^{noC}_{m,t}$	Substation voltage target in absence of CVC (pu).

The planning problem is formulated as a MINLP where binary variables are used to denote investment decisions. In particular, the planner has the choice to invest in reconductoring (conventional investment) and in smart technologies (CVC, DSR, and SOP). According to the nomenclature, the decision for investment in CVC, DSR, and SOP is denoted by the binary variables C_m,$D_{m,n}$, and $S_{m,c}$ respectively. A DSR scheme can be deployed at any load bus, SOPs can be installed at any NOP and CVC can be installed at the substation. The planner can also optimally perform active power generation curtailment (APGC), which involves paying the DG owners for curtailing their output. In addition, a nonlinear ACOPF formulation has been adopted to capture both thermal and voltage constraints [76].

Uncertainty is modelled in the form of a multi-epoch scenario tree consisting of $|\Omega_{\mathrm{M}}|$ nodes and spanning $|\Omega_{\mathrm{E}}|$ epochs capturing the possible system states across the planning horizon, where each node represents a multi-year period over which the system state remains unchanged. The mathematical formulation presented below is of the node-variable type [54] i.e. variables are associated with decision points (scenario tree nodes) rather than scenarios. As such, each scenario-specific decision variable has an associated index m, denoting the scenario tree node to which it pertains as well as the corresponding epoch (denoted by ε_m). As demonstrated in [55], node-variable formulations can result in significant computational benefits compared to their scenario-variable counterparts due to eliminating redundant variables and removing the need for non-anticipativity constraints. The problem's mathematical formulation follows.

$$min\left\{\sum_{m\in\Omega_M}\pi_m\left(r^I_{\varepsilon_m}\omega^I_m + r^O_{\varepsilon_m}\omega^O_m\right)\right\} \tag{2.24}$$

$$\omega^I_m = C_m\gamma_C + \sum_{l\in\Omega_L} B_{m,l}\gamma_B + \sum_{n\in\Omega_N} D_{m,n}\gamma_D + \sum_{c\in\Omega_C} S_{m,c}\gamma_S \tag{2.25}$$

$$\omega^O_m = \sum_{q\in\Omega_Q}\sum_{t\in\Omega_{T_q}} N_q\delta_t c^c \sum_{g\in\Omega_{DG}}\left(P^{max}_{m,g}\zeta_{t,g} - P_{m,t,g}\right) + \sum_{q\in\Omega_q}\sum_{t\in\Omega_{T_q}}\sum_{n\in\Omega_N} N_q\delta_t\xi^d_{m,t,n}\lambda \tag{2.26}$$

$$\left(P_{m,t,g}\right)^2 + \left(Q_{m,t,g}\right)^2 \le \left(S^{max}_{m,g}\zeta_{t,g}\right)^2 \qquad \forall m,t,\ \forall g\in\Omega_{TH}U\Omega_{DG} \tag{2.27}$$

$$\tilde{F}_{m,l} = \sum_{\varphi\in\Phi_{k_L}(m)} B_{\varphi,l}\,F_{max} \qquad \forall m,l \tag{2.28}$$

$$\tilde{B}_{m,l} = \sum_{\varphi\in\Phi_{k_L}(m)} B_{\varphi,l} \qquad \forall m,l \tag{2.29}$$

$$\tilde{C}_m = \sum_{\varphi\in\Phi_{k_C}(m)} C_\varphi \qquad \forall m \tag{2.30}$$

$$\widetilde{D}_{m,n} = \sum_{\varphi\in\Phi_{k_D}(m)} D_{\varphi,n} \qquad \forall m,n \tag{2.31}$$

$$\tilde{S}_{m,c} = \sum_{\varphi \in \Phi_{kS}(m)} S_{\varphi,c} \qquad \forall m, c \quad (2.32)$$

$$\begin{aligned} P^{s}_{m,t,l} = \left(1 - \tilde{B}_{m,l}\right)[V^2_{m,t,u_l} g^A_l - V_{m,t,u_l} V_{m,t,v_l} g^A_l \cdot \\ cos\left(\theta_{m,t,u_l} - \theta_{m,t,v_l}\right) - V_{m,t,u_l} V_{m,t,v_l} b^A_l \, sin\left(\theta_{m,t,u_l} - \theta_{m,t,v_l}\right)] \\ + \tilde{B}_{m,l}[V^2_{m,t,u_l} g^N_l - V_{m,t,u_l} V_{m,t,v_l} g^N_l \, cos\left(\theta_{m,t,u_l} - \theta_{m,t,v_l}\right) \\ - V_{m,t,u_l} V_{m,t,v_l} b^N_l \cdot sin\left(\theta_{m,t,u_l} - \theta_{m,t,v_l}\right)] \end{aligned} \qquad \forall m, t, l \quad (2.33)$$

$$\begin{aligned} P^{r}_{m,t,l} = \left(1 - \tilde{B}_{m,l}\right)[V^2_{m,t,v_l} g^A_l - V_{m,t,v_l} V_{m,t,u_l} g^A_l \cdot \\ cos\left(\theta_{m,t,v_l} - \theta_{m,t,u_l}\right) - V_{m,t,u_l} V_{m,t,v_l} b^A_l \, sin\left(\theta_{m,t,v_l} - \theta_{m,t,u_l}\right)] \\ + \tilde{B}_{m,l}[V^2_{m,t,v_l} g^N_l - V_{m,t,u_l} V_{m,t,v_l} g^N_l \, cos\left(\theta_{m,t,v_l} - \theta_{m,t,u_l}\right) \\ - V_{m,t,u_l} V_{m,t,v_l} b^N_l \cdot sin\left(\theta_{m,t,v_l} - \theta_{m,t,u_l}\right)] \end{aligned} \qquad \forall m, t, l \quad (2.34)$$

$$\begin{aligned} Q^{s}_{m,t,l} = \left(1 - \tilde{B}_{m,l}\right)[-V^2_{m,t,u_l} b^A_l - V_{m,t,u_l} V_{m,t,v_l} g^A_l \cdot \\ sin\left(\theta_{m,t,u_l} - \theta_{m,t,v_l}\right) + V_{m,t,u_l} V_{m,t,v_l} b^A_l \, cos\left(\theta_{m,t,u_l} - \theta_{m,t,v_l}\right)] \\ + \tilde{B}_{m,l}[-V^2_{m,t,u_l} b^N_l - V_{m,t,u_l} V_{m,t,v_l} g^N_l \, sin\left(\theta_{m,t,u_l} - \theta_{m,t,v_l}\right) \\ + V_{m,t,u_l} V_{m,t,v_l} b^N_l \cdot cos\left(\theta_{m,t,u_l} - \theta_{m,t,v_l}\right)] \end{aligned} \qquad \forall m, t, l \quad (2.35)$$

$$Q^r_{m,t,l} = \left(1 - \tilde{B}_{m,l}\right)[-V^2_{m,t,v_l} b^A_l - V_{m,t,u_l} V_{m,t,v_l} g^A_l \cdot$$
$$sin\left(\theta_{m,t,v_l} - \theta_{m,t,u_l}\right) + V_{m,t,u_l} V_{m,t,v_l} b^A_l \, cos\left(\theta_{m,t,v_l} - \theta_{m,t,u_l}\right)]$$
$$+\tilde{B}_{m,l}[-V^2_{m,t,v_l} b^N_l - V_{m,t,u_l} V_{m,t,v_l} g^N_l \, sin\left(\theta_{m,t,v_l} - \theta_{m,t,u_l}\right)$$
$$+V_{m,t,u_l} V_{m,t,v_l} b^N_l \cdot cos\left(\theta_{m,t,v_l} - \theta_{m,t,u_l}\right)] \qquad \forall m, t, l \quad (2.36)$$

$$\left(P^s_{m,t,l}\right)^2 + \left(Q^s_{m,t,l}\right)^2 \leq \left[F_l + \tilde{F}_{m,l}\right]^2 \qquad \forall m, t, l \quad (2.37)$$

$$\left(P^r_{m,t,l}\right)^2 + \left(Q^r_{m,t,l}\right)^2 \leq \left[F_l + \tilde{F}_{m,l}\right]^2 \qquad \forall m, t, l \quad (2.38)$$

$$V_{min} \leq V_{m,t,n} \leq V_{max} \qquad \forall m, t, n - \{1\} \quad (2.39)$$

$$V_{m,t,1} = V^{cvc}_{m,t} + V^{noc}_{m,t} \qquad \forall m, t \quad (2.40)$$

$$V^{cvc}_{min} \cdot \tilde{C}_m \leq V^{cvc}_{m,t} \leq V^{cvc}_{max} \cdot \tilde{C}_m \qquad \forall m, t \quad (2.41)$$

$$V^{noc}_{m,t} = V_{set_m} \cdot \left(1 - \tilde{C}_m\right) \qquad \forall m, t \quad (2.42)$$

$$\sum_{t \in \Omega_{T_q}} (\xi^d_{m,t,n} - \xi^c_{m,t,n}) = 0 \qquad \forall m, n, q \quad (2.43)$$

$$\xi^d_{m,t,n} \leq \widetilde{D}_{m,n} \cdot f_{t,n} \cdot d_{t,n} \qquad \forall m, t, n \quad (2.44)$$

$$\xi^{c}_{m,t,n} \leq \widetilde{D}_{m,n}\overline{D}_{t,n} \qquad \forall m,t,n \qquad (2.45)$$

$$G_{m,t,c} \leq P^{max}_{c} \cdot \tilde{S}_{m,c} \qquad \forall m,t,c \qquad (2.46)$$

$$|H^{Q}_{m,t,c,n}| \leq Q^{max}_{c} \cdot \tilde{S}_{m,c} \qquad \forall m,t,c \qquad (2.47)$$

$$\sum_{g\in\Omega_{Dg}U\Omega_{TH}} P_{m,t,g}I_{n,g} - \sum_{l\in\{\Omega_L|v_l=n\}} P^{r}_{m,t,l} - \sum_{l\in\{\Omega_L|u_l=n\}} P^{s}_{m,t,l} = \\ +d_{t,n} - \xi^{d}_{m,t,n} + \xi^{c}_{m,t,n} + \sum_{c\in\{\Omega_c|n=n^{a}_{c}\}} G_{m,t,c} + \sum_{c\in\{\Omega_c|n=n^{b}_{c}\}} (-G_{m,t,c}\,\eta_f) \qquad \forall m,t,n \qquad (2.48)$$

$$\sum_{g\in\Omega_{Dg}U\Omega_{TH}} Q_{m,t,g}I_{n,g} - \sum_{l\in\{\Omega_L|v_l=n\}} Q^{r}_{m,t,l} - \sum_{l\in\{\Omega_L|u_l=n\}} Q^{s}_{m,t,l} = \\ +\Psi_{n,t}(d_{t,n} - \xi^{d}_{m,t,n} + \xi^{c}_{m,t,n}) + \sum_{c\in\{\Omega_C|n=n^{a}_{c}\ or\ n=n^{b}_{c}\}} H^{Q}_{m,t,c,n} \qquad \forall m,t,n \qquad (2.49)$$

The objective function (2.24) describes the minimization of the discounted expected investment (2.25) and operational (2.26) cost. The former is equal to the sum of the investment cost of all smart and conventional technologies, while the latter includes the cost of DG curtailment as well as the cost of paying the consumers for their DSR participation. Notice the parameter N_q that is the number of days of type q along one year. Constraint (2.27) ensures that the real and reactive power drawn from the grid are within the limits of the substation transformer; the substation is located at $n = 1$ and corresponds to $g = 1$ having $\zeta_{t,g} = 1\ \forall t$. Regarding DG units ($g \neq 1,\ 0 \leq \zeta_{t,g} \leq 1\ \forall t$), their maximum real and reactive output is defined in terms of their installed capacity $S^{max}_{m,g}$ and resource variability

as dictated by the time-variable parameter $\zeta_{t,g}$ that captures hourly and seasonal variability. In addition, cumulative discount factors $r^I_{\varepsilon_m}$ and $r^O_{\varepsilon_m}$ are used to appropriately weight investment and operation costs incurred in each node m in terms of the time value of money and epoch duration. For example, $r^I_{\varepsilon_m}$ accounts for the fact that annual capital payments are to be made from the year an investment decision is made until the final year of the study.

Constraints (2.28)-(2.32) define the state variables that aggregate all investment decisions taken in the past considering their corresponding build times, i.e. the number of epochs between the epoch when the investment decision is made (and the investment cost in (2.25) is incurred) and the epoch when the investment becomes operational.

Constraints (2.33)-(2.36) define the real and reactive power flows in polar form. A disjunctive formulation has been implemented to capture the effect that reconductoring has on a line's characteristics b_l and g_l; if an existing line is reconductored ($\tilde{B}_{m,l} = 1$) then these parameters change from g^A_l, b^A_l to g^N_l, b^N_l. Note that knowing the line resistance and reactance, one can easily compute line conductance $g = r/(r^2 + x^2)$ and susceptance $b = -x/(r^2 + x^2)$. Different variables are used to model the flow at the sending and receiving ends of each line similar to [77]; differences between these variables represent losses over the line. Demonstration of these power flows in a small system is shown in Figure 2.21 for a particular time period t at some node m. In this figure there are four lines: l_0, l_1, l_2, l_3 and five buses $0-4$. Each line is defined in the form (u_l, v_l) as follows: $(0,1), (1,2), (2,3), (3,4)$. By default the power flows $P^s_{m,t,l}$, $P^r_{m,t,l}$ take positive values when they are modelled as depicted in the figure. Thus, in a normal situation where the power flows from generation to load, the receiving power flows $P^r_{m,t,l}$ receive negative values. In this case, the losses at some line are equal to the summation of $P^s_{m,t,l}$, $P^r_{m,t,l}$.

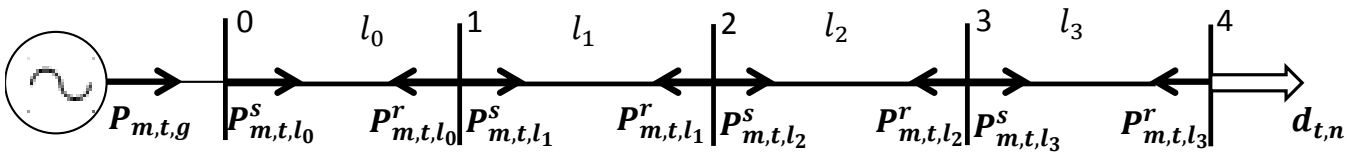


Figure 2.21 Illustration of the entire set of power flows per line as modelled in the formulation.

Constraints (2.37)-(2.38) state that real and reactive power flows are bounded by the line's thermal rating. This rating can be increased from its initial value F_l to the value $F_l + \tilde{F}_{m,l}$ after line reconductoring has taken place. Constraint (2.39) imposes the statutory voltage limits V_{min}, V_{max} on voltage magnitudes $V_{m,t,n}$ across all buses, with the exception of the voltage magnitude at the substation ($n = 1$) that is defined in (2.40) to be equal to the voltage target value of the automatic voltage control (AVC) relay of the On Load Tap Changer (OLTC) transformer located at the substation. This is because when the CVC scheme has not been deployed ($\tilde{C}_m = 0$) a fixed voltage-target policy for the OLTC at the substation is assumed [72], where $V_{m,t,1} = V_{m,t}^{noc} = V_{set_m}$ and $V_{m,t}^{cvc} = 0$ according to (17)-(19). If a CVC scheme has been implemented ($\tilde{C}_m = 1$), then the substation voltage target no longer follows a fixed voltage-target policy. Rather, it can be controlled optimally based on real-time information about system voltages; in this case it is $V_{m,t,1} = V_{m,t}^{cvc}$, with $V_{m,t}^{cvc}$ taking on values in the continuous domain $V_{min}^{cvc} \leq V_{m,t}^{cvc} \leq V_{max}^{cvc}$ according to (2.40)-(2.42).

Constraints (2.43)-(2.45) model the operation of all deployed DSR schemes. In particular, energy equality (2.43) ensures that all flexible load is eventually served within the period of a typical day (i.e. no load is lost); bounds on this load are defined in (2.44) and (2.45) respectively. In (2.44) the load that is disconnected at period t from bus n at node m is zero if no DSR has been deployed at bus n i.e. if $\widetilde{D}_{m,n} = 0$. Otherwise, it can attain the maximum value of $\mathrm{f_{t,n}} \cdot \mathrm{d_{t,n}}$, which is the total amount of flexible load available at time period t. The same logic applies for (2.45).

The SOP installed at normally-open point (NOP) c enables the transfer of active power from bus n_c^a to n_c^b with efficiency η_f. This transfer has to respect the SOP active power transfer limits according to constraint (2.46). According to this constraint, if the SOP has not been deployed at c (i.e. $\tilde{S}_{m,c} = 0$) then the corresponding controlled power flow must be zero i.e. $G_{m,t,c} = 0$. Otherwise, this power flow can reach the limit of P_c^{max}. Note that SOPs can perform reactive compensation at any of their two terminals (n_c^a or n_c^b) as well. In this regard, constraint (2.47) imposes the upper bound Q_c^{max} on the reactive power that a SOP can absorb ($H_{m,t,c,n}^{Q} > 0$) or generate ($H_{m,t,c,n}^{Q} < 0$). Finally, (2.48) and (2.49) impose system balance for real and reactive power respectively, while considering actions from smart assets. In (2.48), the last two terms state that at bus n_c^a an amount of $G_{m,t,c}$ is drawn by the SOP and is later released at bus n_c^b, taking into account the efficiency η_f.

These two terms do not appear in (2.49) because SOPs are not capable of transferring reactive power. Also, note the term $\Psi_{n,t}(d_{t,n} - \xi^{d}_{m,t,n} + \xi^{c}_{m,t,n})$ which is based on the fact that real and reactive powers are related according to equation $Q = P \cdot tan\phi$, where $tan\phi$ is represented by $\Psi_{n,t}$ at bus n and in period t.

2.2.4 ***Solution Methodology***

As mentioned in section 2.2.1, the analysis is focused on five typical days, which are used to represent the duration of one year. Approximating the year with typical days is a common approach taken to alleviate the computational load of planning studies (e.g. see [14]).This is necessary because as the investment cost is expressed in annual terms, so should the operational cost be. Obviously, it would be ideal to consider the network operation across 8760 hourly periods. However, in a nonlinear settting this method leads to intractability. Also, clearly the greater the number of typical days, the better is the approximation of the annual operational cost. However, with relatively larger number of typical days, the solution times become unacceptably higher. When employing five typical days, the solution times for the stochastic case studies range from half an hour to a little less than a day depending on the number of technologies available to the planner. The increased computational burden is due to the non-linear ACOPF formulation (e.g. constraints (2.33)-(2.36)), introduction of inter-temporal constraints to simulate DSR operation (see constraint (2.43)), binary variables related to investment decisions and the use of stochastic optimization. For instance, when solving the deterministic version of the problem and with all technologies available to the planner the solution times drop to at most two hours for each of the four scenarios.

Note that the model presented in section 2.2.3 is utilized to perform a number of deterministic and stochastic studies. This generic model includes both thermal (e.g. (2.27), (2.37) and (2.38)) and voltage constraints (e.g. (2.39)). In the case study presented in section 2.2.1 the value selected for parameter F_l (thermal capacity of the existing lines) is sufficiently high so that the system is bounded only by voltage constraints. This obviously has favourable effect on solution times as the thermal constraints (2.37) and (2.38) are actually redundant and can be ignored. Also, it is important to highlight that it is possible to simplify the quadratic constraint (2.27) by replacing it with box constraints (i.e. (2.50)-

(2.51)) as demonstrated in [78]. As expected, this relaxation leads to improved computational performance.

$$P_{m,t,g} \leq P_{m,g}^{max} \zeta_{t,g} \qquad \forall m, t, \; \forall g \in \Omega_{TH} U \Omega_{DG} \tag{2.50}$$

$$Q_{m,t,g} \leq Q_{m,g}^{max} \zeta_{t,g} \qquad \forall m, t, \; \forall g \in \Omega_{TH} U \Omega_{DG} \tag{2.51}$$

All models are developed using FICO Xpress 7.8 [79] and all studies are carried out on a Xeon 3.46GHz computer. For the solution of the MINLP that arises, FICO Xpress uses the Xpress-NLP optimization engine that allows for a solution strategy that includes a combination of Sequential (also known as Successive) Linear Programing (SLP) and the traditional Branch and Bound (B&B) technique. The solution process starts with the user providing an estimate of the optimal solution and, as the problem is nonlinear (nonconvex), the quality of the initial estimate is of high importance as the final solution is sensitive to it. In the study shown in Figure 2.16 the initial estimate that was given to the solver was based on expert opinion. Then, FICO starts to solve the problem by initially ignoring all integer constraints (linear relaxation) and performing multiple SLP iterations (first – order approximations around the initial estimate by Taylor series expansion) to approximate non-linear constraints. The linearized problem can be solved via Simplex as a usuall linear programming problem. This is essentially the solution of node 0 (the first node) of the Branch and Bound tree. As this is a minimization problem, the solution of the root solve (node 0) acts as a lower bound to the original problem's objective function based on the fact that linear relaxations always yield better (or equally good) solutions than the integer versions of the problem.

After node 0 has been solved, the process continues as a usual B&B methodology. That is, a variable is selected that has a fractional solution and branch constraints are created giving birth to two children nodes. Each node involves a linear relaxation by ignoring any integer constraints and by using SLP for approximation of the nonlinear elements of the formulation. This process continues and new nodes of the B&B tree are explored. When an

integer solution is found, the corresponding objective function acts as an upper bound to the original problem's objective function. Note that the initial value of the upper bound is plus infinity. However, this is updated to the objective value of a problem solved at a node that yields an integer solution (i.e. a solution where all variables attain integer values). The algorithm converges when the gap between the upper and lower bounds is sufficiently small (in this case, it was selected to be 0.1%). Note that although an exhaustive search is necessary to guarantee global optimality, extensive studies were carried out with different initial estimates to ensure comprehensive exploration of the solution space and guarantee the its high quality.

Chapter 3 Option Value under Endogenous Uncertainty with Immediate Resolution

3.1 *Immediate & Local DDU resolution (applied to distribution)*

In this section a case study is presented that applies to a distribution network that undergoes load and DG capacity growth over a ten-year horizon. In order to accommodate the resulting rising power flows the planner has the possibility to invest in conventionally upgrading lines and / or investing in DSR technology. However, the way by which optimal investment decisions will be made is not straightforward due to uncertainty. In particular, the source of uncertainty, which is the level of consumer participation in DSR, is of decision-dependent or endogenous type (i.e. does not resolve with the passage of time but requires action taken from the planner) and resolves immediately (i.e. at the same epoch when the investment is made) and locally (i.e. only at the bus where the corresponding investment is made). The results show that the deployment of DSR in the system allows not only for accommodating the rising power flows but also for generating significant cost savings while emphasizing the importance of investing in DSR as early as possible or otherwise costs are higher. This happens because by investing in DSR early, uncertainty resolves early thereby resulting in future investment decisions that are targeted to the realized system state i.e. stranding risk is minimized.

Conducting the studies involves modelling the problem in a stochastic optimization programming formulation and using various Benders decomposition techniques (e.g. multicut, monocut, sequential, parallel etc) to produce results within reasonable solution times. Additionally, a novel algorithm embedded within the Benders decomposition methodology is presented (Intelligent Filtering) that takes advantage of the specific characteristics of decision-dependent formulations and results in faster solution times. Finally, the methodology for obtaining the option value of DSR under decision dependent uncertainty is presented with relevant insights and explanations being provided.

3.1.1 *Problem description*

Despite the significant advantages of DSR technology, it is widely recognized that the participation of the consumers in the scheme is highly uncertain [80] because of the lack of precise knowledge about their responsiveness to the available financial incentives. Particularly, every consumer has individual preferences and perceptions that cannot be known a priori with certainty. Furthermore, it is highly unlikely that any socioeconomic study will be able to capture the entire spectrum of societal, cultural and personal factors that influence consumer choices [81], [82]. This uncertainty is classified as DDU as it cannot be resolved simply with the passage of time. Rather, the deployment of DSR will trigger the resolution of uncertainty because it will give the opportunity to consumers to choose whether they wish to participate or not.

Figure 3.1 depicts the reference overhead radial distribution network under study. There are eleven buses, with bus 1 representing the substation which allows energy imports from the main system, while some of the remaining buses accommodate load whose annual peak (in the first epoch) is 60kW. From the second epoch onwards the peak load at buses 5 and 8 grows over the study horizon, as shown in Table 3.1, while in all other buses it remains the same as that in the first epoch. Note that all load-buses have identical demand profiles as in Figure 2.3. Note also that since the peak load grows from one epoch to the next and the load pattern remains the same as in Figure 2.3, the hourly load (kW) grows as well from one epoch to the next. Furthermore, the eleventh bus starts to accommodate a DG-wind unit from the second epoch onwards (i.e. the DG unit is not operational in the first epoch) with installed capacity that grows as shown in Table 3.1; the deterministic time series used to represent its operational pattern is shown in Figure 2.4.

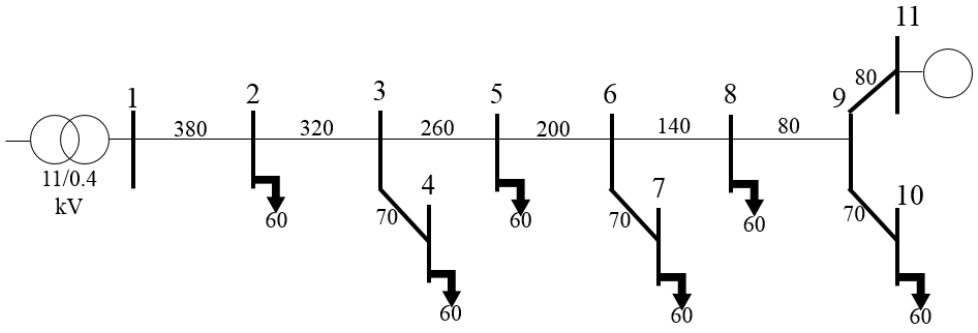


Figure 3.1 Schematic diagram of the distribution network showing line ratings (numbers above each line, in kW), peak load (numbers to which the arcs point, in kW), bus indices (numbers above each bus) and the location of connection of the DG-wind unit (bus 11), which becomes operational at the second epoch.

The study horizon is split in five two-year epochs over which the planner must minimize system costs by choosing to invest in increasing the capacity of the existing lines and/or deploying DSR schemes. Note that the power flows through the lines are modelled according to the DC power flow model.

The load growth leads to increased power flows, the safe accommodation of which requires investments. Without resorting to any investments, a significant amount of load would need to be curtailed over the horizon. Thus, in order to safely accommodate these growing power flows the planner has a range of potential solutions available that are shown in Table 3.2.

Epoch	Capacity of DG-wind unit at bus 11 (kW)	Peak load of each of the buses 5 and 8
1	0	60
2	120	80
3	130	85
4	150	90
5	170	100

Table 3.1 Growth of the installed capacity of the DG-wind unit at bus 11 and growth of the peak load of buses 5 and 8. Note that proportional increases apply not only to the peak load of these buses but to their entire demand pattern.

The DSR scheme, which can be deployed at any bus that accommodates load, allows shifting (for some monetary compensation to the consumer) of the time at which the flexible load was initially set to start its demand. The shifting coverage period is taken to extend across 24 hours. This flexible load is expressed as a percentage of the total hourly load connected to the bus and reflects the consumer participation level (expressed as a percentage of the population of consumers connected to the bus) in the DSR scheme. In other words, the more people participate in the scheme (i.e. the higher the consumer participation), the greater the amount of flexible load that can be controlled.

It is assumed that the level of consumer participation is uncertain at some buses and this uncertainty can be resolved only by deploying a DSR scheme. Thus, this is a case of *decision-dependent uncertainty*. Once such an investment is made, the DDU will completely resolve within one epoch (*immediate resolution*), and *locally* (*local resolution*) at the bus where the DSR is deployed. In particular, assume that m, n are buses exhibiting DDU around the consumer participation and a DSR scheme gets deployed at n. As the DDU

resolves only locally at n, the DSR deployment does not affect the uncertainty resolution at m.

Technology	Build time (epochs)	Investment cost (£k)
Conventional reinforcement alternative #1 (+50 kW)	1	80 /year/line
Conventional reinforcement alternative #2 (+100 kW)	1	120 /year/line
DSR	0	50 /year - bus

Table 3.2 Investment cost and build time for the available technologies for investment.

In Figure 3.1 there are six load-buses i.e. six candidate locations for DSR deployment. Load-buses 2, 4, 7 and 10 do not exhibit uncertainty around the participation level, which is there a priori set at 20%; it is generally possible for a system not to exhibit DDU at every location. For instance, in [48] only some of the considered oilfields are assumed to be uncertain in their properties. On the other hand, buses 5 and 8 exhibit DDU with the degree of consumer participation becoming known only after DSR deployment there. Following DSR installation, the consumer participation can take on two possible values: 10% (with 30% probability) and 50% (with 70% probability). Thus, four possible scenarios are formed, each with a corresponding probability as shown in Table 3.3. Notice that the most likely scenario has been selected to correspond to the high DSR uptake (S1) in order to reflect the increasing interest in smart technologies; $\pi_1 = 70\% \cdot 70\% = 49\%, \pi_2 = \pi_3 = 30\% \cdot 70\% = 21\%, \pi_4 = 30\% \cdot 30\% = 9\%$. Note also, that the values 10%, 20% and 50% are upper bounds; clearly the optimal amount of load shifting may be lower at some periods.

The network planner's objective is to determine the investment decisions that minimize the sum of the total expected investment and operational cost, so as to guarantee that the total system load is supplied at all times. The latter cost consists of the cost of curtailing the output of the DG-wind unit and the cost of payments to consumers for their participation in the DSR scheme as in Table 3.4.

Scenarios	Buses 2, 4, 7, 10	Bus 5	Bus 8	Scenario Probability
Scenario S1	20%	50%	50%	49%
Scenario S2	20%	50%	10%	21%
Scenario S3	20%	10%	50%	21%
Scenario S4	20%	10%	10%	9%

Table 3.3 Consumer participation in the DSR scheme at each load-bus, per scenario.

	Costs
Curtailment of the output of the DG unit	100 £/MWh
Compensation to consumers for participating in DSR scheme	10 £/MWh

Table 3.4 Costs relevant to the operation of the power system.

3.1.2 *Results of the optimization studies*

Figure 3.2 displays the optimal investment strategy if only the conventional technology is available to the planner. The resulting total expected system cost is £3.63m where £3.62m is the investment component and £13k the component due to wind curtailment cost .

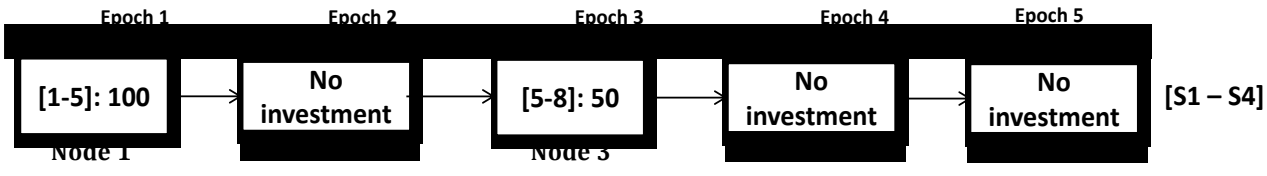


Figure 3.2 Optimal investment strategy in the case where only the conventional technology is available to the planner. The [x-y]:100 means that the decision is taken to reinforce each of the lines between buses x and y by 100kW. Thus [1-5]:100 means [1-2]:100, [2-3]:100, [3-5]:100, and [5-8]:50 means [5-6]:50, [6-8]:50. Such conventional investment decisions become operational in the subsequent epoch. The brackets at the rightmost corner show to which scenarios the depicted investment paths correspond.

Notice that the depicted investment plan is similar to that of a deterministic study, where no branching is present; this is because uncertainty resolution (i.e. branching) can only be triggered by investment in DSR. Thus, all four scenarios remain undifferentiated and subject to the same unconditional investment decisions. The logic behind the investment decisions is shown in Table 3.5. For example, the decision to reinforce line 1-2 by 100kW is taken in the first epoch so that it becomes operational in the second epoch due to the one-epoch build-time delay. However, as the maximum power flow in the second epoch exceeds the thermal limit by only 12kW, it would make sense to select the 50kW investment alternative. This does not happen because it has been assumed that at most one investment decision per line can be made across a scenario. This assumption has been made in order to simplify the resulting investment strategy and allow the reader to focus on the essence of the chapter. Thus, with 100kW investment the power flows along line 1-2 are accommodated in all subsequent epochs. The same logic applies for all other conventional decisions. It can also be observed that lines closer to the DG-wind unit require less investment because of its alleviating presence (the loads that are close to the DG unit are fed by it thereby requiring less power from the main grid). Hence, lines [5-6] and [6-8] are upgraded later in time and with 50kW.

	[1-2]:380	**[2-3]:320**	**[3-5]:260**	**[5-6]:200**	**[6-8]:140**
Epoch 2	392	332	272	194	134
Epoch 3	404	344	284	200	140
Epoch 4	415	355	295	205	145
Epoch 5	439	379	319	217	157

Table 3.5 Maximum power flows (kW) per line for each epoch. Underlined are the flows that exceed the initial (shown in bold at the top row) line thermal limit.

Figure 3.3 shows the optimal investment strategy for a network planner who has the DSR and the conventional technologies available for investment. A first observation to make when comparing this strategy with the previous one is that they do not only entail different investment, but their branching structure is also radically different. In addition, it is evident that the availability of DSR to the planner involves fewer decisions to invest in conventional assets, with the planner opting for DSR deployment instead. The resulting total

expected system cost is £655k consisting of £642k (investment component) and £13k (wind curtailment cost).

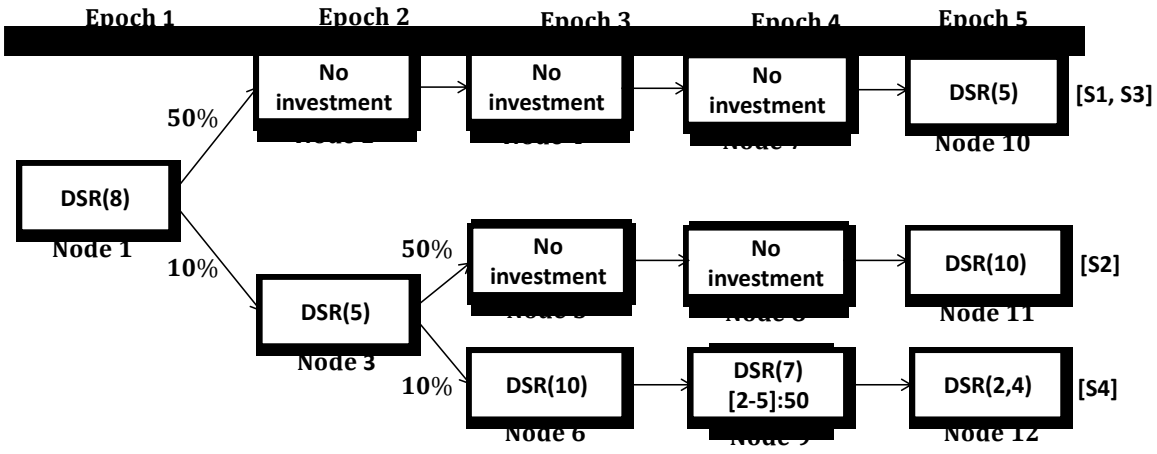


Figure 3.3 Optimal investment strategy for a network planner with two investment technologies available: DSR and conventional reinforcement. The DSR(X) signifies the decision to invest in DSR at bus X. Percentages refer to consumer participation levels for the buses to which the DSRs have been deployed (these percentagesremain the same across a single path ie when no branching exists because consumer participation per bus does not change). The [x-y]:50 signifies the decision to reinforce the lines between buses x and y by 50kW each. For example, [2-5]:50 is equivalent to [2-3]:50 and [3-5]:50. The brackets at the rightmost corner show to which scenarios the depicted investment paths correspond.

The DSR scheme has two functions. The first is the uncertainty resolution, which allows for conditional investment, and the second is load shifting that prevents exceeding line thermal limits and leading toconventional investment deferral.

Regarding the shifting operation of DSR technology in Figure 3.3, it serves the purpose of countering the consequences of low wind output (due to low wind resource availability). In particular, DSR operation involves disconnecting load at times of very low availability of wind resource and very high demand. In such periods the DG-wind unit has insignificant output. As a result, the system demand is mostly satisfied through imports from the substation leading to increased power flows through the lines of the main feeder (eg 1-2, 2-3, 3-5, 5-6, 6-8). The load is then connected back at periods when it is safe for system operation (ie medium to small load factor and medium to high wind output). This is the essence of the DSR operation at every node of Figure 3.3 and this load-shifting operation does not increase or reduce the curtailment of wind output.

For example, at node 2 (in Figure 3.3) the DSR at bus 8 disconnects load at times when the DG-wind unit can output less than 4% of its installed capacity, due to very low wind availability, and the demand at all buses is at peak levels. This way the DSR operation prevents power flows from exceeding the corresponding thermal limits of lines 1-2, 2-3 and 3-5 and the disconnected load is then connected back to bus 8 at periods that are safe for the operation of the system. Similar description applies to nodes 4 and 7 whereas at node 10 an extra DSR at bus 5 is needed for the same purpose. Regarding node 3 the DSR investment allows for distinguishing scenarios S2 and S4 (local uncertainty resolution – see description further below) which allows for pursuing a different investment strategy across each one. In addition at node 3 both the DSR at bus 5 and that at bus 8 perform load shifting achieving safe accommodation of power flows (since the DSR at bus 8 cannot shift the entire necessary load by itself, despite using up its maximum available consumer participation level of 10%, the DSR at bus 5 is assisting also by disconnecting the extra necessary load) . In other words at node 3 both uncertainty resolution and load shifting operation are performed.. Regarding nodes 6/9/12 the simultaneous operation of three/four/six DSR schemes is required for the safe accommodation of power flows. Many DSR units are needed because the flexible load per bus is limited and the sum of these flexible loads is required in order to respect line ratings. For example, at a certain period characterized by low wind output (3% of its installed capacity) and high demand (99.9% of the peak demand at all buses) without these DSR units a flow of 438kW would need to pass through line 1-2 whose ratings is 380kW ie 58kW over the rating. Thus, the DSR units disconnect the maximum flexible load that is available per bus i.e. 10kW from bus 5, 10kW from bus 8, 12kW from bus 10, 12kW from bus 2 and 12kW from bus 4 and the remaining 2kW from bus 7.

Figure 3.4, Figure 3.5 and Figure 3.6 show the operation of DSR schemes (buses 5, 8 and 10 respectively for node 11) over 24 hours with the goal of accommodating the increased power flows through the lines of the main feeder (Figure 3.7shows the effect that the combined operation of these DSR schemes has on the power flows through line 3-5). It can be seen that during periods when the DG-wind unit output is low (see the dotted line that corresponds to the right axis), line 3-5 becomes overloaded in the absence of the DSRschemes thereby requiring disconnection of flexible load from the aforementioned buses (5,8,10). This load is connected during hours when the DG-wind unit output is high (or when the load in the system is low) because during these periods the problematic lines

(such as 3-5) are not overloaded because much of the system load is fed by the DG output and so less power is imported via the substation. Similar operation takes place during other 24-hour periods. Note that load growth takes place only at buses 5 and 8 and the DSR schemes at buses 5, 8 and 10 have consumer participation 50%, 10% and 20%.

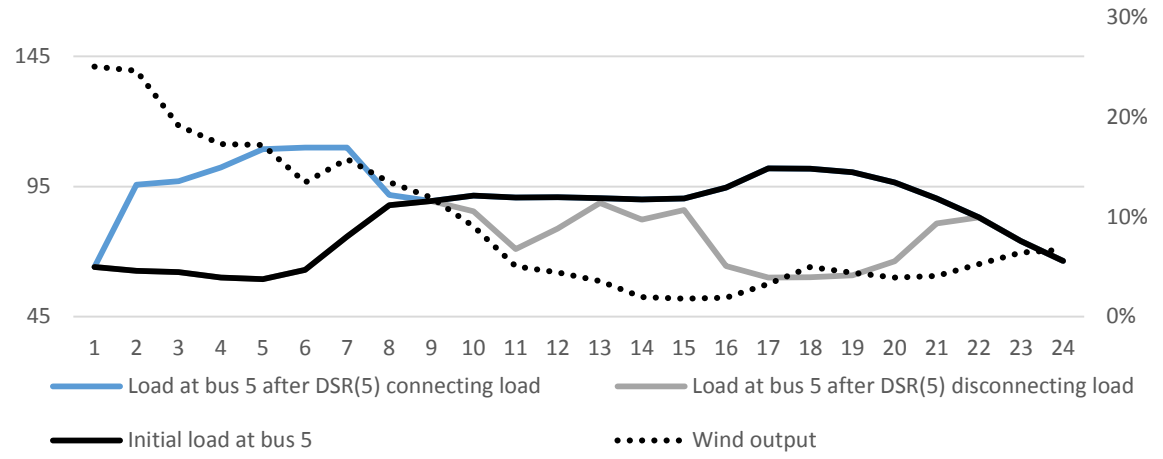


Figure 3.4. Load shifting operation by the DSR scheme at bus 5 (referring to node 11, Figure 3.3) over 24 hours, where load is disconnected during periods of low wind output, and is then connected back (so that no load is lost) during periods of high wind output thereby avoiding / deferring conventional reinforcement of the lines of the main feeder. Note that the dotted line corresponds to the right axis while the others correspond to the left axis. Note that power flows follow the DCOPF model.

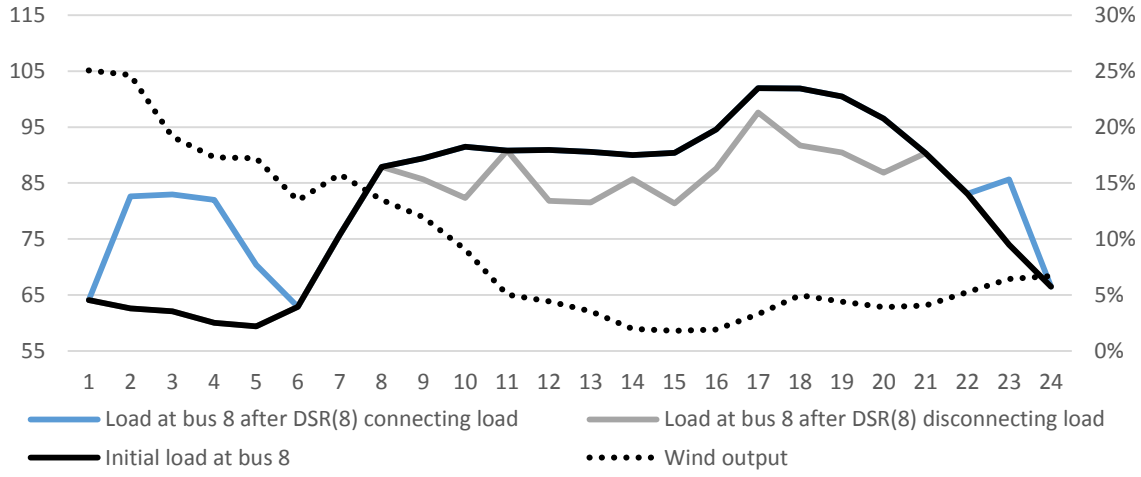


Figure 3.5. Load shifting operation by the DSR scheme at bus 8 (referring to node 11, Figure 3.3) over 24 hours, where load is disconnected during periods of low wind output, and is then connected back (so that no load is lost) during periods of high wind output (some is also connected during periods when the initial load is small) thereby avoiding / deferring conventional reinforcement of the lines of the main feeder. Note that the dotted line corresponds to the right axis while the others correspond to the left axis. Note that power flows follow the DCOPF model.

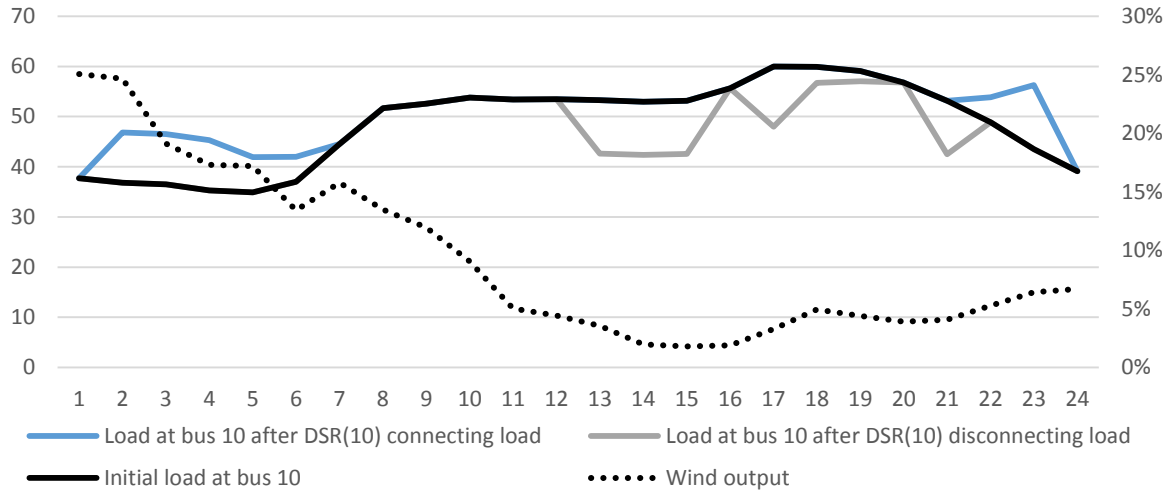


Figure 3.6. Load shifting operation by the DSR scheme at bus 10 (referring to node 11, Figure 3.3) over 24 hours, where load is disconnected during periods of low wind output, and is then connected back (so that no load is lost) during periods of high wind output (some is also connected during periods when the initial load is small) thereby avoiding / deferring conventional reinforcement of the lines of the main feeder. Note that the dotted line corresponds to the right axis while the others correspond to the left axis. Note that power flows follow the DCOPF model.

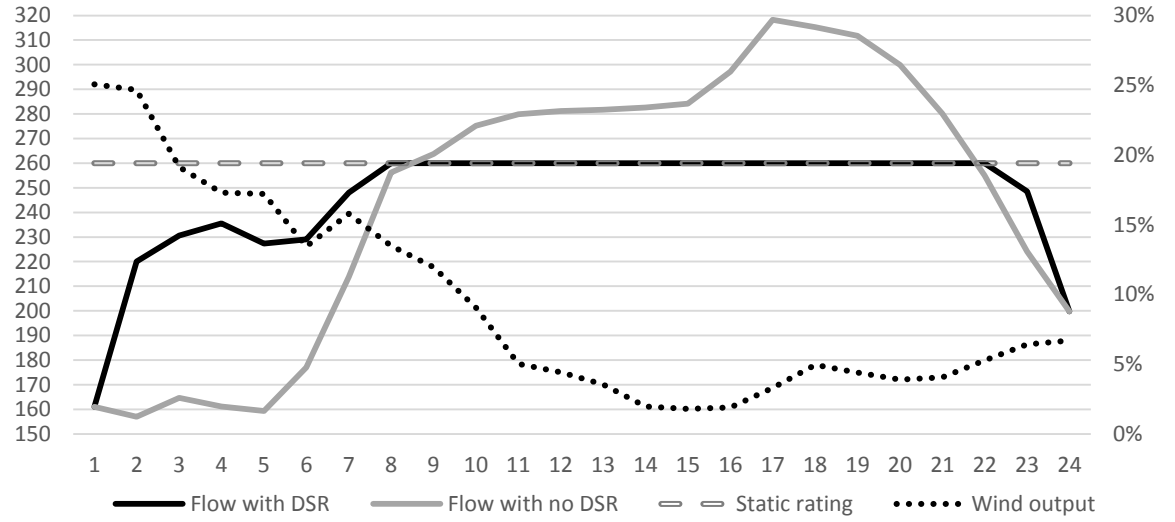


Figure 3.7. Power flow pattern through line 3-5 (referring to node 11, Figure 3.3) over 24 hours, before and after the combined operation of the DSR schemes connected to buses 5, 8 and 10 (see the previous three figures). The dotted line corresponds to the right axis while the others correspond to the left axis. Note that power flows follow the DCOPF model.

Regarding the uncertainty resolution process, in the first epoch the DSR gets deployed at bus 8 allowing the planner to completely resolve the uncertainty around the

consumer participation at bus 8. Complete resolution means that there is no more uncertainty at bus 8 to resolve. Also, since the uncertainty is resolved completely at the same epoch as when the investment decision is made, the resolution can be characterized as *immediate*. In addition, the planner learns the value for the consumer participation at bus 8, but not at bus 5, since the resolution of uncertainty is *local.* Following uncertainty resolution at bus 8 the participation levels become known and if they turn out to be favourable i.e. 50% then the need for further investments is alleviated (only a DSR at bus 5 is deployed at node 10). If the adverse case of 10% consumer participation materializes, the planner proceeds with deploying a DSR scheme at bus 5 in the second epoch, where an additional branching occurs. At bus 5 a customer participation of 50% is sufficient to ensure unconstrained operation until the last epoch, when a DSR is deployed at bus 10. In the adverse case of 10% consumer participation, the planner needs to adjust the network by carrying out numerous line upgrades and deploy DSR schemes in subsequent epochs. Notice, again, that the resolution of uncertainty in buses 5 and 8 is completely independent of each other.

The option value [11] of investing in the DSR technology under DDU is equal to the difference in the total expected system cost in the resulting strategies where the DSR is available (Figure 3.3) and where it is not (Figure 3.2). This difference amounts to £3.633m - £655k= £2.978 m representing the expected value of the net benefit accrued from optimally investing in DSR. This net benefit stems from the ability of the DSR to perform load shifting (which can allow for deferral or avoidance of conventional reinforcement) and to resolve uncertainty (which can permit conditional investments).

It is remarkable that in Figure 3.3 in the first epoch there is no DSR load shifting operation because network constraints only arise from the second epoch onwards (because load growth takes place from the second epoch onwards). This highlights the fact that DSR deployment takes place in the first epoch in order to trigger DDU resolution early enough so that conditional investments can take place further resulting in reduced total expected investment cost. To demonstrate this, an optimization study is conducted in which the planner can consider both technologies in all epochs except for the first one, when only the conventional technology is considered (see Figure 3.8). This results in 11% increase in total expected system cost (comparing to the strategy shown in Figure 3.3) i.e. the total expected system cost amounts to £727k consisting of £713k (investment component) and £13k (wind curtailment cost). This cost increase can be attributed to the fact that in Figure 3.8 the DSR

at bus 5 is deployed in the second epoch and unconditionally applies to all four scenarios as opposed to Figure 3.3 where a similar investment in the second epoch applies to two scenarios. This happens because a first-epoch DSR investment (as in in Figure 3.3) allows for uncertainty resolution at the first epoch which allows for subsequent investments that are more efficient than making the first investment in the second epoch (as in Figure 3.8). The rule that applies to this decision-dependent uncertainty problem is that 'investing in DSR early leads to a more economical investment strategy.

Regarding Figure 3.3, note that although the DSR at bus 8 does not need to perform load-shifting operation in the first epoch, this investment is justified from the perspective of the minimization of total expected system costs. In the first epoch the DSR at bus 8 may have the form of a pilot DSR scheme whose operation is not aimed at accommodating the power flows (after all, these are safely accommodated) but at the uncertainty resolution which can happen by observing customer participation levels in the pilot DSR scheme. In other words, this pilot DSR scheme must be designed as an experiment at the end of which meaningful and realistic conclusions can be extracted about actual consumer participation levels in this novel technology. It is assumed here that setting up this pilot scheme has the same investment cost as setting up any other DSR scheme in the system and that the uncertainty can be resolved by asking consumers to allow control of their flexible load (despite no need from the system perspective may exist in reality).

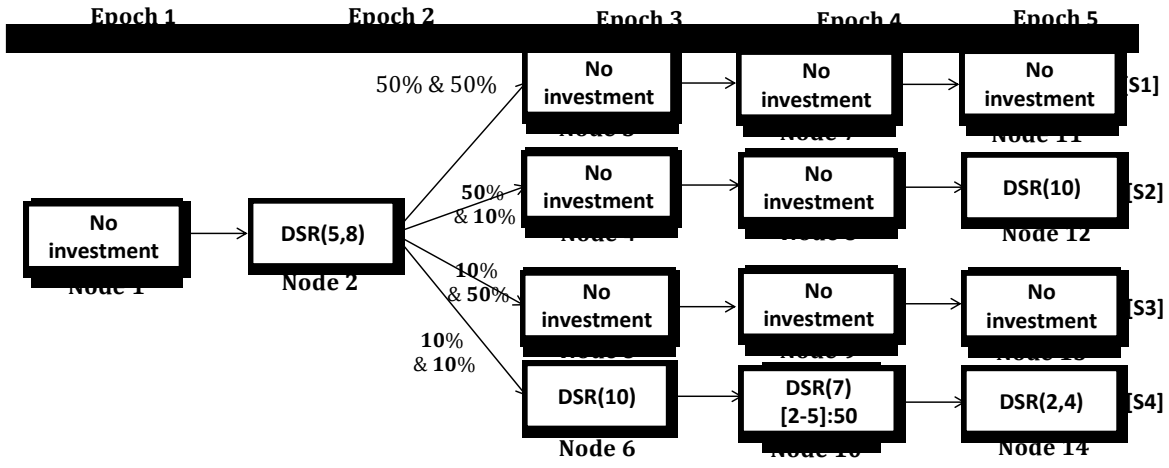


Figure 3.8 Optimal strategy for a planner with two technologies available: DSR and conventional line upgrade. The planner does not have the possibility to invest in DSR in the first epoch, but has this possibility in all other epochs. The percentage values correspond to the values for the consumer participation at buses 5 and 8 respectively.

3.1.3 *Mathematical Formulation*

The nomenclature for the mathematical formulation follows.

Sets and indices

Ω_S	Set of scenarios, indexed s, s'.
Ω_{DG}	Set of renewable distributed-generation (DG) units, indexed g^*.
Ω_E	Set of epochs, indexed e.
Ω_L	Set of distribution lines, indexed l.
Ω_G	Set of all generation units and substations, indexed g. It is $\Omega_{DG} \subseteq \Omega_G$.
Ω_N	Set of system buses, indexed n.
Ω_O	Set of conventional investment alternatives indexed o.
Ω_T	Set of demand periods in a year, indexed t.

Input Parameters

γ_D	Investment cost for a DSR scheme $(£/year)$
γ_o	Investment cost for a line upgrade with o $(£/year)$
δ_t	Duration of one period (hours).
π_s	Probability of scenario s occurring.
$\zeta_{t,g}$	Intermittency of g as a percentage of its installed capacity. For $g \in \Omega_G - \Omega_{DG}$ (i.e. substations, and thermal units), it is $\zeta_{t,g} = 1, \forall t$. Otherwise, it is a real number $\in [0,1]$.
Λ	Consumer payments for DSR flexibility $(£/kWh)$.
c	Cost of curtailing DG output $(£/kWh)$.
$d_{s,e,t,n}$	Demand at n, in s, e, t (kW).
D	Table of dimensions $\|\Omega_s\| x \|\Omega_s\|$ where each element is a set, denoted by $D_{s,s'}$, that corresponds to scenarios s, s' and consists of buses n for which $f_{s,n} \neq f_{s',n}$.

$\overline{D}_{t,}$ Max load that can be shifted to t at bus n (kW).

F_l Initial capacity of l (kW).

$f_{s,n}$ Consumer participation in the DSR scheme at s, n. It is equal to the percentage of the load connected to bus n that can be shifted from one period to another.

$I_{n,g}$ Bus-to-generation incidence matrix. Its elements are equal to 1 when g is connected to n. Otherwise, they are equal to zero. For example, in the network of Figure 3.1 it is $I_{1,1} = I_{11,2} = 1$, with all other zero.

k_D Build time for the deployment of the DSR scheme at a bus (epochs).

k_L Build time for conventional upgrade (epochs).

$K_{s,e,g}$ Installed capacity of g at s, e (kW).

$L_{n,l}$ Bus-to-line incidence matrix. Its elements are equal to 1 when n is the receiving bus of l, and -1 when it is the sending bus. Otherwise they are 0. Example values for the network of Figure 3.1 include $L_{11,10} = 1$ and $L_{9,10} = -1$ while $L_{1,2} = 0$.

M Large positive number.

Q_o Capacity corresponding to o (kW).

r_e Cumulative discount factor for investment cost corresponding to e.

τ_e Cumulative discount factor for operational cost corresponding to e.

u_l Sending bus of line l.

v_l Receiving bus of line l.

X_l Reactance for line l (pu).

Decision Variables

a^i Variable $\in \mathbb{R}_+$ used for the approximation of the operational cost.

$\theta_{t,n}$ Voltage angle at t corresponding to bus n (rad). It is $\theta_{t,1} = 0$.

$\lambda^{i}_{s,e,l,o}$	Dual variable $\in \mathbb{R}$ yielded from the operational subproblem for s, e, l, o at Benders iteration i.
$\mu^{i}_{s,e,n}$	Dual variable $\in \mathbb{R}$ yielded from the operational subproblem for s, e, n, at Benders iteration i.
$\omega^{i}_{s,e}$	Objective function of the operational subproblem for s, e at iteration i.
ω^{i}_{s}	Objective function of the operational subproblem for s at iteration i.
Δ_n	Continuous variable representing $\widetilde{D}_{s,e,n}$ in the operational subproblem.
ξ^{I}_{s}	Total investment cost for s.
σ_n	Consumer participation (flexible load) at bus n.
$T_{t,n}$	Variable $\in \mathbb{R}_+$ for load at bus n, shifted to t from another period (kW).
$\Xi_{t,n}$	Variable $\in \mathbb{R}_+$ for load at bus n shifted away from period t (kW).
$\Phi_{l,o}$	Continuous variable representing $\tilde{F}_{s,e,l,o}$ in the operational subproblem.
$B_{s,e,l,o}$	Binary decision to upgrade line l by o at s, e.
$\mathbb{B}_{s,e,l,o}$	Boolean representation for $B_{s,e,l,o}$.
$D_{s,e,n}$	Binary decision to invest in DSR at bus n at s, e.
$\mathbb{D}_{s,e,n}$	Boolean representation for $D_{s,e,n}$.
$\widetilde{D}_{s,e,n}$	Continuous state variable aggregating all investment decisions $D_{s,e,n}$ while considering their corresponding build times.
$\widetilde{\mathbb{D}}_{s,e,n}$	Boolean representation for $\widetilde{D}_{s,e,n}$.
$F_{s,e,l,o}$	Continuous variable for the capacity (on top of the initial capacity) by which line l is upgraded by o at s, e (kW).
$\tilde{F}_{s,e,l,o}$	Continuous state variable aggregating all investment decisions $F_{s,e,l,o}$ while considering their corresponding build times.
$F_{t,l}$	Variable $\in \mathbb{R}$ for the power flow across line l at t (kW).
$P_{t,g}$	Continuous variable $\in \mathbb{R}_+$ for the output of g at t (kW).

$Z_e^{s,s'}$	Continuous variable stating whether or not scenarios s, s' are indistinguishable by the end of epoch e.
$\mathbb{Z}_e^{s,s'}$	Boolean representation for $Z_e^{s,s'}$.
$\aleph_{s,s'}$	Number of elements in the set $D_{s,s'}$

The planning problem is formulated as a mixed integer linear problem, where binary variables are used to denote investment decisions. The planner's objective is to minimize the total expected system cost while having the choice to invest in conventional line reinforcement and /or in DSR (note that at most one DSR investment can be made per bus and a line can be upgraded at most once across each scenario in the sense that one major line upgrade is to be considered).

The mathematical formulation is based on Benders Decomposition, in which the original problem is decomposed into a master problem and several operational subproblems; one per epoch and per scenario. The former problem models investment and approximates operation, while the latter problems solely model the operation of the power system; Figure 3.9 depicts the decomposition procedure. At every iteration of the algorithm the master problem is first solved and the 'trial' investment decisions it yields are passed as inputs onto the operational subproblems that are solved in parallel after the master problem has been solved. In turn, these generate Lagrangian multipliers that are used by the master problem of the subsequent iteration to construct one extra constraint known as the Benders cut; this cut approximates the optimal value of the operation subproblem. As the Benders iteration index increases, more Benders cuts are gradually appended to the master problem. Ultimately, the algorithm converges when the difference between the lower and the upper bounds, to the original problem's objective function, is sufficiently close to zero. The lower bound (3.1) is essentially the objective function of the master problem, while the upper bound (3.2) is equal to the objective function of the original problem. To the knowledge of the author, this is the first application of Benders decomposition in problems with DDU.

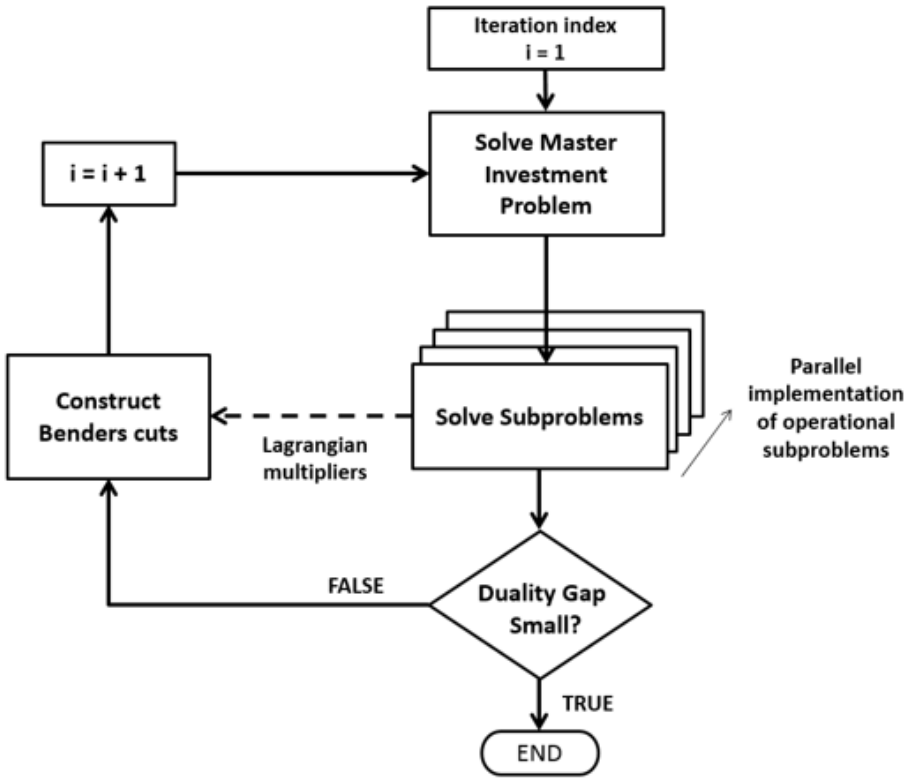


Figure 3.9 Principle of operation of the Benders Decomposition Algorithm (parallel implementation of operational subproblems) for the problem described in section 3.1.1.

$$z_{lower}^{i} = \sum_{s} \pi_s r_e \xi_s^i + a^i \tag{3.1}$$

$$z_{upper}^{i} = \sum_{s} \pi_s r_e \xi_s^i + \sum_{s} \pi_s \omega_s^i \tag{3.2}$$

At each Benders iteration i, the master problem contains all investment-related variables and constraints as follows:

$$\min\left\{\sum_{s} \pi_s r_e \xi_s^I + a^i\right\} \tag{3.3}$$

$$\xi_s^I = \sum_{e}\left(\sum_{l}\sum_{o} B_{s,e,l,o}\gamma_o + \sum_{n} D_{s,e,n}\gamma_D\right) \qquad \forall s \tag{3.4}$$

$$\tilde{F}_{s,e,l,o} = \sum_{z=1}^{e-k_L} F_{s,z,l,o} \qquad \forall s,e,l,o \qquad (3.5)$$

$$\widetilde{D}_{s,e,n} = \sum_{z=1}^{e-k_D} D_{s,z,n} \qquad \forall s,e,n \qquad (3.6)$$

$$F_{s,e,l,o} = Q_o B_{s,e,l,o} \qquad \forall s,e,l,o \qquad (3.7)$$

$$B_{s,1,l,o} = B_{s',1,l,o} \qquad \forall s,s',l,o \qquad (3.8)$$

$$D_{s,1,n} = D_{s',1,n} \qquad \forall s,s',n \qquad (3.9)$$

$$\mathbb{Z}_e^{s,s'} = True \Leftrightarrow \left(\bigwedge_{n \in D_{s,s'}} \neg \widetilde{\mathbb{D}}_{s,e,n} \right) = True \qquad \forall s,s',e \qquad (3.10)$$

$$\mathbb{Z}_e^{s,s'} = True \Leftrightarrow \left\{ \begin{matrix} \mathbb{B}_{s,e+1,l,o} = \mathbb{B}_{s',e+1,l,o} & \forall l,o \\ \mathbb{D}_{s,e+1,n} = \mathbb{D}_{s',e+1,n} & \forall n \end{matrix} \right\} \qquad \begin{matrix} \forall s \neq s' \\ \forall e \end{matrix} \qquad (3.11)$$

$$a^i \geq \sum_s \pi_s \omega_s^{i-1} + \sum_s \sum_e \sum_l \sum_o \pi_s \lambda_{s,e,l,o}^{i-1} \left(\tilde{F}_{s,e,,l,o} - \tilde{F}_{s,e,,l,o}^{i-1} \right) + \sum_s \sum_e \sum_n \pi_s \mu_{s,e,n}^{i-1} (\widetilde{D}_{s,e,n} - \widetilde{D}_{s,e,n}^{i-1}) \qquad (3.12)$$

The objective function (3.3) describes the minimization of the sum of the discounted expected investment cost and the approximation of the total expected operational cost,

denoted by a^i. The total investment cost per scenario is shown in (3.4). Equations (3.5)-(3.6) define the state variables for the investment decisions taking into account the corresponding build-time required until the investment becomes operational. Constraint (3.7) allows the variable $F_{s,e,l,o}$ to take on a value equal to the capacity (kW) of one of the available conventional investment alternatives. Constraints (3.8)-(3.9) constitute the first-epoch non-anticipativity constraints (NACs), which force the first-epoch investment decisions to be identical across all scenarios because of the absence of information that will distinguish s, s'.

Constraints (3.10)-(3.11) are presented using logic symbols as in [48] where $\wedge$ and $\neg$ denote logical conjunction and logical negation respectively. This form, which is frequent in mathematical formulations of problems with DDU, allows for faster comprehension of the essence of the constraint and is especially useful in complicated constraints (see, for example, [53]). Constraint (3.10) states that by epoch e scenarios s, s' are indistinguishable ($\mathbb{Z}_e^{s,s'} = True$) if there has been no DSR deployment ($\neg\widetilde{\mathbb{D}}_{s,e,n} = True$) across any of the buses $n \in D_{s,s'}$. If across s there has been no investment in DSR at some bus $n \in D_{s,s'}$ until and including epoch e, then it is $\widetilde{\mathbb{D}}_{s,e,n} = False$ i.e. $\neg\widetilde{\mathbb{D}}_{s,e,n} = True$. In order to have $Z_e^{s,s'} = True$ it must be $\neg\widetilde{\mathbb{D}}_{s,e,n} = True\ \forall n \in D_{s,s'}$.

Set $D_{s,s'}$ contains those buses where the consumer participation differentiates s, s' i.e. $D_{s,s'} = \{n \in \Omega_N | f_{s,n} \neq f_{s',n}\}$. Obviously, it is $D_{s,s'} = D_{s',s}\ \forall s, s'$. Also $D_{s,s'} \neq \emptyset$ otherwise it should have been $s = s'$ (i.e. it makes no sense to have two separate scenarios that have the same values for $f_{s,n}$ because by default a scenario constitutes a unique trajectory for the values of $f_{s,n}$). Table D, for the case study presented in 3.1.1, is shown in Table 3.6 and is populated by sets $D_{s,s'}$ that are selected according to Table 3.3. For instance, it is $f_{s_1,n} \neq f_{s_4,n}\ for\ n \in \{5,8\}$ i.e. the values for the consumer participation in DSR are different between S1 and S4 for buses 5 and 8. Thus $D_{s_1,s_4} = \{5,8\}$. Note that it would be redundant to have $\bigwedge_{n\in\Omega_n} \neg\widetilde{\mathbb{D}}_{s,e,n}$ in (3.10) because for all $n \in (\Omega_n - D_{s,s'})$ it is $f_{s,n} = f_{s',n}$. Thus, only for $n \in D_{s,s'}$ it is necessary to check if $\neg\widetilde{\mathbb{D}}_{s,e,n} = True$.

Scenarios	S1	S2	S3	S4
S1	-	{8}	{5}	{5,8}
S2	{8}	-	{5,8}	{5}
S3	{5}	{5,8}	-	{8}
S4	{5,8}	{5}	{8}	-

Table 3.6 Table *D* for the case study presented in 3.1.1. Each element of the table contains a set $D_{s,s'}$.

Constraint (3.10) can be expressed in an equivalent linear form, as in (3.13)-(3.14), based on the linear modelling of the multiplication of binary variables [83]. In particular, the product of n binary variables $\prod_1^n d_i$ can be equivalently written using the set of constraints: $0 \leq d \leq d_n \; \forall n$ and $d \geq \sum_n d_i - (n-1)$ where d continuous variable. Similarly, in (3.10) it is $\bigwedge_{n \in D_{s,s'}} (\neg \widetilde{\mathbb{D}}_{s,e,n}) = (\neg \widetilde{\mathbb{D}}_{s,e,1}) \wedge (\neg \widetilde{\mathbb{D}}_{s,e,2}) \wedge \ldots \wedge (\neg \widetilde{\mathbb{D}}_{s,e,n}), n \in D_{s,s'}$ which can be seen as the product $(1 - \widetilde{D}_{s,e,1}) \cdot (1 - \widetilde{D}_{s,e,2}) \cdot \ldots \cdot (1 - \widetilde{D}_{s,e,n}),\ n \in D_{s,s'}$ where each factor $(1 - \widetilde{D}_{s,e,k})$ can take values 0 or 1 i.e. a product of binary variables. Note that $\aleph_{s,s'} = |D_{s,s'}|$ i.e. the number of variables $(1 - \widetilde{D}_{s,e,k})$.

$$Z_e^{s,s'} \leq 1 - \widetilde{D}_{s,e,n} \qquad \begin{matrix} \forall s, s', e \\ \forall n \in D_{s,s'} \end{matrix} \qquad (3.13)$$

$$Z_e^{s,s'} \geq \sum_{n \in D_{s,s'}} \{(1 - \widetilde{D}_{s,e,n})\} - (\aleph_{s,s'} - 1) \qquad \forall s, s', e \qquad (3.14)$$

For example in Figure 3.3 it is $\mathbb{Z}_e^{1,3} = True, \forall e \in \{1..4\}$ and $\mathbb{Z}_1^{2,4} = True$. Further examples follow to demonstrate the computation of $Z_{e^*}^{s_1,s_4}$ and $Z_{e^*}^{s_4,s_1}$ at some epoch e^* given that $D_{s_1,s_4} = \{5,8\}$ (see Table 3.6) i.e. $\aleph_{s_1,s_4} = 2$.

Assuming $\widetilde{D}_{s_1,e^*,5} = \widetilde{D}_{s_1,e^*,8} = 0$, (3.13) yields $\begin{Bmatrix} Z_{e^*}^{s_1,s_4} \leq 1 - 0 \ , for\ n = 5 \\ Z_{e^*}^{s_1,s_4} \leq 1 - 0 \ , for\ n = 8 \end{Bmatrix}$ while (3.14) yields $Z_{e^*}^{s_1,s_4} \geq (1-0) + (1-0) - (2-1) = 1$ i.e. $Z_{e^*}^{s_1,s_4} = 1$ i.e. identical

scenarios. As (3.13)-(3.14) are applied $\forall s, s^{'}$, (3.13) yields $\begin{Bmatrix} Z_{e^*}^{s_4,s_1} \leq 1-0, \text{ for } n=5 \\ Z_{e^*}^{s_4,s_1} \leq 1-0, \text{ for } n=8 \end{Bmatrix}$ while (3.14) yields $Z_{e^*}^{s_4,s_1} \geq (1-0)+(1-0)-(2-1)=1$ (concluding that $Z_{e^*}^{s_4,s_1}=1$) based on the fact that since $\widetilde{D}_{s_1,e^*,5} = \widetilde{D}_{s_1,e^*,8}=0$ it is also $\widetilde{D}_{s_4,e^*,5} = \widetilde{D}_{s_4,e^*,8}=0$ and this is proven as follows: The $\widetilde{D}_{s_1,e^*,5} = \widetilde{D}_{s_1,e^*,8}=0$ is equivalent to $D_{s_1,e^*,5}=D_{s_1,e^*,8}=0$ and $D_{s_1,e^*-1,5}=D_{s_1,e^*-1,8}=0$, …, $D_{s_1,1,5}=D_{s_1,1,8}=0$.

According to (3.9) it is $D_{s_1,1,5}=D_{s_4,1,5}$ and $D_{s_1,1,8}=D_{s_4,1,8}$ for which the master's solution yields zero. So according to (3.10) it is $Z_1^{s_4,s_1}=1$ and according to (3.11) it is $D_{s_1,2,5}=D_{s_4,2,5}$ and $D_{s_1,2,8}=D_{s_4,2,8}$ which are all equal to 0 (this value is optimally decided as a result of the optimization). Then from (3.10) it is $Z_2^{s_4,s_1}=1$. This process continues so that $\widetilde{D}_{s_4,e^*,5} = \widetilde{D}_{s_4,e^*,8}=0$ yielding $Z_{e^*}^{s_1,s_4}=1$.

Assuming $\widetilde{D}_{s_1,e^*,5}=1, \widetilde{D}_{s_1,e^*,8}=0$, (3.13) yields $\begin{Bmatrix} Z_{e^*}^{s_1,s_4} \leq 1-1, for\ n=5 \\ Z_{e^*}^{s_1,s_4} \leq 1-0, for\ n=8 \end{Bmatrix}$ while (3.14) yields $Z_{e^*}^{s_1,s_4} \geq (1-1)+(1-0)-(2-1)=0$ i.e. $Z_{e^*}^{s_1,s_4}=0$ i.e. distinguishable scenarios. As (3.13)-(3.14) are applied $\forall s, s^{'}$, (3.13) yields $\begin{Bmatrix} Z_{e^*}^{s_4,s_1} \leq 1-1 \text{ , for } n=5 \\ Z_{e^*}^{s_4,s_1} \leq 1-0 \text{ , for } n=8 \end{Bmatrix}$ while (3.14) yields $Z_{e^*}^{s_4,s_1} \geq (1-1)+(1-0)-(2-1)=0$ (concluding that $Z_{e^*}^{s_4,s_1}=0$) based on the fact that since $\widetilde{D}_{s_1,e^*,5}=1, \widetilde{D}_{s_1,e^*,8}=0$ it is also $\widetilde{D}_{s_4,e^*,5}=1, \widetilde{D}_{s_4,e^*,8}=0$ and this is proven as follows: The $\widetilde{D}_{s_1,e^*,5}=1, \widetilde{D}_{s_1,e^*,8}=0$ may, without loss of generality, mean $D_{s_1,e^*,5}=1, D_{s_1,e^*,8}=0$ and $D_{s_1,e^*-1,5}=D_{s_1,e^*-1,8}=0$, …, $D_{s_1,1,5}=D_{s_1,1,8}=0$. According to (3.9) it is $D_{s_1,1,5}=D_{s_4,1,5}$ and $D_{s_1,1,8}=D_{s_4,1,8}$ for which the master's solution yields zero. So according to (3.10) it is $Z_1^{s_4,s_1}=1$ and according to (3.11) it is $D_{s_1,2,5}=D_{s_4,2,5}$ and $D_{s_1,2,8}=D_{s_4,2,8}$. This process goes on until $Z_{e^*-1}^{s_4,s_1}=1$ which according to (3.11) gives $D_{s_4,e^*,5}=D_{s_1,e^*,5}$ that are equal to 1 and $D_{s_4,e^*,8}=D_{s_1,e^*,8}$ being equal to 0. Thus $\widetilde{D}_{s_4,e^*,5}=1,\ \widetilde{D}_{s_4,e^*,8}=0$.

The aforementioned examples show that it is $\mathbb{Z}_e^{s,s'}=\mathbb{Z}_e^{s',s}$ which intuitively means that if s, s' are identical then s', s are also identical and vice versa. This fact is guaranteed through (3.13)-(3.14) and this is why no explicit constraint stating $\mathbb{Z}_e^{s,s'}=\mathbb{Z}_e^{s',s}$ is incorporated in the formulation.

Constraint (3.11) represents the conditional non-anticipativity constraints; the equalities on the right-hand side of the equivalence sign are applied on the condition that $\mathbb{Z}_e^{s,s'} = True$. If this condition holds then it means that at the end of epoch e scenarios s, s' are identical and so the investment decisions (that are made at the beginning of epoch $e+1$) for s and s' must be identical to each other. The terminology 'at the end of the epoch' and 'at the beginning of the epoch' is used in every problem exhibiting DDU [48] and is based on that (3.10) suggests that $\mathbb{Z}_e^{s,s'}$ is calculated after $\widetilde{\mathbb{D}}_{s,e,n}$.

If $\mathbb{Z}_e^{s,s'} = False$ then the investment decisions of epoch $e+1$ are not forced to be identical i.e. the NACs do not apply. Constraint (3.11) can be expressed in mixed integer linear form as in (3.15)-(3.16), where $M \geq 1$. In particular, when $Z_e^{s,s'} = 1$ it is $B_{s,e+1,l,o} \geq B_{s',e+1,l,o}$ and $D_{s,e+1,n} \geq D_{s',e+1,n}$ and since (3.11) applies $\forall s, s'$ it must be $B_{s',e+1,l,o} \geq B_{s,e+1,l,o}$ and $D_{s',e+1,n} \geq D_{s,e+1,n}$ given that $Z_e^{s,s'} = Z_e^{s',s}$. Hence, when $Z_e^{s,s'} = 1$ it is $B_{s,e+1,l,o} = B_{s',e+1,l,o}$ and $D_{s,e+1,n} = D_{s',e+1,n}$. Conversely, when $Z_e^{s,s'} = 0$ the constraints become redundant (i.e. they do not affect the feasible region of the problem) allowing $B_{s,e+1,l,o}, B_{s',e+1,l,o}$ and $D_{s,e+1,n}, D_{s',e+1,n}$ to be equal or unequal to each other. Note that since the left-hand side of (3.11) can take the lowest value of $0-1=-1$ and since $Z_e^{s,s'} = 0$ (the two scenarios must have been differentiated for such solutions to be possible) it must be $M \geq 1$. Note that when $B_{s,e+1,l,o} = B_{s',e+1,l,o}$ and $D_{s,e+1,n} = D_{s',e+1,n}$ this does not necessarily mean that $Z_e^{s,s'} = 1$ (two scenarios may be different but at some point involve identical decisions).

Note that different values for M were simulated and the results showed that M has had no effect on the optimal solution presented in 3.1.2. Note also that (3.16) applies $\forall n$ and not only $\forall n \in D_{s,s'}$ as in this case the solution could, for some bus $x \in \Omega_N - D_{s,s'}$ include $D_{1,2,x} = 0,\ D_{2,2,x} = 1, Z_1^{s_1,s_2} = 1$ which cannot hold.

$$B_{s,e+1,l,o} - B_{s',e+1,l,o} \geq -M\left(1 - Z_e^{s,s'}\right) \qquad \begin{matrix}\forall s \neq s', \\ \forall e, l, o\end{matrix} \qquad (3.15)$$

$$D_{s,e+1,n} - D_{s',e+1,n} \geq -M\left(1 - Z_e^{s,s'}\right) \qquad \begin{matrix}\forall s \neq s', \\ \forall e, n\end{matrix} \qquad (3.16)$$

Note that all NACs (3.8)-(3.9) and (3.11) involve investment variables and not operational ones. Applying the NACs to operational variables would be incorrect and this is explained as follows. Assume that in the first epoch a DSR is deployed at a bus $n \in D_{s,s'}$ resulting in $Z_1^{s,s'} = 0$. Hence, the first-epoch operational decisions will be different for s, s' as they are based on $f_{s,n}$ (amount of load shifted to another period). By not applying the NACs to operational variables these variables do not couple any pair of scenarios s, s', thereby allowing for parallel implementation of the operational subproblems.

Finally, (3.12) represents the Benders cut where α^i is the estimate of the total expected operational cost at iteration i. In the right-hand-side of the inequality the first term $\sum_s \pi_s \omega_s^{i-1}$ is the total expected operational cost corresponding to iteration $i-1$ and $\omega_s^{i-1} = \sum_e \omega_{s,e}^{i-1} \ \forall\ s$ where $\omega_{s,e}^i$ is the objective value yielded by each operational subproblem as in (3.17). The second and third terms in the right hand side of (3.12) incorporate the information about the impact that the change (between iterations i and $i-1$) in the investment decisions has on the operational cost.

The formulation for the operational subproblem corresponding to Benders iteration i with scenario s and epoch e as inputs follows.

$$\omega_{s,e}^i = min\left\{\sum_t \sum_{g^*} \tau_e\ \delta_t c(K_{s,e,g^*}\zeta_{t,g^*} - P_{t,g^*}) + \sum_t \sum_n \tau_e\ \delta_t \Xi_{t,n}\Lambda\right\} \tag{3.17}$$

$$T_{t,n} \leq \Delta_n \overline{D}_{t,n} \qquad \forall t, n \qquad (3.18)$$

$$\Xi_{t,n} \leq \Delta_n f_{s,n} d_{s,e,t,n} \qquad \forall t, n \qquad (3.19)$$

$$\sum_t (T_{t,n} - \Xi_{t,n}) = 0 \qquad \forall n \qquad (3.20)$$

$$P_{t,g} \leq K_{s,e,g}\zeta_{t,g} \qquad \forall t, g \qquad (3.21)$$

$$F_{t,l} = \frac{\theta_{t,u_l} - \theta_{t,v_l}}{X_l} \qquad \forall t, l \qquad (3.22)$$

$$|F_{t,l}| \leq F_l + \sum_o \Phi_{l,o} \qquad \forall t, l \qquad (3.23)$$

$$\sum_g P_{t,g} I_{n,g} + \sum_l F_{t,l} L_{n,l} = d_{s,e,t,n} + T_{t,n} - \Xi_{t,n} \qquad \forall t, n \qquad (3.24)$$

$$\Delta_n = \widetilde{D}^i_{s,e,n} : \mu^i_{s,e,n} \qquad \forall n \qquad (3.25)$$

$$\Phi_{l,o} = \tilde{F}^i_{s,e,l,o} : \lambda^i_{s,e,l,o} \qquad \forall l, o \qquad (3.26)$$

According to (3.17) the objective function is equal to the sum of the discounted cost of curtailment of the output of the renewable DG unit and that of the payments to consumers who participate in the DSR scheme. Note that in (3.3) and (3.17) cumulative discount factors are used as the costs are expressed per annum. For example, when a DSR unit is deployed at a certain epoch its annual cost needs to be paid until the end of the horizon. Summing these discounted annual investment costs leads to the calculation of the total investment cost corresponding to the investment decision. This discount factor is expressed as in (3.27), where k is the number of years per epoch (e.g. in the problems presented in this chapter it is $k = 2$) and $|\Omega_E|$ is the number of epochs. Thus $k \cdot |\Omega_E|$ is the number of years in the horizon, $k \cdot e$ is the year at which the investment decision is made and r is annual the interest rate. For example, assume that an investment decision is made in the third epoch ($e = 3$) of a six-epoch horizon ($i.e. |\Omega_E| = 6$ meaning that there are $k \cdot |\Omega_E|$ =12 years in the horizon, from year 0 to year 11), then $r_e = \frac{1}{(r+1)^4} + \cdots + \frac{1}{(1+r)^{11}}$, with r=5% yields 5.58.

That is, the first epoch consists of years 0 (currently) and 1, the second epoch consists of years 2 and 3, so on.

$$r_e = \sum_{i=k\cdot e}^{k|\Omega_E|-1} \frac{1}{(r+1)^{i-k}} \qquad \forall e \qquad (3.27)$$

Regarding the operational costs, the cumulative discounting factor is defined by (3.28) accounting for the fact that payments corresponding to epoch e are paid for all years that make up the epoch. For example $\tau_1 = \frac{1}{(1+r)^0} + \frac{1}{(1+r)^1}$, and with $r = 0.05$ it yields 1.95.

$$\tau_e = \sum_{i=k\cdot e}^{ke+1} \frac{1}{(r+1)^{i-k}} \qquad \forall e \qquad (3.28)$$

Constraints (3.18), (3.19) and (3.20) model the operation of all deployed DSR schemes. In particular, (3.18) sets $\overline{D}_{t,n}$ as the upper bound for the load that can connect to bus n at t, provided that a DSR has been deployed at this bus ($\Delta_n = 1$). This upper bound can be any large positive value. According to (3.19), the maximum load that can disconnect from bus n at t is equal to $f_{s,n} d_{s,e,t,n}$. Energy equality (3.20) ensures that the entire flexible load is eventually served within 24 hours (i.e. no load is lost in the rescheduling process).

According to (3.21) and when g refers to the substation (in this case it is $\zeta_{t,g} = 1, \forall t$), it is ensured that the power drawn from the grid is within the limits of the transformer, whereas when g refers to a renewable DG unit, (3.21) states that the maximum output of the unit is defined in terms of its installed capacity and resource variability as dictated by parameter $\zeta_{t,g}$. Constraint (3.22) defines the power flows according to the DC power flow model. Note that the developed DDU methodology can be readily applicable to nonlinear AC power flow problems at the expense of greater complexity. Constraint (3.23) states that power flows are bounded by the line's thermal rating. In addition, (3.24) imposes system energy balance while considering actions from DSR assets: The active power flows coming into a bus are equal to those coming out of the bus, at every period. Finally, in (3.25)-(3.26), the output of the master problem informs the corresponding variables in the operational subproblem; Lagrangian multipliers are obtained from these constraints and are

used to construct the Benders cut to be applied to the next iteration. Note that the value of these multipliers is negative (to indicate a reduction in the objective value of the operational subproblem) or zero.

3.1.4 *Solution Methodology*

In the classic version of Benders Decomposition (CBD) parallel implementation may not have been so easy to apply due to hardware restrictions in terms of computer processor capabilities. Most likely, there were also memory restrictions as well. In this case, every iteration of CBD would involve sequential execution of all operational subproblems.

In this paragraph, a modification of Benders algorithm has been developed taking advantage of the unique elements of the formulation of DDU problems. Such problems have a scenario-variable formulation, giving rise to a large number of subproblems, while at each Benders iteration it is highly likely that the same investment decisions apply to multiple subproblems that correspond to the same epoch. As such, it is possible to screen the investment decisions and determine which subproblems are equivalent and do not warrant separate solution, selecting to only solve those that add new information. This screening is performed via Intelligent Filtering Implementation (IFI), which is an algorithm that is embedded in Benders and is executed immediately after the master problem of iteration i has been solved. Without including the IFI in the formulation, the total number of operational subproblems to be solved per iteration is equal to $|\Omega_S||\Omega_E|$. Under IFI, a subset of $|\Omega_S||\Omega_E|$ is executed per iteration and the number of elements of this subset is determined after the master problem has been solved (i.e. this number is not fixed for all iterations but can vary). The IFI algorithm corresponding to a single Benders iteration and applying to four scenarios, as in 3.1.2, is presented in 13 steps as follows.

Step 1.	Solve master problem for iteration $\boldsymbol{i}$ and store the values for $\boldsymbol{Z_e^{s,s'}}$.
Step 2.	Define set $K_1 = \{(s,e)\mid s = s_1,\ \forall e \in \Omega_E\}$.
Step 3.	Store all operational subproblems corresponding to $(s,e) \in K_1$ in set $\mathbb{P}$.

Step 4.	Define set $K_2 = \{(\mathrm{s},\mathrm{e})|\ \mathrm{s} = \mathrm{s}_2,\ \forall \mathrm{e} \in \Omega_\mathrm{E}:\ \mathrm{Z}_\mathrm{e}^{s_2,s_1} = 0\}$.
Step 5.	Store all operational subproblems corresponding to $(\mathrm{s},\mathrm{e}) \in \mathrm{K}_2$ in set $\mathbb{P}$.
Step 6.	Define set $\mathrm{K}_3 = \{(\mathrm{s},\mathrm{e})|\mathrm{s} = \mathrm{s}_3,\ \forall \mathrm{e} \in \Omega_\mathrm{E}: \mathrm{Z}_\mathrm{e}^{s_3,s_1} = \mathrm{Z}_\mathrm{e}^{s_3,s_2} = 0\}$.
Step 7.	Store all operational subproblems corresponding to $(\mathrm{s},\mathrm{e}) \in \mathrm{K}_3$ in set $\mathbb{P}$.
Step 8.	Define set $\mathrm{K}_4 = \{(\mathrm{s},\mathrm{e})|\mathrm{s} = \mathrm{s}_4,\ \forall \mathrm{e} \in \Omega_\mathrm{E}: \mathrm{Z}_\mathrm{e}^{s_4,s_1} = \mathrm{Z}_\mathrm{e}^{s_4,s_2} = \mathrm{Z}_\mathrm{e}^{s_4,s_3} = 0\}$.
Step 9.	Store all operational subproblems corresponding to $(\mathrm{s},\mathrm{e}) \in \mathrm{K}_4$ in set $\mathbb{P}$.
Step 10.	Solve all operational subproblems in set $\mathbb{P}$, in parallel and store their solution.
Step 11.	For each operational subproblem corresponding to (s_k, e) that was not called: equalize its corresponding costs and dual variables to those of a problem solved (denoted by (s_m, e)) for which $Z_e^{s_k,s_m} = 1$.
Step 12.	Benders iteration i ends. If the algorithm converged then go to Step 13. Otherwise Benders iteration $i + 1$ begins and go to Step 1.
Step 13.	End.

Steps 2-3 guarantee solution of <u>all operational subproblems corresponding to the first scenario without any conditions</u>. Whereas steps 4-5, 6-7 and 8-9 guarantee that only those subproblems that correspond to distinguishable scenarios will be solved; there is no value in solving subproblems $(s_i, e), (s_j, e),\ \forall i, j \in \Omega_S$ for which s_i, s_j have not been distinguished. An example for five epochs is presented. In particular, after the master problem has been solved and the $Z_e^{s,s'}\ \forall (s, s') \in \Omega_s, \forall e \in \Omega_E$ have become known, the subproblems corresponding to $(s, e) \in K_1 = \{(s_1, e_1), (s_1, e_2), (s_1, e_3), (s_1, e_4), (s_1, e_5)\}$ are placed in set $\mathbb{P}$.

Regarding the operational subproblems corresponding to s_2 assume that the master's solution yields $\mathrm{Z}_{\mathrm{e}_1}^{s_2,s_1} = 1$ i.e. s_1, s_2 involve identical investment decisions and, therefore, correspond to identical resolution of uncertainty (value for consumer participation) meaning that the operational decisions for subproblems $(s_1, e_1), (s_2, e_1)$ are also identical; this is

because with identical investments and consumer participation the operation of all DSR schemes will be identical (load rescheduling) as well as the generation outputs and the power flows. For this reason, the subproblem corresponding to (s_2, e_1) is not called and the dual variables as well as the corresponding costs are equalized to those of (s_1, e_1), which is called, as follows:

- $Cost_{s_2,e_1} = Cost_{s_1,e_1}$, for each operational cost; namely wind curtailment cost and DSR operational cost. This equality is required for the estimation of $\omega^i_{s,e}\ \forall s, e$ used in (3.12) where $\omega^i_s = \sum_e \omega^i_{s,e}$.

- $\lambda^i_{s_2,e_1,l,o} = \lambda^i_{s_1,e_1,l,o}\ \forall l, o$. This equality is required as these dual variables are used in (3.12).

- $\mu^i_{s_2,e_1,n} = \mu^i_{s_1,e_1,n} \cdot \frac{f_{s_2,e_1}}{f_{s_1,e_1}}\ ,\quad \forall n$. This division takes place so that the effect of f_{s_1,e_1} is removed from $\mu^i_{s_1,e_1,n}$ and that of f_{s_2,e_1} is added (see constraints (3.19) and (3.25)). Obviously for buses that do not involve any uncertainty (i.e. buses other than 5 or 8, referring to paragraph 3.1.1) it is $\frac{f_{s_2,e_1}}{f_{s_1,e_1}} = 1$.

However, if $\mathrm{Z}_{\mathrm{e}_1}^{s_2,s_1} = 0$ then the subproblem corresponding to (s_2, e_1) is stored in set $\mathbb{P}$. This logic applies to all remaining subproblems (i.e. for $e_2, \dots, e_5$) corresponding to s_2.

Regarding the operational subproblems corresponding to s_3, if the master's solution has yielded $\mathrm{Z}_{\mathrm{e}_1}^{s_3,s_1} = 1\ or\ \mathrm{Z}_{\mathrm{e}}^{s_3,s_2} = 1$ (or both) then it means that the operational subproblem (s_3, e_1) does not need to be solved since another that is identical to it will. The subproblem corresponding to (s_3, e_1) will only be solved if $\mathrm{Z}_{\mathrm{e}_1}^{s_3,s_1} = \mathrm{Z}_{\mathrm{e}}^{s_3,s_2} = 0$. A similar logic applies to operational subproblems corresponding to scenario s_4.

Table 3.7 displays the performance of various solution methodologies, all of which give the output presented in Figure 3.3; one year is represented with 8760 hourly periods i.e.$|\ \Omega_T| = 8760, \delta_t = 1$ according to the nomenclature of section 3.1.3. Regarding performance metrics, observe that IFI converges 83% faster than the CBD due to parallel implementation of operational subproblems as well as the inner mechanics of the algorithm that require 35% fewer subproblems are called.

Note that constraint (3.12) suggests that one extra cut is formed per iteration and appended to the set of existing cuts that includes all cuts appended from the first iteration

until the current one. This applies to both IFI and CBD. However, just one extra cut per iteration may not bring enough amount of information (from the operational subproblems to the master) for the algorithm to converge fast. It follows that a greater amount of information may lead to more accurate investments per iteration, thereby reducing solution times significantly. This is achieved with a '*multicut'* version of the algorithm (symbolized as IFI_s and CBD_s in Table 3.7) in which $|\Omega_S|$ number of Benders cuts are appended to the set of existing cuts per iteration. This multicut modelling is achieved by replacing (3.12) with (3.29). In this case, (3.1) and (3.3) are replaced by (3.30) and (3.31) respectively. This denser gradient information results in IFI_s achieving 75% improvement in solution times and 81% reduction in the number of operational subproblems solved (and Benders iterations) when compared to IFI.

$$a_s^i \geq \pi_s \omega_s^{i-1} + \sum_e \sum_l \sum_o \pi_s \lambda_{s,e,l,o}^{i-1} \left(\tilde{F}_{s,e,,l,o} - \tilde{F}_{s,e,,l,o}^{i-1}\right) + \sum_e \sum_n \pi_s \mu_{s,e,n}^{i-1} (\tilde{D}_{s,e,n} - \tilde{D}_{s,e,n}^{i-1}) \qquad \forall s \qquad (3.29)$$

$$z_{lower}^i = \sum_s \pi_s r_e \xi_s^i + a_s^i \qquad (3.30)$$

$$\min \sum_s (\pi_s r_e \xi_s^i + a_s^i) \qquad (3.31)$$

It is important to note that the total number of operational subproblems is $|\Omega_\text{S}||\Omega_\text{E}|$, and this applies to all decomposition methods (CBD,CBD_s, IFI and IFI_s). At each iteration, each operational subproblem that is solved sends a dual variable (e.g. $\lambda_{s,e,l,o}$) to the master problem with the difference between IFI and IFI_s being in how this information applies to master: for all scenarios together (IFI), or for each scenario separately (IFI_s).

Note also the difference in performance between the decomposed versions and the nondecomposed version of the problem. There is an impressive reduction in memory consumption achieved through decomposition that can be attributed to the fact that the operational variables of the nondecomposed problem are four-dimensional as in $P_{s,e,t,l}$ as

opposed to two-dimensional (e.g. $P_{t,l}$). In particular, IFI_S is around 93% faster than ND and achieves 75% smaller memory consumption.

	Benders iterations	**Operational subproblems solved**	**Solution time**	**Average memory consumption**
IFI	142	1828	35 min	~7.5 GB
CBD	142	2840	3 hours & 20 minutes	~7.5 GB
CBD_S	27	540	45 min	~7.5 GB
ND	-	-	2 hours and 10 minutes	~35 GB
IFI_S	27	364	9 min	~7.5 GB

Table 3.7 Comparison of IFI, CBD, CBD_S, ND and IFI_S solution methodologies, all of which yield the same output as the one depicted in Figure 3.3. The IFI and CBD stand for 'Intelligent Filtering Implementation' and 'Classic Benders Decomposition' variations of Benders decomposition algorithm. The ND stands for the 'nondecomposed' problem, while IFI_S and CBD_S refer to the *multicut* versions of the corresponding algorithms. Note that "average memory consumption" refers to the average GB of RAM consumed from the beginning until the end of the execution of the optimization study. The symbol ~ reads 'approximately' in order to account for the inner mechanics of the memory allocation process.

3.2 *Immediate & Global DDU resolution*

In this section a case study is presented that applies to a distribution network that undergoes load and DG capacity growth over a ten-year horizon. In order to accommodate the resulting rising power flows the planner has the possibility to invest in conventionally upgrading lines and / or investing in DSR technology. However, the way by which optimal investment decisions will be made is not straightforward due to uncertainty. In particular, the source of uncertainty, which is the level of consumer participation in DSR, is of decision-dependent or endogenous type (i.e. does not resolve with the passage of time but requires action taken from the planner) and resolves immediately (i.e. at the same epoch when the investment is made) and globally (i.e. not only at the bus where the corresponding investment is made but across the system). The results show that the deployment of DSR in the system allows not only for accommodating the rising power flows but also for generating significant cost savings while emphasizing the importance of investing in DSR as

early as possible or otherwise costs are higher. This happens because by investing in DSR early, uncertainty resolves early thereby resulting in future investment decisions that are targeted to the realized system state i.e. stranding risk is minimized.

Conducting the studies involves modelling the problem in a stochastic optimization programming formulation and using various Benders decomposition techniques (e.g. multicut, monocut, sequential, parallel along with the novel Intelligent Filtering implementation) and relevant comparisons are made. Finally, the methodology for obtaining the option value of DSR under decision dependent uncertainty is presented with relevant insights and explanations being provided.

3.2.1 *Problem description*

The distribution network shown in Figure 3.1 is studied across five two-year epochs with input data as in Table 3.1, Table 3.2, Table 3.4, Figure 2.3 and Figure 2.4. The new elements in this section relate to the characterization of the resolution of uncertainty i.e. Table 3.3 no longer applies in this case study and it is replaced by Table 3.8 as described below.

In this case study all candidate DSR locations (i.e. all load-buses: 2, 4, 5, 7, 8 and 10) are characterized by uncertainty around the consumer participation level in the DSR scheme. The first decision that the planner can make is whether or not to deploy a DSR pilot scheme at a predetermined location (bus n^*). There is only one such predetermined location and this has been arbitrarily selected to be bus $n^* = 8$. If the planner decides to proceed with this deployment, then the pilot DSR scheme must be operated for the entire epoch before the uncertain consumer participation is resolved at n^* according to the possible customer participation scenarios, depicted in Table 3.8. That is, the responsiveness of the consumers to the DSR scheme deployed at n^* will be measured for an entire epoch before extracting the final average value (uncertainty resolution). After resolution, the value will apply to all other system buses (i.e. *globally* across the system). In other words it has been assumed that the eventual participation level in the pilot scheme is a perfect predictor of the willingness of the consumers to participate in the DSR scheme in the other parts of the system. Note that if the planner decides not to invest in the pilot scheme at n^* then this will be equivalent to

0% consumer participation and , subsequently, no DSR will subsequently be deployed anywhere else in the system as the consumers will not have gained the confidence to participate in the scheme; hence, they will have no interest in supporting it.

Notice that this is a type of *decision-dependent uncertainty* because uncertainty can be resolved only after an investment in DSR (at n^*) has been made and not by the simple passage of time (as it is the case in the type of exogenous uncertainty). In addition, the uncertainty resolution is *immediate* because within one epoch all uncertainty has been resolved and it is *global* because the uncertainty resolves across the entire system.

Scenarios	Consumer participation	Scenario Probability
Scenario S1	35%	49%
Scenario S2	20%	21%
Scenario S3	5%	21%
Scenario S4	2.5%	9%

Table 3.8 Scenarios for the consumer participation in DSR.

3.2.2 *Results of the optimization studies*

Figure 3.2 displays the optimal investment strategy if only the conventional technology is available to the planner. Since, in the absence of DSR in the system, the input data are identical between the two studies, the two figures are the same. However, this is no longer the case once DSR technology is also considered. Figure 3.10 shows the optimal investment strategy for a planner who has both the DSR and the conventional technologies available for investment. Note that the availability of DSR allows for a fundamentally different investment approach. In particular, not only does this figure radically differ in branching from Figure 3.2, but the entire investment philosophy has changed with the most remarkable change being that the first-epoch conventional investments have been replaced by a first-epoch smart-technology investment. The resulting total expected system cost is £1.087m where the investment component stands at £1.074 m and £13k is the wind curtailment cost.

The DSR scheme has two functions. The first is the uncertainty resolution, which allows for conditional investment, and the second is load shifting that prevents exceeding line thermal limits and leading toconventional investment deferral.

In terms of uncertainty resolution, as shown in Figure 3.10, the planner decides to deploy DSR at bus 8 (pilot scheme) from the very first epoch, aimed at resolving the uncertainty around customer participation level. This DSR scheme operates for the entire first epoch, at the end of which the uncertainty resolves at all buses i.e. *globally*. Subsequently, if 35% consumer participation is observed at bus 8, then no further investment is required until the last epoch where a DSR at bus 5 is deployed. This largely is the case for scenario S2 as well, which also warrants a DSR investment in the third and fifth epochs. However, in the event of lower consumer participation, the need for additional investment becomes binding. In both scenarios S3 and S4, characterized by 5% and 2.5% participation respectively, three line upgrades in the second epoch (lines 1-2, 2-3 and 3-5) as well as two additional upgrades (5-6 and 6-8) in the fourth epoch are required to accommodate load growth at least cost; since the consumer confidence is low, no DSR investment takes place across these two scenarios for the remaining study horizon. This optimal strategy suggests that it is worth pursuing the investment in DSR *as early as possible* even though there is some probability (corresponding to S3 and S4) that consumers will be very little (2.5% and 5% participation) willing to participate. This early investment will allow for making future investments on a conditional basis depending on how uncertainty resolves thereby achieving minimum cost.

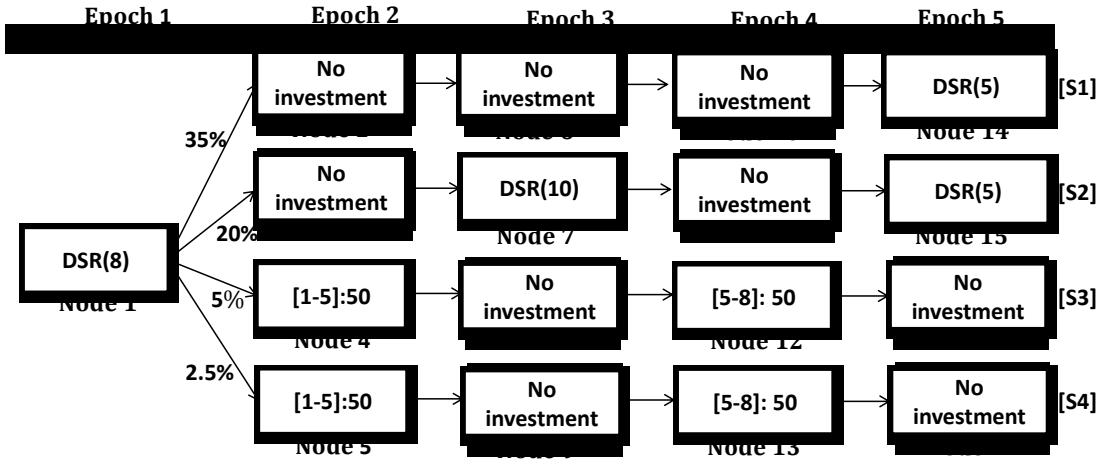


Figure 3.10 Optimal investment strategy for a network planner with two investment technologies available: DSR and conventional reinforcement. The DSR(X) means that the decision to invest in DSR at bus X is made. Note that the DSR becomes operational at the same

epoch at which the decision to invest in it is made. The [x-y]: 50 means that the decision is taken to reinforce the lines between buses x and y by 50 kW each. The numbers above the arcs correspond to the consumer participation that is revealed. For example 20% means that this participation level applies to all buses that can accommodate a DSR (ie buses 2,4,5,7,8,10) and, hense, to buses5, 8, 10 (see scenario S2).

Regarding the load shifting operation performed by deployed DSR schemes, this is done for the same reasons as the ones explained in paragraph 3.1.2 i.e. disconnecting load at times of very low availability of wind resource and very high demand. In such periods the DG-wind unit has insignificant output resulting in the system demand being mostly satisfied through imports from the substation causing increased power flows through the lines of the main feeder (eg 1-2, 2-3, 3-5, 5-6, 6-8). For instance at node 15 all DSR schemes are needed in the system and at each bus the consumer participation is 20% allowing for accommodation of the power flows along the aforementioned lines. Figure 3.11 and Figure 3.12 show the operation of DSR schemes (bus 8 and 5 respectively for node 14) over 24 hours with the goal of accommodating the increased power flows through the lines of the main feeder (Figure 3.13shows the effect that the combined operation of these DSR schemes has on the power flows through line 3-5). It can be seen that during periods when the DG-wind unit output is low (see the dotted line that corresponds to the right axis), line 3-5 becomes overloaded in the absence of the DSRschemes that are present in node 11 (seeFigure 3.13) thereby requiring disconnection of flexible load from the aforementioned buses (5,8). This load is connected during hours when the DG-wind unit output is high (or when the load in the system is low) because during these periods the problematic lines (such as 3-5) are not overloaded because much of the system load is fed by the DG output and so less power is imported via the substation. Similar operation takes place throughout the year.

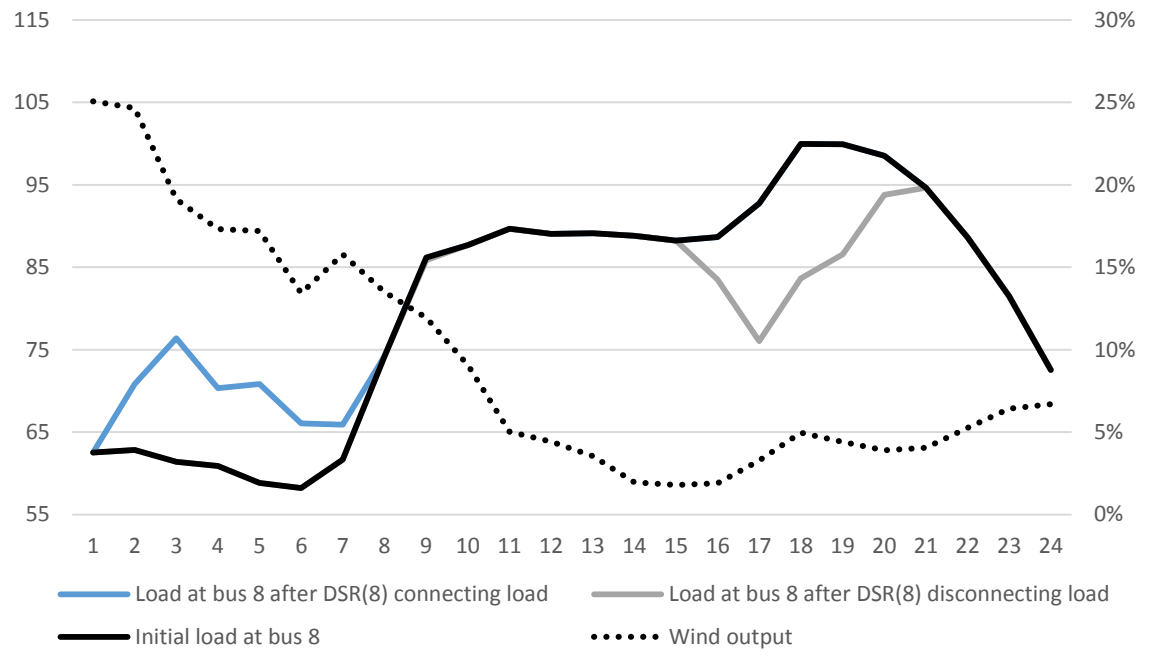


Figure 3.11. Load shifting operation by the DSR scheme at bus 8 (referring to node 14, Figure 3.10) over 24 hours, where load is disconnected during periods of low wind output, and is then connected back (so that no load is lost) during periods of high wind output thereby avoiding / deferring conventional reinforcement of the lines of the main feeder. The dotted line corresponds to the right axis while the others correspond to the left axis. Note that power flows follow the DCOPF model.

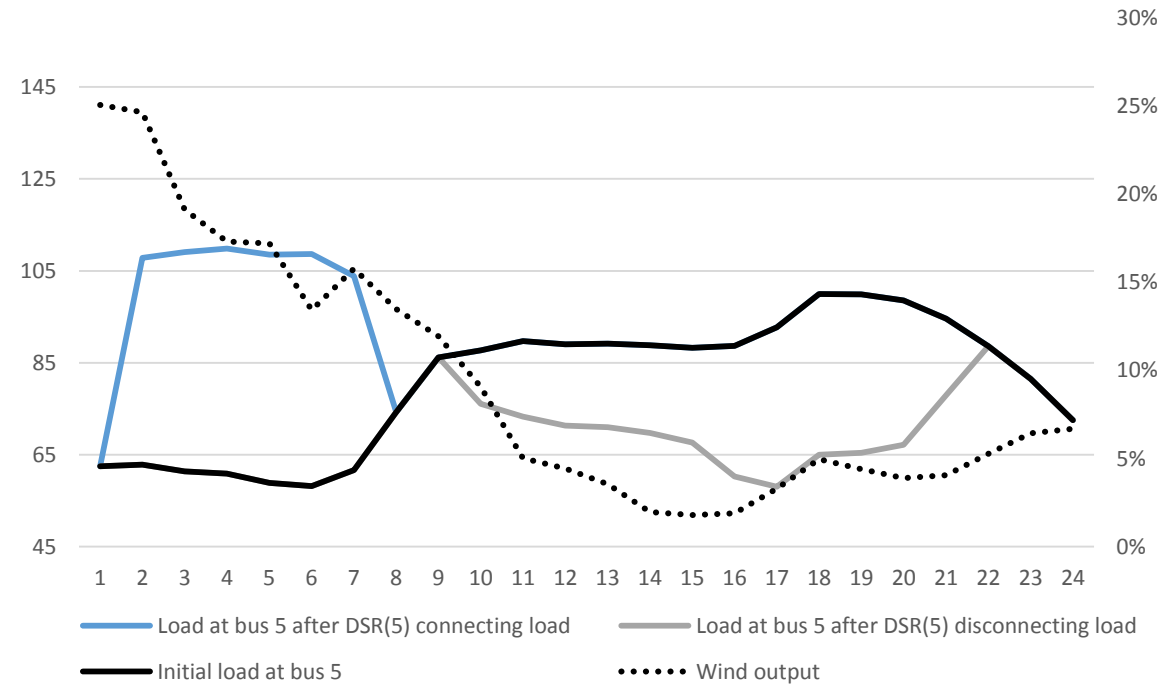


Figure 3.12. Load shifting operation by the DSR scheme at bus 5 (referring to node 14, Figure 3.10) over 24 hours, where load is disconnected during periods of low wind output, and is then

connected back (so that no load is lost) during periods of high wind output thereby avoiding / deferring conventional reinforcement of the lines of the main feeder. The dotted line corresponds to the right axis while the others correspond to the left axis. Note that power flows follow the DCOPF model.

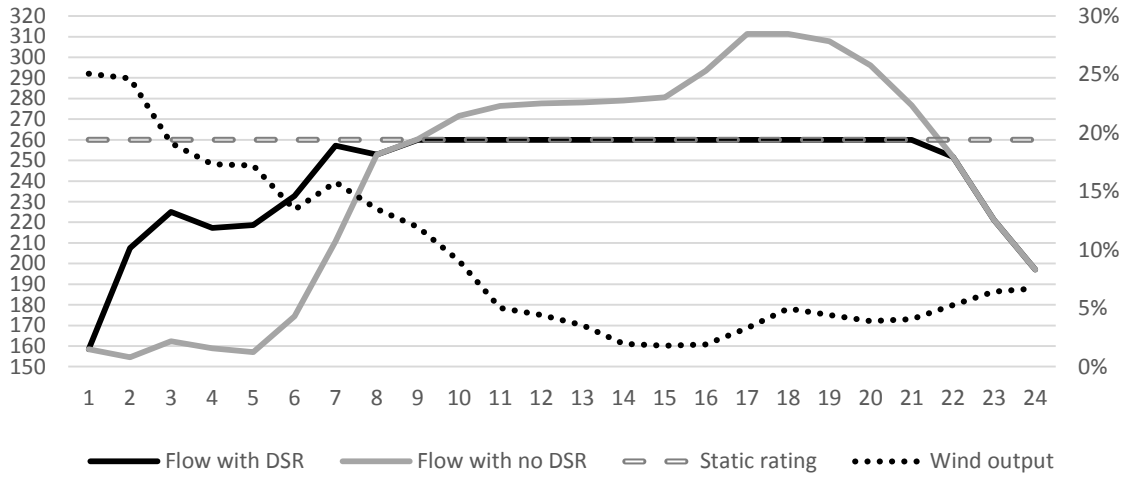


Figure 3.13. Power flow pattern through line 3-5 (referring to node 14, Figure 3.10) over 24 hours, before and after the combined operation of the DSR schemes connected to buses 5 and 8 (see the previous two figures). The dotted line corresponds to the right axis while the others correspond to the left axis. Note that power flows follow the DCOPF model.

The option value [11] of investing in the DSR technology under DDU is equal to the difference in the total expected system cost in the resulting strategies where the DSR is available (Figure 3.10) and where it is not (Figure 3.2). This difference can be calculated at £3.6m - £1.07m= £2.53m representing the total economic benefit, including investment deferral and uncertainty resolution that the ability to deploy DSR offers.

Regarding Figure 3.10, it is important to emphasize that all of the DSR schemes perform load-shifting operations not only in the epoch at which they are deployed but also in all subsequent epochs across the corresponding scenario. However, there is one exception; namely the first-epoch DSR at bus 8. In particular, as in the case of local DDU resolution, the system is unconstrained in the first epoch because load growth takes place from the second epoch onwards. Thus, the pilot scheme is deployed early solely for the purpose of resolving uncertainty around customer participation. By doing so, the subsequent investments can be made conditionally on the learning obtained regarding consumer participation, leading to substantial cost savings. As explained in paragraph 3.1.2, this first-

epoch DSR scheme's operation is not aimed at accommodating the power flows (after all, these are safely accommodated) but at the uncertainty resolution which can happen by observing customer participation levels in the pilot DSR scheme. In other words, this pilot DSR scheme will be designed so that at the end of which realistic conclusions can be extracted about actual consumer participation levels in this novel technology. It is assumed here that setting up this pilot scheme has the same investment cost as setting up any other DSR scheme in the system and that the uncertainty can be resolved by asking consumers to allow control of their flexible load (despite no need from the system perspective may exist in reality).

In order to comprehend the importance of such an investment, a further optimization study is carried out in which the planner can consider both technologies (DSR and conventional reinforcement) in all epochs except for the first one, when only the conventional technology is considered. The results indicate that if this early DSR investment is not possible to undertake then, according to Figure 3.14, the resultant strategy involves second-epoch investment decisions in DSR and three line upgrades; all these investments are made *unconditionally* as in the beginning of the second epoch the uncertainty has not been resolved thereby leading to all scenarios being identical to each other.

As a result, the total expected system cost amounts to £1.931 m (with £1.918m being the investment component and £13k the wind curtailment cost) which equates to a rise of around 80% comparing to the cost of the investment strategy depicted in Figure 3.10. The fact that these second-epoch conventional investments are made unconditionally is the sole reason for this significant growth in cost. Notice that in Figure 3.10 the three line upgrades are made conditionally only for scenarios S3 and S4 rather than for all four scenarios. In addition, notice the similarities that S3 and S4 have when compared between Figure 3.10 and Figure 3.14 and the effect that the second-epoch conventional investments in Figure 3.14 have on the investments across scenarios S1 and S2;while these two scenarios are dominated by DSR investments in Figure 3.10 this is no longer the case in Figure 3.14 as the increased power flows are taken care of by the upgraded lines. As a result, the absence of the first-epoch DSR investment leads to far fewer DSR investments across the system and significantly increased costs.

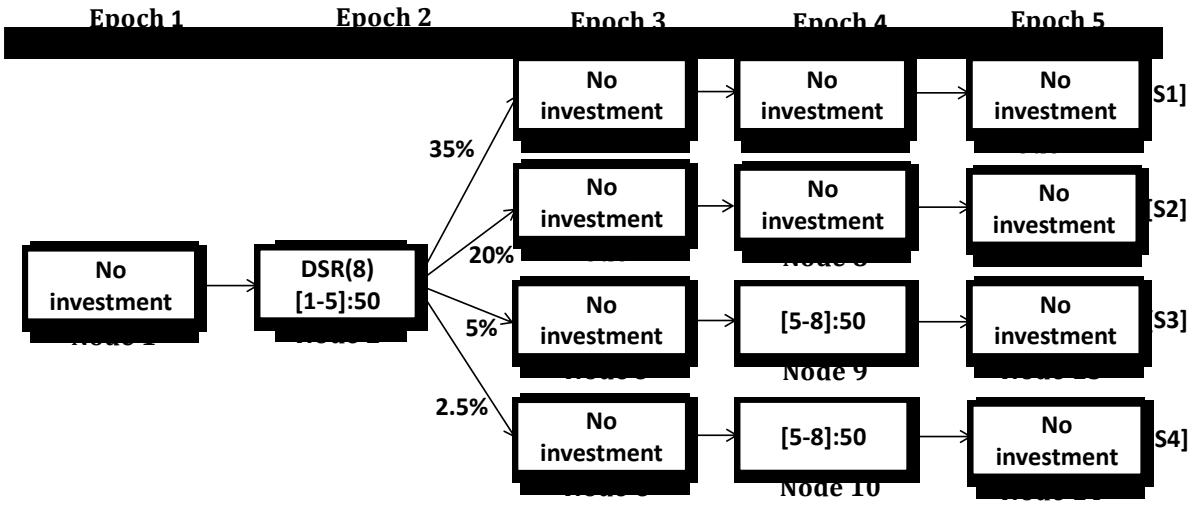


Figure 3.14 Optimal strategy for a planner with two technologies available: DSR and conventional line upgrade. The planner does not have the possibility to invest in DSR in the first epoch, but has this possibility in all other epochs. The percentage values correspond to the values for the consumer participation at buses 5 and 8 respectively.

3.2.3 *Mathematical Formulation*

A DSR scheme deployed at bus $n^* \in \Omega_N$ is a pilot scheme with the objective to measure the participation of the consumers in the DSR scheme. It is assumed that after the scheme has operated for the duration of one epoch, the consumer participation observed at n^* will apply to all buses across the system (*globally*) rather than only at n^* (*locally*). The problem formulation is decomposed, via Benders, into a master subproblem and many operational subproblems. The formulation for the operational subproblems consists of (3.17)-(3.26) except for (3.19), which is replaced by (3.32)-(3.33), where the decision variable σ_n represents the consumer participation in DSR at bus n.

In particular, inequality (3.32) sets the upper limit for the flexible load that can be shifted from period t to a different period within 24 hours. This upper limit is equal to the consumer participation at n multiplied by the current level of demand. Then, (3.33) states that if a DSR scheme is deployed at n (i. e. $\Delta_n = 1$) then the consumer participation at n is equal to that in n^* (i.e to f_{s,n^*}) provided that a pilot scheme was deployed by the previous epoch. The latter is catered for by including in the master problem, which for this case also consists of (3.3)-(3.12), the additional constraint (3.34) stating that if a pilot scheme has not

been deployed by epoch $e-1$ it is impossible to deploy a DSR at e at any bus across the system (equivalently there will be no support among the consumers in favor of DSR).

$$\Xi_{t,n} \leq \sigma_n d_{s,e,t,n} \qquad \forall t,n \qquad (3.32)$$

$$\sigma_n = \Delta_n f_{s,n^*} \qquad \forall n \qquad (3.33)$$

$$D_{s,e,n} \leq \widetilde{D}_{s,e-1,n^*} \qquad \forall s,e,n \qquad (3.34)$$

3.2.4 ***Solution Methodology***

Table 3.9 displays the performance of various solution methodologies, all of which give the output presented in Figure 3.10; it is $\delta_t = 1$ hour and $|\Omega_T| = 8760$ hours (duration of a year). The first obvious advantage of decomposition relates to reduced memory consumption; an improvement of 75% can be witnessed. Another remarkable observation has to do with the superior advantage of IFI_s over all other solution methodologies in terms of solution times. When compared to ND this improvement amounts to 95% and it is around 100% when compared to IFI or CBD reflecting how great an effect the number of cuts generated per iteration and the call-implementation (whether the operational subproblems are called in a sequential or parallel manner) have on solution times. Note that both IFI and CBD have the cut shown in (3.12) as opposed to (3.29) that applies to IFI_s and CBD_s; obviously the number of appended cuts has the greatest impact given that both IFI and IFI_s call the operational subproblems in the same manner.

Hence, it can be seen that *inefficient decomposition formulations* may turn out slower than the nondecomposed formulation of the problem because solution times in the former are affected by parameters that are not present in the latter, namely the number of appended cuts and the way by which the operational subproblems are called. If these parameters are not modelled efficiently then it is reasonable to anticipate poor performance. However, efficient decomposition formulations should theoretically result in faster solution times. Note that even inefficient decomposition formulations can guarantee lower memory consumption because they involve decision variables of lower dimensionality that the

nondecomposed formulation where all operational decision variables are also a function of scenario s and epoch e (e.g. $\sigma_{s,e,n}$, $\Xi_{s,e,t,n}$).

	Benders iterations	**Operational subproblems solved**	**Solution time**	**Average memory consumption**
IFI	1157	22,218	20 hours	~8 GB
CBD	1157	23,140	36 hours	~8 GB
CBD_S	39	780	1 hour	~8 GB
ND	-	-	5 hours & 10 minutes	30 GB
IFI_S	39	719	15 minutes	~8 GB

Table 3.9 Comparison of IFI, CBD, CBD_S, ND and IFI_S solution methodologies, all of which yield the same output as the one depicted in Figure 3.10. The IFI and CBD stand for 'Intelligent Filtering Implementation' and 'Classic Benders Decomposition' variations of Benders decomposition. The ND stands for 'nondecomposed'. IFI_s and CBD_S refer to the multicut formulations of the problem.

In addition, by comparing Table 3.7 with Table 3.9 it can be seen that in the former case IFI calls 35% fewer operational subproblems, while in the latter case the reduction is only 5%. The reason for this lies in how the scenario tree expands when uncertainty resolves; by comparing Figure 3.3 with Figure 3.10 it is obvious that in the latter case after the initial uncertainty resolution all nodes get distinguished resulting in the need for calling a greater number of operational subproblems. In addition, the application of IFI_S results in small solution times in both cases while IFI has very poor performance under global resolution because of greater complexity as the master problem has the extra set of constraints (3.34) that apply $\forall s, e, n$ while the operational subproblem formulation contains (3.32)-(3.33) that imply that the consumer participation is a decision variable for all buses. This greater complexity requires more than just one cut generated per iteration (achieved via IFI_S) for the accurate representation of the operational subproblem; otherwise the process of convergence becomes much slower.

Finally, note that different values for parameter M were tested and found to have no effect whatsoever on the optimal solution shown in Figure 3.10 or on the solution times.

3.3 *Immediate & Local DDU resolution (applied to transmission)*

In this section a case study is presented that applies to a transmission system that undergoes load and wind generation capacity growth over a fifteen-year horizon. In order to accommodate the resulting rising power flows the planner has the possibility to invest in conventionally upgrading lines and / or investing in DSR technology. However, the way by which optimal investment decisions will be made is not straightforward due to uncertainty. In particular, the source of uncertainty, which is the level of consumer participation in DSR, is of decision-dependent or endogenous type (i.e. does not resolve with the passage of time but requires action taken from the planner) and resolves immediately (i.e. at the same epoch when the investment is made) and locally (i.e. only at the bus where the corresponding investment is made). The results show that decision-dependent uncertainty formulations can be effectively applied to transmission system planning and that the deployment of DSR in the system allows not only for accommodating the rising power flows but also for generating significant cost savings while emphasizing the importance of investing in DSR as early as possible or otherwise costs are higher. This happens because by investing in DSR early, uncertainty resolves early thereby resulting in future investment decisions that are targeted to the realized system state i.e. stranding risk is minimized.

Conducting the studies involves modelling the problem in a stochastic optimization programming formulation and using various Benders decomposition techniques (e.g. multicut, monocut, sequential, parallel along with the novel Intelligent Filtering implementation) and relevant comparisons are made. Finally, the methodology for obtaining the option value of DSR under decision dependent uncertainty is presented with relevant insights and explanations being provided.

3.3.1 *Problem description*

Figure 3.15 depicts the reference GB transmission system under study that has been developped by Imperial College London and has been extensively used on many occasions [84] [85]. The total peak demand amounts to 52 GW [86] distributed across sixteen buses, where each bus represents a GB zone and each branch (or corridor) represents a system boundary, which is a concept invented by National Grid for assisting in calculating

transmission system requirements; boundaries cross important power-flow paths where there are limitations to capability or where it is expected that additional bulk power transfer capability will be needed [87]. Corridor lengths (km) [85] and thermal ratings [84] are shown in Table 3.10.

Four generic types of generators are used: marginal thermal (i.e. gas/coal), nonmarginal thermal (i.e. gas/coal), nuclear and wind, with the total installed capacity of the generating units across the system being approximately 74GW (corresponding to the first epoch of the study horizon) out of which 31GW are nonmarginal thermal, 30.8GW are marginal thermal, 6GW are wind and 6.4GW nuclear units i.e. around 70GW conventional capacity [84]. The location of connection, fuel cost and installed capacity of these generating units is included in Table 3.11 [84].

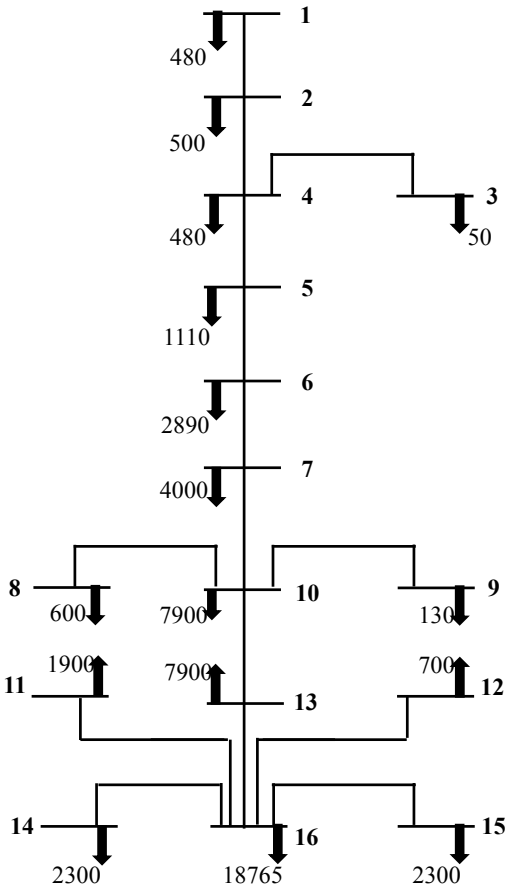


Figure 3.15 Schematic diagram of the tranmission system showing peak load per bus (numbers to which the arcs point), in MW. The depicted peak load corresponds to the first epoch of the study horizon.

The study horizon is split in five three-year epochs over which the planner must minimize system costs by choosing to invest in increasing the capacity of corridors and/or deploying DSR schemes. Note that the power flows through the lines are modelled according to the DC power flow model.

Corridor	Length (km)	Thermal limit (MW)
1-2	60	5000
2-4	100	6000
3-4	50	346
4-5	120	6000
5-6	35	6000
6-7	150	6000
7-10	150	8000
8-10	79	3000
9-10	40	5500
10-13	93	11403
11-16	75	3500
12-16	80	2800
13-16	155	10273
14-16	195	3500
15-16	60	7000

Table 3.10 Length (km) and thermal rating (MW) for each corridor of the transmission system.

The main assumption for the system under study is that significant wind generation capacity is to connect in the North (Scotland) as shown in Table 3.12 [84] resulting in approximately a total of 21GW installed capacity by the early 2020s, which is in accordance with the projections of the Central wind energy scenario formulated by the European Wind Energy Association [88]. Notice that the installed capacity of all non-wind units remains at the same level as in the first epoch (i.e. no new connections or decomissions are modelled) across the horizon. Also, the installed capacity of wind units deployed at buses other than buses 1, 2 and 4 stays the same across the horizon.

Bus of connection	Generator Type	Fuel cost (£/MWh)	Installed capacity (MW)
1	Wind	0	1000
1	Marginal Thermal	80	800
2	Wind	0	1050
2	Nonmarginal thermal	30	1100
2	Marginal Thermal	80	436
4	Wind	0	100
5	Wind	0	210
5	Nonmarginal thermal	30	1200
5	Marginal Thermal	80	1300
6	Wind	0	1450
6	Nuclear	20	1200
6	Marginal Thermal	80	250
7	Nuclear	20	4000
7	Nonmarginal thermal	30	1020
7	Marginal Thermal	80	5380
8	Wind	0	833
9	Wind	0	500
9	Marginal Thermal	80	2000
9	Nonmarginal thermal	30	3200
10	Nonmarginal thermal	30	7800
10	Marginal Thermal	80	5753
11	Nonmarginal thermal	30	2172
11	Marginal Thermal	80	900
12	Nuclear	20	1200
13	Nonmarginal thermal	30	5863
13	Marginal Thermal	80	4086
14	Nonmarginal thermal	30	905
15	Wind	0	792
15	Nonmarginal thermal	30	4500
15	Marginal Thermal	80	3300
16	Nonmarginal thermal	30	3005
16	Marginal Thermal	80	6900

Table 3.11 Types of generator technologies connected to the system along with the bus of connection, fuel cost and installed capacity, the latter corresponding to the first epoch.

Furthermore, the load is set to grow at every bus in the system; however, at large demand centres located in the south and centre (England) this growth will take place at a higher pace than at load centres in the north (see Table 3.13). This rapid increase in peak demand is in line with the underlying assumptions of National Grid's Gone Green scenario [89] that the decarbonisation of heat and transport sectors along with the uptake of electric vehicles (mostly happening in large demand centres) will lead to significant peak increases. In Table 3.13 it can be seen that the annual average increase across the system is 6% from epoch 1 to epoch 2 and then it drops to 1% (Epoch 2 → Epoch 3) and 0.5% (Epoch 3 →Epoch 4 and Epoch 5). ~~This sudden rise followed by a drop can be attributed to the initial effect just after decarbonisation of a large portion of heat and trasport sectors and connections of electric vehicles.~~

Thus, with the aim of the planner being to minimize the total expected investment and generation cost, generation from wind units is particularly valuable as it corresponds to zero fuel cost and by replacing energy from thermal units it can considerably contribute to the reduction of the total expected system costs.

Bus	Epoch 1	Epoch 2	Epoch 3	Epoch 4	Epoch 5
1	1000	1500	5000	7000	9500
2	1050	1550	5050	7050	9550
4	100	600	4100	6100	8600

Table 3.12 Installed capacity (MW) of wind generation connected to each of the mentioned buses per epoch. The capacities shown for epoch 1 are taken from Table 3.11.

Area	Epoch 1	Epoch 2	Epoch 3	Epoch 4	Epoch 5
1	1.000	1.070	1.080	1.085	1.090
2	1.000	1.300	1.370	1.400	1.450

Table 3.13 Factor by which the peak load per bus grows corresponding to diagram shown in Figure 3.15. Area 1 consists of buses 1 to 10, while the remaining buses (11…16) constitute Area 2.

The need to accommodate the increasing power flows from the north to the south prompts the planner to consider the following technologies (see Table 3.14) as potential candidates for investments.

Technology	Build time (epochs)	Investment cost (£)
Conventional reinforcement alternative #1 (+1500 MW)	1	20/MW/km/year
Conventional reinforcement alternative #2 (+6000 MW)	1	70/MW/km/year
Conventional reinforcement alternative #2 (+12000 MW)	1	120/MW/km/year
DSR	0	200,000 /bus/year

Table 3.14 Investment cost and build time for the available technologies for investment.

The DSR scheme can be deployed at any bus taking into account that all buses exhibit uncertainty around the consumer participation level in DSR and only after DSR deployment this uncertainty resolves per bus to be either 0% or 20% or 60%. Four possible scenarios are formed, each with a probability 25% as shown in Table 3.15. Since the uncertainty can be resolved only by deploying a DSR scheme, it can be characterized as DDU. In addition, once such an investment is made the DDU will completely resolve in one epoch and *locally* at the bus where the DSR is deployed. Thus, this is the case of *immediate* and *local* DDU resolution.

The network planner's objective is to determine the investment decisions that minimize the sum of the total expected investment and operational cost, so as to guarantee that the total system load is supplied at all times. The latter cost consists of the generation cost which is a direct function of the fuel cost presented in Table 3.11.

Scenarios	Buses Group A	Buses Group B	Scenario Probability
Scenario S1	60%	60%	25%
Scenario S2	20%	0%	25%
Scenario S3	60%	60%	25%
Scenario S4	20%	0%	25%

Table 3.15 Consumer participation in the DSR scheme per bus and per scenario. Group A consists of buses {1,3,5,7,9,11,12} while group B contains buses {2,4,6,8,10,13,14,15,16}.

3.3.2 *Results of the optimization studies*

Figure 3.16 displays the optimal investment strategy if only the conventional technology is available to the planner. The resulting total expected system cost amounts to £99.10 bn, with the total expected investment cost being £2.26bn and the total expected generation cost standing at £96.83bn.

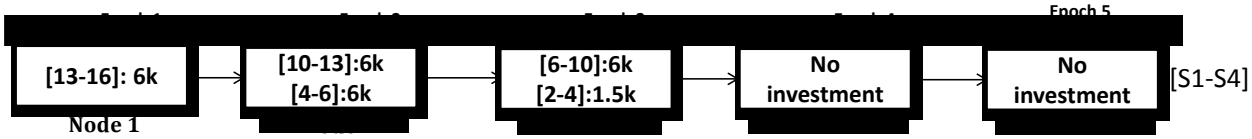


Figure 3.16 Optimal investment strategy in the case where only the conventional technology is available to the planner. The [x-y]:6k means that the decision is taken to reinforce each of the lines between buses x and y by 6000MW. For example [6-10]:6k means [6-7]:6k and [7-10]:6k while [4-6]: 6k means [4-5]: 6k and [5-6]: 6k. Conventional investment decisions become operational in the subsequent epoch. The brackets at the rightmost corner show to which scenarios the depicted investment path corresponds.

It can be observed that initially the enhancement of section 13-16 is decided so as to help accommodate the rising demand of bus-16 load. Further investments take place with the aim of bringing cheap wind generation to the southern parts that exhibit high demand so that by epoch 4 the entire corridor from bus 2 to bus 16 is upgraded. Note that each corridor can be upgraded at most once across a scenario. The level of upgrade is decided based on the cost minimization objective i.e. by upgrading the corridors some cost will be incurred,

which has to be smaller than the benefits accrued from reducing the generation cost through the investment.

Notice that the depicted investment plan is similar to that of a deterministic study, where no branching is present; this is because uncertainty resolution (i.e. branching) can only be triggered by investment in DSR. Thus, all four scenarios remain undifferentiated and subject to the same unconditional investment decisions.

Scenarios	Total Investment Cost per scenario	Total Generation Cost per scenario
S1-S4	£2.26bn	£96.83bn

Table 3.16 Total costs per scenario for the study shown in Figure 3.16.

Figure 3.17 shows the optimal investment strategy for a network planner who has the DSR and the conventional technologies available for investment. Note that a series of DSR investments are made in the first epoch to allow for the distinction of the scenarios (i.e. resolve uncertainty) as well as perform necessary load shifting that reduces the generation cost (i.e. the DSR schemes connect the previously disconnected load at times of low wind speed i.e. low wind generation). The DSR schemes are deployed accordingly to those buses so that in the event of unfavourable realization of uncertainty they do not exhibit 0% consumer participation levels.

Notice that due to the higher consumer participation across S1-S3, a reduction of 30% in the amount of conventional investment is made (i.e. 24k MW) than across S2-S4 (i.e. 33.5k MW) resulting in reduced investment cost per scenario. In addition, the greater DSR activity (due to higher consumer participation) leads to reduced generation costs as regards to S1 and S3. The resulting total expected system cost is £94.39bn, with the total expected investment cost being £1.53bn and the total expected generation cost at £92.86bn.

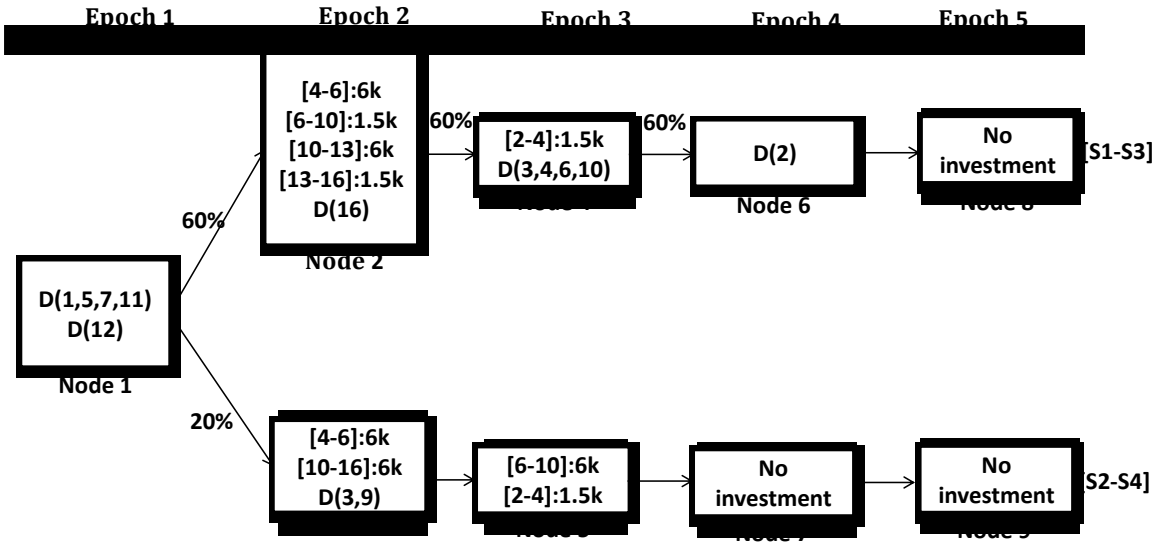


Figure 3.17 Optimal investment strategy for a network planner with two investment technologies available: DSR and conventional reinforcement. The D(X,Y,Z) signifies the decision to invest in DSR at buses X,Y,Z. The brackets at the rightmost corner show to which scenarios the depicted investment paths correspond. Percentage values indicate consumer participation levels per bus.

The following table presents the investment and generation costs per scenario.

Scenarios	Total investment cost per scenario (£)	Total generation cost per scenario (£)
S1	0.99bn	90.9bn
S2	2.094bn	94.81bn
S3	0.99bn	90.9bn
S4	2.094bn	94.81bn

Table 3.17 Investment and generation costs per scenario for the study shown in Figure 3.17.

From the difference in total expected system costs, one can calculate the option value of DSR technology to be equal to £99.10bn - £94.39bn = £4.71bn representing the net investment and generation savings accrued from investing in DSR technology across the GB transmission system. These savings can be attributed to both the fact that DSR investment resolves uncertainty, thereby allowing for conditional investment, and to the fact that DSR performs load shifting operations that allow peak shaving.

In conclusion, this case study demonstrates that DDU modelling can be applied to investment decision making problems in the transmission system and showcases the scalability of the developped stochastic planning tool. In addition, the significant contribution of DSR technology is emphasized when it comes to reducing investment and generation costs under DDU on a transmission level advocating in favour of its early deployment.

3.3.3 *Mathematical formulation*

The mathematical formulation for the master problem consists of (3.5)-(3.11) with (3.38) representing the total investment cost per scenario (as in (3.4)) with l_l being the length (km) of corridor l and $F_{s,e,l,o}$ the extra thermal capacity (MW). Regarding the type of Benders cut, notice that (3.12) defines the monocut version of Benders algorithm in which one cut per iteration is generated, while in (3.29) a number of $|\Omega_S|$ cuts are generated per iteration and appended to the master. In order to transfer greater amount of information from the operational subproblems to the master problem, constraint (3.35) is used in this case for the Benders cut representation, thereby generating a number of $|\Omega_s||\Omega_E|$ cuts per iteration which results in improved solution times. In this case, the objective function of the master problem becomes (3.37) with (3.36) and (3.2) being the lower and upper bounds to the original problem's objective function respectively.

$$a_{s,e}^{i} \geq \pi_s \omega_{s,e}^{i-1} + \sum_{l}\sum_{o} \pi_s \lambda_{s,e,l,o}^{i-1}\left(\tilde{F}_{s,e,,l,o} - \tilde{F}_{s,e,,l,o}^{i-1}\right) + \sum_{n} \pi_s \mu_{s,e,n}^{i-1}(\tilde{D}_{s,e,n} - \tilde{D}_{s,e,n}^{i-1}) \qquad \forall s, e \qquad (3.35)$$

$$z_{lower}^{i} = \sum_{s} \pi_s r_e \xi_s^i + \sum_{s,e} a_{s,e} \qquad (3.36)$$

$$\min\left\{\sum_{s} \pi_s r_e \xi_s^i + \sum_{s,e} a_{s,e}\right\} \qquad (3.37)$$

$$\xi_s^I = \sum_e \left(\sum_l \sum_o F_{s,e,l,o} \gamma_o l_l + \sum_n D_{s,e,n} \gamma_D \right) \qquad \forall s \qquad (3.38)$$

Regarding the formulation for the operational subproblem, it consists of (3.18)-(3.26), with the corresponding objective function being formulated as in (3.39) where f_g is the fuel cost of generating unit g and Λ is the remuneration paid to consumers for allowing load shifting of their flexible load. Notice that (3.39) does not need to include the cost of curtailment of wind generation as this is implied in the objective of minimizing the generation from thermal units.

$$\omega_{s,e}^i = min \left\{ \sum_t \sum_g \tau_e \, \delta_t f_g P_{t,g} + \sum_t \sum_n \tau_e \, \delta_t \Xi_{t,n} \Lambda \right\} \qquad (3.39)$$

3.3.4 ***Solution Methodology***

Table 3.18 displays the performance of various solution methodologies, yielding the output presented in Figure 3.17; it is $\delta_t = 1$ hour and $|\Omega_T| = 840$ hours where the duration of the year is represented by five typical weeks rather than 8760 hourly periods (as in paragraphs 3.1 and 3.2) that results in intractability. The use of typical weeks leads to the reduction of the time-domain from 8760 hours to 840 hours (each week contains $24 \cdot 7 = 168$ hours). Note that four typical weeks are used to represent the four seasons of the year (each week corresponds to each season) and an extra week is used to capture the peak loading conditions (corresponds to the week that includes the peak load period). The flow diagram for the algorithm is shown in Figure 3.18.

Both $\text{IFI}_{s,e}$ and $\text{CBD}_{s,e}$ are similar to IFI and CBD with the difference being that the $a_{s,e}$ type of Benders cut is used as in (3.35). This allows for $|\Omega_s||\Omega_E|$ number of Benders cuts appended to the master problem leading to dramatic reductions in solution time comparing to the cases where α_s and a types of cuts are used. In addition, notice that all decomposition methodologies achieve more than 90% decrease in average memory

consumption as the nondecomposed problem involves operational variables with dimensions of the form (s, se, e, t, n), where $s \in \Omega_S$, se being the index for the five typical weeks, $e \in \Omega_E$, $t \in \{1,..,168\}$ and $n \in \Omega_N$, where $|\Omega_s| = 4, |\Omega_E| = 5, |\Omega_N| = 16$ for the problem presented in paragraph 3.3.1. Whereas the decomposed versions involve operational variables with dimensions of the form (t, n) as each operational subproblem is solved only for the duration of a typical week.

Figure 3.19 shows the total number of operational subproblems for the problem presented in paragraph 3.3.1; four scenarios and five epochs make up twenty nodes (i.e. combinations of scenarios and epochs) and since five typical weeks are used (illustrated in Figure 3.19 by the five areas that each node is divided), the total number of operational subproblems grows to 100. Then, depending on the characteristics of the CPU a number of operational subproblems are called for simultaneous implementation. In this case the CPU characteristics allow for twenty operational subproblems being implemented simultaneously. Thus, the implementation begins by calling these twenty subproblems corresponding to the first typical week and, after they are solved, the second batch of twenty subproblems corresponding to the second typical week is called and so on (this process is repeated for all five typical weeks). Note that each operational subproblem yields dual variables and costs that correspond to a typical week. The determination of the respective quantities that correspond to the corresponding year is made as follows.

- $Cost_{s,e} = \sum_{\psi} w_{\psi} Cost_{s,e,\psi} \ \ \forall s, e$: The nodal operational cost (i.e. the cost corresponding to $scenario\ s, epoch\ e$) is equal to summing the product of the assumed number of typical weeks in a year by the corresponding operational cost; namely thermal generation cost and DSR operational cost. A similar relation applies to dual variables.

The nodal quantities are then passed on to the master problem of the subsequent iteration for the formation of the Benders cut constraint (see (3.35)).

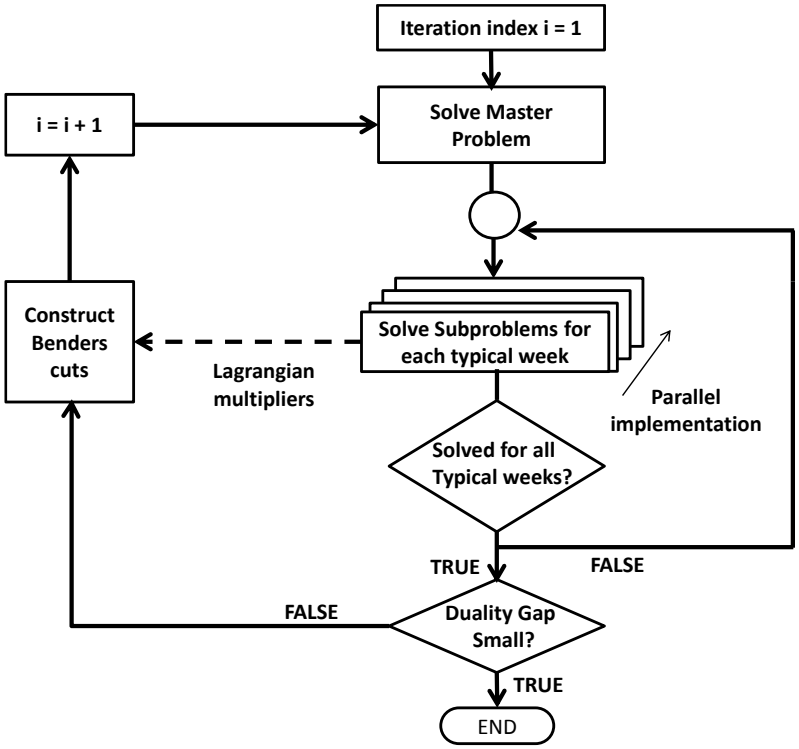


Figure 3.18. Principle of operation of Benders Decomposition when using a number of typical weeks to represent a year.

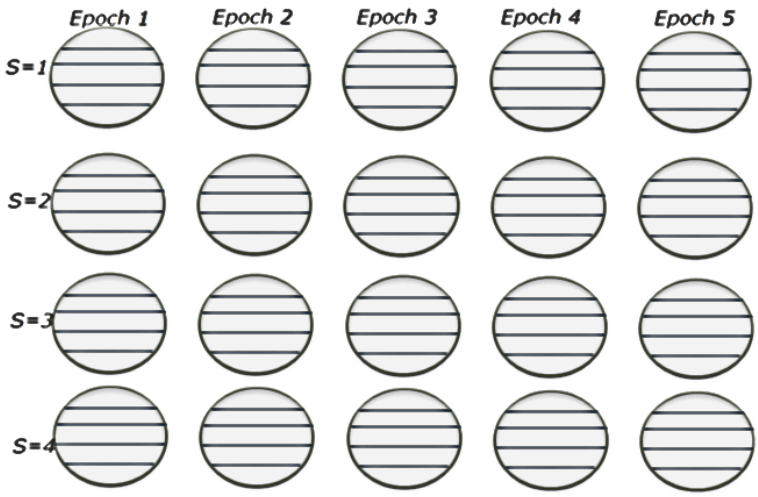


Figure 3.19. Operational subproblems for the problem presented in paragraph 3.3.1 (five epochs, four scenarios and five typical weeks). Each node is divided in five areas (corresponding to the five typical weeks), each of which is an operational subproblem.

	Benders iterations	Operational subproblems solved	Solution time	Average memory consumption
IFI	-	-	> 2 days	N/A
$IFI_{s,e}$	152	7,625	45 minutes	~1.5 GB
$CBD_{s,e}$	152	15,200	1 hour and 50 minutes	~1.5 GB
ND	-	-	4 hours & 40 minutes	60 GB
IFI_s	-	-	> 2 days	N/A

Table 3.18 Comparison of IFI, $I_{s,e}$,$CBD_{s,e}$, ND and IFI_s solution methodologies, all of which yield the same output as the one depicted in Figure 3.17. $IFI_{s,e}$ and $CBD_{s,e}$ refer to the multicut version which involves $|\Omega_s|$ $|\Omega_E|$ Benders cuts appended per iteration to the master subproblem.

Chapter 4 Option Value under Endogenous Uncertainty with Gradual Resolution

4.1 *Gradual & Global DDU resolution*

In this section a case study is presented that applies to a distribution network that undergoes load and DG capacity growth over a twelve-year horizon. In order to accommodate the resulting rising power flows the planner has the possibility to invest in conventionally upgrading lines and / or investing in Storage technology. However, the way by which optimal investment decisions will be made is not straightforward due to uncertainty. In particular, there are three sources of uncertainty (the invesment cost in £k/year, the power in kW, and energy capability of storage technology in kWh) which are caused by a primary source of uncertainty that surrounds the amount of innovation funding that this technology can attract. All three sources of uncertainty are of decision-dependent or endogenous type (i.e. do not resolve with the passage of time but only after some action has been taken from the planner) and resolve gradually (i.e. across a number of epochs after many investment decisions are made) and globally (i.e. not only at the bus where the corresponding investment is made but across the system). The results show that the deployment of Storage in the system allows not only for accommodating the rising power flows but also for generating significant cost savings while emphasizing the importance of investing in Storage as early as possible or otherwise costs are higher. This happens because by investing in Storage early, uncertainty resolves early thereby resulting in future investment decisions that are targeted to the realized system state i.e. stranding risk is minimized.

Conducting the studies involves modelling the problem in a stochastic optimization programming formulation and using various Benders decomposition techniques (e.g. multicut, monocut, sequential, parallel as well as the novel Intelligent Filtering Implementation) to produce results within reasonable solution times. Finally, the methodology for obtaining the option value of Storage under decision dependent uncertainty is presented with relevant insights and explanations being provided.

4.1.1 *Problem description*

The distribution network shown in Figure 3.1 is studied across six two-year epochs with Table 3.1 displaying the load growth as well as the growth in DG capacity across the first five epochs. For the sixth epoch, the corresponding values applying in the current case study are 105 kW (for each of the buses 5 and 8) and 180kW for the DG capacity respectively. Note that the cost of wind curtailment is shown in the first row of Table 3.4. In addition, the load pattern for each load-bus is illustrated in Figure 2.3. The investment technologies that are available to the planner are shown in Table 4.1. Notice that storage technology has zero build time meaning that it becomes operational at the same epoch at which the corresponding investment decision is taken, whereas conventional line upgrades require one extra epoch due to required time-consuming planning permissions and civil works. In addition, observe that storage technology costs around 35% and 100% more than the most expensive and cheapest conventional solution respectively, indicating that the storage technology under study corresponds to a newly introduced and expensive model. Note however that the storage unit modelled in this work is a generic storage device. This allows to capture the benefits of storage operation regardless of any particular technology and this approach has been used in other works also [84][90].

Technology	Build time (epochs)	Investment cost (£k)
Conventional reinforcement alternative #1 (+50 kW)	1	80 /year/line
Conventional reinforcement alternative #2 (+100 kW)	1	120 /year/line
Storage 15kW/30kWh	0	160 / year / unit

Table 4.1 Investment cost and build-time for the available technologies for investment.

The significant advantages of storage technology have strengthened the prospects for innovation and newer models are expected to emerge in the future [90]. However, as for every new technology there is significant amount of uncertainty around the level of innovation funding that this technology may attract as such funding will depend on whether or not pilot tests and corresponding demonstration projects will be considered successful. In turn, uncertainty around the level of innovation funding directly translates into uncertainty

around techno-economical characteristics of future storage investments given that innovation leads to cost reductions and technical improvements.

Table 4.2 shows the uncertainty around techno-economic parameters of storage technology including the investment cost of storage, the maximum power (kW) that can be charged/discharged and the energy capacity (kWh) of each storage unit. Uncertainty is represented by four scenarios, with each one depicting a different path for the uncertainty resolution of the aforementioned parameters. The first scenario corresponds to the case where insufficient innovation funding is given to storage leading to no techno-economical improvements. On the other hand, S4 corresponds to a situation where storage technology continuously attracts funding that leads to significant improvements. More specifically, once a storage unit gets deployed at any bus across the system it possesses techno-economic characteristics, as indicated in Table 4.2, and these characteristics remain fixed until the end of the horizon. Units that will be deployed in future epochs may have improved or identical (but not worse) characteristics comparing to units deployed in previous epochs; this depends on the level of received innovation funding. The modelling of this techno-economical evolution can be facilitated through the concept of *levels of uncertainty resolution*.

A level of uncertainty resolution, denoted by p, characterizes a system state spanning one or more epochs where the deployed storage units possess identical techno-economical characteristics. For example, all units deployed across S1 correspond to the same level p (see Table 4.2) due to insufficient innovation funding. Furthermore, a storage unit can correspond to exactly one level p; this value is fixed for the particular unit (as its characteristics are fixed) and is taken the moment it is deployed in the system. More generally, in any epoch there may be many storage units in the system with each corresponding to a different p. However, all units deployed in the same epoch correspond to the same p (i.e. all have identical characteristics).

Note that the described uncertainty does not present exogenous characteristics because the passage of time does not have any effect on its resolution, which can be accomplished only through storage investments. Thus, it can be characterized as *decision-dependent* or *endogenous*. In addition, the uncertainty resolution applies *globally* (i.e. at all buses) rather than *locally* (i.e. at a certain bus only) and takes place *gradually* since a series of investments spread out over a number of epochs are required for full uncertainty clearance.

	Investment Cost Evolution as a function of the level of uncertainty resolution	P/C evolution as a function of the level of uncertainty resolution	Scenario Probability
Scenario S1	160	15/30	20%
Scenario S2	160→80	15/30→25/50	20%
Scenario S3	160→80→40	15/30→25/50→50/100	20%
Scenario S4	160→80→40→20	15/30→25/50→50/100→100/200	40%

Table 4.2 Possible scenarios for the investment cost (£k/year) of storage technology, the maximum power P (kW) that can be charged/discharged by a storage unit on an hourly basis and the hourly storage capacity C (kWh) (two hours are required for charging or discharging between zero and full capacity). The value of these parameters, per scenario, depends on the level of uncertainty resolution.

4.1.2 *Results of the optimization studies*

Figure 4.1 displays the optimal investment solution if only the conventional technology is available to the planner. The resulting total expected system cost amounts to £4.6m. Notice that the depicted investment plan is similar to that of a deterministic study because branching (uncertainty resolution) can only be triggered by investment in storage technology. Hence, since only conventional reinforcement is available to the planner, all four scenarios S1 – S4 collapse to one i.e. remain indistinguishable until the end of the horizon.

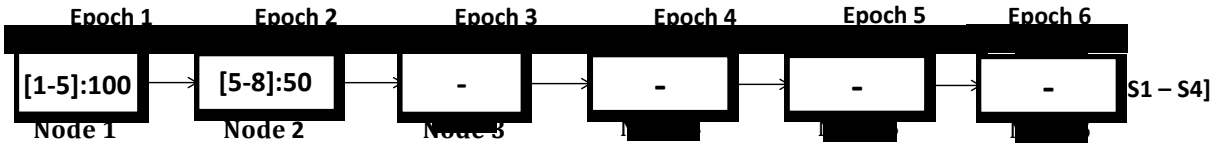


Figure 4.1 Optimal investment decisions in the case where only the conventional technology is available to the planner. The [x-y]:100 means that the decision is taken to reinforce each of the lines between buses x and y by 100kW. Such a conventional investment decision becomes operational one epoch after the corresponding decision is made. The brackets at the rightmost corner show to which scenarios the depicted investment paths correspond.

Figure 4.2 illustrates the optimal investment strategy for a network planner with both storage and conventional technologies available. The resulting total expected system cost is £3.0m.

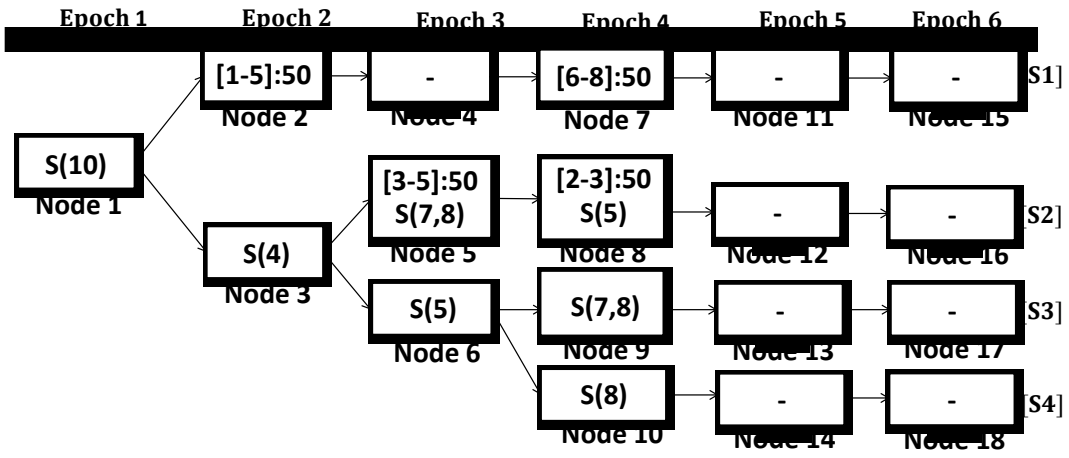


Figure 4.2 Optimal investment strategy for a network planner with two technologies available: storage and conventional reinforcement. The S(x) means that the decision to invest in storage at bus x is made.

Notice that the availability of storage allows for a fundamentally different investment approach due to the capability of making conditional investments. According to this figure, no storage investment takes place across S1 as at the end of epoch 1 it becomes known that no innovation funding will become available leaving the storage unattractive as a candidate technology for investment and leading to an amount of 200kW of conventional reinforcement taking place by the end of the horizon. This is, however, not the case for the remaining scenarios where more investments in storage and less to none conventional investments are made. In particular, the first investment that is made is in a storage unit at bus 10 costing £160,000/year with 30kWh capacity and 15kW maximum hourly power capability. Such an investment leads to the partial uncertainty resolution with the appearance of two branches in the decision tree. The first branch (realization of scenario S1) involves innovation funding that is insufficient to generate any techno-economical improvements meaning that it becomes known that the next storage unit deployed in the system will possess exactly the same characteristics as the first one Thus, in the second epoch of S1, an investment of 50kW at each of the lines 1-2, 2-3 and 3-5 takes place. This investment becomes operational in the third epoch. Thus, all flows in the second epoch are

accommodated by the storage unit at bus 10; no further storage investments are made across S1.

After the deployment of the first-epoch storage unit, the other alternative is to attract innovation funding resulting in techno-economical improvements of storage technology. As a result, a further storage unit is deployed at bus 4 (node 3), for half the cost (£80,000 per annum) and almost twice the capacity (50kWh) and power capability (25kW). This investment leads to a further uncertainty resolution around storage technology. In other words, it is revealed whether additional innovation funding is attracted (node 3 → node 6) or not (node 3→node 5). In any case, the same number of storage investment are made (see S2 and S3) with the difference being that in S3 no conventional investments take place given that the future storage units come with enhanced capabilities (nodes 6,9) i.e. storage investment at node 6 has a cost of £40,000/year, 100kWh capacity and 50kW power capability. This further reduces the uncertainty resulting in two realizations: node 6→ node 9 and node 6→ node 10. In the former case the innovation funding stops. However, the storage technology has already become very competitive in terms of cost, power and energy capabilities thereby leading to additional investments. In the latter case (node 6→ node 10), one additional storage investment at node 10, having enhanced capabilities (100kW, 200kWh) suffices for achieving safe system operation.

In Figure 4.2 it can be observed that an early storage investment (first epoch) allows for early uncertainty resolution, which is very beneficial for system economics especially for scenario S4. Expectedly, as the total innovation funding rises (scenarios S1 towards S4), the number of conventional reinforcement decisions reduces. Across scenario S1 (nodes 1→2→4→7→11→15) there are 200kW of conventional reinforcement and 100kW across S2 (nodes 1→3→5→8→12→16), while in S3 (nodes 1→3→6→9→13→17) and across S4 (nodes 1→3→6→10→14→18) there are no conventional reinforcement decisions.

In Figure 4.2 it can be observed that at some nodes there are many storage units that operate simultaneously. For example, at node 17, all deployed storage units operate simultaneously (i.e. those located at buses 4,5,7,8, and 10). In particular, at some period of relatively low load factor the units charge with energy so that at another period of high load they extract this power (acting as generators, causing the reduction of local load) thereby relieving stress on the lines that bring power from the substation. Note that over a typical day of operation the algebraic sum of the total power charged by a single unit plus that

discharged is equal to zero i.e. no losses. Figure 4.3 shows the effect that the storage unit at bus 8 has on contributing to the safe accommodation on power flows across line 3-5 over the duration of a day.

The option value of investing in storage technology under gradual DDU is equal to the difference in the total expected system cost in the resulting strategies where the DSR is available (Figure 4.2) and where it is not (Figure 4.1). This difference amounts to £4.6m - £3.0m = £1.6m, representing the expected value of the net benefit accrued from optimally investing in storage technology. This net benefit stems from the ability to conditionally invest based on the resolution of uncertainty (i.e. in Figure 4.1 all investment decisions are unconditional), which brings economic benefits to the system given that storage technology exhibits gradually improved techno-economical characteristics making it more attractive than conventional line upgrades. For example, in Figure 4.2 there are no 100kW line upgrades and any conventional investment decision is made only in particular scenarios and away from the first epoch (first-epoch decisions cost more due to higher cumulative discounting factor), thereby leading to savings in total expected investment cost, which are the driver behind the option value.

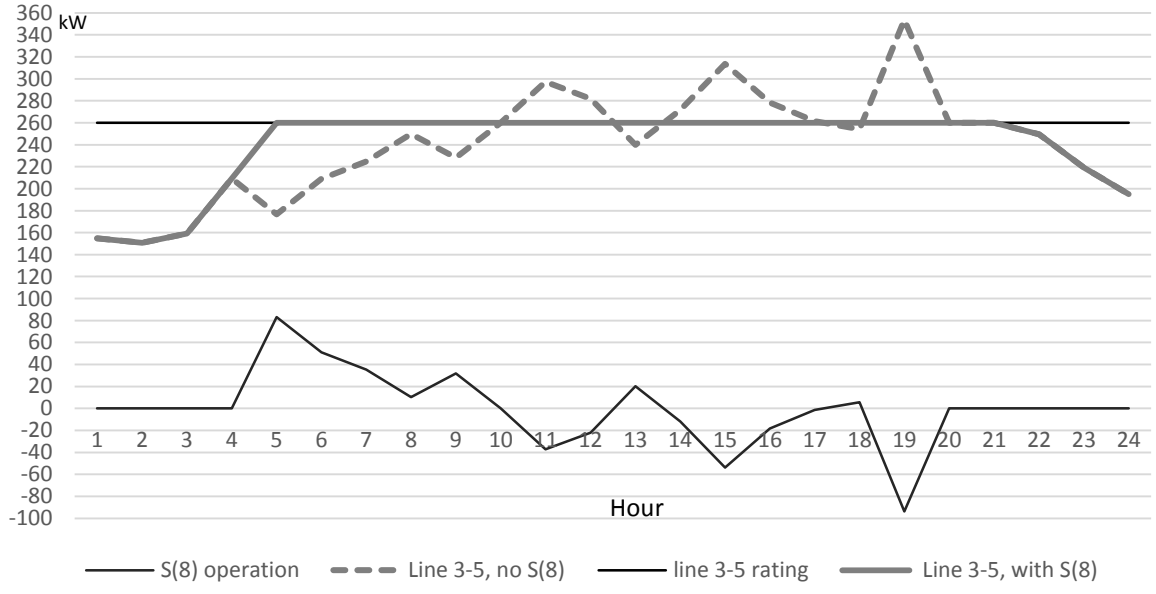


Figure 4.3. Power flo
w pattern (thick grey lines) and operation of storage unit at bus 8 (thin black line), referring to node 18 of Figure 4.2, for line 3-5 (whose rating is 260kW – see the network in Figure 3.1) with/without the storage unit of bus 8.

As a result, examining investments in storage technology under DDU around its techno-economical characteristics leads to two important conclusions. First, it is considered optimal to invest in storage technology as early as possible and, secondly, to continue investing in the technology as long as innovation funding continues to arrive.

In order to emphasize the importance of the first-stage storage investment, a further study is solved where there is no possibility for such an investment. Figure 4.4 displays the resulting optimal investment strategy that yields a total expected system cost increased by approximately 12% and amounting to £3.35m.

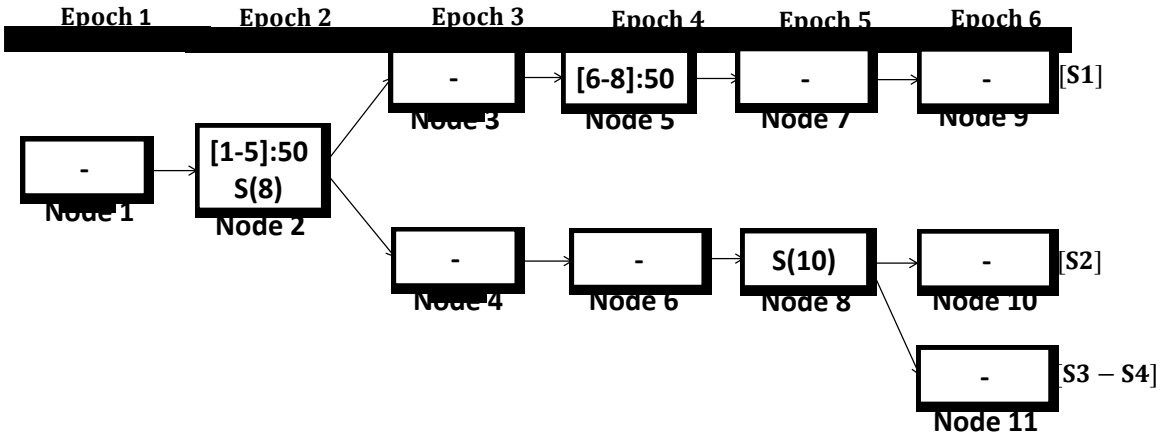


Figure 4.4. Optimal investment strategy for a network planner with two technologies available: storage and conventional reinforcement, with the extra condition that the planner does not have the possibility to invest in storage in the first epoch.

4.1.3 *Mathematical Formulation*

The nomenclature for the mathematical formulation follows and is complemented by the nomenclature presented in paragraph 3.1.3.

Sets and indices

Ω_{DG} Set of renewable distributed-generation (DG) units, indexed g^*.

Ω_G Set of generation units and substations, indexed g.

Ω_P Ordered set of levels of uncertainty resolution, indexed p, where $p > 0$ and integer. All storage units corresponding to the same p have identical

values for their uncertain characteristics.

Ω_T Set of demand periods in a typical day, indexed t.

$\aleph_p$ Set consisting of scenario pairs (s, s') and defining the way by which the gradual DDU becomes resolved as a function of storage investments.

Input Parameters

Γ_s^p Investment cost for the deployed storage unit corresponding to p across s $(£/year)$.

$\zeta_{t,g}$ Intermittency of g as a percentage of its installed capacity. For $g \in \Omega_G - \Omega_{DG}$ (i.e. substations, and thermal units), it is $\zeta_{t,g} = 1, \forall w, t$. Otherwise, it is a real number $\in [0,1]$.

Ψ_s^p Energy capacity of a storage unit corresponding to p at (kWh).

$\overline{\Psi}_s^p$ Maximum power that a storage unit, corresponding to p, can absorb/release at scenario s (kW).

$d_{t,n}$ Demand at n, in t (kW).

$I_{n,g}$ Bus-to-generation incidence matrix. Its elements are equal to 1 when g is connected to bus bn. Otherwise, they are equal to zero.

k_D Build time for a storage unit (epochs).

$L_{n,l}$ Bus-to-line incidence matrix. Its elements are equal to 1 when n is the receiving bus of l, and -1 when it is the sending bus. Otherwise they are 0.

M Large positive number.

Decision Variables

Δ_n^p Continuous variable representing $\tilde{D}_{s,e,n}^p$ in the operational subproblem.

$E_{t,n}$ Continuous variable representing energy capacity at t for the storage

	unit located at (kWh).
$B_{s,e,l,o}$	Binary decision to upgrade line l by o at s, e.
$\mathbb{B}_{s,e,l,o}$	Boolean representation for $B_{s,e,l,o}$.
$D^{p}_{s,e,n}$	Binary decision to invest in a storage unit corresponding to p at s, e, n.
$\mathbb{D}^{p}_{s,e,n}$	Boolean representation for $D^{p}_{s,e,n}$.
$\widetilde{\widetilde{D}}^{p}_{s,e,n}$	Continuous state variable for $D^{p}_{s,e,n}$.
$\widetilde{\widetilde{\mathbb{D}}}^{p}_{s,e,n}$	Boolean representation for $\widetilde{\widetilde{D}}^{p}_{s,e,n}$.
$J_{t,n}$	Continuous variable $\in \mathbb{R}$ representing power that is charged/discharged at t by a storage unit located at (kW).
$P_{t,g}$	Continuous variable for the output of g at t (kW).
$F_{t,l}$	Power flow $\in \mathbb{R}$ across line l at t (kW).
$w^{p}_{s,e}$	Binary variable signifying investment in at least one storage unit corresponding to p by epoch e.
$\mathbb{w}^{p}_{s,e}$	Boolean representation for $w^{p}_{s,e}$.
$Z^{s,s'}_{e}$	Binary variable stating whether or not scenarios s, s' are indistinguishable by e.
$\mathbb{Z}^{s,s'}_{e}$	Boolean representation for $Z^{s,s'}_{e}$.

The following mathematical model pertains to network planning under DDU around techno-economic storage characteristics (investment cost, maximum absorbable/releasable power and energy capacity). The uncertainty in all these characteristics resolves simultaneously after undertaking an investment in a storage unit at any bus across the system (*globally*). Note that a line can be upgraded at most once across any scenario and at most one storage unit can be deployed per bus. Complete resolution of uncertainty happens after a series of storage investments (*gradual resolution*).

The problem formulation is presented in a decomposed form using Benders algorithm, with (3.36), (3.2) being the lower and upper bounds respectively. The

formulation for the master problem follows taking into account that equation (3.37) is the objective function of the master problem.

$$\xi_s^I = \sum_e \left(\sum_l \sum_o B_{s,e,l,o} \gamma_o + \sum_n \sum_p D_{s,e,n}^p \Gamma_s^p \right) \qquad \forall s \qquad (4.1)$$

$$\widetilde{D}_{s,e,n}^P = \sum_{z=1}^{e-k_D} D_{s,z,n}^P \qquad \forall s, e, n, p \qquad (4.2)$$

$$B_{s,1,l,o} = B_{s\prime,1,l,o} \qquad \forall s, s', l, o \qquad (4.3)$$

$$D_{\mathrm{s},1,n}^P = D_{\mathrm{s}',1,n}^P \qquad \forall s, s', n, p \qquad (4.4)$$

$$\mathbb{w}_{\mathrm{s},e}^P = True \Leftrightarrow \bigvee_n \left(\widetilde{\mathbb{D}}_{s,e,n}^p = False \right) \qquad \forall s, e \qquad (4.5)$$

$$\mathbb{Z}_e^{s,s\prime} = True \Leftrightarrow \begin{Bmatrix} \mathbb{B}_{s,e+1,l,o} = \mathbb{B}_{s',e+1,l,o} \ \forall l, o \\ \bigwedge \\ \mathbb{D}_{s,e+1,n}^p = \mathbb{D}_{s',e+1,n}^p \ \forall n, p \end{Bmatrix} \qquad \forall s, s', e \qquad (4.6)$$

$$\mathbb{Z}_e^{s,s\prime} = True \Leftrightarrow \begin{Bmatrix} \mathbb{w}_{s,e}^p = True \\ \bigwedge \\ \mathbb{w}_{s',e}^p = True \end{Bmatrix} \qquad \begin{matrix} \forall e, p, \\ \forall s, s' \in \aleph_p \end{matrix} \qquad (4.7)$$

$$\bigvee_{n} \mathbb{D}_{s,e+1,n}^{p+1} = True \Rightarrow \bigvee_{n} \widetilde{\mathbb{D}}_{s,e,n}^{p} = True \qquad \forall s, e, p \qquad (4.8)$$

$$a^{i} \geq \sum_{s} \pi_s \, \omega_s^{i-1} + \sum_{s}\sum_{e}\sum_{l}\sum_{o} \pi_s \lambda_{s,e,l,o}^{i-1}\left(\tilde{F}_{s,e,l,o} - \tilde{F}_{s,e,l,o}^{i-1}\right) + \sum_{s}\sum_{e}\sum_{n}\sum_{p} \pi_s \mu_{s,e,n}^{p,i-1}\left(\widetilde{D}_{s,e,n}^{p} - \widetilde{D}_{s,e,n}^{p,i-1}\right) \qquad (4.9)$$

Equation (4.1) skotos describes the total investment cost per scenario s with Γ_s^p being the uncertain parameter representing the investment cost of storage technology. Constraints (3.5) and (4.2) define the state variables that aggregate all investment decisions taken in the past while considering their corresponding build-times, with variable $F_{s,e,l,o}$ taking its values according to (3.7). Constraints (4.3)-(4.4) constitute the initial non-anticipativity constraints, which force the first-epoch investment decisions to be identical across s, s' as no information has arrived to allow for their distinction.

Constraints (4.5)-(4.8) are presented using logic symbols as in [48], where $\wedge$ denotes logical conjunction and $\vee$ logical disjunction. In particular, (4.5) states that $\mathbb{w}_{s,e}^{p} = True$ if and only if there has been no investment (across the system) in any storage unit corresponding to p in all epochs from 1 to e and the moment when one such storage unit is deployed at any bus across the system (*globally*) it becomes $\mathbb{w}_{s,e}^{p} = False$; since it is not possible to remove a storage unit after its deployment the $\mathbb{w}_{s,e}^{p}$ cannot change from its $False$ value. This constraint can be expressed in a mixed integer linear form as follows:

$$\sum_{n} \widetilde{D}_{s,e,n}^{p} \geq 1 - w_{s,e}^{p} \qquad \forall s, e \qquad (4.10)$$

$$\sum_{n} \widetilde{D}_{s,e,n}^{p} \leq M(1 - w_{s,e}^{p}) \qquad \forall s, e \qquad (4.11)$$

According to (4.10)-(4.11), when $w_{s,e}^{p} = 1$ it is $\sum_n \widetilde{D}_{s,e,n}^{p} = 0$ i.e. no investment has taken place in a storage unit of level p. Conversely, when $\sum_n \widetilde{D}_{s,e,n}^{p} = 0$ it must be $w_{s,e}^{p} = 1$. Similarly, when $w_{s,e}^{p} = 0$ it is $M \geq \sum_n \widetilde{D}_{s,e,n}^{p} \geq 1$ and, conversely, when $M \geq \sum_n \widetilde{D}_{s,e,n}^{p} \geq 1$ it is $w_{s,e}^{p} = 0$.

Constraint (4.6) represents the conditional non-anticipativity constraints i.e. they are applied only when $\mathbb{Z}_e^{s,s'} = True$. In this case, the investment decisions made at $e+1$ must be identical between s and s' since no information will have arrived to distinguish them. Similarly to constraints (3.15)-(3.16), constraint (4.6) can be expressed in mixed integer linear form as follows. Note that the value of M does not affect the solution time or the optimal solution.

$$B_{s,e+1,l,o} - B_{s',e+1,l,o} \geq -M\left(1 - Z_e^{s,s'}\right) \qquad \forall s, s', e, l, o \qquad (4.12)$$

$$D_{s,e+1,n}^{p} - D_{s',e+1,n}^{p} \geq -M\left(1 - Z_e^{s,s'}\right) \qquad \forall s, s' e, n, p \qquad (4.13)$$

Constraint (4.7) determines whether scenarios s, s' are indistinguishable (i.e. $Z_e^{s,s'} = 1$) at epoch e. Set $\aleph$ is defined having as its elements all the unique possible scenario-pairs i.e. $\aleph = \{(s,s') : \forall s, s' \in \Omega_S \; and \; s < s'\}$ and it is partitioned in subsets $\aleph_p, \forall p \in \Omega_p$ where each element of $\aleph$ belongs to exactly one $\aleph_p, p \in \Omega_p$. Sets $\aleph_p$ facilitate the modelling of gradual uncertainty resolution. For instance, every scenario pair in $\aleph_1$ contains the scenarios that will become distinguished after the first storage unit of level $p = 1$ gets deployed in any of them (i.e. there may be many level-1 storage units, but the first of them is that which separates the scenarios from each other). Similarly, every scenario pair in $\aleph_2$ contains scenarios that will separate after the deployment of the first storage unit of level $p = 2$. I.e. storage units of level $p = 1$ do not affect any of the scenario pairs in $\aleph_2$. The same explanation applies to $\aleph_3$ and so on. It becomes evident that the consideration of subsets $\aleph_p$ is a core element of the formulation for problems with gradual DDU resolution as it allows to make the uncertainty resolve only for a subset of the scenarios. Without these subsets the uncertainty will resolve immediately in one epoch as in section 3.2, in which a single investment in DSR resolves the uncertainty everywhere (globally).

As an example, for the problem presented in paragraph 4.1.1 the corresponding set $\aleph = \{(s_1, s_2), (s_1, s_3), (s_1, s_4), (s_2, s_3), (s_2, s_4), (s_3, s_4)\}$, and the subsets are defined as $\aleph_1 = \{(s_1, s_2), (s_1, s_3), (s_1, s_4)\}$, $\aleph_2 = \{(s_2, s_3), (s_2, s_4)\}$, $\aleph_3 = \{(s_3, s_4)\}$ i.e. it is $|\Omega_p| = 3$. Obviously, if more than four scenarios were defined then one could form a greater number of sets $\aleph_p$. Note that the number $|\Omega_p|$ of levels of uncertainty resolution as well as the elements of $\aleph_p \; \forall p$ are predefined and given as an input to the problem. Note also that the reason why every element of $\aleph$ belongs to exactly one subset $\aleph_p$ is that if it belonged to more than one subsets then this duplication would be redundant. For example assume $\aleph_1 = \{(s_1, s_2), (s_1, s_3), (s_1, s_4)\}, \aleph_2 = \{(s_2, s_3), (s_2, s_4), (s_1, s_2)\}$ i.e. (s_1, s_2) belongs to both $\aleph_1$ and $\aleph_2$. After the deployment of the first $level - 1$ unit in any of s_1, s_2, these will separate. Thus, it is redundant to have this scenario pair in $\aleph_2$ because this set has all the scenario pairs that become distinguishable after the deployment of the first $level - 2$ unit (which can only be deployed only after a level 1 unit has been deployed, and by then scenarios s_1, s_2 will have already separated).

Figure 4.5 shows the general form of the resulting gradual uncertainty resolution tree over a finite number of epochs (nodes that are vertically aligned belong to the same epoch) and with the subsets defined for the problem presented in paragraph 4.1.1 i.e. $\aleph_1 = \{(s_1, s_2), (s_1, s_3), (s_1, s_4)\}$, $\aleph_2 = \{(s_2, s_3), (s_2, s_4)\}$, $\aleph_3 = \{(s_3, s_4)\}$. Nodes that contain a dash signify that no storage investment is made (any other investment or no investment at all are both possible) as opposed to those with 'S'. Notice that the resolution of uncertainty takes place after an investment in storage occurs. For instance, if there is no investment in storage at any epoch then the resulting tree will have the shape of a deterministic plan as in Figure 4.1. Similarly if the last storage investment is at node k, then after node m there will be no branching and the nodes will continue on a single path until the end of the horizon. In both the aforementioned cases, the uncertainty will not have resolved completely. Note that the three dots represent any number of nodes in between and, obviously, this number of nodes depends on the number of epochs making up the horizon under study. For example, with six epochs the fully revealed tree (i.e. the one showing the complete resolution of uncertainty) is identical to the one shown in Figure 4.2.

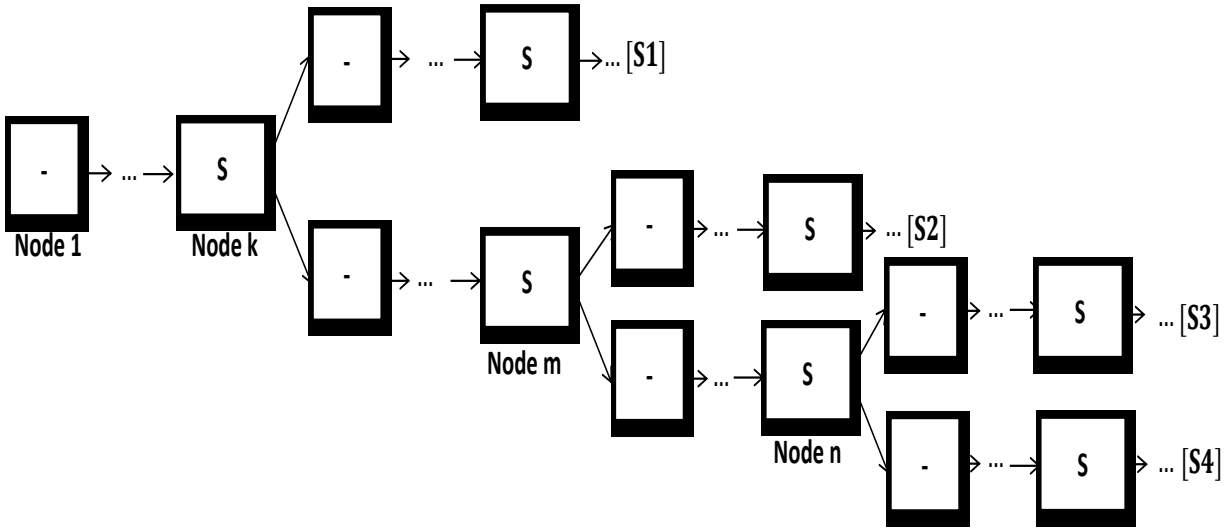


Figure 4.5 Tree illustrating the uncertainty that has resolved completely for a problem with four scenarios and finite number of epochs and with $\aleph_1 = \{(s_1, s_2), (s_1, s_3), (s_1, s_4)\}, \aleph_2 = \{(s_2, s_3), (s_2, s_4)\}, \aleph_3 = \{(s_3, s_4)\}$. White rectangular nodes with the letter S symbolize the decision to invest in storage, while a dash represents the absence of a storage investment (such a node can have a conventional investment decision instead, or no decision at all). The three dots represent a finite number of nodes that do not lead to tree branching. These nodes can be 'S' or '-'depending on the scenario to which they belong.

By populating the sets $\aleph_p$ with different elements from the ones mentioned previously one can create different shapes for the resulting tree as shown in Figure 4.6, for which it is $\aleph_1 = \{(s_1, s_3), (s_1, s_4), (s_2, s_3), (s_2, s_4)\}, \aleph_2 = \{(s_1, s_2), (s_3, s_4)\}$. In this tree, the first level-one storage unit is deployed at node k resulting in the tree expansion (branching) with scenarios S1-S2 and S3-S4 being identical (indistinguishable) to each other. A further investment in storage results in the complete resolution of uncertainty. For example, node m corresponds to the first level-two storage investment meaning that between nodes k and m there must be no other storage investments. However, between nodes m and r there can be further storage investments because the uncertainty resolved completely at node m. That is, if along a particular scenario the uncertainty has resolved then all future storage investments will correspond to the same level p of uncertainty resolution (i.e. will have identical characteristics). See for example scenario S1 in Figure 4.2.

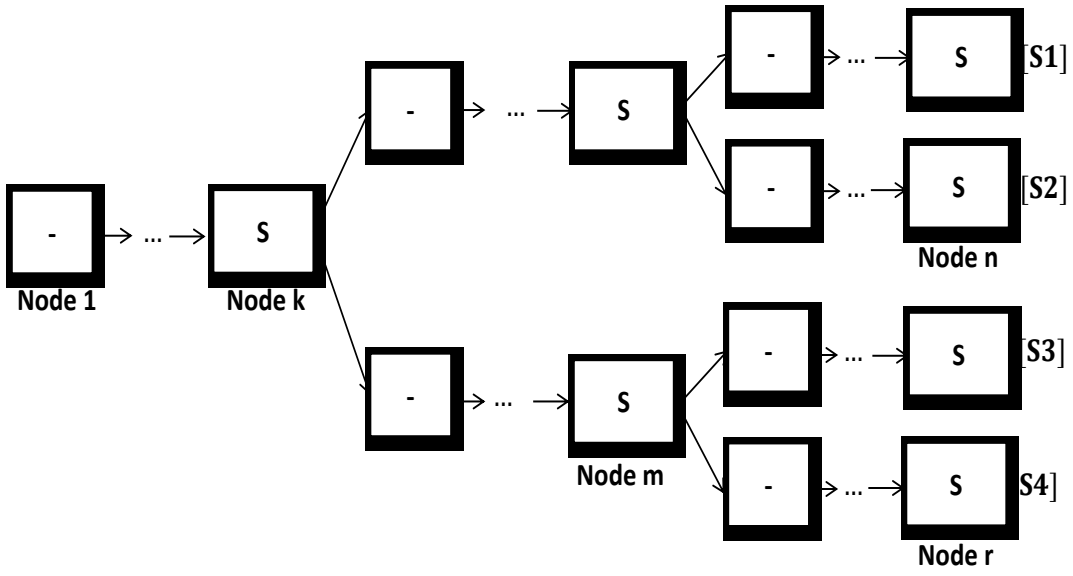


Figure 4.6 Tree illustrating the uncertainty that has resolved completely for a problem with four scenarios and finite number of epochs when $\aleph_1 = \{(s_1, s_3), (s_1, s_4), (s_2, s_3), (s_2, s_4)\}, \aleph_2 = \{(s_1, s_2), (s_3, s_4)\}$.

Constraint (4.7) is analysed as follows. Each element of $\aleph$ is checked to figure out the subset $\aleph_p$ to which it belongs. For instance, (s_1, s_2) belongs to $\aleph_1$. Then, the values for $\mathrm{w}_{\mathrm{s,e}}^{p=1}$ are found for both s_1 and s_2 in order to finally come up with the value for $Z_e^{s_1,s_2}$ that can be 0 (i.e. the two scenarios become distinguishable) or 1 (the two scenarios are indistinguishable). This way the values for all $Z_e^{s_1,s_2}$ are obtained resulting in the shape of the tree. For instance, in Figure 4.2 the S(10) is a level-1 unit and after its deployment the scenario pairs belonging to $\aleph_1$ get distinguished and $\mathbb{w}_{s,e=1}^{p=1} = False\ \forall s$, i.e. across all scenarios at least one (or exactly one) storage unit corresponding to level $p = 1$ has been deployed. Note that it is $\mathbb{w}_{s,e=1}^{p} = True, \forall p \geq 2$. Then, $\mathbb{Z}_{e=1}^{s,s'}$ is computed $\forall (s, s') \in \aleph_1$ to indicate whether or not s, s' are to be differentiated. For example, $\mathbb{Z}_{e=1}^{s_1,s_2} = False$ resulting in the separation of the two scenarios. For the same reason it is $\mathbb{Z}_{e=1}^{s_1,s_3} = False$. Whereas, for the pair (s_2, s_3) that belongs to $\aleph_2$ it is $\mathbb{Z}_{e=1}^{s_2,s_3} = True$ because no first –epoch storage units of level-2 have been deployed. Then, S(4) is a level-2 unit resulting in the scenario pairs $\in \aleph_2$ to be distinguished. Note that S(7), S(8) and S(5) across scenario s_2 are all level-2 units as they all possess identical techno-economical characteristics. The S(5) at node 6 is a level-3 unit leading to separation of scenarios s_3 and s_4 both of which belong to $\aleph_3$. The S(7) and

S(8) across s_3 are also level-3 units while S(8) at Node 10 is a level-4 unit. The equivalent mixed integer linear representation of this constraint is the following.

$$\left(1 - w_{s,e}^{p}\right) + \left(1 - w_{s',e}^{p}\right) + Z_e^{s,s'} \geq 1 \qquad \begin{matrix} \forall e, p \\ \forall s, s' \in \aleph_p \end{matrix} \tag{4.14}$$

$$w_{s,e}^{p} \geq Z_e^{s,s'} \qquad \begin{matrix} \forall e, p \\ \forall s, s' \in \aleph_p \end{matrix} \tag{4.15}$$

$$w_{s',e}^{p} \geq Z_e^{s,s'} \qquad \begin{matrix} \forall e, p \\ \forall s, s' \in \aleph_p \end{matrix} \tag{4.16}$$

According to (4.14)-(4.16) if at least one of $w_{s,e}^{p}, w_{s',e}^{p}$ is equal to zero, then $Z_e^{s,s'} = 0$. That is, if at any of the two scenarios at least one storage unit, corresponding to p, has been deployed then the two scenarios must be distinguished (i.e. uncertainty resolved). Conversely, if $Z_e^{s,s'} = 0$, then it is impossible for both $w_{s,e}^{p}, w_{s',e}^{p}$ to be 1 (see (4.14)); however, it is possible that exactly one (or no one) of $w_{s,e}^{p}, w_{s',e}^{p}$ is 1 meaning that if s, s' are distinguishable then at one of them a storage unit must have been deployed. If $Z_e^{s,s'} = 1$ then it must be that both $w_{s,e}^{p}, w_{s',e}^{p}$ are 1 i.e. if s, s' are identical then it means that in both of these scenarios no storage unit, corresponding to p, has been deployed. Conversely, if both $w_{s,e}^{p}, w_{s',e}^{p}$ are equal to one then it must be $Z_e^{s,s'} = 1$, i.e. if at both scenarios no storage unit has been deployed, then they must be identical.

Constraint (4.8) states that one or more storage units corresponding to level $p + 1$ can be deployed in the system at the earliest in epoch $e + 1$, where e is the epoch when at least one storage unit corresponding to level p has been deployed in the system. For instance, in Figure 4.2 at node 5 the S(7) and S(8) are both level-2 storage units so they can be deployed in the same epoch. Whereas, at nodes 1, 3, 6 and 10 there are units corresponding to different levels deployed in the system and so they are separated by one

epoch. It has been assumed that one epoch is the required time duration for technoeconomical improvements to potentially materialize. The equivalent mixed-integer linear representation of this constraint is the following.

$$\sum_{n} D_{s,e+1,n}^{p+1} \leq M \sum_{n} \widetilde{D}_{s,e,n}^{p} \qquad \forall s, e, p \qquad (4.17)$$

According to (4.17), across a particular scenario s if a level p storage unit has not been deployed in the system (at any bus) by epoch e then no level $p+1$ unit can be deployed at the next epoch i.e. the left-hand side is zero. On the other hand, if at least one level p storage unit has been deployed by epoch e then at least one level $p+1$ storage unit can be deployed in the subsequent epoch. Notice that this formulation allows the unit deployed at $e+1$ to be of the same or of lower level of uncertainty resolution than that deployed at e i.e. this is allowed: $D_{s,e+1,n}^{p-1} \leq M \sum_n \widetilde{D}_{s,e,n}^{p}$. However, given that the objective function involves cost minimization it is clear that higher-level units are always preferred as they possess improved technoeconomical characteristics.

Constraint (4.9) describes the Benders cut that is appended to the master problem at each Benders iteration. Note the similarities with (3.36).

The formulation for the operational subproblem corresponding to Benders iteration i for a particular scenario s, and epoch e consists of (3.21), (3.22) (for DC power flow model), (3.23) and (3.26). It also consists of constraints (4.18)-(4.23) that are presented below.

$$\omega_{s,e}^{i} = \min\left\{\sum_{t,g^*} \tau_e \delta_t c(K_{s,e,g^*}\zeta_{t,g^*} - P_{t,g^*})\right\} \qquad (4.18)$$

$$E_{t,n} = \delta_t J_{t,n} + E_{t-1,n} \qquad \forall t, n \qquad (4.19)$$

$$E_{t,n} \leq \sum_{p} \Delta_n^p \Psi_s^p \qquad \forall t, n \qquad (4.20)$$

$$|J_{t,n}| \leq \sum_{p} \Delta_n^p \overline{\Psi}_s^p \qquad \forall t, n \qquad (4.21)$$

$$\sum_{g} P_{t,g} I_{n,g} + \sum_{l} P_{t,l} L_{n,l} = J_{t,n} + d_{t,n} \qquad \forall t, n \qquad (4.22)$$

$$\Delta_n^p = \widetilde{D}_{s,e,n}^{p,i} : \mu_n^{p,i} \qquad \forall n \qquad (4.23)$$

The objective function for the operational subproblem is equal to the discounted cost of curtailment of the output of the renewable DG unit; the product $K_{s,e,g^*}\zeta_{t,g^*}$ constitutes the maximum possible output of the unit (determined by the availability of the wind resource for the DG-wind unit g^* denoted by ζ_{t,g^*}) while P_{t,g^*} is its actual output. Notice that there is no cost involved for storage operation. Constraint (4.19) determines the energy capacity of a storage unit at t as being equal to its capacity at $t-1$ plus/minus the energy charged/discharged, assuming no losses when transferring the stored energy from period $t-1$ to t. The bounds for storage capacity $E_{t,n}$ and storage power $J_{t,n}$ are shown in (4.20)-(4.21) respectively. Uncertain parameter Ψ_s^p (maximum storage energy capacity) is the upper bound for $E_{t,n}$ while $\overline{\Psi}_s^p$ (maximum storage power capability) is the upper bound for $|J_{t,n}|$; both upper bounds are uncertain, as they are functions of s. Notice that $E_{t,n}$ can assume nonnegative real values, while $J_{t,n}$ can take on positive (signifying charging of the storage unit i.e. it behaves like a load thereby increasing local demand) and negative (for power discharged by the storage unit i.e. reduction of demand at the bus) real values. Regarding the summation (over all p) appearing in the right-hand side of both (4.20)-(4.21) it is targeted to yield the storage unit located at bus n. This is because every bus can accommodate at most one such unit (regardless of the level p), which is defined by the value of $\widetilde{D}_{s,e,n}^{p}$. Thus, instead of employing variables $E_{t,n}^p$ and $J_{t,n}^p$ that are also functions of p, these are defined only for the combination (t, n). Finally, (4.22) imposes system

energy balance (per bus) while considering actions from storage assets, while (3.26)-(4.23) generate the Lagrangian multipliers.

4.1.4 *Solution Methodology*

Table 4.3 displays the performance of various solution methodologies, yielding the output presented in Figure 4.2. In particular, ND signifies the nondecomposed version of the problem, and IFI, IFI_s, $\text{IFI}_\text{s,e}$ signify the decomposed version where 1, $|\Omega_s|$ and $|\Omega_{s,e}|$ cuts are generated per iteration respectively.

Clearly, the advantage of all decomposed versions is the reduced memory consumption; 95% reduction is achieved. However, among all decomposed versions only $\text{IFI}_\text{s,e}$ manages to converge as it involves the transfer of a larger amount of gradient information between the master and the operational subproblems.

	Number of Benders iterations	**Operational subproblems solved**	**Solution time**	**Average memory consumption**
ND	-	-	3 hours	15 GB
IFI	-	-	>2 days	N/A
IFI_s	-	-	>2 days	N/A
$\text{IFI}_{s,e}$	44	4000	13 minutes	0.6 GB

Table 4.3 Comparison of solution methodologies. Solution times '>2 days' indicate that running of the algorithm was stopped after 48 hours as there were no signs of an imminent convergence. The ND and $\text{IFI}_\text{s,e}$ converge at the output depicted in Figure 4.2.

Table 4.4 provides insight into why the type of Benders cut (α_s versus $\alpha_{s,e}$) is so important when it comes to solution times. In particular, as the iteration index increases there is *insignificant* increase in the solution time of the operational subproblems because the formulation remains the same as no additional constraints are added. However, the master, which is an MILP problem solved via the Branch and Bound method, takes more time to solve as more and more Benders cuts are added to its formulation. For instance, in order to find the solution to the master when α_s type of cut is used, a search tree of 223,000 nodes is created and the solution is found in 540 seconds (iteration 850). However, this does

not happen with an $\alpha_{s,e}$ type of cut because it involves greater amount of information passed from one iteration to the next (a number of $|\Omega_S||\Omega_E|$ cuts are appended to the master problem per iteration) resulting in a more accurate way of shaping the feasible space allowing for fast tracking of the optimal solution. Thus, the algorithm converges before the master grows in size significantly enough. On the other hand, the a_s type of cut does not provide sufficiently accurate amount of information per iteration that would restrict the feasible region sufficiently. Thus, it takes longer for the search tree to find solutions.

	IFI$_s$						**IFI$_{s,e}$**					
Iteration	**20**		**620**		**850**		**5**		**20**		**44 (final)**	
Master	15	387	370	144k	540	223k	5	739	10	1053	40	32k
Operational	0.5		4.3		4.6		0.5		0.5		1.1	

Table 4.4 Comparison of IFI_s and $IFI_{s,e}$ yielding the solution depicted in Figure 4.2. The second row shows the iteration index. The third row shows the number of seconds required for the master to be solved at that iteration, and the number of nodes explored in the Branch and Bound search tree, respectively. The last row shows the number of seconds it takes for all operational subproblems to be solved.

For tractability reasons the duration of the year is represented using typical days. Note that this approximation is important in order to estimate the annual operational costs (the investment costs are expressed in annual terms as well). Figure 4.7 illustrates the principle of Benders decomposition using typical days for the representation of the year. This method is similar to that of typical weeks (see Figure 3.18); five typical days represent the four seasons of the year (winter, spring, summer, autumn) plus an extra typical day for the representation of the peak day (occuring in winter). Each day has a certain frequency of occurrence within a year (e.g. 90 is the frequency corresponding to the autumn typical day meaning that this typical day is assumed to occur 90 times in a year) with the condition that the sum of the annual frequencies equals 365. Notice that there has been no time-coupling among the typical days i.e.(4.19) applies only within the duration of a typical day and this is actually the benefit of using typical days in the first place. Figure 4.7 also depicts the way by which the master and operational subproblems are solved. In particular, since the master problem is a mixed-integer linear problem (MILP) it is solved via Branch and Bound, while each operational subproblem is solved via Simplex as it is a linear programming problem.

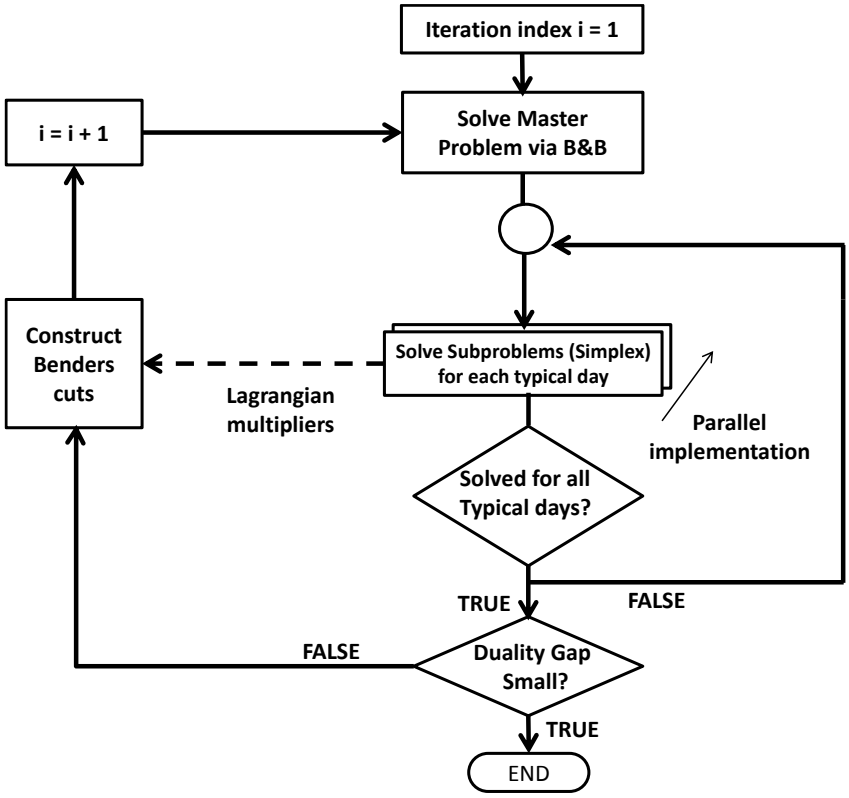


Figure 4.7. Principle of operation of Benders Decomposition when using a number of typical days to represent the full time-domain of a year.

4.2 *Gradual & Local resolution of DDU*

In this section a case study is presented that applies to a distribution network that undergoes load and DG capacity growth over a ten-year horizon. In order to accommodate the resulting rising power flows the planner has the possibility to invest in conventionally upgrading lines and / or investing in DSR technology along with conducting a marketing study that leads to increased consumer participation in DSR). However, the way by which optimal investment decisions will be made is not straightforward due to uncertainty. In particular the source of uncertainty, which is the consumer participation in DSR, is of decision-dependent type (i.e. does not resolve with the passage of time but only after some action has been taken from the planner) and resolves gradually (i.e. across a number of epochs after many investment decisions are made) and globally (i.e. not only at the bus where the corresponding investment is made but across the system). The results show that the deployment of DSR in the system allows not only for accommodating the rising power flows but also for generating significant cost savings while emphasizing the importance of

investing in DSR as early as possible or otherwise costs are higher. This happens because by investing in DSR early, uncertainty resolves early thereby resulting in future investment decisions that are targeted to the realized system state i.e. stranding risk is minimized.

Conducting the studies involves modelling the problem in a stochastic optimization programming formulation and using various Benders decomposition techniques (e.g. multicut, monocut, sequential, parallel as well as the novel Intelligent Filtering Implementation) to produce results within reasonable solution times. Finally, the methodology for obtaining the option value of DSR under decision dependent uncertainty is presented with relevant insights and explanations being provided.

4.2.1 *Problem description*

The distribution network shown in Figure 3.1 is studied across five two-year epochs with input data as in Table 3.1, Table 3.2, Table 3.4, Figure 2.3 and Figure 2.4. Out of all candidate DSR locations (i.e. load-buses: 2, 4, 5, 7, 8 and 10), buses 5 and 8 are characterized by uncertainty ('uncertain buses') around the consumer participation level in a deployed DSR scheme as shown in Figure 4.8. At each uncertain bus there are three levels of uncertainty resolution: The first describes the situation where the DSR has not been deployed. The second characterizes the state of learning immediately after the DSR deployment and the third applies after a marketing campaign has been conducted (at a cost equal to one third of the DSR investment cost as mentioned below) with the aim of increasing the observed consumer participation (i.e. the consumers have more flexible than they were initially willing to shift). Note that the marketing campaign can be conducted one epoch after the corresponding DSR investment in order to first allow the DSR to operate for one epoch and then extract conclusions about the observed customer participation levels. This information is illustrated in a tree-structure using four scenarios ($S_1 \dots S_4$), each with a corresponding probability (20%, 20%, 25%, and 35%). Note that all buses other than 5 and 8 have an a-priori known negligible consumer participation which stays fixed for the remaining of the horizon.

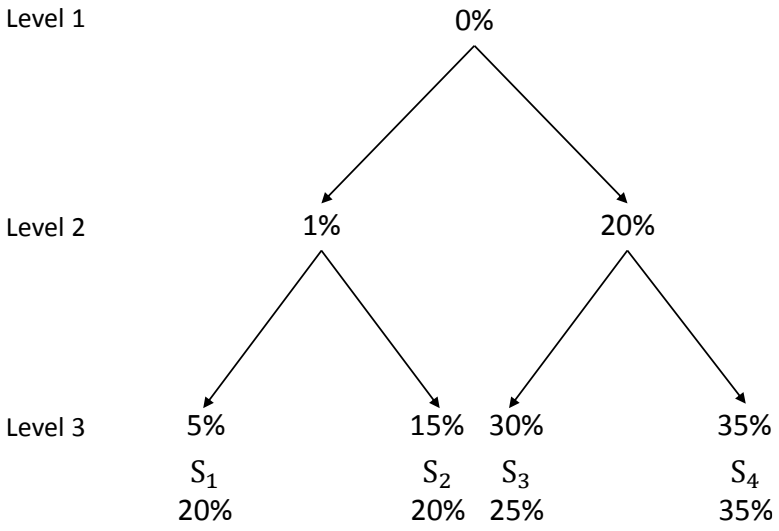


Figure 4.8 Consumer participation in the DSR scheme for an uncertain bus. In this example, uncertain are buses 5 and 8. There are three levels of uncertainty resolution and four scenarios ($S_1 \dots S_4$), each with a corresponding probability (20%, 20%, 25%, and 35%).

Notice that this is a type of *decision-dependent uncertainty* because it can be resolved only after an investment in DSR (at an uncertain bus) has been made. Its resolution is *gradual* because multiple investments conducted over more than one epoch are required for complete resolution. Finally, the resolution is *local* because each investment does not lead to uncertainty resolution across the system but only at a particular location.

4.2.2 *Results of the optimization studies*

The network planner's objective is to determine the investment decisions that minimize the sum of the total expected investment and operational cost, so as to guarantee that the total system load is supplied at all times. The latter cost consists of the cost of curtailing the output of the DG-wind unit and the cost of payments to consumers for their participation in the DSR scheme as in Table 3.4. Figure 3.2 displays the optimal investment strategy if only the conventional technology is available to the planner. Figure 4.9 shows the optimal investment strategy for a network planner who has the DSR and the conventional technologies available for investment. The availability of DSR allows for a radically different investment approach leading to total expected system cost of £1.25m.

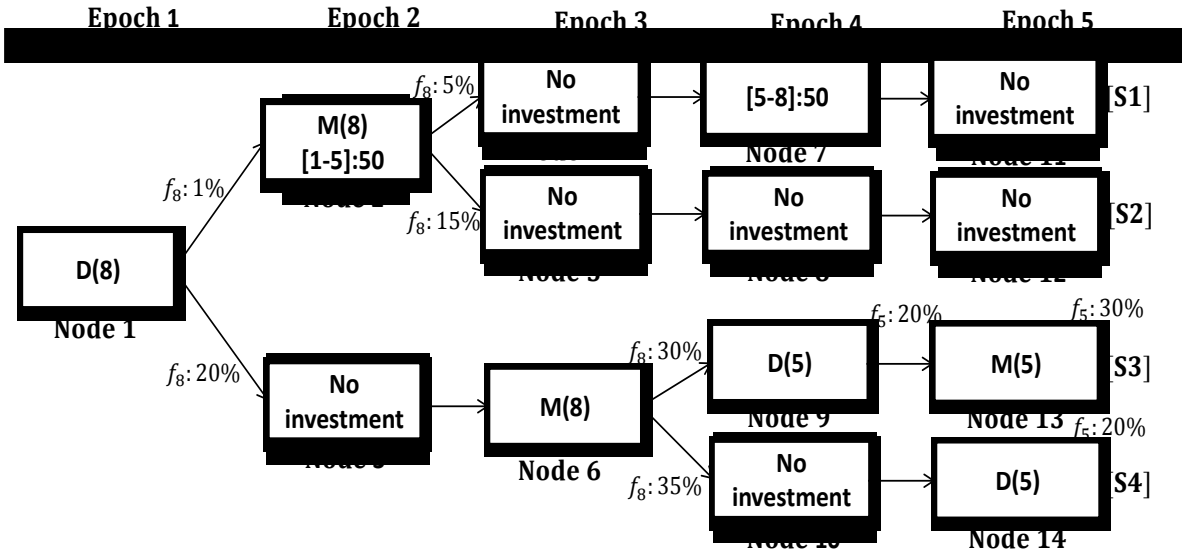


Figure 4.9 Optimal investment strategy for a network planner with two technologies available: DSR and conventional reinforcement. The D(x) means that the decision to invest in DSR technology at bus x is made. The M(x) means that the decision to conduct a marketing campaign at bus x is made. The f_8: 20% signifies that at bus 8 the consumer participation is 20%. The [x-y]:50 means that the decision is taken to reinforce each of the lines between buses x and y by 50kW. Thus [1-5]:50 means [1-2]:50, [2-3]:50, [3-5]:50. Conventional investments become operational in the subsequent epoch. The brackets at the rightmost corner show to which scenarios the depicted investment paths correspond.

The DSR scheme has two functions. The first is the uncertainty resolution, which allows for conditional investment, and the second is load shifting that prevents exceeding line thermal limits and leading toconventional investment deferral.

Regarding uncertainty resolution, the DSR scheme that gets deployed at bus 8 (node 1) leads to the resolution of the uncertainty around consumer participation at bus 8; this quantity stands either at 1% (scenarios S1, S2) or 20% (S3, S4). Seeing that 1% is insufficient to cover the increasing power flows the planner decides to run a marketing campaign at the same bus at node 2 along with a 50kW upgrade of each of the lines 1-2, 2-3, 3-5 (as a reminder the network diagram is shown in Figure 3.1). The marketing campaign increases the participation at bus 8 to either 5% (scenario S1) or 15% (scenario S2). In the former case the planner optimally decides to resort to a total of 100kW of line upgrades at node 7 (i.e. lines 5-6 and 6-8 are upgraded with 50kW each) which becomes operational in the last epoch (node 11). However, in the event of 15% participation no further investment is taking place. Also, at node 6 the marketing campaign leads to the distinction of scenarios S3 and S4 at 30% (S3) or 35% (S4) according to Figure 4.8. with a decision to deploy a

DSR at bus 5 at node 9 (operating at 20%) followed by a marketing campaign conducted at node 13 leading to an increase of the participation value to 30% at bus 5. At node 14, the DSR at bus 5 operates at 20%.

Notice that in the presented case study the uncertain bus that is first fit with a DSR scheme leads to complete uncertainty resolution as per Figure 4.8. Particularly, bus 8 is first fit with a DSR resulting in partial uncertainty resolution (second level) at the end of epoch 1 and complete uncertainty resolution (third level) at nodes 2 and 6. If bus 5 was first fit with DSR then the same observation would be made. However, for the uncertain bus that is fit with DSR after the first one has been fit the same observation does not apply; investment in DSR at bus 5 (node 9) does not lead to a branching similar to that at node 1, as Figure 4.8 suggests. Similarly, the investment in marketing campaign at the same bus (node 13) does not lead to a branching similar to that at node 2. This discrepancy lies in a modelling simplification, adopted in the current example for tractability purposes, according to which when the second uncertain bus (whichever it is) is deployed with DSR then the revealed value of consumer participation will be the one revealed in the case of the first uncertain bus at the current scenario. Thus, at node 9 the second level value (20%) is the one revealed for bus 8 (node 1) while the third-level value (30%) is the one revealed at node 6 (for scenario S3). Without this modelling simplification it would be necessary to consider far greater number of scenarios rather than just four (as per Figure 4.8) in order to account for all possible combinations of uncertainty resolution cases, resulting in intractable solution times with the currently developped solution algorithms; future work on this research may produce algorithms allowing for this modelling capability to be included.

Regarding load-shifting operations, these are performed for the exact same purpose as described in paragraphs 3.1.2 and 3.2.2 i.e. during periods of small wind output, the DSR schemes disconnect load so that less power has to be imported through the substation and, thus, keep the power flows within the corresponding thermal limits.

The option value of investing in DSR technology under this type of DDU is equal to the difference in the total expected system cost in the resulting strategies where the DSR is available (Figure 4.9) and where it is not (Figure 3.2). This difference amounts to £3.63m - £1.25m = £2.38m, representing the expected value of the net benefit accrued from optimally investing in DSR technology. This net benefit stems from the ability of DSR technology to

perform load-shifting operations as well as to resolve uncertainty which allows conditionally investments.

It is important to mention that in the first epoch (node1) no DSR operation takes place. In other words, this investment is made solely for purposes of uncertainty resolution. Figure 4.10 shows the resulting investment strategy if the planner opts to not allow investment in DSR in the first epoch. The resulting total expected cost amounts to £2.37m. It can be seen that lines 1-2, 2-3 and 3-5 are set to be upgraded by 50kW each in the first epoch. Then, a DSR investment takes place at bus 8 at epoch 3, with a marketing campaign being conducted only in case that the participation levels are 1% along with an upgrade of line 5-8. The reason for the first-epoch conventional reinforcement decision is the fact that at epoch 2 all lines between buses 1 and 5 need to accommodate the rising power flows and the DSR at bus 8 alone would be insufficient (the addition of a DSR at bus 5 would not help either in the event of 1% participation levels).

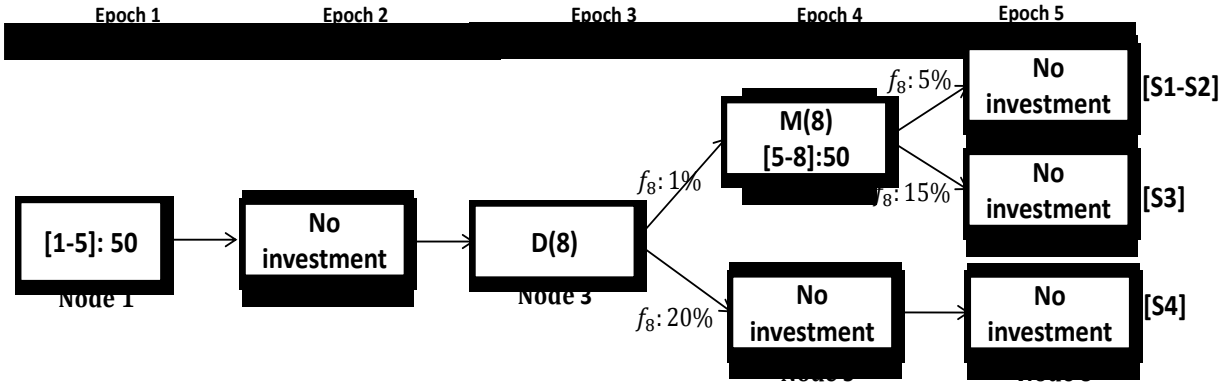


Figure 4.10 Optimal strategy for a planner with two technologies available: DSR and conventional line upgrade. The planner does not have the possibility to invest in DSR in the first epoch, but has this possibility in all other epochs. The percentage values correspond to the values for the consumer participation.

In conclusion this case study corroborates the conclusions observed in sections 3.1 and 3.2 indicating that an early DSR investment (initially operating as a pilot scheme aiming to gauge the consumer participation levels in DSR) can yield considerably reduced total expected system costs by allowing early resolution of the endogenous uncertainty which will provide information about how to optimally reinforce the network. These studies reveal the significant option value embedded in DSR technology under DDU.

4.2.3 *Mathematical Formulation*

The nomenclature for the mathematical formulation follows.

Sets and indices

Ω_E	Set of epochs, indexed e.
Ω_L	Set of distribution lines, indexed l.
Ω_N	Set of system buses, indexed n.
Ω_{NU}	Set of uncertain system buses i.e. buses that exhibit DDU, indexed n^*.
Ω_O	Set of conventional investment alternatives indexed o.
Ω_P	Set of levels of local uncertainty resolution, indexed $\mathbb{p} \in \{1,2,3\}$.
$\mathbb{C}_{s,s'}$	Set defined as $\left\{(s,s') \middle\| \left(f_s^{(2)} = f_{s'}^{(2)}\right), \forall s,s' \in \Omega_S\right\}$.

Input Parameters

γ_D	Investment cost for a DSR scheme $(£/year)$
γ_o	Investment cost for a line upgrade with o $(£/year)$
γ_N	Investment cost for a marketing campaign for DSR $(£/year)$
k_N	Build time for a marketing campaign (epochs).
$d_{s,e,t,n}$	Demand at n, in s,e,t (kW).
$f_s^{(3)}$	Consumer participation (flexible load) after the marketing campaign has been conducted.
$f_s^{(2)}$	Consumer participation (flexible load) after the DSR deployment but before the marketing campaign has been conducted.
$\bar{\bar{f}}$	Consumer participation (flexible load) for buses that are not uncertain.
$A_{s,s'}$	It is $A_{s,s'} = 1 \Leftrightarrow (s,s') \in \mathbb{C}_{s,s'}$. Otherwise, it is zero.I.e. this parameter informs about whether or not two scenarios are identical in terms of

the value of flexible load at the second level of uncertainty resolution.

Decision Variables

$a_{s,e}^{i}$	Approximate operational cost at s, e for Benders iteration i.
Δ_n	Continuous variable representing $\widetilde{D}_{s,e,n}$ in the operational subproblem.
M_n	Continuous variable representing $\widetilde{N}_{s,e,n}$ in the operational subproblem.
$\omega_{s,e}^{i}$	Objective function of the operational subproblem for s, e at Benders iteration i.
ξ_s^I	Total investment cost for s.
$\lambda_{s,e,l,o}^{i}$	Dual variable $\in \mathbb{R}$ yielded from the operational subproblem for s, e, l, o at Benders iteration i.
$\mu_{s,e,n}^{i}$	Dual variable $\in \mathbb{R}$ yielded from the operational subproblem for DSR at s, e, n, at Benders iteration i.
$m_{s,e,n}^{i}$	Dual variable $\in \mathbb{R}$ yielded from the operational subproblem for marketing campaign at s, e, n, at Benders iteration i.
$B_{s,e,l,o}$	Binary decision to upgrade line l by o at s, e.
$\mathbb{B}_{s,e,l,o}$	Boolean representation for $B_{s,e,l,o}$.
$D_{s,e,n}$	Binary decision to invest in a DSR scheme at s, e, n.
$\mathbb{D}_{s,e,n}$	Boolean representation for $D_{s,e,n}$.
$\widetilde{\mathbb{D}}_{s,e,n}$	Boolean representation for $\widetilde{D}_{s,e,n}$.
$\widetilde{D}_{s,e,n}$	Continuous state variable for $D_{s,e,n}$.
$e_{e,n}^{\mathbb{p},s}$	Binary variable indicating whether $\mathbb{p}$ represents the current level of uncertainty resolution at bus n in epoch e for scenario s.
$\tilde{e}_{e,n^*}^{\mathbb{p},s,s'}$	Binary variable assuming the value '1' if $e_{e,n^*}^{\mathbb{p},s} = 1 = e_{e,n^*}^{\mathbb{p},s'}$.

$\mathbb{e}_{e,n}^{\mathbb{p},s}$ Boolean representation for $e_{e,n}^{\mathbb{p},s}$.

$F_{s,e,l,o}$ Continuous variable for the capacity (on top of the initial capacity) by which line l is upgraded by o at s, e (kW).

$\tilde{F}_{s,e,l,o}$ Continuous state variable aggregating all investment decisions $F_{s,e,l,o}$ while considering their corresponding build times.

$H_{e,n}^{s,s'}$ Binary variable indicating whether scenarios s, s' differ in $f_s^{(2)}$ after DSR deployment (at n) and prior to conducting the marketing campaign there. If this is true, then it takes the value of zero.

$\mathbb{H}_{e,n}^{s,s'}$ Boolean representation for $H_{e,n}^{s,s'}$.

$N_{s,e,n}$ Binary decision to invest in marketing campaign at s, e, n.

$\widetilde{N}_{s,e,n}$ Continuous state variable for $N_{s,e,n}$.

$\mathbb{N}_{s,e,n}$ Boolean representation for $N_{s,e,n}$.

$\widetilde{\mathbb{N}}_{s,e,n}$ Boolean representation for $\widetilde{N}_{s,e,n}$.

$T_{e,n}^{s,s'}$ Binary variable in the master problem for determining the distinguishability of two scenarios..

$\mathbb{T}_{e,n}^{s,s'}$ Boolean representation for $T_{e,n}^{s,s'}$.

$Z_e^{s,s'}$ Binary variable stating whether or not scenarios s, s' are indistinguishable by e.

$\mathbb{Z}_e^{s,s'}$ Boolean representation for $Z_e^{s,s'}$.

The problem formulation is presented in a decomposed form using Benders algorithm, with (3.36), (3.2) being the lower and upper bounds respectively. The formulation for the master problem follows.

$$\xi_s^I = \sum_e \left(\sum_l \sum_o B_{s,e,l,o} \gamma_o + \sum_n (D_{s,e,n} \gamma_D + N_{s,e,n} \gamma_N \right) \qquad \forall s \qquad (4.24)$$

$$N_{s,e,n} \leq \widetilde{D}_{s,e-1,n} \qquad \forall s,e,n \qquad (4.25)$$

$$\widetilde{N}_{s,e,n} = \sum_{z=1}^{e-k_N} N_{s,z,n} \qquad \forall s,e,n \qquad (4.26)$$

$$N_{s,1,n} = N_{s',1,n} \qquad \forall s,s',n \qquad (4.27)$$

$$\mathbb{Z}_e^{s,s'} = True \Leftrightarrow \mathbb{N}_{s,e+1,n} = \mathbb{N}_{s',e+1,n} \qquad \forall s,s',e,n \qquad (4.28)$$

$$\mathbb{e}_{e,n^*}^{p,s} = True \Leftrightarrow \widetilde{\mathbb{D}}_{s,e,n^*} = False \qquad \forall s,e,n^*, \ \mathbb{p} = 1 \qquad (4.29)$$

$$\mathbb{e}_{e,n^*}^{\mathbb{p},s} = True \Leftrightarrow (\widetilde{\mathbb{D}}_{s,e,n^*} = True \bigwedge \widetilde{\mathbb{M}}_{s,e,n^*} = False) \qquad \forall s,e,n^*, \ \mathbb{p} = 2 \qquad (4.30)$$

$$\bigoplus_p \mathbb{e}_{e,n^*}^{\mathbb{p},s} = True \qquad \forall s,e,n^* \qquad (4.31)$$

$$\mathbb{H}_{e,n^*}^{s,s'} = True \Leftrightarrow \left\{ \begin{array}{c} \mathbb{e}_{e,n^*}^{2,s} = True \\ \bigwedge \\ \mathbb{e}_{e,n^*}^{2,s'} = True \\ \bigwedge \\ A_{s,s'}^{e} = 1 \end{array} \right\} \qquad \forall s,s',e,n^* \qquad (4.32)$$

$$\mathbb{T}_{e,n^*}^{s,s'} = True \Leftrightarrow \left\{ \begin{array}{c} \left\{ \mathbb{e}_{e,n^*}^{1,s} = True \bigwedge \mathbb{e}_{e,n^*}^{1,s'} = True \right\} \\ \bigvee \\ \mathbb{H}_{e,n^*}^{s,s'} = True \end{array} \right\} \qquad \forall s, s', e, n^* \qquad (4.33)$$

$$\mathbb{Z}_{e}^{s,s'} = True \Leftrightarrow \bigwedge_{n^*} \mathbb{T}_{e,n^*}^{s,s'} = True \qquad \forall s, s', e \qquad (4.34)$$

$$a_{s,e}^{i} \geq \pi_s \omega_{s,e}^{i-1} + \sum_{l} \sum_{o} \pi_s \lambda_{s,e,l,o}^{i-1} \left(\tilde{F}_{s,e,,l,o} - \tilde{F}_{s,e,,l,o}^{i-1} \right) + \sum_{n} \pi_s \mu_{s,e,n}^{i-1} (\widetilde{D}_{s,e,n} - \widetilde{D}_{s,e,n}^{i-1}) + \sum_{n} \pi_s m_{s,e,n}^{i-1} (\widetilde{N}_{s,e,n} - \widetilde{N}_{s,e,n}^{i-1}) \qquad \forall s, e \qquad (4.35)$$

Equation (3.37) is the objective function of the master problem, with (4.24) describing the total investment cost per scenario s, including the cost of DSR deployment γ_D and the cost γ_N of conducting a marketing campaign with the aim of further increasing the consumer participation at the bus. Notice that across every scenario each line can be upgraded at most once (by any of the available capacities), at most one DSR scheme can be deployed per bus and at most one marketing campaign can be conducted per bus. Constraint (4.25) states that at least one epoch needs to have passed after DSR deployment so that a decision for conducting a marketing campaign can be considered, reflecting the fact that some minimum amount of time is required for the DSR to operate at an area before measures for increasing consumer responsiveness are considered (thus, in the first epoch it is $N_{s,e,n} = 0$). Constraint (4.26), similar to (3.5) - (3.6) that are also included in the formulation, define the state variables that aggregate all investment decisions taken in the past while considering their corresponding build times, with variable $F_{s,e,l,o}$ linked to $B_{s,e,l,o}$ according to (3.7). Constraint (4.27), similar to (3.8)-(3.9) that are also both included in the formulation, constitute the initial non-anticipativity constraints, which force the first-epoch investment decisions to be identical across s, s' as no information has arrived to allow for their distinction. Constraint (4.28) is similar to (3.11), which is also incorporated in this formulation, representing the conditional non-anticipativity constraint i.e. the equality is

applied only when $\mathbb{Z}_e^{s,s'} = True$. In this case, the investment decisions made at $e+1$ must be identical between s and s' since no information will have arrived to distinguish them. This constraint can be expressed in mixed integer linear form as in (4.36) in the same way as (3.15)-(3.16).

$$N_{s,e+1,n} - N_{s',e+1,n} \geq -M\left(1 - Z_e^{s,s'}\right) \qquad \begin{matrix} \forall s \neq s', \\ \forall e, n \end{matrix} \qquad (4.36)$$

Constraints (4.29)-(4.31) determine the three levels of local DDU resolution for any uncertain bus n^* ; since no uncertainty exists in other buses, these constraints do not apply anywhere else. Specifically, (4.29) states that $\text{e}_{e,n}^{1,s} = True$ (i.e the current level of DDU resolution is the first) only if by epoch e (current epoch) a DSR scheme has not been deployed at n^*. This constraint can be written in a mixed integer linear form as follows.

$$1 - e_{e,n^*}^{\mathbb{p},s} \leq \widetilde{D}_{s,e,n^*} \qquad \begin{matrix} \forall s, e, n^*, \\ \mathbb{p} = 1 \end{matrix} \qquad (4.37)$$

$$\widetilde{D}_{s,e,n^*} \leq M(1 - e_{e,n^*}^{\mathbb{p},s}) \qquad \begin{matrix} \forall s, e, n^*, \\ \mathbb{p} = 1 \end{matrix} \qquad (4.38)$$

According to (4.37)-(4.38), if no DSR has been deployed ($\widetilde{D}_{s,e,n^*} = 0$) by the current epoch then it must be $e_{e,n^*}^{1,s} = 1$. On the other hand, if $\widetilde{D}_{s,e,n^*} = 1$ then it must be $e_{e,n^*}^{1,s} = 0$. Note that there is no reference to $\widetilde{N}_{s,e,n}$ because the value for $e_{e,n}^{1,s}$ depends on $\widetilde{D}_{s,e,n}$ but not on $\widetilde{N}_{s,e,n}$. Constraint (4.30) states that $\text{e}_{e,n}^{2,s} = True$ (i.e. current level of uncertainty resolution is the second) only if by the current epoch a DSR scheme has been deployed at n^* but without having conducted a marketing campaign there. This constraint can be expressed in mixed integer linear form as follows.

$$1 - e_{e,n^*}^{\mathbb{p},s} \leq 1 - \widetilde{D}_{s,e,n^*} + \widetilde{N}_{s,e,n^*} \qquad \begin{matrix} \forall s, e, n^*, \\ \mathbb{p} = 2 \end{matrix} \qquad (4.39)$$

$$1 - \widetilde{D}_{s,e,n^*} + \widetilde{N}_{s,e,n^*} \leq M(1 - e_{e,n^*}^{\mathbb{p},s}) \qquad \forall s, e, n^*, \; \mathbb{p} = 2 \tag{4.40}$$

According to (4.39)-(4.40), if $\widetilde{D}_{s,e,n^*} = \widetilde{N}_{s,e,n^*} = 0$, then it must be $e_{e,n^*}^{2,s} = 0$. Similarly, with $\widetilde{D}_{s,e,n} = \widetilde{N}_{s,e,n} = 1$ it is $e_{e,n}^{2,s} = 0$. Note that the combination of values $\widetilde{D}_{s,e,n} = 0, \widetilde{N}_{s,e,n} = 1$ is not possible (a marketing campaign can be waged only after DSR deployment). However, having $\widetilde{D}_{s,e,n} = 1, \widetilde{N}_{s,e,n} = 0$ is possible and results in $e_{e,n}^{2,s} = 1$.

Constraint (4.31), where $\oplus$ is the symbol for the eXclusive OR, states that exactly one of the variables $\mathbb{e}_{e,n}^{\mathbb{p},s}$ must be $True$ (i.e. the summation of $e_{e,n^*}^{1,s}$, $e_{e,n^*}^{2,s}$, $e_{e,n^*}^{3,s}$ is one) meaning that every operating point s, e, n has to correspond to exactly one level of uncertainty resolution. Note that the third level $\mathbb{p} = 3$ pertains to the situation where both DSR and marketing campaign have been made by epoch e. For example, some indicative values corresponding to Figure 4.9 are $e_{e_1,n_5}^{1,s} = 1, \forall s$, $e_{e_1,n_8}^{2,s} = 1, \forall s$, $e_{e_2,n_8}^{3,s} = 1, \forall s \in \{S_1, S_2\}, e_{e_4,n_5}^{2,s_3} = 1, \forall s$. .

According to (4.32), it is $\mathbb{H}_{e,n^*}^{s,s'} = True$ when the current level of uncertainty resolution at $n^*$is the second (i.e. $\mathbb{e}_{e,n^*}^{2,s} = True$ and $\mathbb{e}_{e,n^*}^{2,s'} = True$. This is equivalently expressed as $\tilde{e}_{e,n^*}^{2,s,s'} = True$ and means that a DSR has been deployed at n^* but a marketing campaign has not been waged|) and $f_s^{(2)} = f_{s'}^{(2)}$ (i.e. $A_{s,s'} = 1$). For instance, in Figure 4.8 at level 2 it is $f_{S_1}^{(2)} = f_{S_2}^{(2)} = 1\%$ and $f_{S_3}^{(2)} = f_{S_4}^{(2)} = 20\%$. Thus, it is $\mathbb{C}_{s,s'} = \{(S_1, S_2), (S_3, S_4)\}$. This information is passed in the formulation via parameter $A_{s,s'}$ meaning that $A_{S_1,S_2} = 1, A_{S_3,S_4} = 1$. Notice that the fact that $A_{S_1,S_2} = 1$ does not mean that $e_{e,n^*}^{2,s} = 1$ as the former is a parameter (i.e. constant value) and the latter is a decision variable. In particular the values of these two are independent; being in the second level of uncertainty resolution does not guarantee that $f_s^{(2)} = f_{s'}^{(2)}, \forall s, s'$ and, so, variable $\mathbb{H}_{e,n}^{s,s'}$ helps this identification. This constraint can be expressed in mixed integer linear form as follows.

$$1 + H_{e,n^*}^{s,s'} \geq \tilde{e}_{e,n^*}^{2,s,s'} + A_{s,s'} \qquad \forall s, s', e, n^*, \tag{4.41}$$

$$\tilde{e}_{e,n^*}^{2,s,s'} \geq H_{e,n^*}^{s,s'} \qquad \forall s, s', e, n^*, \qquad (4.42)$$

$$A_{s,s'} \geq H_{e,n^*}^{s,s'} \qquad \forall s, s', e, n^*, \qquad (4.43)$$

Where $\tilde{e}_{e,n^*}^{2,s,s'} = 1$ means that $e_{e,n^*}^{2,s} = 1 = e_{e,n^*}^{2,s'}$ and is expressed in a mixed integer linear form as follows:

$$1 + \tilde{e}_{e,n^*}^{2,s,s'} \geq e_{e,n^*}^{2,s} + e_{e,n^*}^{2,s'} \qquad \forall s, s', e, n^*, \qquad (4.44)$$

$$e_{e,n^*}^{2,s} \geq \tilde{e}_{e,n^*}^{2,s,s'} \qquad \forall s, s', e, n^*, \qquad (4.45)$$

$$e_{e,n^*}^{2,s'} \geq \tilde{e}_{e,n^*}^{2,s,s'} \qquad \forall s, s', e, n^*, \qquad (4.46)$$

According to (4.41)-(4.43), if $\tilde{e}_{e,n^*}^{2,s,s'} = 0$ or $A_{s,s'} = 0$ or both, then $H_{e,n}^{s,s'} = 0$, otherwise ($\tilde{e}_{e,n^*}^{2,s,s'} = A_{s,s'} = 1$) it becomes $H_{e,n}^{s,s'} = 1$. This variable takes the following values corresponding to Figure 4.9: $H_{e_1,n_8}^{S_1,S_2} = 1 = H_{e_1,n_8}^{S_2,S_1} = H_{e_1,n_8}^{S_3,S_4} = H_{e_1,n_8}^{S_4,S_3}$ and $H_{e_2,n_8}^{S_3,S_4} = 1 = H_{e_2,n_8}^{S_4,S_3}$. For example $H_{e_2,n_8}^{S_3,S_4} = 1$ indicates that $f_{s_3}^{(2)} = f_{s_4}^{(2)}$, a DSR has been deployed at bus n_8 for both s, s' and a marketing campaign has not been waged in any of s, s'. The variable is ultimately useful for the determination of $Z_e^{s,s'}$ (see further below). Note that it is essential to use $\tilde{e}_{e,n^*}^{2,s,s'}$ rather than $e_{e,n^*}^{2,s}$ in order to avoid having $H_{e,n}^{s,s'} = 1$ with one of $e_{e,n^*}^{2,s}, e_{e,n^*}^{2,s'}$ being zero.

Constraint (4.33) states that $\mathbb{T}_{e,n^*}^{s,s'} = True$ if the current level of uncertainty resolution at n is the first ($\mathbb{e}_{e,n^*}^{1,s} = True = \mathbb{e}_{e,n^*}^{1,s'}$. This is equivalently expressed as $\tilde{e}_{e,n^*}^{1,s,s'} = 1$, i.e. no DSR has been deployed across both s, s') or is the second but with identical scenarios ($\mathbb{H}_{e,n^*}^{s,s'} = True$). That is, $\mathbb{T}_{e,n^*}^{s,s'} = True$ reflects that s, s' are identical for the uncertain bus n^* (i.e. if the tree does not have any DSR investments in other critical buses,

the two scenarios will be indistinguishable) either because a DSR has not been deployed or because a marketing campaign has not been made. For example, some indicative values corresponding to Figure 4.9 are $T_{e_1,n_5}^{s,s'} = 1\ \forall s \neq s'$, $T_{e_1,n_8}^{S_1,S_2} = 1$. The equivalent mixed integer linear representation of the constraint is the following.

$$T_{e,n^*}^{s,s'} \geq \tilde{e}_{e,n^*}^{1,s,s'} \qquad \forall s, s', e, n^*, \qquad (4.47)$$

$$T_{e,n^*}^{s,s'} \geq H_{e,n^*}^{s,s'} \qquad \forall s, s', e, n^*, \qquad (4.48)$$

$$T_{e,n^*}^{s,s'} \leq H_{e,n^*}^{s,s'} + \tilde{e}_{e,n^*}^{1,s,s'} \qquad \forall s, s', e, n^*, \qquad (4.49)$$

where $\tilde{e}_{e,n^*}^{1,s,s'}$ is defined as $\tilde{e}_{e,n^*}^{2,s,s'}$ above. According to (4.47)-(4.49), if $H_{e,n}^{s,s'} = \tilde{e}_{e,n^*}^{1,s,s'} = 0$, then $T_{e,n}^{s,s'} = 0$. However, if at least one of $H_{e,n}^{s,s'} = 1, \tilde{e}_{e,n^*}^{1,s,s'} = 1$ holds then $T_{e,n}^{s,s'} = 1$. In other words, if no DSR has been deployed at the uncertain bus n^* ($\tilde{e}_{e,n^*}^{1,s,s'} = 1$) then, obviously it will be $H_{e,n^*}^{s,s'} = 0$ (i.e.the second level of DDU resolution is not the current one) and $T_{e,n^*}^{s,s'} = 1$. Similarly, if $H_{e,n^*}^{s,s'} = 1$, then obviously it is $\tilde{e}_{e,n^*}^{1,s,s'} = 0$ and $T_{e,n^*}^{s,s'} = 1$. It is not possible to have $H_{e,n^*}^{s,s'} = 1 = \tilde{e}_{e,n^*}^{1,s,s'}$.

Constraint (4.34) states that if it is $T_{e,n^*}^{s,s'} = 1$ at all critical buses n^*then the two scenarios are identical by epoch e i.e. $\mathbb{Z}_e^{s,s'} = True$. In other words, for two scenarios to be identical, at both of them it must be that i) no DSR investment has taken place at any uncertain bus, or ii) such a DSR investment has taken place but the flexible load is still identical. This constraint can be written in mixed integer linear form in the following way, where (4.50) - (4.51) inform that if $T_{e,n^*}^{s,s'} = 0$ for at least one bus n^* then s, s' become distinguishable.

$$Z_e^{s,s'} \leq T_{e,n^*}^{s,s'} \qquad \forall s, s', e, \ \forall n^* \qquad (4.50)$$

$$\sum_{n^*}\left(1 - T_{e,n^*}^{s,s'}\right) + Z_e^{s,s'} \geq 1 \qquad \forall s, s', e \qquad (4.51)$$

Finally, constraint (4.35) describes the Benders cut appended to the master problem at each Benders iteration.

Note that in order to keep the number of scenarios to four it has been assumed that the tree in Figure 4.8applies to all uncertain buses (i.e. buses 5 and 8) and that the level of consumer participation at both buses will follow the same path. For example, if a marketing campaign has been conducted at bus 8 with the consumer participation there resulting in 35% (i.e. path 20% → 35%) then a potential DSR deployment at bus 5 will also follow the same path (20% → 35%) and vice versa (see Figure 4.9). This is achieved in the mathematical formulation by defining $f_S^{(2)}, f_S^{(3)}$ for four scenarios each $(s_1, \dots, s_4)$ and one table $\mathbb{C}_{s,s'}$that actually states that at level 2 the pairs (s_1, s_2) and (s_3, s_4) contain identical scenarios. This problem in its full dimension will need to have a tree similar to that shown in Figure 4.8 for every uncertain bus (i.e. buses 5 and 8) and thus define 16 scenarios in total (combination of each of the four values in level-3 of both trees). This way the second deployment of DSR (e.g. at bus 5 in scenario 3 and epoch 4 in Figure 4.9) will lead to branching of the tree as this happens in the first epoch after the DSR deployment at bus 8and this does not happen in Figure 4.9 because there are only four scenarios defined in the problem. This small number of scenarios allows for a small-sized problem and better comprehension of the corresponding logic.

The formulation for the operational subproblem corresponding to Benders iteration i for a particular scenario s, and epoch e consists of (3.17), (3.18), (3.20), (3.21), (3.22), (3.23), (3.24), (3.25), (3.26). It also consists of (4.52), (4.53), (4.54), where the first determines that the upper bound for the amount of load (kW) that can be disconnected during period t at the uncertain bus n^* is $f_s^{(2)} d_{s,e,t,n^*}$ after a DSR is deployed ($\Delta_{n^*} = 1$), or $f_s^{(3)} d_{s,e,t,n^*}$after a marketing campaign is conducted ($M_{n^*} = 1$). Constraint (4.53) states that for buses that are not uncertain, the upper bound for the disconnected load is $\bar{f} d_{s,e,t,n}$ whether or not a marketing compaign is conducted, where $\bar{f}$ is a fixed value for the consumer participation. Finally, (4.54) is in the same logic as (3.25) and (3.26) but applies to M_n, where $m_{s,e,n}^i$ is the Lagrange multiplier.

$$\Xi_{t,n^*} \leq \Delta_{n^*} f_s^{(2)} d_{s,e,t,n^*} + M_{n^*}(f_s^{(3)} - f_s^{(2)}) d_{s,e,t,n^*} \qquad \forall t, n^* \qquad (4.52)$$

$$\Xi_{t,n} \leq \Delta_n \bar{f} \cdot d_{s,e,t,n} \qquad \begin{matrix} \forall t, \\ \forall n \in \Omega_N - \Omega_{NU} \end{matrix} \qquad (4.53)$$

$$M_n = \widetilde{N}_{s,e,n}^i : m_{s,e,n}^i \qquad \forall n \qquad (4.54)$$

4.2.4 ***Solution Methodology***

The problem is solved using five typical weeks and Benders decomposition with $\alpha_{s,e}$ type of Benders cut (i.e. $IFI_{s,e}$). This results in obtaining the solution in less than 30 minutes.

Chapter 5 Concluding remarks and further work

5.1 *Summary of findings and future goals*

This thesis proposes models for identifying the optimal investment strategy towards alleviating network constraints that may arise due to uncertain DG penetration and/or load growth. The models consider conventional reinforcement (line redonctoring and line upgrades) and a range of smart technologies (SOP, CVC, DSR, DLR, storage, APGC). In addition, exogenous and endogenous types of uncertainty are modelled with particular emphasis on possible categories of DDU resolution. Through case studies on networks it is demonstrated that smart technologies considerably alleviate the need for anticipatory (especially tied to the first epoch) conventional commitments as the planner can take advantage of the strategic flexibility embedded in such technologies; application of deterministic approaches systematically undervalues this benefit and may lead to unnecessarily high levels of risk of stranded assets and basically hinder the transition to the smart grid as smart assets are completely ignored in the resulting optimal solution. The strategic flexibility of smart technologies is crystallized in the concept of option value.

This thesis also proposes a new class of optimization models for identifying the optimal investment strategy under endogenous uncertainty. This type of modelling can be useful in yielding policy and investment decisions around future innovation developments since most new technologies are characterized by DDU. Applications focus on the uncertain consumer participation in DSR schemes and on the uncertainty surrounding technoeconomic characteristics of storage technology with four assumptions for the uncertainty resolution being considered; local or global, and, immediate or local resolution. These applications highlight the fact that resolving the uncertainty early may entail significant strategic benefits, thus making a strong case for the earliest possible deployment of smart technologies in the power system.

An important insight of the present work is that the increasing uncertainty in combination with the lack of regulatory frameworks that consider a candidate technology's option value are bound to hinder the deployment of smart grid assets and favor long-term capital commitments at the detriment of flexibility. The presented methods can be

instrumental in enabling a shift towards strategic distribution network planning, thereby contributing to the reduction of stranding risk and to the generation of net savings for consumers and network planners alike. Below, a list of findings follows.

- The option value of investing in a smart technology can be quantified by solving two stochastic programming formulations that consider identical technologies but one of these formulations does not consider the technology whose option value is to be determined.

- The option value of investing in a smart technology represents the expected net benefit (investment and operational) accrued from considering this technology in the investment solution. It is a nonnegative value that reflects the flexibility that the corresponding smart technology holds to deal with uncertainty. Also, the magnitude of option value is problem-specific and it is determined by the properties assigned to the particular technology in the formulation.

- Smart technologies are shown to result in the eradication of first-epoch risk of stranded assets as they alleviate the need for first-epoch conventional reinforcement decisions.

- Coordinated Voltage Control and Soft Open Point technologies are shown to hold considerable option value as their operation can affect large areas of a network ('non localized effects') in addition to the relatively small associated build times (comparing to conventional technologies).Similar conclusions hold for other smart technologies including DLR, DSR and Storage.

- Deterministic planning approaches are shown to yield investment solutions that systematically ignore smart technologies, potentially hindering the transition to the smart grid. In addition, given the increasing levels of uncertainty, deterministic planning approaches are no longer relevant and lead to decisions characterized by high levels of stranding risk.

- Problems characterized by decision-dependent uncertainty (or endogenous uncertainty) can be decomposed via Benders Decomposition, applications of which that rely on greater number of cuts appended to the master subproblem are shown to yield considerable benefits in terms of solution times.

- Decision –dependent uncertainty can be resolved in four ways, namely locally, globally, gradually and immediately. All of these formulations are characterized by a dependence relationship between uncertainty resolution and decision variables, which requires scenario variable stochastic formulation application.

- Problems exhibiting decision-dependent uncertainty allow for embedding within the Benders decomposition algorithm a novel extension that exploits the dependence between uncertainty resolution and decision variables yielding faster solution times.

- Problems exhibiting decision-dependent uncertainty require the application of non-anticipativity constraints (NACs) in both of their forms: Unconditionally in the first epoch and conditionally in subsequent epochs. The recognition of the fact that NACs need only apply to investment variables allows for parallel implementation of the operational subproblems that are independent of each other.

- Stochastic optimization planning under DDU leads to the conclusion that smart grid technologies need to be deployed as soon as possible because such an investment allows for early resolution of uncertainty.

- The DDU concept can be applied not only to distribution planning but also to transmission planning yielding the same conclusions.

5.2 *Prospects for future work*

The focus of work in the midterm future lies in the development and application of novel decomposition and linearization techniques (e.g. linearization of ACOPF as in [91]) for achieving more efficient solution times as outlined in the recent literature. For example, the combination of temporal decomposition with tight relaxation schemes has already been demonstrated to offer impressive computational gains in the context of stochastic transmission planning [92]. Extending this scheme to the non-linear ACOPF paradigm will be imperative for rendering the proposed modelling approach scalable to larger systems and scenario trees.

Implementing new decomposition methodologies may allow for the study of larger networks with the availability of a wider range of conventional reinforcement options such as different conductor types (each with its own technical characteristics) as well as of smart technologies that will be modelled also in greater detail. For instance, the modelling of different storage technologies will offer the possibility for the computation of the option value of each one of them. Moreover, notice that in this thesis no differentiation to the load profile between different load buses exists. This is also the case for the PV generation

pattern in section 2.2, as the same pattern applies to all PV units. Although multi-area profile diversification could in fact create a challenge of potential intractability due to the rapid increase of possible operating points, there is expectation that the application of new decomposition schemes could allow for overcoming this challenge.

Another future goal is to model the operation of smart technologies under a wider variety of system conditions. The current thesis investigates the voltage rise effect and the accommodation, within thermal limits, of increased power flows. However, the flexibility of smart technologies may well be observed on other occasions such as the operation of SOP technology to assist in maintaining the supply of loads after the occurrence of faults that caused the tripping of critical supply lines.

Another area for improvement is the consideration of uncertainty at operating timescales both for wind and load profiles. Note that uncertainty around demand growth has been incorporated in section 2.1, but it spans investment timescales. Modelling demand level uncertainty at operating timescales would not only make the case study more realistic (as at each hourly period more than one values for demand per bus would be possible) but could also affect the optimal investment decisions.

A further goal for future work involves the consideration of extra sources of uncertainty including market prices for coal (thereby affecting the cost of conventional reinforcement) or the cost of power electronic components, which may affect the optimal investment decisions for particular smart technologies such as SOPs. In the case of the transmission system, uncertainty around the market price for oil and gas may result in changes of the merit order dispatch while also directly impacting the power flow patterns across various corridors.

There is also much potential for future work in the area of DDU with specific emphasis on the modelling of new types of DDU. Particularly, the authors in [48] classify endogenous uncertainty in two categories: First, as analyzed in the current thesis, the planner makes some decisions that lead to resolution of uncertainty, which is depicted through the expansion of the decision tree in more scenarios. Secondly, the planner makes some decisions that may alter the probability distribution (see [93]) by making one outcome more probable than others. Notice that the current thesis investigates four possible types (namely local, global, immediate and gradual) of resolution of DDU of the first category

because no investment decision is shown to alter the probability distributions. An application of the second category of endogenous uncertainty would be to make certain investment decisions that would make it more likely for DG units to connect to certain areas than areas. Note that all this analysis – concerning both endogenous and exogenous sources of uncertainty – can be performed also within a minimax-regret modelling framework, in which probability parameters are no longer used with the eventual goal then being to minimize the maximum associated regret.

It is also very much interesting to analyse how the operation of smart technologies may affect the higher voltage grid. Such an analysis will try to respond to questions such as "How the optimal operation of smart technologies will change if all distribution voltage levels are taken into account along with those of the transmission system?", "will the optimal operation of CVC become suboptimal when the resulting transmission system effects are taken into consideration?".

Note that specifically for CVC a further goal includes conducting system-wide sensitivity analysis as this may lead to significant reductions in cost of installing this technology in the system. In particular, such a sensitivity analysis will allow selection of critical buses that will be used as sources of information and will at the same time be the positions of measurement for feeding the CVC technology with the appropriate information, thereby removing the need for collecting information on a system-wide basis, as is the case in this thesis.

There is also much interest in combining exogenous with endogenous types of uncertainty in one formulation. That would pose significant challenges with respect to the computational load and this difficulty may lead to innovative ideas around new algorithmic methodologies that reduce the solution times. Another topic of interest is the application of DDU to transmission system planning, as in section 3.3, but in a more detailed way involving decommissions of units and a wide variety of assets relevant to the transmission system e.g. FACTS.

Finally, it is necessary to underline that this thesis is part of attempts made to investigate the field of real options. Extracting the option value of smart technologies may be possible by using multiple approaches stemming both from the fields of mathematical finance and mathematical optimisation. In the current thesis, the option value is obtained

using mathematical optimization theory but it would be interesting to apply new ideas from other research areas that would enhance or even modify the meaning of option value. The investigation of new ideas for application to computationally calculate the option value constitutes a fundamental goal of future work.

References

[1] *Autonomic Power System*, 2016. [Online]. Available: www.imperial.ac.uk/electrical-engineering/research/control-and-power/research/autonomic-power-system-aps/. [Accessed: 02- Oct- 2016].

[2] *Autonomic Economics*, 2016. [Online]. Available: http://autonomicpowersystem.org.uk/projects/ae.html#ae13-12. [Accessed: 02- Oct- 2016].

[3] UK Governmet, Climate Change Act, TSO, London 2008.

[4] Council of the European Union, Energy and Climate Change – Elements of the final compromise, Dec. 2008.

[5] G. Strbac, I. Konstantelos, M. Pollitt, R. Green, *Delivering future-proof energy infrastructure: Report for National Infrastructure Commission*, Feb. 2016.

[6] OFGEM, "Strategy decision for the RIIO-ED1 electricity distribution price control," 04/03/2013.

[7] O. Brewin, S.C.E. Jupe, M. G. Bartlett, K.T. Jackson and C. Hanmer, "New Technologies for Low Voltage Distribution Networks", *ISGT Europe*, Manchester, 2011.

[8] Eurelectric *Active Distribution System Management– Full Discussion Paper*, Feb. 2013.

[9] J.M. Bloemink and T.C. Green, "Benefits of distribution-level power electronics for supporting distributed generation growth", *IEEE Trans. Power Del.*, vol. 28, no.2, pp. 911–919, Apr. 2013.

[10] J. M. Bloemink and T. C. Green, "Increasing distributed generation penetration using soft normally-open points," *IEEE PES General Meeting*, Minneapolis, MN, 2010, pp. 1-8.

[11] S. Giannelos, I. Konstantelos and G. Strbac, “Option value of Soft Open Points in distribution networks,” *PowerTech, 2015 IEEE,* Eindhoven, 2015, pp 1-6.

[12] L. Y. Seng and P. Taylor, "Innovative Application of Demand Side Management to Power Systems," *First International Conference on Industrial and Information Systems*, Peradeniya, 2006, pp. 185-189.

[13] G. Strbac, “Demand side management: Benefits and challenges,” *Energy Policy,* vol. 36, no. 12, pp. 4419-4426, 2008.

[14] S.N. Liew and G. Strbac, “Maximizing Penetration of Wind Generation in Existing Distribution Networks”, *IEE Proceedings -Generation, Transmission and Distribution,* vol. 149, no. 3, pp. 256-262, May 2002.

[15] V. Stanojevic, V. Silva, G. Strbac, D. Pudjianto, P. Lang and D. MacLeman, "Application of storage and demand side management to optimise existing network capacity," *Electricity Distribution - Part 2, 2009. CIRED 2009. The 20th International Conference and Exhibition on*, Prague, 2009, pp. 1-1.

[16] C. R. Black and W. A. Chisholm, "Key Considerations for the Selection of Dynamic Thermal Line Rating Systems," in *IEEE Transactions on Power Delivery*, vol. 30, no. 5, pp. 2154-2162, Oct. 2015.

[17] S. Mohtashami; D. Pudjianto; G. Strbac, "Strategic Distribution Network Planning With Smart Grid Technologies," in *IEEE Transactions on Smart Grid* , vol.PP, no.99, pp.1-1

[18] A. A. Rahim, I. Z. Abidin, F. Tarlochan and M. F. Hashim, "Thermal rating monitoring of the TNB overhead transmission line using line ground clearance measurement and weather monitoring techniques," *Power Engineering and Optimization Conference (PEOCO), 2010 4th International*, Shah Alam, 2010, pp. 274-280.

[19] T. O. Seppa, "FACTS and real time thermal rating - synergistic network technologies," *IEEE Power Engineering Society General Meeting, 2005*, 2005, pp. 2416-2418 Vol. 3.

[20] J. Black, S. Connor and J. Colandairaj, "Planning network reinforcements with Dynamic Line Ratings for overhead transmission lines," *Universities Power Engineering Conference (UPEC), 2010 45th International*, Cardiff, Wales, 2010, pp. 1-6.I.

[21] Statutory Instrument No. 2665 - *Electricity Safety, Quality and Continuity of Supply Regulations*, http://www.berr.gov.uk, 2002.

[22] C. Masters, "Voltage rise: the big issue when connecting embedded generation to long 11 kV overhead lines", *Power Engineering Journal*, vol. 16, no. 1, pp. 5-12, 2002.

[23] G. Strbac, N. Jenkins, P. Djapic, G. Nicholson and M. Hird, "Integration of operation of embedded generation and distribution networks", *Manchester Centre for Electrical Energy*, Manchester, 2002.

[24] T. Sansawatt, J. O'Donnell, L. F. Ochoa, and G. P. Harrison, "Decentralised voltage control for active distribution networks," in *2009 Proc. 44th Int. Universities Power Eng. Conf. (UPEC)*, pp. 1–5.

[25] P. N. Vovos, A. E. Kiprakis, A. R. Wallace and G. P. Harrison, "Centralized and Distributed Voltage Control: Impact on Distributed Generation Penetration," in *IEEE Transactions on Power Systems*, vol. 22, no. 1, pp. 476-483, Feb. 2007.

[26] W. Cao, J. Wu, N. Jenkins, C. Wang and T. Green, "Operating principle of Soft Open Points for electrical distribution network operation", *Applied Energy*, vol. 164, pp. 245-257, 2016.

[27] S. You, H. W. Bindner, J. Hu and P. J. Douglass, "An overview of trends in distribution network planning: A movement towards smart planning", *T&D Conference and Exposition*, 2014 IEEE PES, Chicago, pp. 1-5, 2014.

[28] R. Hidalgo, C. Abbey and G. Joós, "A review of active distribution networks enabling technologies," *IEEE PES General Meeting*, Minneapolis, MN, 2010, pp. 1-9.

[29] F. Maciej, "Modelling, evaluation and demonstration of novel active voltage control schemes to accomodate distributed generation in distribution networks", Brunel University School of Engineering and Design, 2010.

[30] Smith, C.A.; Redfern, M.A.; Potts, S., "Improvement in the performance of on-load tap changer transformers operating in series," *Power Engineering Society General Meeting, 2003, IEEE*, vol.3, no., pp.,1910 Vol. 3, 13-17 July 2003.

[31] Thomson M., "Automatic voltage control relays and embedded generation," *Power Engineering Journal*, vol.14, no.2, pp.71, 76, April 2000.

[32] X. Tao and P. Taylor, "Voltage Control Techniques for Electrical Distribution Networks Including Distributed Generation", in *17th International Federation of Automatic Control World Congress*, 2008.

[33] Elkhatib, M.E.; El-Shatshat, R.; Salama, M.M.A., "Novel Coordinated Voltage Control for Smart Distribution Networks with DG," *IEEE Transactions on Smart Grid*, vol.2, no.4, pp.598, 605, Dec. 2011.

[34] X. Liu, A. Aichhorn, L. Liu and H. Li, "Coordinated Control of Distributed Energy Storage System With Tap Changer Transformers for Voltage Rise Mitigation Under High Photovoltaic Penetration," in *IEEE Transactions on Smart Grid*, vol. 3, no. 2, pp. 897-906, June 2012.

[35] Konstantelos and G. Strbac, "Valuation of flexible investment options under uncertainty", *IEEE Trans. Power Syst*., vol. 30, no. 2, pp. 1047-1055, Mar. 2015.

[36] E. Buzarquis, G. A. Blanco, F. Olsina, and F. F. Garces, "Valuing investments in distribution networks with DG under uncertainty," *T&D Conference and Exposition: Latin America*, 2010 *IEEE PES*, Sao Paulo, pp. 341-348, 2010.

[37] G. Strbac and D. Kirschen, Fundamentals of Power System Economics: John Wiley & Sons, Ltd, 2004.

[38] T.A.Luehman, "Strategy as a portfolio of real options," *Harvard Bus. Rev.,* pp. 76-99, 1998.

[39] G. Blanco, F.Olsina, F. Garces, and C. Rehtanz, "Real option valuation of FACTS investments based on the least square Monte Carlo Method," *IEEE Trans. Power Syst.,* vol. 26, no. 3, pp. 1389-1398, Aug. 2011.

[40] Y. Kitapbayev, J. Moriarty and P. Mancarella, "Stochastic control and real options valuation of thermal storage-enabled demand response from flexible district energy systems", *Applied Energy*, vol. 137, pp. 823-831, 2015.

[41] B. Ramanathan and S. Varadan, "Analysis of Transmission Investments using Real Options," *2006 IEEE PES Power Systems Conference and Exposition*, Atlanta, GA, 2006, pp. 266-273.

[42] Triantis A.J., "Real Options," in *Handbook of Modern Finance,* D1-D32, 2003.

[43] S. Giannelos, I. Konstantelos and G. Strbac, "Stochastic optimization-based valuation of smart grid options under firm DG contracts," accepted for presentation in IEEE EnergyCon, Leuven, 2016.

[44] P. Vasquez and F. Olsina, "Valuing Flexibility of DG Investments in Transmission Expansion Planning," *Power Tech, 2007 IEEE Lausanne*, Lausanne, 2007, pp. 695-700.

[45] Ofgem*, Real Options and Investment Decision Making*, Mar. 2012.

[46] Frontier Economics, A *framework for the evaluation of smart grids: A report prepared for Ofgem*, Mar. 2012.

[47] P. S. Georgilakis and N. Hatziargyriou, "Optimal distributed generation placement in power distribution networks: models, methods, and future research", *IEEE Trans. Power Syst.,* vol. 28, no. 3, Aug. 2013.

[48] V. Goel and I.E. Grossman, “A stochastic programming approach to planning of offshore gas field developments under uncertainty in reserves,” *Computers and Chemical Engineering 28 (8),* 1409-1429, 2004.

[49] V. Goel and I. Grossmann, "A Class of stochastic programs with decision dependent uncertainty", *Mathematical Programming*, vol. 108, no. 2-3, pp. 355-394, 2006.

[50] B. Tarhan, I. Grossmann and V. Goel, “Stochastic Programming Approach for the Planning of Offshore Oil or Gas Field Infrastructure under Decision-Dependent Uncertainty”, *Industrial & Engineering Chemistry Research*, vol. 48, no. 6, pp. 3078-3097, 2009.

[51] V. Gupta and I. Grossmann, "Multistage stochastic programming approach for offshore oilfield infrastructure planning under production sharing agreements and endogenous uncertainties", *Journal of Petroleum Science and Engineering*, vol. 124, pp. 180-197, 2014.

[52] S. Solak, J. Clarke, E. Johnson and E. Barnes, "Optimization of R&D project portfolios under endogenous uncertainty", *European Journal of Operational Research*, vol. 207, no. 1, pp. 420-433, 2010.

[53] B. Tarhan and I. Grossman, “A multistage stochastic programming approach with strategies for uncertainty reduction in the synthesis of process networks with uncertain yields,” *Computers and Chemical Engineering*, vol. 32, no. 4-5, pp 766-788, 2008.

[54] A.J. Conejo, M. Carrion, and J.M. Morales, *Decision making under uncertainty in electricity markets*, New York: Springer, 2010.

[55] I. Konstantelos, “A stochastic optimization framework for anticipatory transmission investments,” Ph.D. dissertation, Department of Electrical and Electronic Engineering, Imperial College London, 2012.

[56] A. Conejo, R. Minguez, E. Castillo, R. Garcia-Bertrand, *Decomposition techniques in mathematical programming*. Berlin: Springer, 2006.

[57] V. Hamidi, K. S. Smith, and R. C. Wilson, “Smart grid technology review within the transmission and distribution sector,” *in Proc. ISGTE*, Gothenburg, Sweden, Oct. 11–13, 2010, pp. 1–8.

[58] *RIIO-ED1 Western Power Distribution business plan*, 2014. [Online]. Available: https://www.westernpower.co.uk/docs/About-us/Stakeholder-information/Our-future-business-plan/WPD-RII-ED1-Business-Plan/WPD-RIIO-ED1-Business-Plan.aspx. [Accessed: 05- Oct- 2016].

[59] G. Strbac, M. Aunedi, D. Pudjianto, P. Djapic, F. Teng and A. Sturt, “Strategic Assessment of the Role and Value of Energy Storage Systems in the UK Low Carbon Energy Future”, Energy Futures Lab, Imperial College London, 2012.

[60] G. Strbac *et al*., “Taking an active approach,” in *IEEE Power and Energy magazine*, vol. 5, no. 4, pp. 68-77, July-Aug. 2007.

[61] “Generation by fuel type”, Elexonportal.co.uk. [Online]. Available: https://www.elexonportal.co.uk

[62] A. McLaughlin, M. Alshamali, J. Colandairaj and S. Connor, "Application of Dynamic Line Rating to Defer Transmission Network Reinforcement due to Wind Generation," *Universities' Power Engineering Conference (UPEC), Proceedings of 2011 46th International*, Soest, Germany, 2011, pp. 1-6.

[63] H. Van der Weidje, B.F. Hobbs, “Planning electricity transmission to accommodate renewables: Using two-stage programming to evaluate flexibility and evaluate uncertainty”, *Cambridge Working Papers in Economics*, Vol. 113, 2011.

[64] J. J. Grainger and J. Stevenson, William D., Power System Analysis. McGraw-Hill, 1994, no. ISBN 0-07-061293-5

[65] S. Haffner, L. F. A. Pereira, L. A. Pereira, and L. S. Barreto, “Multistage model for distribution expansion planning with distributed generation—part I: problem formulation,” *IEEE Trans. Power Del*., vol.23, no. 2, pp. 915–923, Apr. 2008.

[66] “Distributed Generation Connection Guide”, Energy Networks Association, 2014.

[67] P. C. Paiva, H. M. Khodr, J. A. Dominguez-Navarro, J. M. Yusta, and A. J. Urdaneta, “Integral planning of primary-secondary distribution systems using mixed integer linear programming,” *IEEE Trans. Power Syst*., vol. 20, no. 2, pp. 1134–1143, May 2005.

[68] A. Keane, L. F. Ochoa, C. L. T. Borges, G. W. Ault, A. D. Alarcon-Rodriguez, R. A. F. Currie, F. Pilo, C. Dent and G. P. Harrison, “State-of-the-art techniques and challenges ahead for distributed generation planning and optimization”, *IEEE Trans. Power Syst.,* vol. 28, no. 2, pp. 1493-15012, May 2013.

[69] M. Khodr, F. G. Olsina, P. M. Oliveira-De Jesus, and J.M. Yusta, “Maximum savings approach for location and sizing of capacitors in distribution systems,” *Elec. Power Syst. Res.,* vol. 78, no. 7, pp. 1192-1203, 2008.

[70] A. Sallam and O. Malik, *Electric distribution systems*. Wiley-IEEE Press, 2011.

[71] A. Aithal, C. Long, W. Cao, J. Wu and C. E. Ugalde-Loo, "Impact of soft open point on feeder automation," *2016 IEEE International Energy Conference (ENERGYCON)*, Leuven, 2016, pp. 1-6.

[72] M. Fila, D. Reid, G. A. Taylor, P. Lang, and M. R. Irving, “Coordinated voltage control for active network management of distributed generation,” *IEEE PES Gen. Meeting,* Calgary, pp.1-8, Jul. 2009.

[73] E.ON, Network Design Manual v7.7, Dec. 2006.

[74] I. Konstantelos, M. Sun and G. Strbac, *Quantifying demand diversity of households*, Report for the “Low Carbon London” LCNF project, Imperial College London, 2014.

[75] Elexon. Load profiles and their use in electricity settlement, version 2.0, Nov. 2013.

[76] F. Capitanescu, “Critical review of recent advances and further developments needed in AC optimal power flow”, *Elec. Power Syst. Res*., vol. 136, pp. 57-68, 2016.

[77] X. Zhang, G. Karady, K. Piratla, and S. Ariaratnam, “Network capacity assessment of combined heat and power-based distributed generation in urban energy infrastructures,” *IEEE Trans. Smart Grid*, vol.4, no. 4, pp. 2131-2138, Dec. 2013.

[78] R. D. Zimmerman, C. E. Murillo-Sanchez, and R. J. Thomas, “Matpower: steady state operations, planning and analysis tools for power systems research and education,” *IEEE Trans. Power Syst.*, vol. 26, no. 1, pp. 12–19, Feb. 2011.

[79] FICO Xpress Optimization Suite, http://www.fico.com/en/products/fico-xpress-optimization-suite.

[80] T. Holtschneider and I. Erlich, “Modeling demand response of consumers to incentives using fuzzy systems,” *2012 IEEE Power and Energy Society General Meeting,* San Diego, CA, 2012, pp. 1-8.

[81] Frontier Economics, *Demand Side Response in the Domestic Sector – a literature review of major trials*, Aug. 2012.

[82] D. Abi Ghanem, S. Mander, K. Kessels and M. Lombardi, “Consumer engagement with active demand principles and technologies: A review,” *Energy Conference and Exhibition (ENERGYCON), 2012 IEEE International*, Florence, 2012, pp. 687-692.

[83] G. Appa, L. Pitsoulis and H. Williams, Handbook on modelling for discrete optimization. New York: Springer, 2006.

[84] V. Stanojevic, “Enhancing performance of electricity networks through application of demand side response and storage technologies”, Ph.D., Imperial College London, 2012.

[85] Imperial College London and NERA Economic Consulting, "Assessing the Cost Reflectivity of Alternative TNUoS Methodologies", London, 2014.

[86] National Grid, "Electricity Capacity Report", 2015.

[87] National Grid, “Electricity Ten Year Statement”, 2015.

[88] European Wind Energy Association, "Wind Energy Scenarios for 2020", July 2014.

[89] National Grid, "Future Energy Scenarios", 2016.

[90] G. Strbac, M. Aunedi, D. Pudjianto, P. Djapic, F. Teng and A. Sturt, "Strategic Assessment of the Role and Value of Energy Storage Systems in the UK Low Carbon Energy Future", Energy Futures Lab, Imperial College London, 2012.

[91] C. Coffrin, P. Van Hentenryck, and R. Bent, "Approximating line losses and apparent power in AC power flow linearizations", *IEEE PES Gen. Meeting*, San Diego, CA, 2012, pp. 1-8, Jul. 2012.

[92] P. Falugi, I. Konstantelos and G. Strbac, "Application of novel nested decomposition techniques to long-term planning problems," accepted for presentation in PSSC '16, Genoa, 2016.

[93] K. Viswanath, S. Peeta and S. Salman, "Investing in the links of a stochastic network to minimize expected shortest path length", 2004 (Working paper).